

Loughborough University Institutional Repository

Passive acoustic tracking of divers and dolphins

This item was submitted to Loughborough University's Institutional Repository by the/an author.

Additional Information:

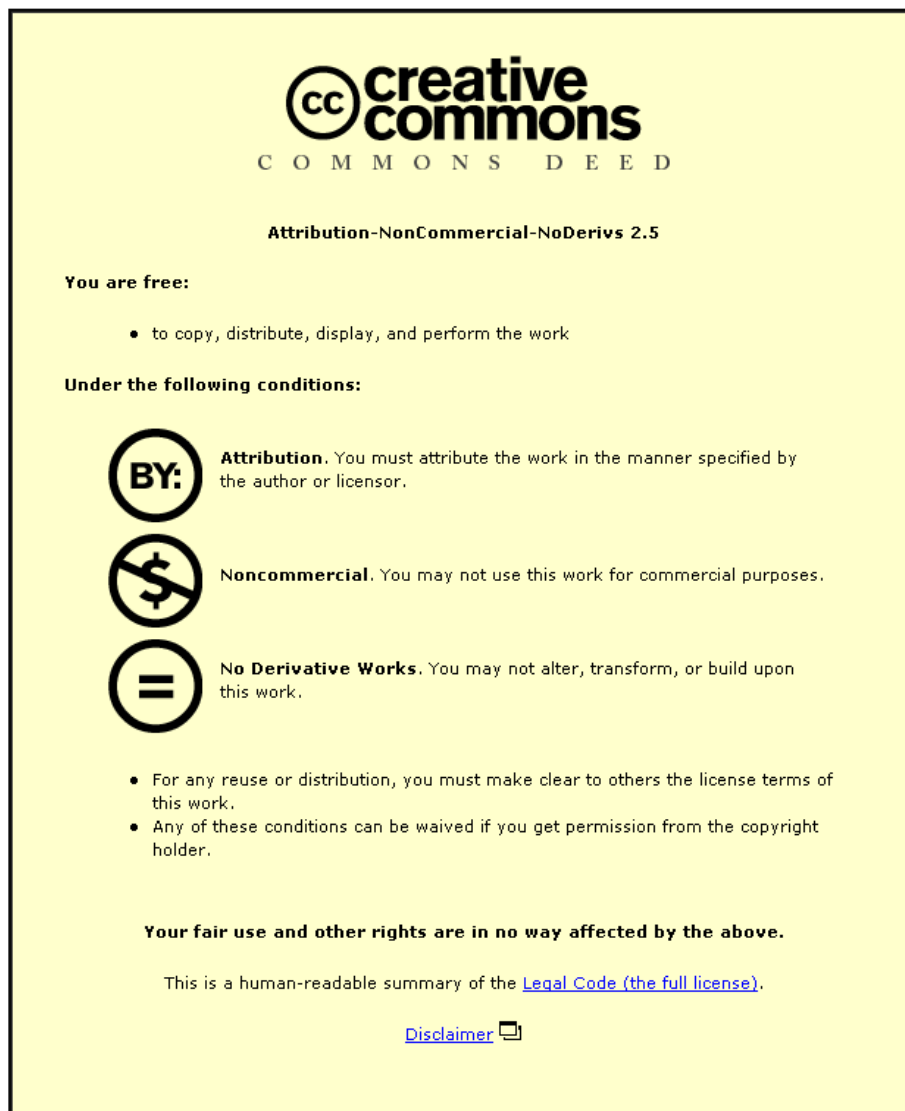
- A Doctoral Thesis. Submitted in partial fulfilment of the requirements for the award of Doctor of Philosophy of Loughborough University.

Metadata Record: <https://dspace.lboro.ac.uk/2134/12883>

Publisher: © Paul Connelly

Please cite the published version.

This item was submitted to Loughborough University as a PhD thesis by the author and is made available in the Institutional Repository (<https://dspace.lboro.ac.uk/>) under the following Creative Commons Licence conditions.



For the full text of this licence, please go to:
<http://creativecommons.org/licenses/by-nc-nd/2.5/>



University Library

Author/Filing Title CONNELLY

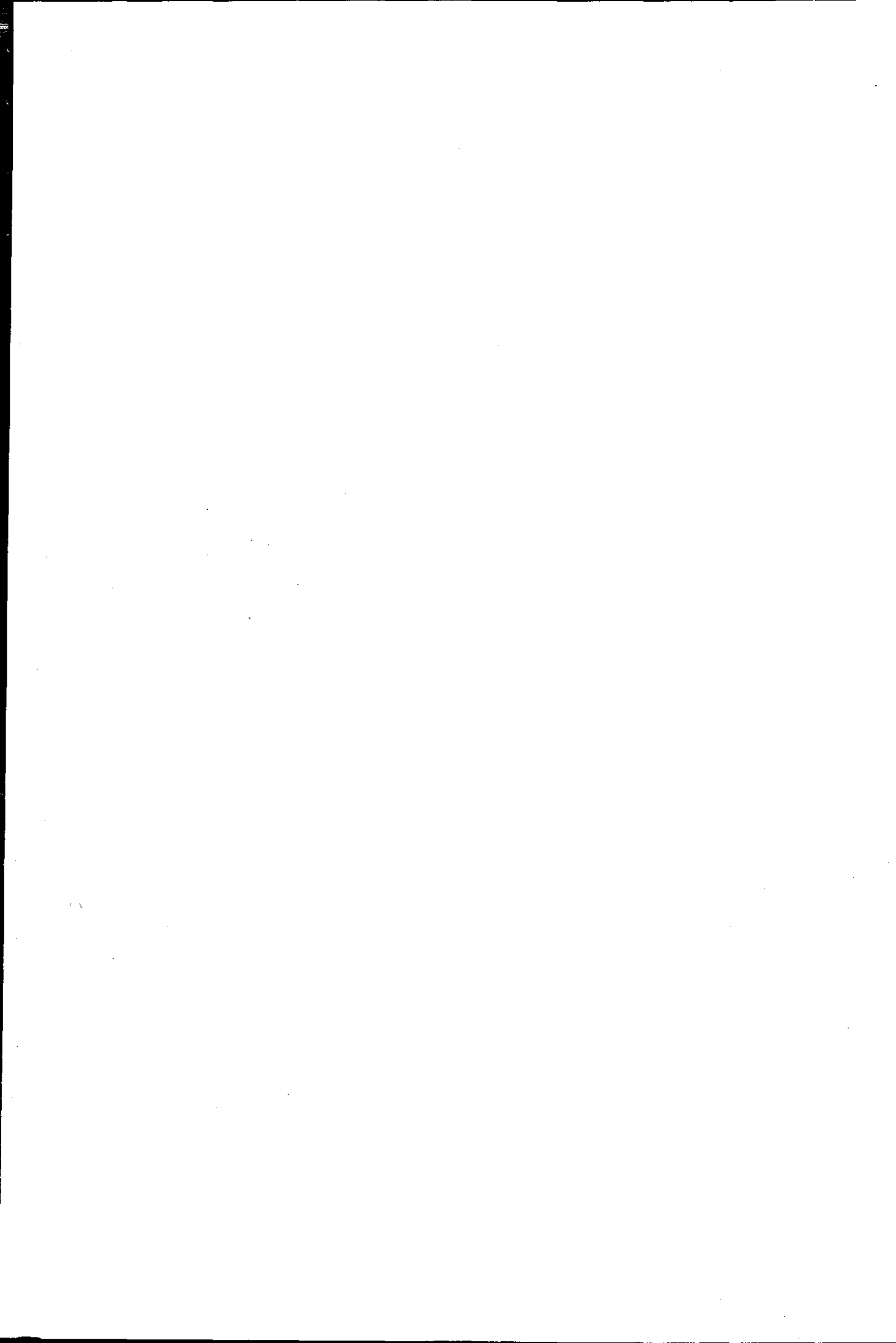
Class Mark

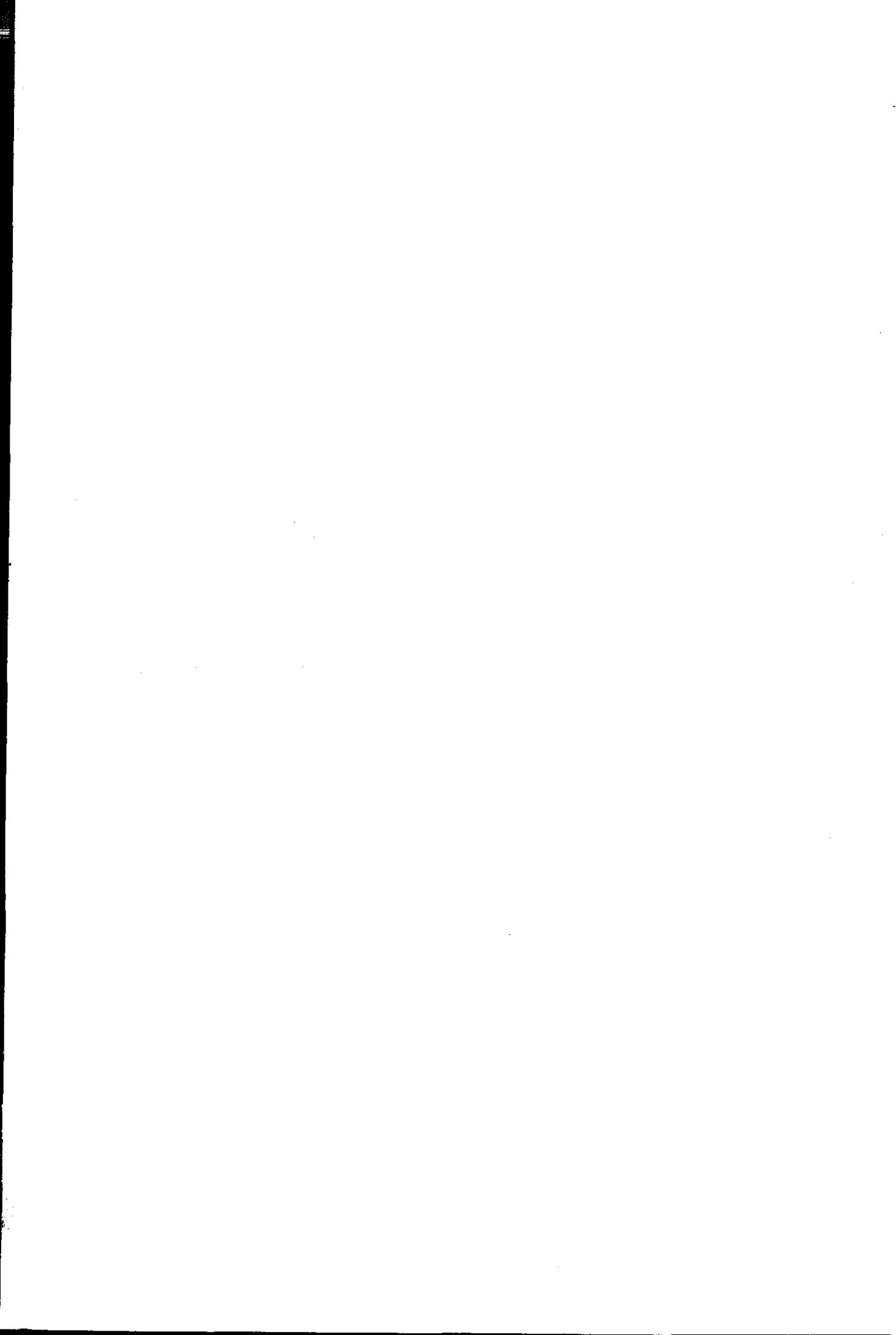
Please note that fines are charged on ALL
overdue items.

--	--	--

0403109752







**PASSIVE ACOUSTIC TRACKING
OF DIVERS AND DOLPHINS**

by


Paul Robert Connelly
MEng, MIEE, PGCE

Thesis submitted in partial fulfilment of the requirements for the award of
Doctor of Philosophy of Loughborough University

June 2004

Supervisor: Professor Bryan Woodward DSc, PhD, DIC, CEng, FIEE, FIOA, FRGS
Underwater Acoustics Research Group
Department of Electrical and Electronic Engineering

© Paul Connelly, 2004

 Loughborough University
Date AUG '05
Class
Acc No. 40310985

ABSTRACT

PASSIVE ACOUSTIC TRACKING OF DIVERS AND DOLPHINS

This thesis describes work performed in the analysis and development of positioning algorithms for self-noise of a known kind; it also describes the development of short base-line systems capable of positioning the sources. Many studies of wild cetaceans rely on tracking the movement of wild animals, often in hostile conditions and with limited contact with these animals. Advanced technology exists for satellite or radio tracking of marine wildlife, but this relies on an animal being first caught and tagged. In situations where random interactions with marine wildlife are to be analysed, it is not practicable to attach devices to an animal, so it is appropriate to use passive techniques, in which the animal's self noise is located and tracked.

Present passive systems usually include a long base-line array, which can be difficult to deploy. The problem may be overcome by reducing the array in size, but it results in an increase in positioning errors. This study attempts to quantify these errors and looks into the practicability of short base-line passive arrays. Two systems are described here, both for tracking impulsive sounds in real time. The first is for use on pelagic trawl nets, the other as a prototype high-speed system to prove the different algorithms developed before and during this study. The prototype systems, each having a minimum of four receivers positioned in various configurations, have been tested in a tank with a controlled sound source. The source is a 'pinger', which allows the systems also to be adopted for diver positioning and tracking.

A survey of unclassified literature has shown characteristics of cetacean acoustic signatures, which have been utilised in the optimisation of the systems. The physiology of cetaceans has also been reviewed to help understand the physical limitations of the systems presented.

ACKNOWLEDGEMENTS

I would like to express my special thanks to my supervisor Professor Bryan Woodward for his encouragement, guidance and endurance. Similarly, I am indebted to my ex-colleagues Dr David Anthony, David Goodson, Dr Paul Lepper, Dr Darryl Newborough and Dr Christopher Richards for their help and support throughout the research work, also to Dr Rob Hay for his help with the development of some of the algorithms.

I am grateful to the European Commission for the funding the research, particularly the FAIR Programme *CETASEL* project and the MAST-II Programme *SIGMA* project. In particular, I would like to thank the partners in the *CETASEL* project for their support, including Dr Mats Amundin (Kolmården Djurpark, Sweden), Dick De Haan (DLO Netherlands Institute for Fisheries Research), Pierre Dremière (IFREMER), Ron Kastelein (Harderwijk Marine Mammal Park) and Kurt Hansen (Danish Institute for Fisheries Technology and Aquaculture). Also, I would like to thank the captain and crew of the Dutch Fisheries Research Vessel *Tridens*.

I must also thank Visiting Professor Tom Curtis and Andy Webb (Qinetiq, previously Defence Evaluation and Research Agency), for their help and advice as well as for the loan of equipment. Further, I would like to thank the technical staff of the Department of Electronic and Electrical Engineering for their help in the construction of the experimental equipment and to the staff of Nortek AS, who have supported me in the later parts of the project.

Finally, I would like to thank my family for their unending support, especially Wendy, Matthew, Inga-Marie and Mum and Dad.

TABLE OF CONTENTS

Title page	i
ABSTRACT	ii
ACKNOWLEDGEMENTS.....	iii
TABLE OF CONTENTS.....	iv
CHAPTER 1 INTRODUCTION.....	1
1.1 <i>SONAR AND UNDERWATER TRACKING SYSTEMS</i>	1
1.1.1 Beginnings of sonar.....	1
1.1.2 From SONAR to tracking systems	2
1.2 <i>BASICS OF ACOUSTICS UNDERWATER</i>	3
1.2.1 Acoustic propagation in water	3
1.2.2 Attenuation due to absorption.....	5
1.2.3 Background noise and signal-to-noise ratios	6
1.2.3.1 Source Level.....	6
1.2.3.2 Background ambient noise level.	6
1.2.3.3 Noise near fishing gear.....	10
1.2.4 Changes in the acoustic velocity in water.....	11
1.2.5 Bioacoustics.....	12
1.2.6 Cetacean echo-location.....	13
1.2.6.1 Sound generation.....	13
1.2.6.2 Sound detection.....	16
1.2.7 Signal processing techniques.....	17
1.2.7.1 Time and phase measurement	18
1.2.7.2 Correlation	18
1.2.7.3 Matched filtering and pulse compression.....	19
1.2.7.4 Streamers.....	20
1.3 <i>TRACKING SYSTEMS AND THEIR USES</i>	20
1.3.1 Traditional tracking methods.....	20
1.3.1.1 Industry / diver systems.....	21
1.3.1.2 Military / covert systems	21
1.3.2 Tracking systems - present technology.....	22
1.4 <i>ACTIVE TRACKING SYSTEMS - ALGORITHMS</i>	24
1.4.1 Spherical tracking systems - mathematics of intersecting spheres	24
1.4.2 Active source / reverberation.....	25
1.5 <i>PASSIVE TRACKING SYSTEMS - ALGORITHMS</i>	26
1.5.1 Three-dimensional array algorithms.....	27
1.5.2 Three dimensions from two?	28
1.5.3 Reverberation method.....	29
1.6 <i>NEW USES FOR PASSIVE TRACKING SYSTEMS</i>	30
1.7 <i>FISHERIES PROBLEM - A TECHNICAL SOLUTION?</i>	30
1.8 <i>THESIS STRUCTURE</i>	33
1.9 References in Chapter 1	34
CHAPTER 2 THEORY	39
2.1 <i>PRE-DEFINED PARAMETERS</i>	39
2.1.1 Physical limitations.....	39
2.1.2 Parameters set by potential users	42
2.2 <i>ACTIVE TRACKING ALGORITHMS</i>	43
2.3 <i>PASSIVE TRACKING ALGORITHMS</i>	46
2.3.1 Absolute algorithms for tracking using hyperbolae.....	49
2.3.1.1 Two-dimensional equation set.....	51
2.3.1.2 Three-dimensional equation set (Method 1).....	53

2.3.2 Absolute method for a flat array (Method 2).....	58
2.4 <i>INACCURACIES IN MEASUREMENTS</i>	61
2.4.1 Tracking using excess receivers (Methods 5 & 6).....	63
2.4.1.1 Linearising the equations	63
2.4.1.2 Least square errors	65
2.4.2 Tabular method (Method 4).....	67
2.5 <i>OTHER TRACKING METHODS</i>	69
2.5.1 The reverberation method (Method 7)	69
2.6 <i>COMPARATIVE ANALYSIS</i>	73
2.7 <i>LIMITATIONS AND PARAMETERS FOR THE SYSTEM</i>	74
2.8 References in Chapter 2	75
CHAPTER 3 SIMULATION	76
3.1 <i>ERROR ANALYSIS</i>	76
3.1.1 Verification of the algorithm being tested.	77
3.1.2 Timing errors.	77
3.1.3 Receiver position analysis	77
3.1.4 Velocity profile variations	77
3.2 <i>ACTIVE TRACKING ALGORITHMS</i>	78
3.3 <i>DIRECTLY-SOLVED PASSIVE TRACKING ALGORITHMS</i>	79
3.3.1 Absolute method – limited receiver positioning (Method 1).....	79
3.3.1.1 No-error simulation	79
3.3.1.2 Timing error	83
3.3.1.3 Receiver positional errors.....	89
3.3.1.4 Errors due to the sound velocity profile	95
3.3.2 Absolute method for a flat arrays (Method2)	99
3.3.2.1 No errors	99
3.3.2.2 Timing errors.....	102
3.3.2.3 Receiver positional errors.....	107
3.3.2.4 Errors due to the velocity profile.....	112
3.4 <i>COMPENSATING PASSIVE TRACKING ALGORITHMS</i>	119
3.4.1 Matrix solved differential equations using singular value decomposition method.....	119
3.4.1.1 No errors	119
3.4.1.2 Timing errors.....	124
3.4.1.3 Receiver positional errors.....	130
3.4.2 Tabular method (Method 4).....	134
3.4.2.1 No errors	134
3.4.2.2 Timing errors.....	139
3.4.2.3 Receiver positional errors.....	140
3.5 <i>OTHER TRACKING METHODS</i>	143
3.5.1 Reverberation method (Method 7).....	143
3.5.1.1 No errors	143
3.5.1.2 Timing errors.....	144
3.5.2.2 Positional errors in the vertical.....	145
3.6 <i>COMPARATIVE ANALYSIS</i>	145
3.7 <i>RECOMMENDATIONS FOR FINAL SYSTEM</i>	147
3.8 References in Chapter 3	147
CHAPTER 4 EXPERIMENTAL SYSTEMS.....	148
4.1 <i>DATA CAPTURE SYSTEMS</i>	148
4.1.1 Filtered amplitude method.....	149
4.1.1.1 Principle	149
4.1.1.2 Method	149
4.1.1.3 Limitations	152
4.1.1.4 Testing.....	152

4.1.1.5 Recommendations	153
4.1.2 Correlation method	153
4.1.2.1 Principle	154
4.1.2.2 Method	154
4.1.2.3 Limitations	157
4.1.2.4 Testing.....	158
4.2 TRACKING SOFTWARE	158
4.2.1 Array method.....	158
4.2.2 High definition system software.....	166
4.2.2.1 Time difference extraction	166
4.2.2.2 Data transfer.....	170
4.2.2.3 System Control.....	170
4.2.2.4 Data logging.....	170
4.2.2.5 Display	171
4.2.2.6 Algorithms	173
4.2.3 Limitations.....	173
4.3 OTHER CONSIDERATIONS	174
4.3.1 Calibration	174
4.3.2 Transmission and pre-distortion	178
4.3.3 Diver and pinger tracking	181
4.3.4 High-Noise situations	181
CHAPTER 5 CASE STUDIES.....	182
5.1 PROJECT CETASEL: BY-CATCH REDUCTION OF SMALL CETACEANS	182
5.1.1 The system.....	184
5.1.1.1 Development of the underwater system	192
5.1.1.2 Power supply unit.....	193
5.1.1.3 Low frequency detector.....	195
5.2 A SIMPLE MEANS OF DETECTING CETACEANS.....	199
5.3 DIRECT DIVER/CETACEAN TRACKING	200
5.3.1 Methodology.....	201
5.3.2 Results	204
5.3.3 Conclusion.....	217
5.4 References in Chapter 5	219
CHAPTER 6 COMPARATIVE ANALYSIS.....	221
6.1 THEORY AND PRACTICE	221
CHAPTER 7 CONCLUSIONS	224
7.1 PASSIVE TRACKING OF DOLPHINS	224
7.1.1 Dynamic deployment.....	224
7.1.2 Static deployment	224
7.2 PASSIVE TRACKING OF DIVERS.....	224
7.3 THREE DIMENSIONS FROM TWO?	225
7.4 SUMMARY.....	225
7.5 FUTURE WORK	226
AUTHOR'S PUBLICATIONS	227
APPENDICES.....	229
Appendix A Expansion of Three-dimensional equation set.	
Appendix B Comprehensive Simulation results.	
Appendix C Single Hydrophone ranging technique.	

Chapter 1

INTRODUCTION

1.1 SONAR AND UNDERWATER TRACKING SYSTEMS

The seas throughout history have been feared and respected, and not without reason. The sea was thought to be limitless in magnitude, inhabited by all sorts of strange and dangerous life forms. Today, virtually all the oceans and seas are charted and much of the sea life is known. However, even today sailors respect the sea and although there is little danger of ferocious sea creatures attacking from below, there are still hidden threats, but mainly from man. As technologies developed it became a priority to see exactly what was down there and where.

1.1.1 BEGINNINGS OF SONAR

Although the use of sound underwater has only been extensively exploited fairly recently, it has been experimented with for centuries. In 1490 Leonardo da Vinci wrote [1]: 'If you cause your ship to stop, and place the head of a long tube in the water and place the outer extremity to your ear, you will hear ships at a great distance from you.' The first recorded regular use of sound underwater was to determine the distance to marker buoys. In 1826 Colladon and Sturm [2] recorded the speed of sound underwater in Lake Geneva. They used an underwater bell, striking it at the same instant as a light flashed. By measuring the difference in time of arrival between the light and the sound, the speed of sound in water could be calculated. Underwater bells were in use for navigation by 1900, both as a method of detecting buoys and lightships in fog and as a method of distance measuring. In 1912, a few days after the *Titanic* disaster, the British Patent Office received a patent application for echo-location with airborne sound from L.F. Richardson [3]. A month later he applied for the patent for its use underwater.

The outbreak of the First World War increased the impetus of research into underwater acoustics. A method of locating the direction of a source of sound was being increasingly used, based on Da Vinci's tubes, but with a pair of tubes to make use of the binaural sense of direction. Today, there are three main types of transducer in use for underwater applications. These are: (a) Magnetostrictive, (b) Piezoelectric and (c) Electrostrictive [4]. Magnetostrictive transducers had been tested with limited success early on but the discovery of the piezoelectric effect allowed the first hydrophones to be used. In 1917 Langevin used piezoelectric crystals to replace the condenser versions that had been tested up until then, and in 1918 echoes were received for the first time from a submarine, occasionally at distances as great as 1500 metres. Meanwhile, a top secret system was being developed by the Allies, known as ASDIC [4] (Allied Submarine Devices Investigation Committee). This was a system of echolocation that could determine the distance and bearing to an object, thus determining its position. In the years since then, systems have been developed not only for military work but also for civil navigation. In the United States, the term ASDIC was gradually replaced by SONAR, which stands for **S**ound **N**avigation and **R**anging. This term complements well with **R**ADAR, the term for the electromagnetic ranging developed in Britain just before the Second World War.

1.1.2 FROM SONAR TO TRACKING SYSTEMS

It soon became obvious that just knowing the range and an approximate bearing to an object would not be enough. More accurate methods of locating a fixed or moving point were needed. This was achieved in a number of ways. ASDIC and standard SONAR uses directional hydrophones, or arrays of hydrophones to locate the bearing of the return of an acoustic signal transmitted by the same system. If the target to be tracked is known and can be fitted with a device (a transponder) that receives and retransmits an acoustic signal, then with the aid of a spatial array of hydrophones, the position of the transponder can be fixed without the need for directional hydrophones. This type of system is in wide use for the localisation of oil bore holes and remotely-operated underwater vehicles [5]. A slightly more challenging problem is to track a sound source without knowing the time of flight of the sound from source to receiver, i.e. to track an object's self-noise. This is of obvious use for covert operations and for operations where the user is incapable of attaching any form of transponder, such as tracking the engine noise of ships undetected,

or for tracking the routes taken by echo-locating wildlife. The latter application has been adopted as the theme for this study, and by imitating signals produced by such animals any other beacon can be tracked using the same method.

1.2 BASIC THEORY OF ACOUSTICS UNDERWATER

To design an effective system for acoustic operations underwater, it is important to fully understand the limitations imposed by the different factors of the environment and technology. As with most sets of design parameters, some are more critical than others. The more important factors are explained here.

1.2.1 ACOUSTIC PROPAGATION IN WATER

In any design of underwater acoustic technology, it is important to be able to predict the response of a system. To be able to achieve this, the reaction of the sound with the medium it is travelling through, in this case water, must be characterised. A set of equations, known as the sonar equations, achieves this. If we consider a point source emitting sound equally in all directions, then at a distance, r , from the source, the sound intensity, I , which is equal to the power per unit area, P/A , is

$$I = P / (4 \pi r^2) \quad (1-1)$$

where P is the acoustic power of the source and $4 \pi r^2$ is the area of the sphere of radius r .

The Source Level (SL) expressed in this form is the intensity of the outgoing wave at a standard distance (commonly 1 m). If expressed in dB, the Source Level is given by

$$SL = 10 \log I = (10 \log P - 11) \text{ W / Steradian} \quad (1.2)$$

Where the factor 11 is $10 \log (4 \pi r^2)$ using 1m as the radius

When the signal is not impeded, it spreads with spherical divergence. It is improbable that the signal will travel unimpeded. In practice, as sound passes through a medium, energy is absorbed and converted to heat. The amount is proportional to the density and temperature of the medium, which includes the water itself, fish, plankton, other sea life as well as bubbles in the signal path, all of which can scatter the signal.

Many of these factors are not predictable and make it difficult to draw up rules such that realistic models can be devised. However, some of the factors can be calculated. When a source emits sound in water, it transforms electrical or mechanical energy into acoustic energy by generating an alternating sound pressure that is superimposed on the static ambient water pressure. The following relation exists between the acoustic power, P , and the sound pressure, p :

$$P = p^2 A / \rho c \quad (1-2)$$

where p is the root-mean-square pressure, ρ is the density of water and c is the velocity of sound [6]. Using (1-1) this can be rewritten as:

$$I = p^2 / \rho c \quad (1-3)$$

More commonly the source level is expressed in terms of pressure in micropascals (μPa). From (1-1) and (1-4), a conversion factor between intensity and pressure can be calculated:

$$I = (1 \times 10^{-6}) / \rho c \quad (1-4)$$

So

$$SL = 10 \log I = (10 \log P + 10 \log ((1 \times 10^{-6})^2) + 10 \log (\rho c / 4\pi)) \text{ dB re } 1 \mu\text{Pa}$$

Or

$$SL = 10 \log I = 10 \log P + 170.9 \text{ dB re } 1 \mu\text{Pa @ } 1\text{m} \quad (1-5)$$

Where 170.8 is conversion factor to give re micro-Pascals at 1 m instead of W/Steradian with a typical sea water density of 1030 kg/m^3 and sound speed 1500m/s .

As sound is propagated through a medium, there is a motion of the particles such that the product of the root-mean-square (rms) particle velocity and the rms sound pressure is equal to the intensity

$$I = p v \quad (1-6)$$

which when combined with (1-4) gives:

$$p v = p^2 / \rho c \quad (1-7)$$

and

$$v = p / \rho c \quad (1-8)$$

To calculate a signal pressure level at any point, the Source Level must be known. As the signal spreads out there will be propagation losses. These can take various forms and are influenced by various factors including temperature, salinity and frequency as well as distance. The most significant is spreading loss, due to the sound signal physically spreading out, i.e.

$$\text{Spreading Loss} = 10 \log R^2 = 20 \log R \quad (1-9)$$

1.2.2 ATTENUATION DUE TO ABSORPTION

A significant attenuation loss occurs due to absorption in the water; in general the higher the frequency the larger the attenuation due to absorption. This loss may be written as

$$\text{Attenuation loss} = \alpha R \text{ dB} \quad (1-11)$$

where α is the absorption loss [7] given by

$$\alpha = 0.1f^2 / (1 + f^2) + 40f^2(4100 + f^2) + 2.75 \times 10^{-4} f^2 / 914.4 \text{ dB re 1m} \quad (1-12)$$

for a water temperature of 4.4°C and a salinity of 3.5%.

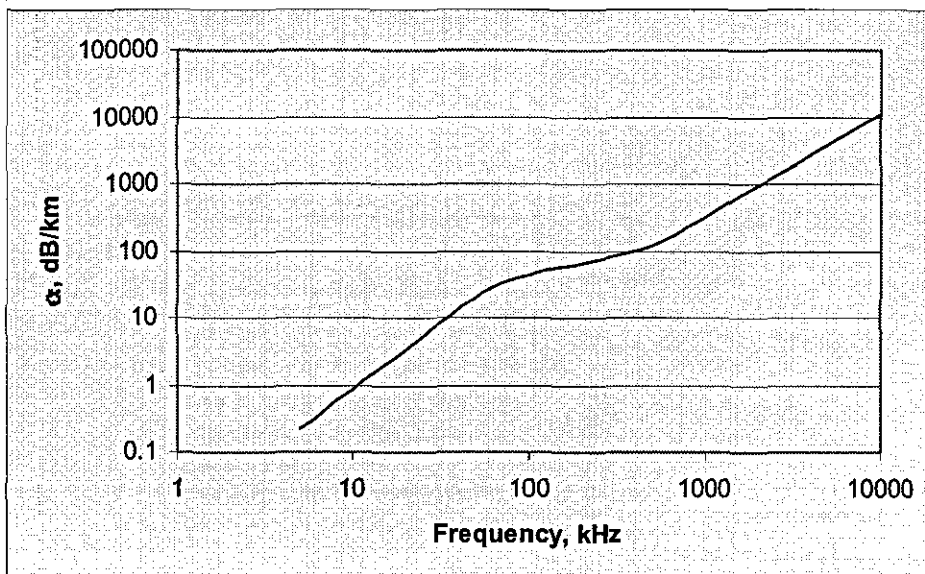


FIGURE 1.2-1 VARIATION OF α WITH FREQUENCY IN SALT WATER RECALCULATED FROM [8]

A general solution for the calculation of α has not yet been produced. Most engineers and scientists use a look-up table, as shown in Figure 1.2-1

Combining these equations gives an expression for transmission loss as:

$$TL = 20 \log R + \alpha R \text{ dB re 1m} \quad (1-13)$$

At short ranges the dominant loss of power is due to spherical spreading but as the range increases, absorption losses become more significant. This assumes nothing will severely impede the flow of the signal. In real life the signal reflects from the sea surface and the sea bed, and reflections and refractions occur wherever temperature (and therefore density) changes in the water; these interfaces are known as thermoclines. In some situations, depending on the water depth, separation of source and receiver, type of source, source pulse length and so on, the transmission loss may fall towards cylindrical spreading. However this effect only happens if the acoustic signal is of sufficient length to allow mixing effects of the reverberant and direct signal.

1.2.3 BACKGROUND NOISE AND SIGNAL-TO-NOISE RATIOS

To show the limitations of a system, we need to calculate the physical constraints. For example, to determine the maximum physical detection range without using special noise reducing signal processing techniques, we need two pieces of information, the Source Level and the background noise level.

1.2.3.1 SOURCE LEVEL

The Source Level is dependant on various factors. For example, an echo-location click detected from an animal may seem to vary with direction due to the animal's sonar directivity pattern and the bearing from which the reading was taken [9,10]. Each click is likely to have slightly differing source levels depending on the animal's activity and its acoustic environment. The source level of the click may also vary with frequency and the repetition rate.

1.2.3.2 BACKGROUND AMBIENT NOISE LEVEL.

The Noise Level at a point is dependent on many factors, including seismic and industrial activity, distant shipping, ocean turbulence, precipitation, and biological and thermal noise sources [7,8,11-13].

Any object vibrating under the water surface produces background noise. This can range from air bubble 'fizz' (cavitation) produced by crashing waves, to stones or sand moving on the sea bed, to machine noise produced by ships or other man-made sources. Although it is difficult to predict exactly what the noise level will be at any place at any moment, it is possible to make some assumptions. In deep water, noise is quite predictable, and generally it increases and becomes less predictable as the water gets shallower. Three of the main factors to which the noise can be attributed are; shipping and industrial noise, wind noise and biological noise, also seasonal variations can be detected. Figure 1.2-2 shows the ambient noise spectrum in deep water, including a noise window between 50 kHz and 200 kHz in which the ambient noise is at its lowest.

Noise below 50 kHz originates from the sea surface in the vicinity of the hydrophone and increases with sea state. Above 200kHz the thermal noise of the sea is dominant.

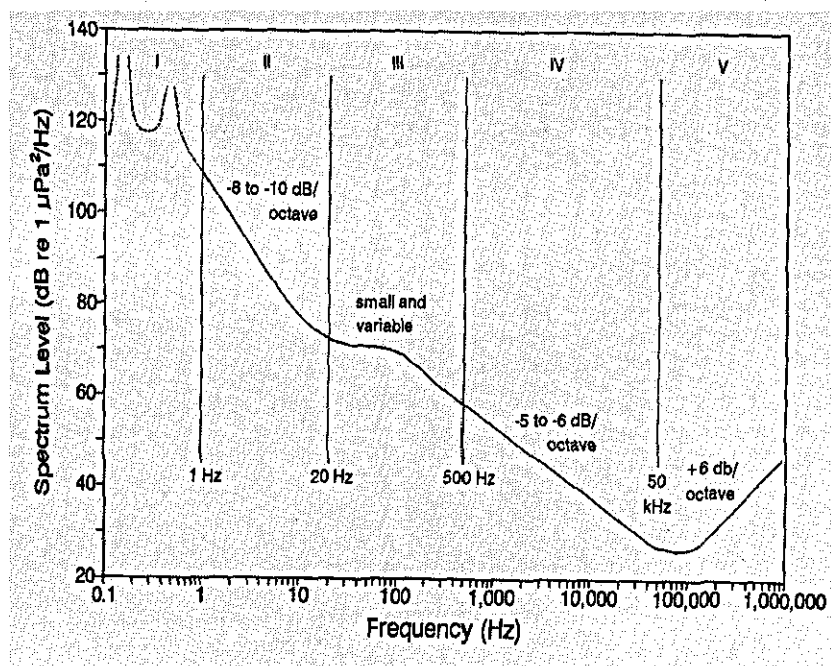


FIGURE 1.2-2 LOW NOISE WINDOW [15]

The equipment measuring the noise can itself produce noise, for example by water flowing over it causing vibrations (hydrodynamic noise), or by the vessel towing the equipment. Noise can also be generated by the local environment, i.e. hydrophone mountings or by noise in the electronic circuitry. This is known as self-noise.

Ambient noise has been measured in the ocean [13,14] for both shallow and deep water. Figures 1.2-3a and 1.2-3b show shallow water noise measured in five different areas and averaged to give a more general solution showing the differences caused by sea conditions or by weather.

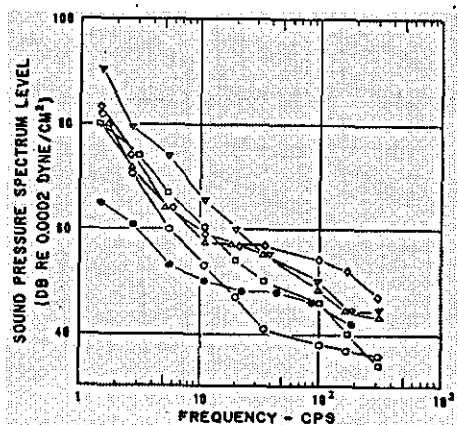


FIGURE 1.2-3A AMBIENT NOISE AVERAGED FROM FIVE DIFFERENT DEEP WATER AREAS, SHOWING DIFFERENCES CAUSED BY SEA CONDITIONS. [13]

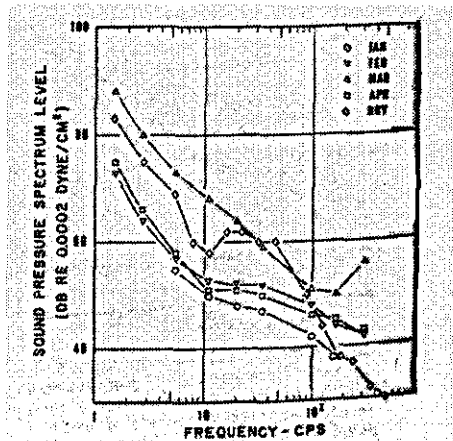


FIGURE 1.2-3B SEASONAL DIFFERENCES IN THE LOW FREQUENCY PART OF THE NOISE SPECTRUM.[13]

If the most dominant noise sources are collated into a single graph (Figure 1.2-4) it can be seen that at low frequencies (<100Hz) intermittent seismic activities are by far the most dominant. As we measure further up the spectrum (100-1000Hz) traffic noise takes priority, then weather conditions and sea state become dominant (600Hz -10 kHz and higher). Above 50kHz thermal noise becomes relevant. As can be seen the average

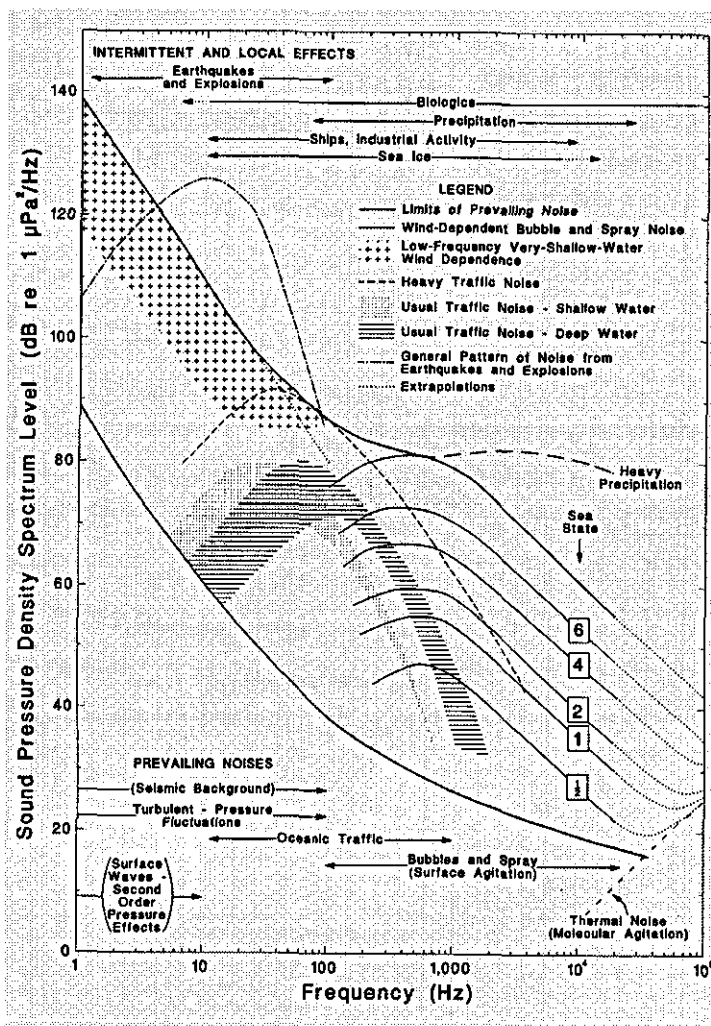


FIGURE 1.2-4 GENERALISED AMBIENT NOISE SPECTRA ATTRIBUTABLE TO VARIOUS SOURCES, TAKEN FROM [13], REDRAWN IN [15]

noise level appears to be lower in the frequency band between approximately 10kHz and 300kHz. This is the part of the acoustic spectrum most commonly used in sonar systems for both man and cetaceans.

1.2.3.3 NOISE NEAR FISHING GEAR

As stated earlier, machines and other man-made sound sources can significantly contribute to the overall noise in a sea environment. In particular, in the vicinity of a

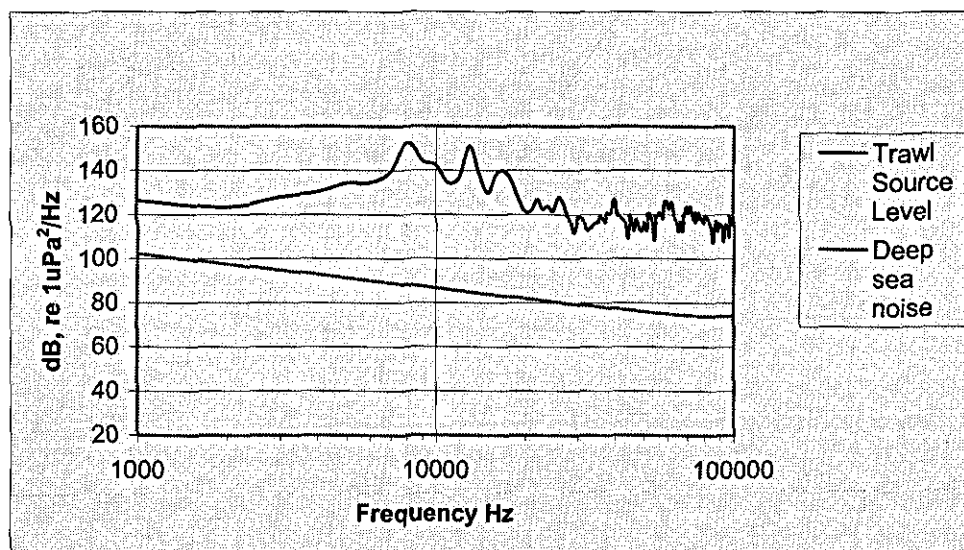


FIGURE 1.2-5 NOISE SPECTRUM OF A FISHING TRAWLER OVERLAID ON THE AMBIENT BACKGROUND NOISE

fishing trawler, the ship's machinery is working hard to tow the nets which themselves make noise in the water.

If acoustic equipment is to be positioned near, or in, such fishing equipment the ship's engines and the noise of the trawl and its associated gear tend to be the greatest contributor to the ambient noise.

Figure 1.2-5 shows the noise of a typical fishing vessel (RV *Tridens*) pulling a pelagic trawl; this has been adjusted to reduce noise from metal objects in the rigging. The lower line shows the deep-sea noise floor.

1.2.4 CHANGES IN THE ACOUSTIC VELOCITY IN WATER

In any large expanse of water the acoustic velocity of sound will undoubtedly change from area to area. In fact, within an area of a few square kilometres with constant bottom and surface conditions the velocity is similar in the horizontal but changes considerably in the vertical. When acoustic measurements are to be made in an area it is therefore important to know these velocities. Three main factors, salinity, pressure and temperature, affect acoustic velocity in water. In most locations the salinity and pressure are predictable but it is temperature as a function of depth that is the most variable and difficult to predict. The vertical section of the sea tends to be split into layers known as thermoclines. Each layer is often considerably different from those above and below.

As would be expected, the greatest temperature variations are close to the surface, and so the velocity stability tends to be worst at the shallow layers, getting progressively more stable with depth. This is reinforced by fresh water run-off that changes the salinity of the surface layer when near land or in wet climates. Figure 1.2-6 shows a typical depth velocity profile with thermoclines, which change within a range of days to many years.

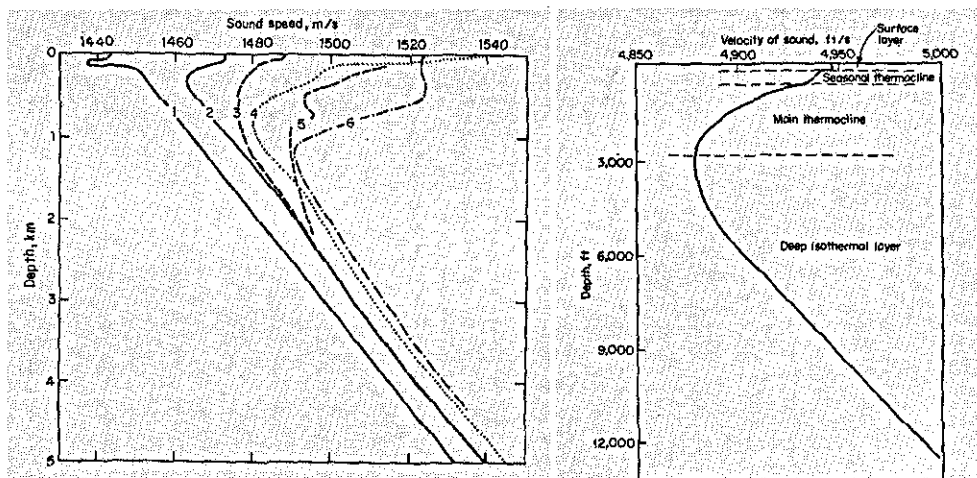


FIGURE 1.2-6 SOUND VELOCITY PROFILES [8] SHOWING A) BOTH GEOGRAPHICAL AND SEASONAL CHANGES RANGING FROM 1-ARCTIC THROUGH WINTER TO TROPICAL SUMMER. B) THE LAYER STRUCTURE OF A TYPICAL OCEAN VELOCITY PROFILE

In practice velocity changes can vary as much as 100 m/s, although the change is gradual. These changes in velocity bend the acoustic waves and the bending is only predictable if the depth profile is known. Most positioning algorithms rely on the sound travelling in straight lines. It is therefore important to predict the errors due to the extended ray path. Figure 1.2-7 shows a model of a ray along with the sound velocity profile.

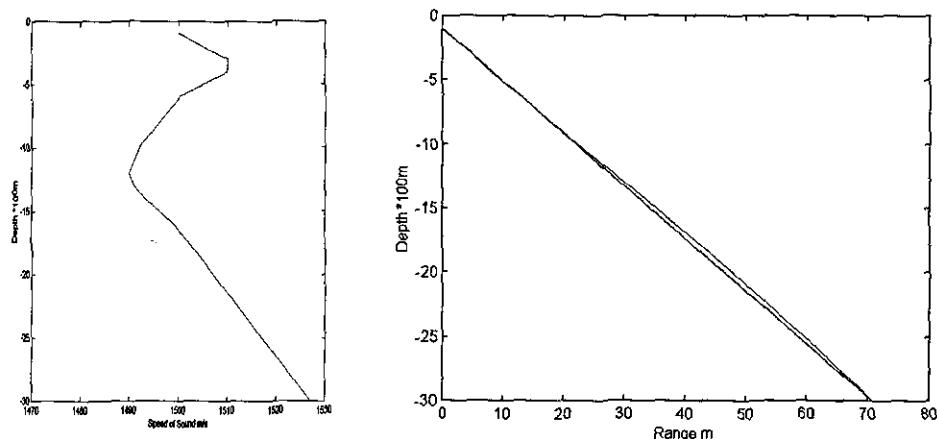


FIGURE 1.2-7 RAY BENDING FROM MATLAB SHOWING A) THE VELOCITY PROFILE AND B) THE BENDING OF THE SIGNAL (BLUE) FROM THE DIRECT PATH (GREEN)

1.2.5 BIOACOUSTICS

Although man has been utilising acoustic techniques underwater for many years, there is very much to be learnt from the 'natives'. In some respects, wildlife in the sea has evolved the use of acoustics to a degree far higher than that of mankind. Much is yet unknown as to the mechanics behind some of the capabilities of oceanic wildlife, or indeed the purposes of their actions. A good example of this is the dolphin family, which is capable of detecting not only the shape or material of a target at distance, but also the thickness of aluminium containers to an accuracy of 0.2 mm [16]. Snapping shrimps are also thought to use sound as a weapon, using the vibrations caused by banging their legs together to stun their prey. Harbour porpoises can penetrate the sea bed with their sound whilst foraging [17]. Sound is not only used for feeding purposes, for example humpback whales are known for their deep melodic 'songs' that are thought to be used to communicate over large distances, and many other cetaceans use the same method. Many species of cetacean use low frequency sound (typically 1 kHz - 20 kHz [18-20],

although recordings have been taken up to 30kHz [21]) to make other individuals in the group aware of their presence or mood [22].

1.2.6 CETACEAN ECHOLOCATION

Cetaceans have evolved their own SONAR systems in many ways similar to man's systems. Their abilities are mainly due to the evolution of two parts of their anatomy.

1.2.6.1 SOUND GENERATION

The animal's head has evolved two sound producing organs in its blow hole capable of producing whistle noises at the lower frequencies and click noises at higher frequencies. A fatty tissue area in front of these organs, known as the melon, contains areas of differing densities and serves as a lens to focus the sound into a beam, which is projected into the water in front of the animal.

Figure 1.2-8a shows the sections that are thought to be linked to the sound generation and reception of the dolphin. Figures 1.2-8b and 1.2-8c show a simulation of the generation of the echolocation clicks taking the physiology of the animal into account.

Cetaceans have sound production and detection capabilities over a very large frequency range in comparison to humans. Certain species produce whistle sounds typically from 3kHz to 24kHz and clicks from about 2kHz to about 140 kHz [25]. The clicks can have a repetition rate up to 800Hz [26] (although up to 300 Hz is more common) and a pulse length in the range of 50 - 100 μ s [27] when homing onto potential food. There is good evidence that cetacean sounds give general information in the wild [26,28-31] and the clicks are generally used for echolocation [32,33], although it is thought that the high frequency clicks may also be involved in communication. This is particularly likely in those animals that do not seem to use the low frequency ranges, for example the harbour porpoise (*Phocoena phocoena*) [34-37], Commerson's dolphin (*Cephalorhynchus commersonii*) and Hector's dolphin (*Cephalorhynchus hectori*) [30]. The sounds emitted from cetaceans have been studied for many years. Early papers describe rasping sounds being produced [38]. These were detected using a variety of instruments ranging from conventional echo sounders [39] to microphones above the water [40].

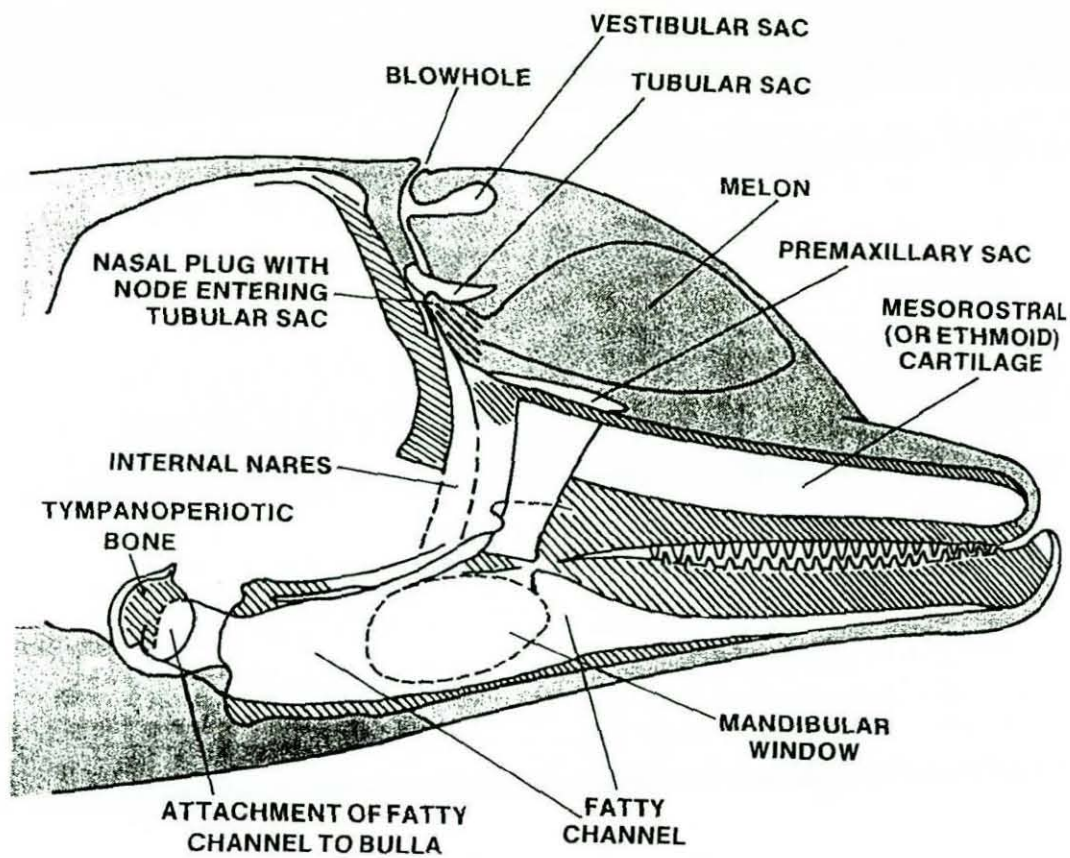


FIGURE 1.2-8A SCHEMATIC OF THE DOLPHIN HEAD SHOWING VARIOUS STRUCTURES ASSOCIATED WITH THE THEORY OF SOUND PRODUCTION IN THE NASAL SAC SYSTEM [23]

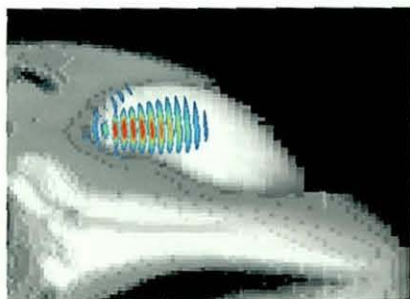


FIGURE 1.2-8B

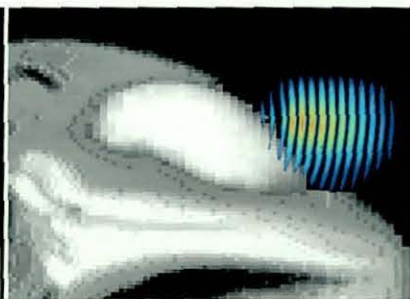


FIGURE 1.2-8C

TLM MODELLING OF THE SOUND GENERATION OF ECHOLOCATION CLICKS IN THE MELON OF A BOTTLENOSE DOLPHIN [24]

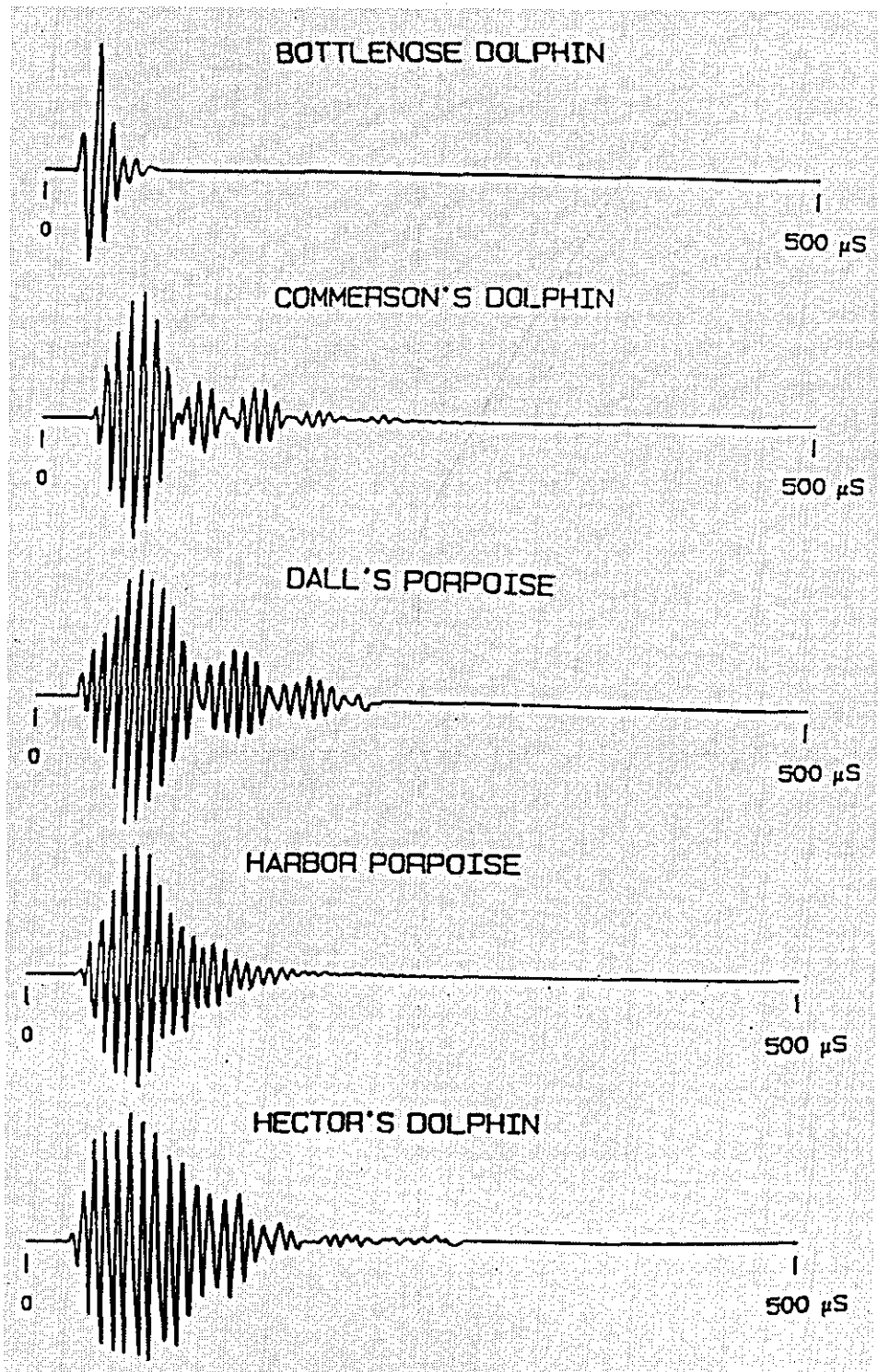


FIGURE 1.2-9 ECHOLOCATION CLICKS FROM VARIOUS CETACEAN SPECIES [41]

The typical cetacean echolocation pulse takes the form of a short (30-100 μ s) [42] raised-cosine type of pulse at frequencies typically between 10 kHz and 170 kHz [43-45], as seen in Figure 1.2-9. It can clearly be seen that the bottlenose dolphin pulse is the shortest, with only one cycle at full amplitude. This is probably to reduce any ambiguities as to arrival time of any echoes, and also to allow greater energy to pass into the water without using up much of the animal's precious life resources. To increase efficiency and to allow the cetacean to look in particular directions, the sound producing organs show some directionality. Cetacean families such as *Phocoena*, in particular the harbour porpoise (*Phocoena phocoena*), have a high directivity of 9° horizontally and 18° vertically [46] although these measurements have not been verified experimentally. Other species, such as the bottlenose dolphin (*Tursiops truncatus*) have slightly lower indexes but tend to use lower frequency sound (70 kHz), giving greater range. Recent evidence has shown that some dolphins (*Tursiops Truncatus*) may have a capability of switching frequency at will, possibly to characterise a target, switching between 40-60 kHz and 100-120 kHz, the higher frequency giving the higher definition [42]. Such dual-bandwidth systems are now also used by man for the same purpose [47].

As with many sonar systems the directionality of the dolphin's sound generation system reduces as the frequency drops from the optimum. This results in some signal at lower frequencies being detectable out of the main beam. This is particularly useful in tracking applications where it cannot be guaranteed that the cetacean will always point at the receiving array. Figure 1.2-10 shows the directivity pattern of a bottlenose dolphin at various frequencies.

1.2.6.2 SOUND DETECTION

There are two main theories as to how dolphins detect the high frequency component used for echolocation. These are cochlear hearing [23] and via the lower jaw and teeth [48,49]. Cetaceans cannot always use their eyesight to locate each other or their surroundings, especially in low light conditions. Instead, they probably use a combination of passive tracking (signal intensity, direction and triangulation) as well as their active echolocation systems to detect ranges.

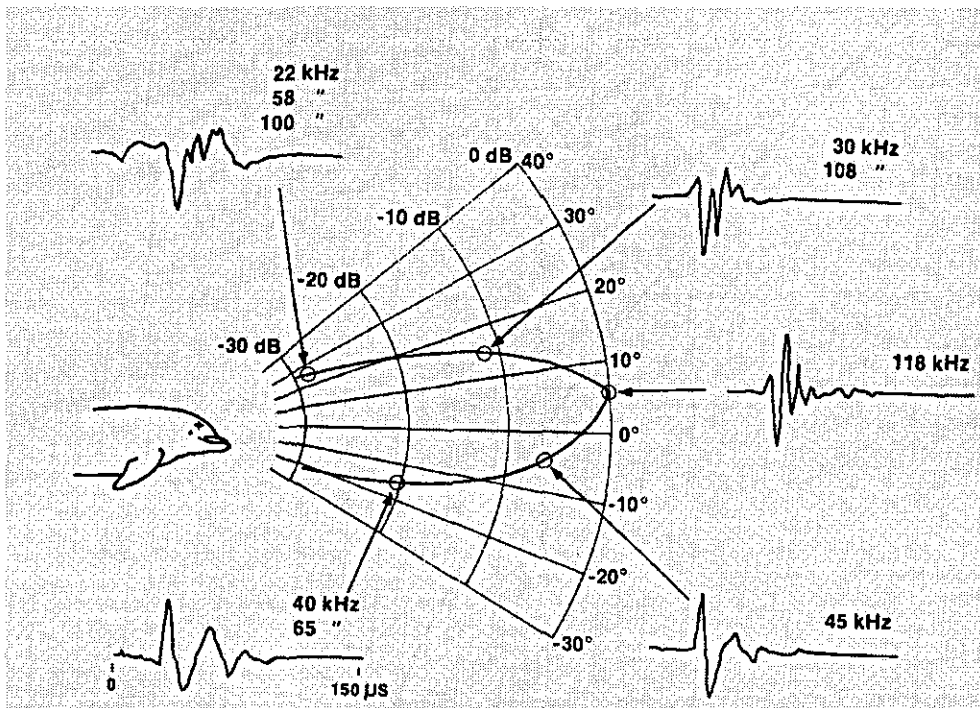


FIGURE 1.2-10 EXAMPLES OF AVERAGE WAVEFORMS AT DIFFERENT AZIMUTHS IN THE HORIZONTAL PLANE FOR VARIOUS PEAK FREQUENCIES. FOR SPECTRA WITH MULTIPLE PEAKS, THE FREQUENCY OF THE PEAKS IS LISTED IN DESCENDING ORDER ACCORDING TO AMPLITUDE [23].

The echolocation system of cetaceans is far better than of any man-made system at present. The U.S. Navy uses dolphins to detect and identify objects under water, in particular mines [50]. Others have tried to simulate the workings of cetacean sonar using various complex computational methods [51], and the cetaceans' methods of identifying objects have also been studied [32,33,52].

1.2.7 SIGNAL PROCESSING TECHNIQUES

The use of signal processing techniques to enhance and improve the results of sound detections has been used for many years. Much can be learnt from techniques designed for RADAR, many of which are directly transposable for use with SONAR

1.2.7.1 TIME AND PHASE MEASUREMENT

As mentioned earlier, arrays of transducers can be used to steer an acoustic beam in desired directions. This is achieved using time or phase delays between each element in the array. The inverse is also true for receiving signals. By adding differing delays (proportional to the position of each element) to the incident acoustic signals, the sensitivity pattern of an array of hydrophones can be made to point in differing directions. If the time difference is calculated instead, a direction relative to the axis of the hydrophones can be calculated. This only works if the time of flight of the acoustic signal is known. If it is not known a hyperbola is described, the source being anywhere on this locus. This principle can be extended to include range and bearing by adding further hydrophones, as explained in Chapter 2.

If the receivers are close together or the source is nearly orthogonal to the two receivers, the time difference will be very small. One technique of measurement in this case is to detect the phase difference in the signals. It is imperative, however, that the time difference should not be greater than one cycle of the signal, as this will result in phase being calculated between different parts of the signal. Timing measurements must therefore be taken between identical parts of the same signal on the two receivers.

1.2.7.2 CORRELATION

If two hydrophones receive a raised cosine pulse from any angle other than the perpendicular, there will be a finite time delay between the arrival times. To calculate the arrival angle to a high degree of accuracy, calculation of this time delay is critical. The simplest method of determining this is to detect a level above the background noise and measure the time delay at this level. For large arrays this may be sufficient, but to achieve greater accuracy, or for smaller arrays, small time difference errors can result in large angular errors (a full analysis of these errors can be found in Chapter 3). To reduce these errors, correlation can be used. In its simplest form, correlation can be written as

$$r_{12} = \frac{1}{N} \sum_{n=0}^{N-1} x_1(n)x_2(n) \quad (1-14)$$

This method is time consuming to calculate, each single correlation requires $2N$ calculations and for a cross correlation needs 2^N calculations, where N is the number of samples taken in a waveform. If there are in excess of 128 data points then it is more efficient to use fast correlation, which requires $12N \log_2 2N + 8N$ calculations. The general equation for fast correlation can be written as

$$r_{12}(j) = \frac{1}{N} F_D^{-1} [X_1^*(k) X_2(k)] \quad (1-15)$$

This method uses both the Discrete Fourier Transforms and its inverse, both of which can be executed using the Fast Fourier Transform (FFT) algorithm.

1.2.7.3 MATCHED FILTERING AND PULSE COMPRESSION

This is a technique used originally in radar to greatly reduce noise, and to increase time accuracy for delays between incident pulses. It is based on correlation and is based on the assumption that the signal is time-limited and has known wave shape. The method comprises a correlation of the incoming signal, $x(i)$, and the time-reversed replica of the signal to be detected, $h(k)$, giving

$$y(i) = \sum_{k=0}^{N-1} h(k)x(i-k) \quad (1-16)$$

The output yields a maximum when the two signals coincide. Pulse compression techniques give an optimum performance with a wideband frequency sweep (chirp) and

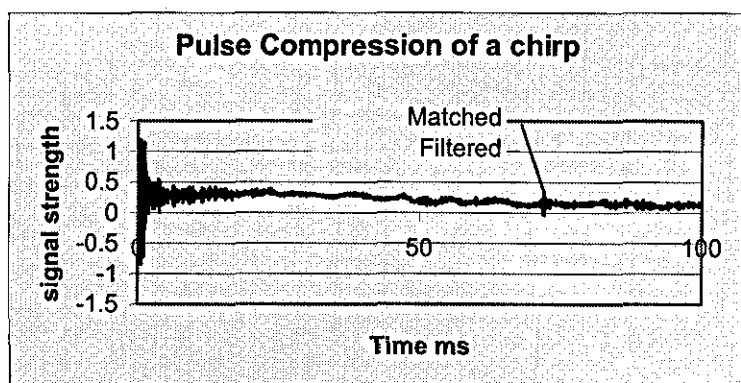


FIGURE 1.2-11 MATCHED FILTER RESPONSE OF AN FM SIGNAL (40MS IN LENGTH).

with a long pulse.

1.2.7.4 STREAMERS

The technology most commonly used to record the signals incorporates streamers, long hydrodynamic oil-filled tubes containing numerous hydrophones, which are either connected together so as to provide a directional line array or are connected individually or in groups to allow beam steering at a later date. These tubes are designed to be towed behind a vehicle and stay in a stable straight line.

1.3 TRACKING SYSTEMS AND THEIR USES

Today, the greatest use for SONAR systems is still as echo-sounders or ranging devices for commercial shipping. The systems nowadays are often used to detect fish in the water column or the range to the sea-bed for navigational purposes. SONAR systems are also used for numerous other navigational tasks such as speed over the ground (using Doppler systems) or for detecting approaching objects and shapes (Scanning SONAR). Often systems are made to switch frequencies depending on range and required resolution; the higher the frequency the greater the resolution but the lower the range. One use of SONAR for commercial shipping is to locate, or relocate, specific areas of interest on the ocean floor. This may be needed to locate lost items (shipwrecks, cargo or pipelines) or to accurately relocate known objects (bore holes). For this type of work high accuracy tracking systems are needed.

1.3.1 TRADITIONAL TRACKING METHODS

In the early days there were few methods of finding lost objects under the sea. If an approximate location was known, and the water was shallow, divers could be sent to find wrecks. At first, eyesight was used to find wrecks, often by towing divers behind boats [53]. However, once the wreck was found a marker buoy or land sightings were often the only way to relocate it. As SONAR technology improved, directional systems using arrays and directional transducers allowed greater accuracy in pinpointing and identifying objects from the surface, and the use of low frequency sound now even allows embedded objects to be viewed. Various SONAR systems exist which can track an object. Most rely on physically moving or steering the sonar beam to give range and bearing. However, the system is not inherently selective in what it detects. Unless a transponder

is used to produce a strong returning signal at either the same frequency, or shifted in frequency to cancel other reflections, the system will see all the reflections, producing a map of the insonified area. To find the bearing many systems steer the transmitted beam either mechanically (moving the transducer with a stepper motor) or electronically (using the phase steering method discussed in section 1.2.7). Other methods include the use of a combination of this method and the array's movement to produce a picture (side-scan).

An important use of SONAR is in the navigation and detection of submarines. Navigation of such vehicles is dependent on sonar systems and accurate charts. However, it is also important to be as inconspicuous as possible. The uses for accurate tracking systems can be summarised into two main categories.

1.3.1.1 INDUSTRY/ DIVER SYSTEMS

The majority of the commercial tracking systems are not concerned with detectability of their signals by third parties. Most systems use a transponder positioned by a diver or Remotely Operated Vehicle (ROV) in the position to be tracked, whether a moving target (diver or ROV) or a static target (bore-hole or wreck). These systems rely on a known time of flight of an acoustic signal from a transponder, the timings giving ranges to a number of receiving hydrophones. In some cases it is not convenient to place a transponder on the target, and then reflectors may be used to increase the detectability of an object using a similar array of hydrophones, the initial acoustic signal being transmitted from the surface. Some systems are available for tracking fish. These rely on an acoustic source being placed on a fish and a more complicated algorithm being used to calculate its position.

1.3.1.2 MILITARY/ COVERT SYSTEMS

As stated earlier, a consideration with military systems is non-detectability. If an active system is used there is a possibility that the signals may be detected by others. The need to be undetectable has led to development of passive systems, which can detect and locate sounds created by other sources. The use of spread spectrum techniques (similar to matched filtering) has allowed active signals to be hidden in noise, with the signal or its reverberations only being recovered if the source signal is known.

1.3.2 TRACKING SYSTEMS-PRESENT TECHNOLOGY

The available tracking systems can be grouped under three main headings [5]:

- Sonar - systems using traditional ranging techniques combined with transducer directionality to give bearing and range.
- Spherical - the use of time of flight to calculate the range to a target, usually using transponders.
- Hyperbolic - when the time of flight is unknown, positions are calculated with an algorithm, usually using pingers or passively.

The spherical and hyperbolic tracking methods can be sub-divided into three categories dependant on their array size:

- i) Super-Short Baseline (SSBL): This arrangement combines all the hydrophones into one physical unit with dimensions of the order of centimetres. Such systems rely on phase measurements within a single cycle.
- ii) Short Baseline (SBL): This is a larger array ranging from 1-20m and relies on phase or time measurements.
- iii) Long Baseline (LBL): This uses a much larger array, often hundreds of metres in size, usually making use of sonobuoys. The upper frequency range of these is limited only by the signal attenuation.

Most research in the public domain has been carried out with the oil industry in mind, with systems to determine the location of bore-holes or objects such as pipelines or the legs of offshore structures, either used in conjunction with an ROV or divers [5]. The systems are used to find the position of a moving object in relation to a fixed object or mother ship, or to position a ship, ROV or diver near a fixed object, i.e. a bore-hole usually marked by a beacon.

Most acoustic tracking systems work by having a stable array of hydrophones, spatially separated, such that the arrival times of any impulse produced by a beacon can produce a position using mathematical models, often to high accuracy ($\pm 0.1\text{m}$). If a transponder is used, it is possible to track with three hydrophones in three-dimensional space, assuming

the transponders are on the surface or on the sea-bed. A pulse can be used to activate the transponder and as long as the processing time of the transponder is known the distance from the transponder to each hydrophone can be calculated, then triangulation is used to find the position. Many systems of this type are commercially available.

If a beacon/pinger is used, the mathematical solutions for the position become more complicated [54] because the time of transmission is not known and so absolute distances cannot easily be calculated. An extra hydrophone is required in this instance. Some systems are available commercially, mainly for use in the fisheries industry.

Each of the above categories has some advantages over the others. The system proposed later in this thesis uses a Short Baseline array, which derives its position from the difference in time of arrival, dt , of the acoustic signal at the hydrophones. This

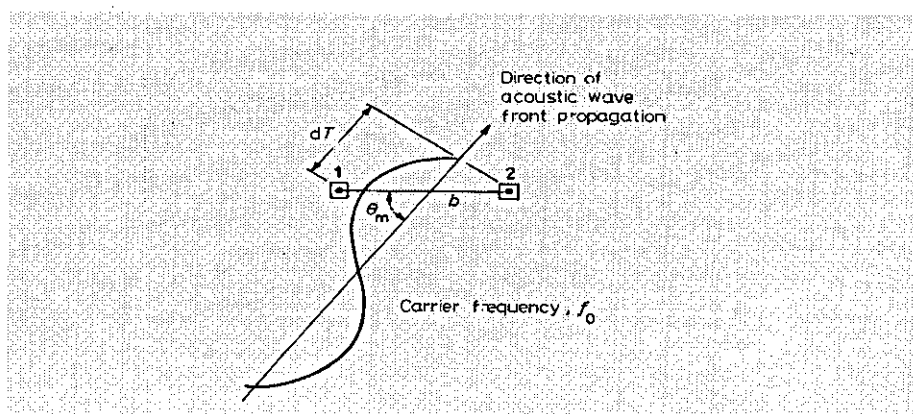


FIGURE 1.3-1 A PULSE ARRIVAL IN A SSBL SYSTEM SHOWING HOW PHASE CAN DETERMINE THE ARRIVAL ANGLE.[5]

information allows bearing and distance to be determined. The use of Short Baseline is convenient, but as with all such systems, its definition is reliant on the accuracy of the time differences measured. As the array gets larger the percentage error due to quantisation is reduced (see section 3.1 for a full analysis).

To make the system compact enough to use on smaller vessels, a Super-Short Baseline can be used. Instead of array spacings of 5-20m [5] as in Short Baseline, Super-Short Baseline typically uses three sensors placed in a single transducer. The method depends

on the relative phase angle of an acoustic pulse arriving at several hydrophones, as shown in Figure 1.3-1; the phase angle corresponds to the direction. If the depth of the beacon is known the position can be calculated easily. If a transponder is used the range information can also be calculated.

If the size of the array is not limited, a Long Baseline system can be used. This works by having an array of transponders at known positions on the sea-bed. Each transponder replies to a specific frequency and is interrogated by a transducer mounted on the hull of a ship or an ROV. The ship can be made to interrogate the array to find ranges to the transponders and hence to find its position. Calibration of the transponder positions can be performed in a number of ways using extra transducers or with one of the other systems, but once in place the system is not dependant on external equipment.

1.4 ACTIVE TRACKING SYSTEMS - ALGORITHMS

An active tracking system is one that generates its own acoustic signal. As the user has control over when the ping occurs and what form the ping takes, they can determine the time of flight of the ping and therefore the range of any returning signals. Assuming the source position and the velocity of sound in the water is known, an array of receivers can determine the position of a transponder or an object reflecting the signal.

1.4.1 SPHERICAL TRACKING SYSTEMS DESCRIPTION OF MATHEMATICS OF INTERSECTING SPHERES

In a two-dimensional space, if a single source transducer (or projector) sends a ping to a transponder, which instantaneously returns the pulse, the time difference between the signal emission and reception corresponds to the range of the object by the equation $d = c \cdot \Delta t$, where c is the velocity of sound in the medium. The transponder could be anywhere on a circle around the transducer. If two transducers are used, spatially separated, then two circles can be drawn around them. Where these circles intersect are the two possible locations of the transponder. Clearly there is an ambiguity but this can be removed by adding a third transducer (Figure 1.4-1).

In three-dimensional space we must now consider spheres instead of circles. It can be seen in Figure 1.4-2 that with three source transducers there is still an ambiguity, which may be eliminated by adding a fourth transducer out of the plane of the other three. If the array is placed in a position where one of the ambiguities is not possible, i.e. at the surface or sea-bed, then the total number of transducers can be reduced by one.

A set of equations for tracking in three-dimensional space is known as the spherical method.

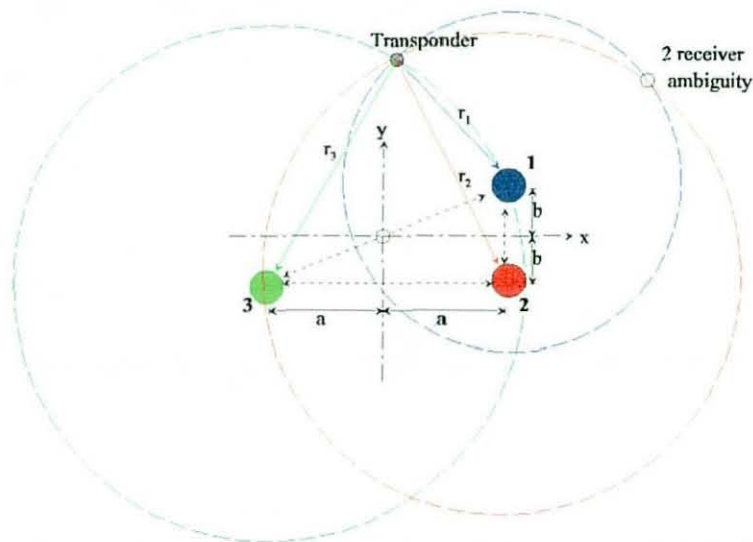


FIGURE 1.4-1 TWO DIMENSIONAL SPACE SHOWING LOCI OF POSSIBLE POSITIONS OF A TRANSPONDER.

1.4.2 ACTIVE SOURCE / REVERBERATION

The method described in 1.4.1 relies on a transponder to return a known signal. It will also work on reflected signals, and with some algorithmic adjustments can be made to work with the source being spatially separated from the receivers. Other methods of active tracking are to use directional systems such as side-scan and move the receiver such that bearing and range can be collated to locate the target. This system allows additional information of the target to be collected, which may provide useful for identification [55].

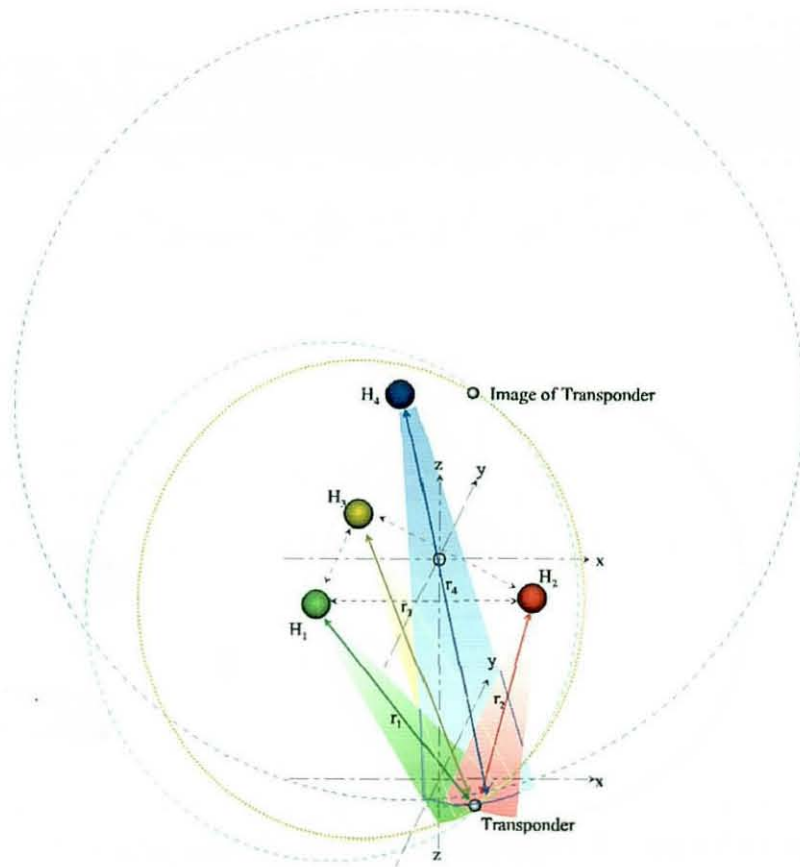


FIGURE 1.4-2 THREE-DIMENSIONAL SPACE SHOWING THE NEED FOR A FOURTH TRANSDUCER

1.5 PASSIVE TRACKING SYSTEMS - ALGORITHMS

A passive tracking system can determine the position of an acoustic source without itself emitting an acoustic signal. The acoustic source could be anything from an engine noise to a marker beacon or even natural marine life noises such as cetacean echolocation. This project has the ultimate aim of tracking cetacean echo-location clicks or other acoustic sources producing similar sounds. There are a number of studies associated with this project [56-58], as well as others that are similar [59-61]. Most independent studies have been in a static situation and have relied on LBL systems, which simplifies the timing circuitry. Such systems suffer from problems if cetacean echo-location clicks are detected, as they tend to be directional at the peak Source Level frequencies, and at lower frequencies where the signals are less directional the SL of the source is reduced. This,

combined with the inter-hydrophone spacings used in LBL makes such a system not ideal for click tracking, but good for tracking the lower frequency whistles.

In many circumstances LBL is not appropriate, for example in any dynamic situation, e.g. on a boat. In this case the array must be fitted to the bow of the vessel, or towed behind the vessel. In this situation SBL or SSBL systems are more suitable. This necessitates a higher accuracy of the timing information.

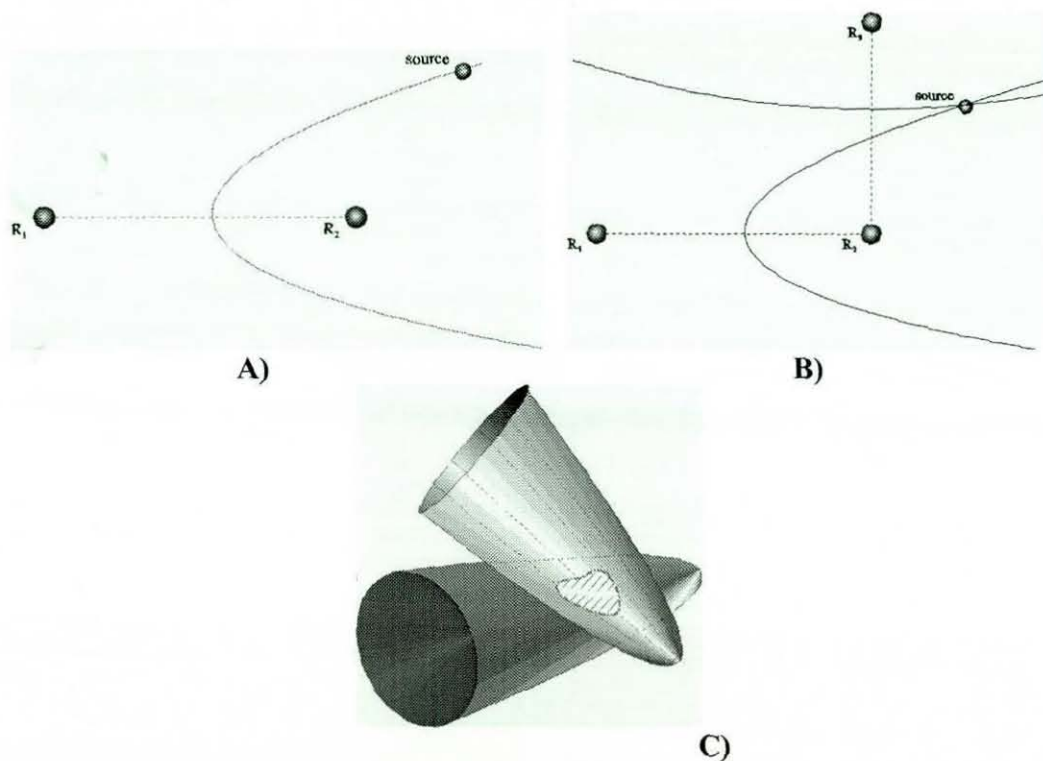


FIGURE 1.5-1 THEORETICAL LINES OF SOLUTIONS FOR A PARTICULAR TIME DIFFERENCE CASE. A) 2-DIMENSIONAL CASE WITH 2 HYDROPHONES. B) 2-DIMENSIONAL CASE WITH 3 HYDROPHONES AND C) 3-DIMENSIONAL CASE WITH 2 HYDROPHONES.

1.5.1 THREE DIMENSIONAL ARRAY ALGORITHMS

Unlike the active case, where ranges are known, the time of sound emission is unknown in the passive situation. The time of flight of the signal is therefore unknown and has to be calculated. This usually entails the use of an extra hydrophone. Unlike the active case, spherical algorithms cannot be used. Instead, any difference in arrival time of an

acoustic signal between hydrophones in two-dimensional space corresponds to a parabola around the hydrophones, as in Figure 1.5-1a. The source can be shown to be on this parabola. By adding more hydrophones further parabolae result and the intersections show the possible solutions (Figure 1.5-1b). In the three-dimensional case these parabolae become paraboloids and instead of intersection points, ellipses are formed (Figure 1.5-1c). The algorithms for such systems are developed and analysed thoroughly in Chapter 2.

1.5.2 THREE DIMENSIONS FROM TWO?

In the practical case of a moving baseline where the array is mounted on, or towed behind, a vessel, it is often very difficult to get a stable hydrophone in the third dimension as this means having a protruding hydrophone in moving water. With adequate hydrophones it is possible to track an object in three dimensions using a two-dimensional array. The array will suffer from an ambiguity in the missing dimension, but if the array

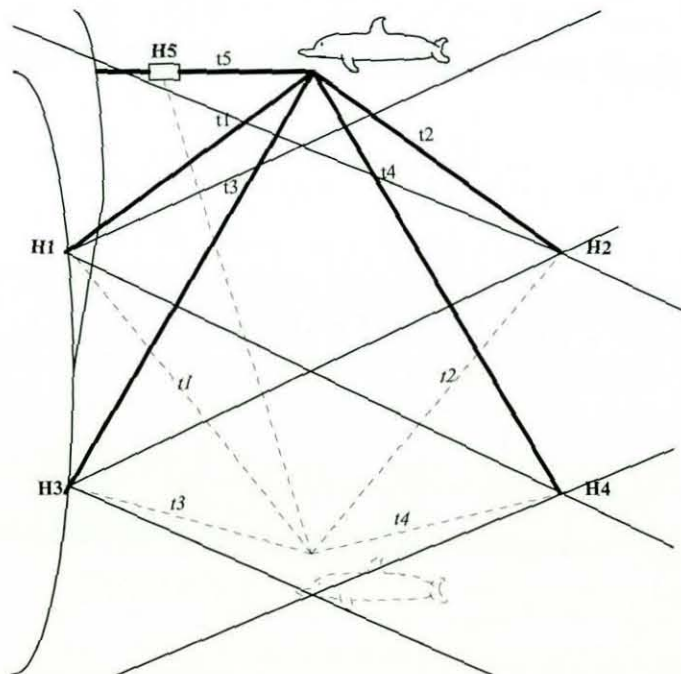


FIGURE 1.5-2 FLAT ARRAY, AMBIGUITY ELIMINATED WITH A FIFTH HYDROPHONE

is on the sea-bed or surface, the ambiguity can be eliminated. If the array is situated mid-water, it would be possible to eliminate this ambiguity using a single hydrophone, as shown in Figure 1.5-2. The same time accuracy is not needed for this device, as it is not

involved in the tracking process. This device also does not require the same position stability as the main array. The algorithm for this system is also analysed in Chapter 2.

1.5.3 REVERBERATION METHOD

In some cases it is not possible to deploy an array of hydrophones. If conditions are correct, a simple method of retrieving some data of the position of a sound source is with the use of standard sonobuoys or hydrophones. The method uses the reverberations of the sound from the surface and the seabed. A system has been developed [57,62,63] whereby the received sounds are analysed in terms of the frequency and time differences between distinct patterns. With the time differences between the first, second and third arrival of a signal, the range and depth of a signal source can be calculated, as shown in Figure 1.5-3. With two such devices a source can be positioned in one of two positions; with three, the exact three-dimensional position can be calculated (assuming the positions of the hydrophones are known).

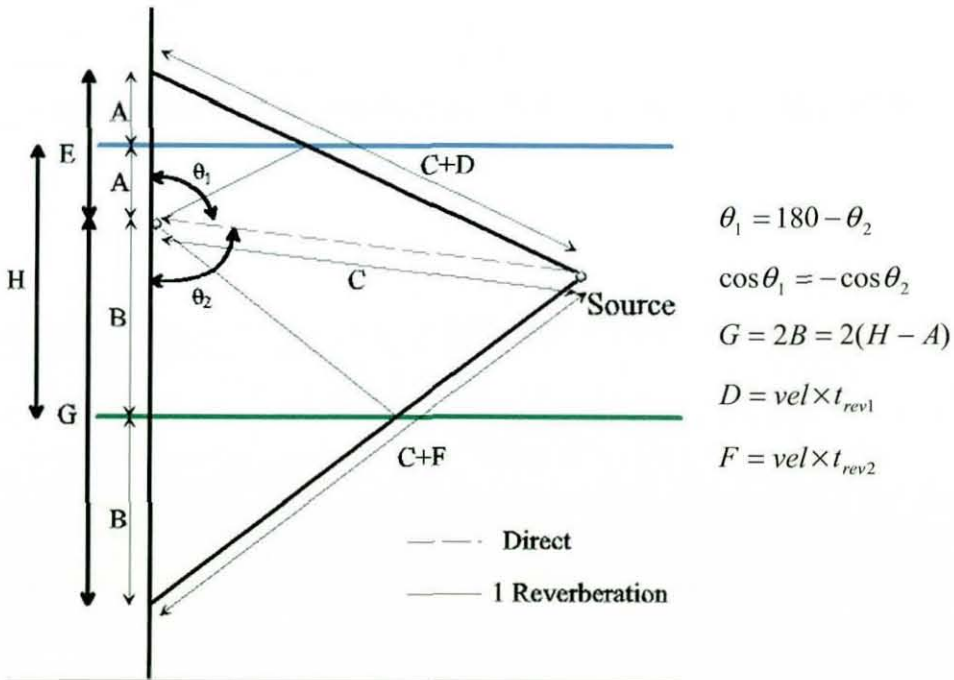


FIGURE 1.5-3 REVERBERATION METHOD, WITH CALCULATION OF RANGE AND DEPTH

Using the cosine rule and the dimensions shown in Figure 1.5-3:

$$\cos \theta_1 = \frac{E^2 + C^2 - (C + D)^2}{2EC} \tag{1-16}$$

and

$$\cos\theta_2 = -\cos\theta_1 = \frac{G^2 + C^2 - (C + F)^2}{2GC} \quad (1-17)$$

Equating these equations gives:

$$C = \frac{G^2E - F^2E + E^2G - D^2G}{2(GD + EF)} \quad (1-18)$$

and

$$\theta_1 = \cos^{-1}\left(\frac{4A^2 - 2CD - D^2}{4AC}\right) \quad (1-19)$$

1.6 NEW USES FOR PASSIVE TRACKING SYSTEMS

Although there are undoubtedly many passive-tracking systems used for military purposes, mostly unpublished, there are many uses for similar systems in the commercial sector. There is a need to understand the movements of animals underwater. Analysis of such data can lead to more effective harvesting of the oceans, or greater protection of endangered species. Minute acoustic tags placed on fish allow researchers to study the spawning habits and migration of many species, allowing them to show the fishing industries where and when to fish. It is generally thought that most fish cannot detect the acoustic signal of the tags [64]. If, however, animals can hear at the frequencies used for tracking, it is important that the system is acoustically passive. The methods used to date to locate cetaceans have mainly involved radio and satellite tagging of individual animals, although some acoustic tags have also been used. It has been shown that this does not appear to affect the animals' behaviour [61]. It is not guaranteed, however, that one animal will behave in an identical fashion to another.

1.7 A FISHERIES PROBLEM - A TECHNICAL SOLUTION?

During the last fifteen years there has been increasing concern about the environmental effects of industrial activities. These concerns also extend to the fisheries industry. Questions have been raised as to the size of cetacean by-catches in particular fisheries. By the end of the 1980s it had become clear that some fisheries were endangering marine mammals [65-67]. A European Commission study (named *CETASEL*) to look into the problem and to find possible solutions was initiated, the aim being to discover the scale

of the cetacean by-catch problem in pelagic trawl nets. This entailed the use of underwater vehicles equipped with cameras and the development of an underwater acoustic tracking system that could be attached to the trawl. The data obtained was expected to show the behaviour of cetaceans around the trawl and then possibly identify a reason why, or if, there are critical moments when the cetaceans are caught. The cetacean species thought to be at risk [68] from this type of trawl are the bottlenose dolphin (*Tursiops truncatus*), common dolphin (*Delphinus delphis*), Atlantic white-sided dolphin (*Lagenorhynchus acutus*), white-beaked dolphin (*Lagenorhynchus albirostris*) and harbour porpoise (*Phocoena phocoena*). Some of these have been studied in detail, others have little written about them. The cetacean that appears to set the acoustic limitations of the proposed system is the harbour porpoise, as the directivity of this particular species' echo-location clicks is narrow and fixed at a high band of frequencies.

This sets the minimum range, R, for the system to work at (depending on array size as

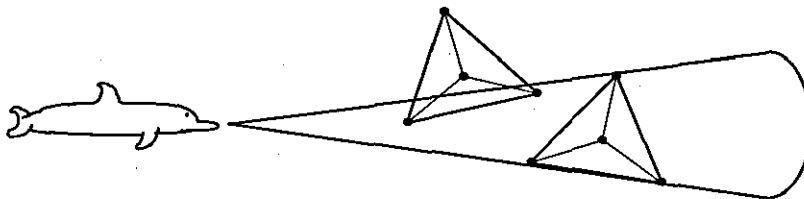


FIGURE 1.7-1 MINIMUM RANGE BETWEEN AN ECHOLOCATING HARBOUR PORPOISE AND AN ARRAY

demonstrated in Figure 1.7-1), which is given by

$$R = \frac{\Delta d}{2 \cdot \tan^{-1}(\theta/2)} \quad (1-20)$$

Cetaceans have been studied in various environments [41,69-72] and the source level of up to 166dB re 1μPa at 1m is generally accepted [70,71] for the harbour porpoise and 217 to 220dB re 1μPa at 1m for the bottlenose dolphin [41,72].

Comparing these figures with the noise figures in section 1.2, adjusted for the bandwidth of the receiver circuitry (47dB/Hz), the absolute maximum range of the tracking system following a harbour porpoise transmitting with a SL of 166dB is 1890m. If the in band sounds of the pelagic trawl are taken into account, the range is reduced to 400m. This

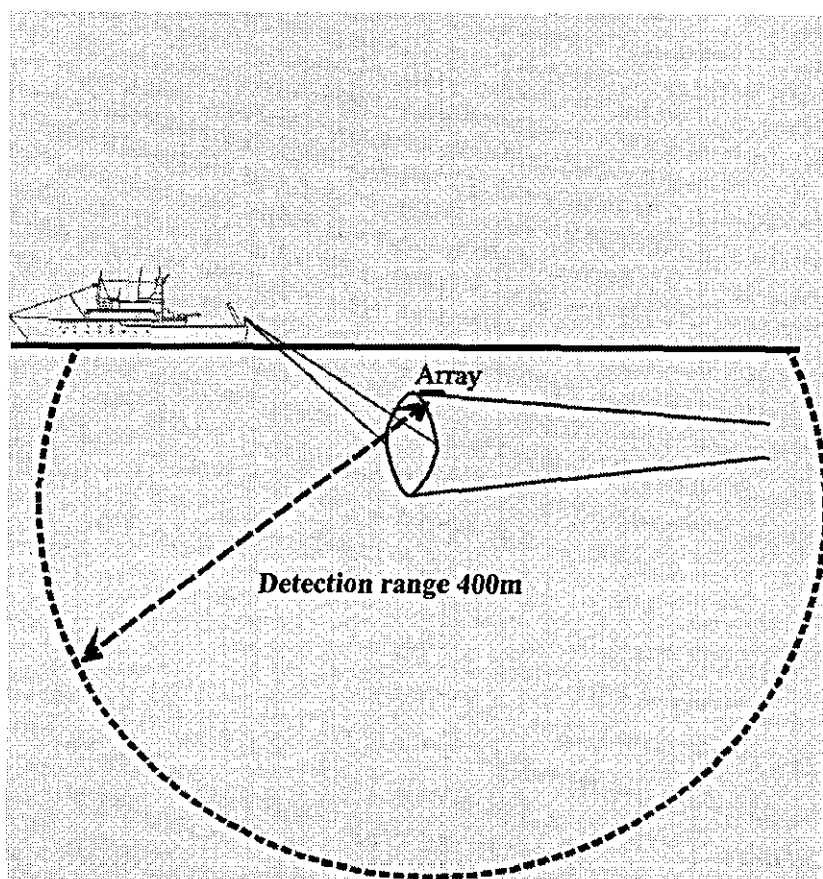


FIGURE 1.7-2 DIMENSIONAL DIAGRAM OF A PELAGIC TRAWL, SHOWING THE RANGE FOR THE HARBOUR PORPOISE AND THE BOTTLENOSE DOLPHIN.

will cover the majority of the pelagic trawl, which has dimensions shown in Figure 1.7-2. A full table of values for the different species of interest can be found in Table 2-1.

Some problems arise with this physical set-up. The trawl is very large and if a three-dimensional SBL array is attached (which is in itself difficult as a rigid structure cannot be used) it is difficult to achieve enough stability in the third dimension. The trawl can also be anything up to a kilometre behind the ship. The signals need to be sent to the ship with a large bandwidth to achieve the accuracy desired.

With these limitations in mind this thesis concentrates on the development of SBL systems capable of tracking wild cetaceans around the pelagic trawl.

1.8 THESIS STRUCTURE

The first three chapters of this thesis follow the same layout, with each of the different tracking system types being analysed in greater depth in each chapter. This chapter gives a general background to the systems. Chapter 2 describes the algorithms used and develops some new algorithms. Chapter 3 presents simulations and performance models of the algorithms.

Chapter 4 describes two systems developed for this project that are capable of running the algorithms described, and is followed in Chapter 5 by two case studies describing the testing of the systems. The results of these studies are compared with the theoretical performance in Chapter 6 and from these results conclusions are drawn as to the suitability and success of the algorithms considered.

1.9 References in Chapter 1

- [1] T.G. Bell, *Sonar and Submarine Detection* 545, 1962. U.S. Navy Underwater Sound Laboratory.
- [2] T.G. Haines, *Sound Underwater*, London: David and Charles, 1974.
- [3] F.V. Hunt, *Electroacoustics*, New York: John Wiley & Sons Inc, 1954.
- [4] D.G. Tucker and B.K. Gazey, Applications of Underwater Acoustics. In: *Applied Underwater Acoustics*, London: Pergamon, 1966.
- [5] P.H. Milne, *Underwater acoustic positioning systems*, London: E & F. N. Spon Ltd, 1983.
- [6] V.M. Albers, *Underwater Acoustics*, New York: Plenum, 1961.
- [7] B. Woodward, W. Forsythe, and S.K. Hole, Estimating backscattering strength for a correlation sonar, *IEEE Journal of Oceanic Engineering*, vol. 19, pp. 476-483, 1994.
- [8] R.J. Urick, *Principles of underwater sound for engineers*, New York: McGraw-Hill, 1967, pp. 181-210.
- [9] A.D. Goodson and R.H. Mayo, Interactions between free-ranging dolphins (*Tursiops truncatus*) and passive acoustic gill-net deterrent devices. In: *Sensory systems of aquatic mammals*, eds. R.A. Kastelein, J.A. Thomas and P.E. Nachtigall. Woerden: De Spil, 1995, pp. 365-379, ISBN 90-72743-05-9.
- [10] G. Pilleri, K. Zbinden, and H. Minglong, The Sonar Field in the Bottlenose Dolphin, *Tursiops truncatus*, pp. 81-94, 1999.
- [11] G.P. Haddle and E.J. Skudrzyk, The physics of flow noise, *J.Acoust.Soc.Am.*, vol. 46, pp. 130-157, 1969.
- [12] L.E. Kinsler and et al., *Fundamentals of acoustics*, London: John Wiley & Sons, 1982.
- [13] G.M. Wenz, Acoustic Ambient Noise in the Ocean: Spectra and Sources, *J.Acoust.Soc.Am.*, vol. 34, no. 12, pp. 1936-1956, 1962.
- [14] C.R. Greene and B.M. Buck, Arctic Ocean Ambient Noise, *J.Acoust.Soc.Am*, vol. 36, pp. 1218-1220, 1964.
- [15] W.J. Richardson, C.R. Greene Jr, C.I. Malme and D.H. Thomson, *Marine mammals and noise*, San Diego: Academic Press, 1995, pp 92-95, 576, ISBN 0-12-588440-0.
- [16] R.G. Busnel and J.F. Fish, *Animal Sonar Systems*, Plenum Press, 1980, pp 747.
- [17] R.A. Kastelein, N.M. Schooneman, W.W.L. Au, W.C. Verboom and N. Vaughan, The ability of a harbour porpoise (*Phocoena phocoena*) to discriminate between objects buried in sand. In: *The Biology of the Harbour Porpoise*, pp. 329-342. eds. A.J. Read, P.R. Wiepkema and P.E. Nachtigall. Woerden: De Spil, 199, ISBN 90-72743-07-05.
- [18] J.J. Dreher, Linguistic considerations of porpoise sounds, *J.Acoust.Soc.Am*, vol. 33, pp. 1799-1800, 1961.

- [19] W.E. Evans and J.H. Prescott, Observations of the sound production capabilities of the bottlenosed porpoise: A study of whistles and clicks. *Zoologica*, vol. 47, pp. 121-128, 1962.
- [20] J.C. Lilly and A.M. Miller, Sounds emitted by the bottlenose dolphin, *Science*, vol. 133, pp. 1689-1693, May 26, 1961.
- [21] S.H. Rigeway, Personal Comment, 1996.
- [22] R.H. Defran and K. Pryor, The Behavior and Training of Cetaceans in Captivity. In: *Cetacean Behavior: Mechanisms and Functions*, pp. 319-362. ed. L.M. Herman. New York: Wiley (Interscience), 1980.
- [23] W.W.L. Au, *The sonar of dolphins*, Springer-Verlag, 1993, pp 277, ISBN 0-387-97835-6.
- [24] A.D. Goodson, J.A. Flint, S.C. Pomeroy, and T.W. Cranford, Bio-Sonar Characteristics Of The Harbour Porpoise (*Phocoena phocoena*), Proceedings of the 5th European Conference on Underwater Acoustics, eds. P. Chevret and M.E. Zakharia, 2000, Lyon, France, pp 979-984, Vol I, ISBN 92-828-9530-0.
- [25] C. Kamminga and H. Wiersma, Investigations on cetacean sonar II, acoustical similarities and differences in odontocete sonar signals, *Aquatic Mammals*, vol. 8, pp. 41-62, 1981.
- [26] J.C. Lilly, Interspecies communication, *McGraw-Hill Yearbook of Science and Technology*, vol. pp. 279-281, 1962.
- [27] M. Amundin, Delfinen - det levande ekolodet
- [28] D.K. Caldwell and M.C., Underwater pulsed sounds produced by captive spotted dolphins, *Stenella plagiodon Cetology*, no. 1, 1971.
- [29] D.K. Caldwell and M.C., Cetaceans. In: *How Animals Communicate*, eds. Sebeok, T A, pp. 794-808, Indiana University Press, 1977.
- [30] S.M. Dawson, Clicks and Communication: The Behavioural and Social Contexts of Hector's Dolphin Vocalizations, *Ethology*, vol. 88, pp. 265-276, 1991, ISSN 0179-1613.
- [31] T.G. Lang and H.A.P. Smith, Communication between dolphins in separate tanks by way of an electronic acoustic link, *Science*, vol. 150, pp. 1839-1844, 1965.
- [32] W.W.L. Au and P.W.B. Moore, Critical ratio and critical bandwidth for the Atlantic bottlenose dolphin, *J. Acoust. Soc. Am*, vol. 88, no. 3, pp. 1635-1638, 1990.
- [33] N.A. Dubrovsky, Dolphin echolocation *Journal De Physique IV*, vol. 2, pp. 875-882, 1992.
- [34] M. Amundin and E.S. Kallin, The study of the sound production apparatus in the harbour porpoise, *Phocoena phocoena*, and the Jacobita, *Cephalorhynchus commersoni* by means of serial cryo-microtome sectioning and 3-D computer graphics, *Animal Sonar*, pp. 61-66, 1988, eds. P.E. Nachtigall and P.E. Moore, Plenum Press.
- [35] M. Amundin and T. Cranford, Forehead anatomy of *Phocoena phocoena* and *Cephalorhynchus commersonii*: 3-dimensional reconstructions with emphasis on the nasal diverticula, *Sensory Abilities of Cetaceans*, vol. pp. 1-18, 1990.
- [36] R.W. Hult, Another function of echolocation for bottlenosed dolphins (*Tursiops truncatus*) *Cetology*, vol. no. 47, pp. 1-7, 1982.

- [37] K. Norris. *Whales, dolphins and porpoises*, Los Angeles: University of California Press, 1966. pp. 638-649.
- [38] F.G. Wood Jnr, Underwater sound production and concurrent behaviour of captive porpoises, *Tursiops truncatus* and *Stenella plagiodo*, *Bulletin of Marine Science of the Gulf and Caribbean*, vol. 3, no. 2, pp. 120-133, 1953.
- [39] V. Valdez, Echo sounder records of ultrasonic sounds made by killer whales and dolphins, *Deep-Sea Research*, vol. 7, no. 1960-61, pp. 289-290, 1961.
- [40] D.L. Hickman and E.M. Grigsby, Comparison of signature whistles in *tursiops truncates*, *Cetology*, vol. 1977.
- [41] W.W.L. Au, Sonar detection of nets by dolphins, IWC Conference on mortality of Cetaceans in passive fishing nets. International Whaling Commission, 1990, La Jolla, California, USA; paper published in IWC Special Issue 15, 1994.
- [42] J.E. Sigurdson, Analyzing the dynamics of dolphin biosonar behavior during search and detection tasks, *Proceedings of the Institute of Acoustics*, vol. 19, no. 9, pp. 123-132, 1997, ISSN 0309-8117.
- [43] R.G. Busnel, A. Dziedic, and S. Andersen, Role de l'impedance d'un cible dans le seuil de sa detection par le systeme sonar de marsouin *Phocoena phocoena*. *Compt.Rend.Soc.Biol.*, vol. 159,, pp. 69-74, 1965.
- [44] R.G. Busnel and A. Dziedic, Resultats mestrologiques experimentaux de l'echolocation chez le *Phocoena phocoena*, et leur comparaison avec ceux de certaines chauvre-souris. In: *Animal Sonar Systems, Biology and Bionics*, pp. 307-336. ed. R.G. Busnel. Jouy-en-Josas, France: Laboratoire de Physiologie Acoustique, 1967.
- [45] W.E. Evans and F.T. Awbrey, Natural history aspects of marine mammal echolocation. In: *Animal Sonar, Processes and performance*, 1988, pp. 521-534.
- [46] G. Pilleri, K. Zbinden, and C. Kraus, Characteristics of the sonar system of cetaceans with pterygoschisis, directional properties of the sonar clicks of the *Neophocaena phocaenoides* and *Phocoena phocoena* (Phocoenidae). *Investigations on Cetacea*, vol. XI, pp. 157-188, 1980.
- [47] TRITECH International Ltd, SeaKing DFP & DFS Dual Frequency Imaging Sonar 2000. Aberdeen.
- [48] R.L. Brill, M.L. Sevenich, T.J. Sullivan, J.D. Sustman, and R.E. Witt, Behavioural evidence for hearing through the lower jaw by an echolocating dolphin (*Tursiops truncatus*) *Marine Mammals Science*, vol. 4, no.3, pp. 223-230, 1988.
- [49] R.L. Brill and P.J. Harder, The effects of attenuating returning echolocation signals at the lower jaw of a dolphin (*Tursiops truncatus*), *J.Acoust.Soc.Am.*, vol. 89, no. 6, pp. 2851-2857, 1991. 0001-4966.
- [50] P.W.B. Moore and L.W. Bivens, The bottlenose dolphin: Nature's ATD in SWMCM autonomous sonar platform technology, *Proceedings of the Vehicle in Mine Countermeasures Symposium*, 1995
- [51] P.W.B. Moore, H.L. Roitblat, R.H. Penner, and P.E. Nachtigall, Recognizing successive dolphin echoes with an integrator gateway network, *Neural Networks*, vol. 4, pp. 701-709, 1991. 0893-6080.

- [52] I.E. Dror, M. Zagaeski, and C.F. Moss, Three-Dimensional Target Recognition via Sonar: A Neural Network Model, *Neural Networks*, vol. 8, no. 1, pp. 149-160, 1995. ISSN 0893-6080.
- [53] K. Jessop, *Goldfinder*, London, Simon & Schuster, 1998.
- [54] P.A. Hardman and B. Woodward, Underwater position fixing by a diver operated acoustic telemetry system *Acustica*, vol. 55, pp. 34-44, 1984.
- [55] H.D. Griffiths, J.W.R. Griffiths, Z. Meng, C.F.N. Cowan, T.A. Rafik, and H. Shafeeu, Interferometric Synthetic Aperture SONAR for High-Resolution 3-D Imaging, *Proceedings of the Institute of Acoustics*, vol. 16, pp. 151-157, 1994.
- [56] C.R. Coggrave, A.D. Goodson, P.A. Lepper, and B. Woodward, An experimental technique for tracking dolphins in the vicinity of a trawl net, Proceedings of the 10th Annual Conference of the European Cetacean Society, Lugano, Switzerland, 1995.
- [57] P.A. Lepper, K. Kaschner, P.R. Connelly, and A.D. Goodson, Development of a simplified ray path model for estimating the range and depth of vocalising marine mammals, *Proceedings of the Institute of Acoustics*, vol. 19, no. 9, pp. 227-234, 1997. ISSN 0309-8117.
- [58] N. Morphett, B. Woodward, and A.D. Goodson, Tracking dolphins by detecting their sonar clicks with an array of hydrophones, *Proceedings of the Institute of Acoustics*, Birmingham, 1993.
- [59] L.E. Freitag and P.L. Tyack, Passive acoustic localization of the Atlantic bottlenose dolphin using whistles and echolocation clicks, *J.Acoust.Soc.Am.*, vol. 93, pp. 2197-2205, 1993.
- [60] J.L. Spiesberger and K.M. Fristrup, Passive localization of calling animals and sensing of their acoustiv environment using acoustic tomography, *The American Naturalist*, vol. 135, pp. 107-153, 1990. 0003-0147.
- [61] W.A. Watkins and et al., Sperm whales tagged with transponders and tracked underwater by sonar, *Marine Mammal Science*, vol. 9, pp. 223-230, 1993.
- [62] K. Kaschner, P.A. Lepper, and A. Goodson, Analysis and interpretation of cetacean sounds obtained from a hydrophone attached to a pelagic trawl, Proceedings of the 11th Annual Conference of the European Cetacean Society, Stralsund, Germany, 10-12 March 1997, eds. U. Siebert and R. Lich, University of Kiel.
- [63] K. Kaschner, A.D. Goodson, P.R. Connelly, and P.A. Lepper, Species characteristic features in communication signals of cetaceans: Source level estimates for some free ranging North Atlantic Odontocetes, *Proceedings of the Institute of Acoustics. Underwater Bio-Sonar and Bioacoustics Symposium*, Loughborough, 1999.
- [64] P.J. Gearin, M.E. Goshu, L. Cooke, R. DeLong, and J. Laake, Acoustic alarm experiment in the 1995 Northern Washington Marine Setnet Fishery: methods to reduce by-catch of harbor porpoise Reports of The International Committee for exploitation of the seas, pp. 1-15, 1996. ICES.
- [65] B. Clausen and S. Andersen, Evaluation of by-catch and health status of the harbour porpoise *Phocoena phocoena* in Danish waters 13(5), *Danish Rev. Game Biol.* pp. 1-20, 1988.
- [66] Y. Morizur, S.D. Berrow, N.J.C. Tregenza, A.S. Couperus, and S. Pouvreau, Incidental catches of marine-mammals in pelagic trawl fisheries of the northeast Atlantic. *Fisheries Research*, vol. 41, pp. 297-307, 1999. 0165-7836.

- [67] S.P. Northridge, Marine mammals and fisheries: a study of conflicts with fishing gear in British waters, Wildlife link. London 1988..
- [68] Y. Morizor, N.J.C. Tregenza, H. Heesen, S. Berrow, and S. Pouvreau, By-catch and discarding in pelagic trawl fisheries Anonymous Final Report, Study contract BIOECO 93/017. European Commission. Brussels. 1995.
- [69] W.W.L. Au, Application of the reverberation-limited form of the sonar equation to dolphin echolocation, *J.Acoust.Soc.Am.*, vol. 92, no. 4, part 1, pp. 1822-1826, 1992.
- [70] A.D. Goodson and C.R. Sturtivant, Sonar characteristics of the harbour porpoise (*Phocoena phocoena*): source levels and spectrum, *ICES Journal of Marine Science*, vol. no. 53, pp. 465-472, 1996.
- [71] A.D. Goodson, R.A. Kastelein, and C.R. Sturtivant, Source levels and echolocation signal signal characteristics of juvenile Harbour porpoises (*Phocoena phocoena*), pp. 41-53 In: *Harbour Porpoises*, eds. P.E. Nachtigall, J. Lien, W.W.L. Au and A.J.Read, Woerden, Netherlands: De Spil, 1999.
- [72] L.B. Poche, L.D. Luker, and P.H. Rogers, Some observations of echolocation clicks from free swimming dolphins in a tank, *J.Acoust.Soc.Am.*, vol. 71, no. 4, pp. 1036-1038, 1982.

CHAPTER 2

THEORY

As stated in Chapter 1, two forms of tracking algorithms exist for tracking short impulse-type signals: spherical algorithms for tracking triggered active sources, and hyperbolic algorithms for tracking passive or unpredictable sources. This chapter describes the theory of each of these in detail, and for the passive case presents a number of methods of achieving the desired solutions. Chapter 1 discussed a number of systems available for tracking cetaceans. Not all are suitable when the limitations of this project are considered. To reduce the number of tracking methods to be analysed for this study, some limits must be imposed on the number of the variables. These include species of animal, form of signal to be detected, minimum and maximum range of signal and the size and shape of the array. Some of these choices have been made by consulting experts in the field, from published literature or first hand by experiment, while others are from simulation results reported in Chapter 3.

2.1 PRE-DEFINED PARAMETERS

For the effective design of a tracking system capable of coping with most situations presented in a particular environment, some parameters must be pre-defined. In this case these consist of physical environmental parameters and user-specific parameters.

2.1.1 PHYSICAL LIMITATIONS

Depending on the method of deployment of the array of receivers, there may be limitations on the size and shape of the array. If the array is to be static and fixed, i.e. attached to a fixed platform, it is possible to keep the receivers in fixed positions relative to each other. This means a three-dimensional array is feasible. If the system is to operate with the minimum possible number of receivers to produce a unique solution, it must have at least three receivers for two-dimensional tracking arranged in a two-

dimensional configuration, or four receivers in the three-dimensional case, usually arranged in a three-dimensional configuration. In the static case it may be possible to place the fourth receiver in the third dimension, i.e. out of the plane of the other three. If this is possible, it allows a number of algorithms to be used in the tracking process. In the dynamic case, with a moving baseline, it may not be simple to place the fourth receiver out of the plane, in this case the information obtainable from the third dimension is limited and other algorithms must be used. The working environment and the quality of the receiving equipment set the maximum range of the system. Assuming a source is transmitting at its maximum source level (SL) the maximum range can be defined by the following equation (explained in 1.2.2):

$$TL = SL - NL - DT$$

where $TL = 20\log R + \alpha R$, $NL =$ combined noise (electronic & environmental) and $DT =$ Detection Threshold. It is simplest to show the range with respect to the signal-to-noise ratio in graphical form (Figure 2.1-1), where each separate line shows the values for a different frequency.

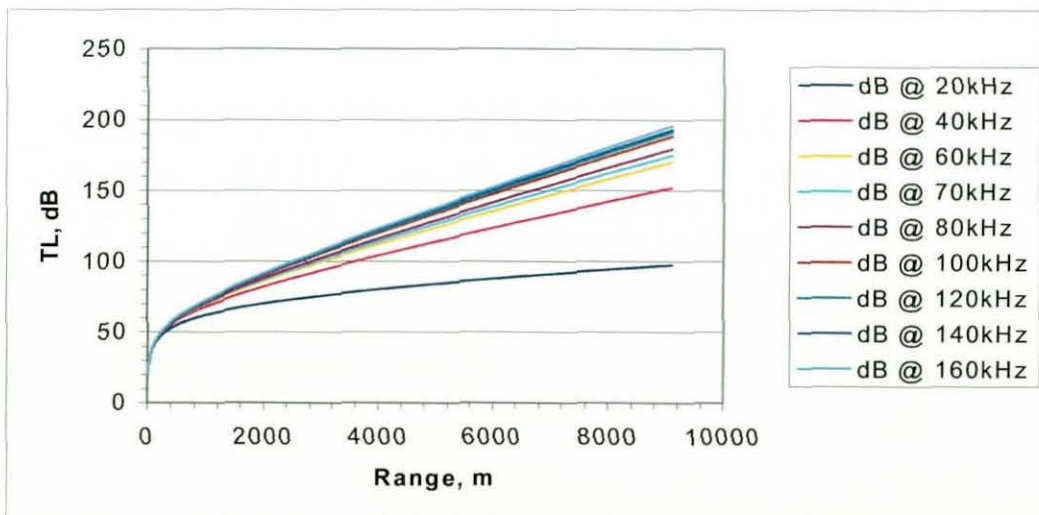


FIGURE 2.1-1 RANGE AGAINST SIGNAL-TO-NOISE RATIO FOR DIFFERENT FREQUENCIES

Taking the Noise Levels shown in Figure 1.2-2 and the maximum cetacean source levels discussed in section 1.2.5, a set of ranges can be calculated using the Figure 2.1-1 (as shown in Table 2-1) for different environments. Shallow water conditions may give a greater noise value, in which case the range will be less.

Source	Max. Source Level, dB ¹	Detectable frequency range, kHz	Ref	Detection Threshold dB for given freq.	Deep water noise, dB re 1 $\mu\text{Pa}^2/\text{Hz}$	Max. theoretical range, m	Pelagic Trawl SL ² , dB re 1 $\mu\text{Pa}^2/\text{Hz}$	Max. theoretical range, m
Bottlenose (Max)	230	20 – 120	[1,2]	10	75 @ 70kHz	7400	114	4160
Bottlenose (typical)	220	20 – 120		10	75 @ 70kHz	6550	114	3380
White Sided (max)	228 ³	30 – 120	[3]	10	75 @ 70kHz	7230	114	4000
White Sided (typical)	220 ¹	30 – 120		10	75 @ 70kHz	6550	114	3380
Harbour porpoise (max)	177	2 & 125 – 140	[4,5]	10	77 @ 140kHz	2550	109 ⁴	530
Harbour Porpoise (typical)	160	2 & 125 - 140		10	77 @ 140kHz	1540	109 ⁴	250
Common Dolphin ⁵ (max)	140	20 – 100	[6]	10	75 @ 70 kHz	730	114	20
Common (typical)	n/a	20 – 100		10			114	

TABLE 2-1 MAXIMUM ACHIEVABLE RANGES FOR DIFFERENT CETACEAN SPECIES

Further references for the SL of cetaceans can be found in Section 1.2.7.

The minimum detection threshold must be taken into account, however; for each dB @ 70 kHz this amounts to approximately 40m. If a trawl produces impulsive noise

¹ SL's are re 1 μPa @1m, and noise is re 1 $\mu\text{Pa}^2/\text{Hz}$. (Deep water noise is adjusted for the system bandwidth of 50kHz (47dB/Hz))

² SPL of trawl detected using trawl system to be found in section 4.1.

³ White sided dolphin figures are assumed to be the same as Bottlenose Dolphin

⁴ Trawl noise was measured only up to 100kHz, the figure is projected from the trend at 100kHz

⁵ Very limited data available and may be limited by recordings

(clinking chains, etc) the detection threshold must be raised to prevent the system tracking the trawl rather than the desired sources.

2.1.2 PARAMETERS SET BY POTENTIAL USERS

The main parameters to be set by the user are to identify and characterise the source, in particular the SL, the frequency, duration and type of pulse. This will allow the tracking system to distinguish between the many acoustic sources in the working area and to filter the desired source. Other important factors include the beamwidth of the source. A typical dolphin echolocation click typically has a beamwidth of 10° to 15° , limiting the minimum range of the source to the receiver. It is essential for the signal to be detected on all receivers. The spacing of the receivers must therefore be as close together as possible to allow the smallest minimum range to the source. Most cetaceans, however, emit a lower level signal at lower frequencies and these tend to have a lower directivity and can be used to detect the animal out of the main beam. If these signals are used the minimum range is less, and the system is less dependant on the animal facing the array.

When a cetacean is concentrating its echolocation on a target, it tends to send pulses as frequently as possible. The repetition rate is then inversely proportional to the range R to the target from the cetacean, i.e. $c/2R$, where c is the sound velocity in the sea.

Repetition rates of the clicks vary from 1 Hz to over 1000 Hz. To track all these points is unnecessary, so a maximum repetition rate must be set. Typical adult cetaceans swim at speeds up to approximately 8m/s, so to give a reasonable idea of their movement, it is necessary to monitor their clicks at up to 2 times per second, although higher update rates may give extra information.

In some cases, such as in the dynamic case, the attachment of the receivers may be complicated, for example in analysing cetacean movements around a trawl net it may only be possible to connect stable receivers in one plane. In this case, algorithms for a flat array must be used as this is a special case, and using conventional algorithms a solution is not possible. Other limitations can include the maximum rate of data transfer

from the receivers to the timing circuitry. If the transfer medium has maximum bandwidth limitations, the accuracy of the algorithms will be limited. Analysis of this will be performed in Chapter 3.

2.2 ACTIVE TRACKING ALGORITHMS

If the time of flight of an acoustic signal is known, and the velocity of sound in the medium is also known, the distance the sound has travelled can be calculated. When the position of the receiver is known, the position of the transmitter can be predicted to be anywhere on the surface of a sphere around the receiver. If several of these receivers are spatially separated, each receiving the same signal, each will have a corresponding sphere, and the intersection of these spheres will correspond to the possible points of transmission. Figure 2.2-1 shows the situation where three receivers are positioned in a plane. It can be seen that with just two receivers there are two possible solutions. If three receivers are used, the ambiguity is removed.

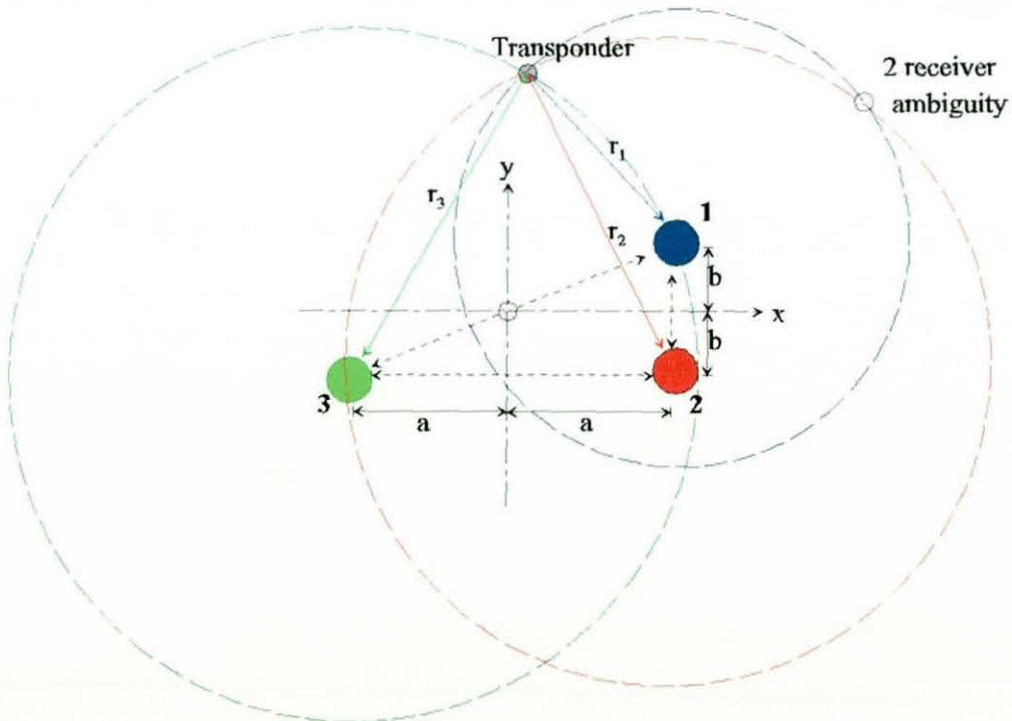


FIGURE 2.2-1 POSITION-FIXING IN TWO DIMENSIONS, KNOWN ACOUSTIC FLIGHT TIME

Errors in measurements may be interpreted as errors in the radii of one or more of these circles. This produces different effects depending on the spatial positions of the receivers. In Figure 2.2-1 circles 1 and 3 cross nearly orthogonal to each other and circles 1 and 2 have a small angle of interception. In the latter case a small error in measurement will produce a larger error in the position. Using the dimensions shown in Figure 2.2-1 the position of the transmitter can be calculated as follows [7]:

The equation of each circle is

$$r^2 = x^2 + y^2$$

Taking into account the spatial offsets we get three equations:

$$r_1^2 = (x-a)^2 + (y+b)^2 \quad (2-1)$$

$$r_2^2 = (x-a)^2 + (y-b)^2 \quad (2-2)$$

$$r_3^2 = (x+a)^2 + (y+b)^2 \quad (2-3)$$

Subtracting pairs of these equations gives:

$$r_3^2 - r_1^2 = 4ax \quad (2-4)$$

$$r_2^2 - r_1^2 = 4by \quad (2-5)$$

From this the solution can be found:

$$x = \frac{r_3^2 - r_1^2}{4a} \quad (2-6)$$

and

$$y = \frac{r_2^2 - r_1^2}{4b}$$

(2-7)

In the underwater tracking situation these equations only really apply in shallow water. If tracking is to be achieved in deeper water the third dimension must be taken into account. Instead of circles, spheres must be constructed to develop the algorithms. Three receivers may give an extra ambiguity in the third dimension, as Figure 2.2-2 shows. A fourth receiver must be added out of the plane of the other three to eliminate this.

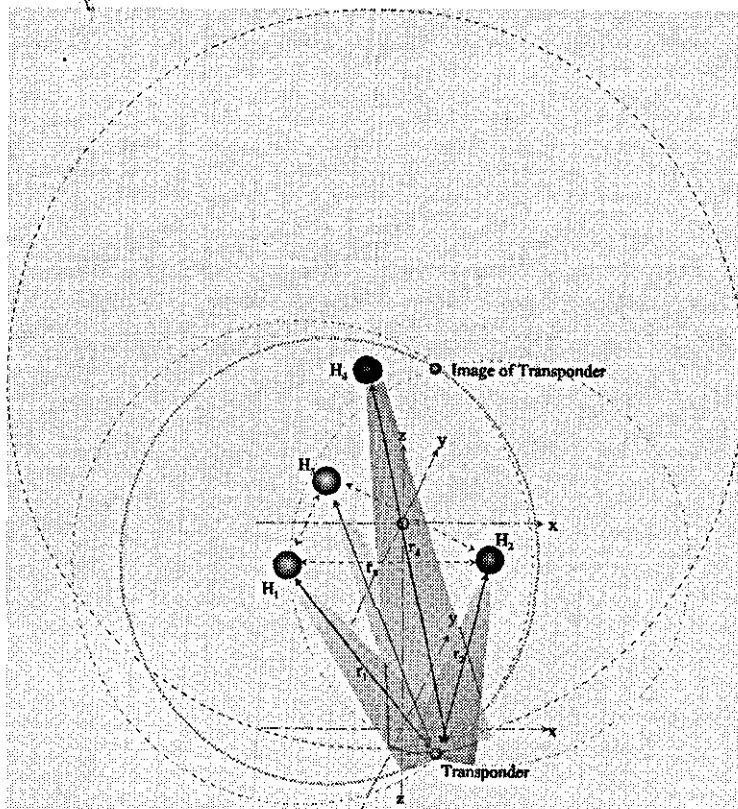


**FIGURE 2.2-2 POSITION-FIXING IN THREE DIMENSIONS,
KNOWN ACOUSTIC FLIGHT TIME**

Again using the dimensions shown in Figure 2.2-2 the position of the transmitter can be calculated. In the simple case where the array is flat:

The equation for a sphere is

$$r^2 = x^2 + y^2 + z^2 \quad (2-8)$$

So equations (2-4) to (2-6) apply if $z = 0$. If x and y are substituted in (2-8) we get:

$$z = \pm \sqrt{r_1^2 - (x-a)^2 - (y-b)^2} \quad (2-9)$$

This method of tracking, though the simplest to calculate, has one large drawback. The algorithms rely on the exact time of transmission. In some cases this parameter is not available and other methods must be used. This form of system is used worldwide in the tracking of man-made acoustic sources, or animals equipped with a transponder. The accuracy of such systems is dependent on the time accuracy, and the positional accuracy of the receivers. Analysis of these parameters is presented in Chapter 3.

2.3 PASSIVE TRACKING ALGORITHMS

If the time of transmission of a signal is not known, spherical algorithms do not apply. Instead a hyperbola is formed around each pair of receivers the, loci of which indicate the possible solutions.

Using dimensions shown in Figure 2.3-1 we can show that the arrival time difference between R_1 and R_2 correspond to a distance d_{12} where

$$d_{12} = \Delta t_{12} \times c$$

(2-10)

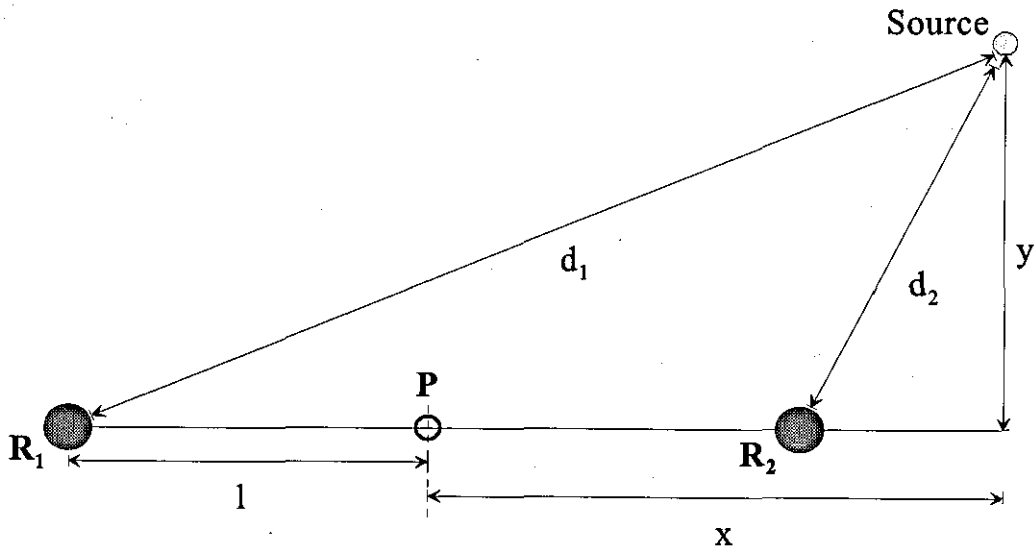


**FIGURE 2.3-1 POSITION-FIXING IN TWO-DIMENSIONS,
UNKNOWN ACOUSTIC FLIGHT TIME, TWO RECEIVERS**

From the geometry of the situation, we see that $d_{12} = d_1 - d_2$, so by Pythagoras' theorem

$$(l+x)^2 + y^2 = d_1^2 = (d_{12} + d_2)^2 \quad (2-11)$$

and

$$(x-l)^2 + y^2 = d_2^2 \quad (2-12)$$

This implies that

$$(l+x)^2 + y^2 = \left[d_{12} + \left((x-l)^2 + y^2 \right)^{\frac{1}{2}} \right]^2 \quad (2-13)$$

which can be rearranged as

$$4lx - d_{12}^2 = 2d_{12} \left((x-l)^2 + y^2 \right)^{\frac{1}{2}} \quad (2-14)$$

Squaring both sides of (2-9) yields

$$16l^2x^2 + d_{12}^4 = 4d_{12}^2(x^2 + l^2 + y^2) \quad (2-15)$$

which can be parameterised and rearranged to give

$$l = \frac{x^2}{p^2} + \frac{y^2}{q^2} \quad (2-16)$$

where

$$p^2 = \frac{d_{12}^2}{4l^2} \quad \text{and} \quad q^2 = \frac{d_{12}^2 - 4l^2}{4l^2}$$

Equation (2-16) is the general definition of a hyperbola, consisting of two curved loci symmetric to each other as shown in Figure 2.3-2. Due to the squaring of (2-14) in order to obtain this equation, the resultant expression does not contain the necessary information to determine which side of the receivers the source is on. This ambiguity can only be removed by repeating the exercise with another pair of receivers and finding the intersection.

If further pairs of receivers are positioned to allow multiple loci, the intersection of these loci will produce the solutions. This process of solving the multiple equations can be performed in a number of ways, some of which are shown in the following sections.

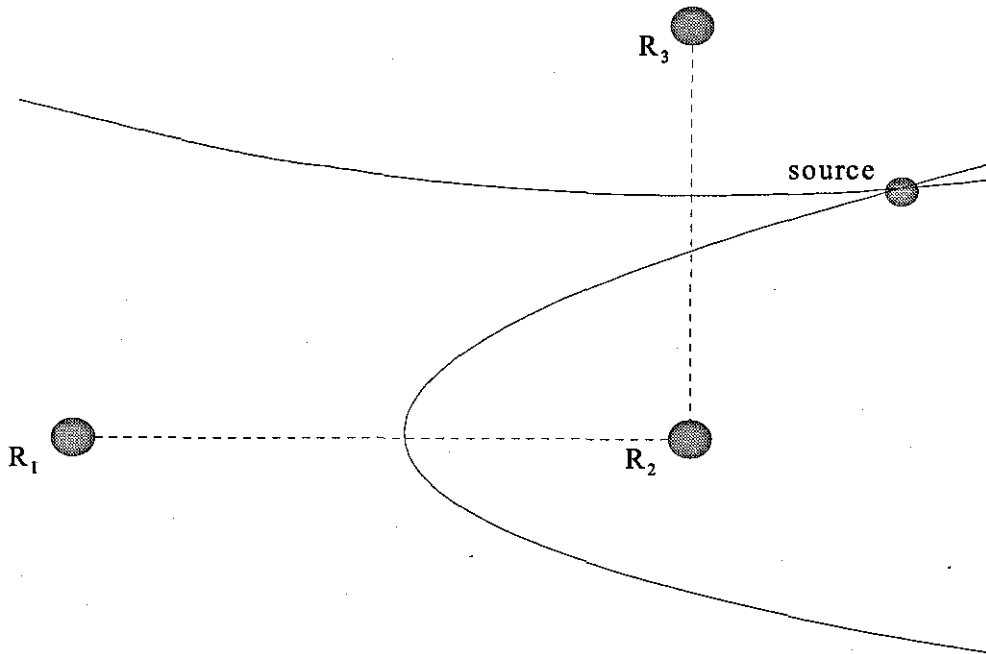


**FIGURE 2.3-2 POSITION-FIXING IN TWO DIMENSIONS,
UNKNOWN ACOUSTIC FLIGHT TIME - HYPERBOLA**

2.3.1 ABSOLUTE ALGORITHMS FOR TRACKING USING HYPERBOLAE

In the two-dimensional case, instead of intersecting circles as with the active case, the intersection of the hyperbolae determines the possible positions. In this case, however, it is possible to have more than a single ambiguity for each pair of hyperbolae. The fourth receiver removes the majority of the ambiguities, although some are still possible. The vulnerable areas for these ambiguities can be calculated (as shown in section 3.3) and in most cases removed with the use of a fifth receiver.

To calculate the position of a source, each hyperbola must be calculated from the time differences available. The total number of hyperbolae can be shown to be:

$$N_{hyp} = \frac{N_R^2 - N_R}{2} \quad (2-17)$$

where N_{hyp} is the number of hyperbolae and N_R is the number of receivers.

If additional 'redundant' receivers are included in the system it is possible to choose which hyperbolae will be used, thus in some cases reducing the complexity of the calculations. The solution of the intersections of a minimum of three hyperbolae rapidly becomes extremely complicated and lengthy, and a general solution is very difficult as there are numerous exceptions when, instead of a hyperbola, a line creates a single set of solutions. In [8] a solution for the general two-dimensional and three-dimensional array was solved using a method in which the spherical solutions are subtracted to eliminate the range and instead give the range difference, and hence the time difference. In effect, each subtraction of circles or spheres produces a hyperbola or hyperboloid respectively. Similar equations are produced for each pair of receivers and these can be solved simultaneously as presented in the following section.

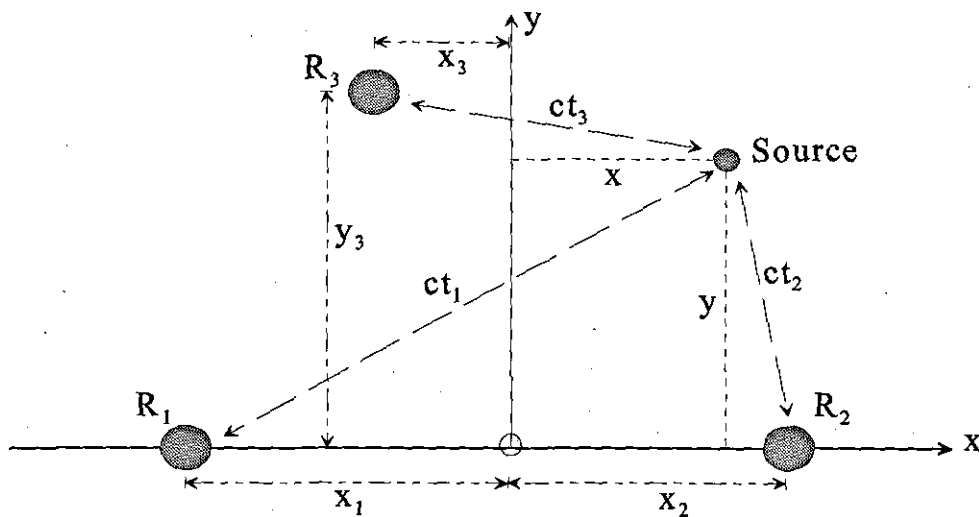


FIGURE 2.3-3 SOLVING A TWO-DIMENSIONAL CASE USING CIRCLES

2.3.1.1 Two-dimensional equation set

Using the dimensions in Figure 2.3-3 the equation for the circle around each receiver can be shown to be:

$$ct_1 = \sqrt{(x-x_1)^2 + y^2} \quad ct_2 = \sqrt{(x-x_2)^2 + y^2} \quad ct_3 = \sqrt{(x-x_3)^2 + (y-y_3)^2}$$

Subtracting pairs of circles creates a hyperbola and eliminates the need for a time of transmission, giving:

$$c\Delta t_{12} = \sqrt{(x-x_1)^2 + y^2} - \sqrt{(x-x_2)^2 + y^2} \quad (2-18)$$

$$c\Delta t_{32} = \sqrt{(x-x_3)^2 + (y-y_3)^2} - \sqrt{(x-x_2)^2 + y^2} \quad (2-19)$$

After simplification we obtain

$$\sqrt{(x-x_2)^2 + y^2} = \frac{2x(x_2 - x_1) + (x_1^2 - x_2^2 - c^2\Delta t_{12}^2)}{2c\Delta t_{12}} \quad (2-20)$$

$$\sqrt{(x-x_2)^2 + y^2} = \frac{2x(x_2 - x_3) - 2yy_3 + (x_3^2 + y_3^2 - x_2^2 - c^2\Delta t_{32}^2)}{2c\Delta t_{32}} \quad (2-21)$$

Substituting $R = \frac{\Delta t_{12}}{\Delta t_{32}}$ gives

$$x = \frac{-(2Ry_3)y}{2[x_2(1-R) - x_1 + Rx_3]} + \frac{R[x_3^2 + y_3^2 - x_2^2 - c^2\Delta t_{32}^2] - [x_1^2 - x_2^2 - c^2\Delta t_{12}^2]}{2[x_2(1-R) - x_1 + Rx_3]} \quad (2-22)$$

which is in the form:

$$x = Ty + S \quad (2-23)$$

Substituting (2-23) into (2-20) we obtain

$$\sqrt{(Ty + S - x_2)^2 + y^2} = \frac{2(Ty + S)(x_2 + x_1) + (x_1^2 - x_2^2 - c^2 \Delta t_{12}^2)}{2c \Delta t_{12}} \quad (2-24)$$

if $K = x_1^2 - x_2^2 - c^2 \Delta t_{12}^2$ then (2.24) can be expanded and rearranged to give

$$\begin{aligned} & y^2 \left(1 + T^2 \frac{[1 - (x_2 - x_1)^2]}{c^2 \Delta t_{12}^2} \right) \\ & + y \left(2T(S - x_2) - T \frac{[2S(x_2 - x_1)^2 + K(x_2 - x_1)]}{c^2 \Delta t_{12}^2} \right) \\ & + (S - x_2)^2 - \frac{K^2 + 4KS(x_2 - x_1) + 4S^2(x_2 - x_1)^2}{4c^2 \Delta t_{12}^2} = 0 \end{aligned} \quad (2-25)$$

which is a quadratic equation in the form $Ay^2 + By + C = 0$, the solution of which can be calculated as follows

$$y = \frac{-B \pm \sqrt{B^2 - 4AC}}{2A} \quad (2-26)$$

This method gives two solutions for y -space, which when substituted in (2-23) will result in two solutions. If the time delays for each solution are calculated, the correct answer will yield the measured delay. As with the spherical case, if the third dimension is introduced, an extra layer of complexity is added. Instead of hyperbolae we must consider hyperboloids, the intersections of which give a ring or 'hyperboloidal section' of solutions, as shown in Figure 2.3-4. Once again a number of ambiguities can be generated, most of which can be removed with an extra receiver out of the plane.

The solution for this situation is again one main algorithm with a number of special cases. Using the spherical equations as a starting point, once again the positions can be calculated as follows[8]:

2.3.1.2 Three-dimensional equation set (method 1)

A full expansion of this algorithm can be found in Appendix A. As in section 2.3.1.1 the solution is found by considering spheres around each receiver, giving four equations:

$$ct_1 = \sqrt{x^2 + (y - y_1)^2 + (z - z_1)^2} \quad (2-27)$$

$$ct_2 = \sqrt{x^2 + (y - y_2)^2 + (z - z_2)^2} \quad (2-28)$$

$$ct_3 = \sqrt{(x - x_3)^2 + (y - y_3)^2 + (z - z_3)^2} \quad (2-29)$$

$$ct_4 = \sqrt{(x - x_4)^2 + (y - y_4)^2 + (z - z_4)^2} \quad (2-30)$$

Subtracting pairs of these to give hyperboloids, hence subtracting (2-27) from (2-28):

$$\sqrt{x^2 + (y - y_2)^2 + (z - z_2)^2} = \frac{2y(y_2 - y_1) + 2z(z_2 - z_1) + y_1^2 - y_2^2 + z_1^2 - z_2^2 - c^2\Delta t_{12}^2}{2c\Delta t_{12}} \quad (2-31)$$

Subtracting (2-29) from (2-28)

$$\sqrt{x^2 + (y - y_2)^2 + (z - z_2)^2} = \frac{-2xx_3 + 2y(y_2 - y_3) + 2z(z_2 - z_3) + x_3^2 - y_2^2 + y_3^2 - z_2^2 + z_3^2 - c^2\Delta t_{32}^2}{2c\Delta t_{32}} \quad (2-32)$$

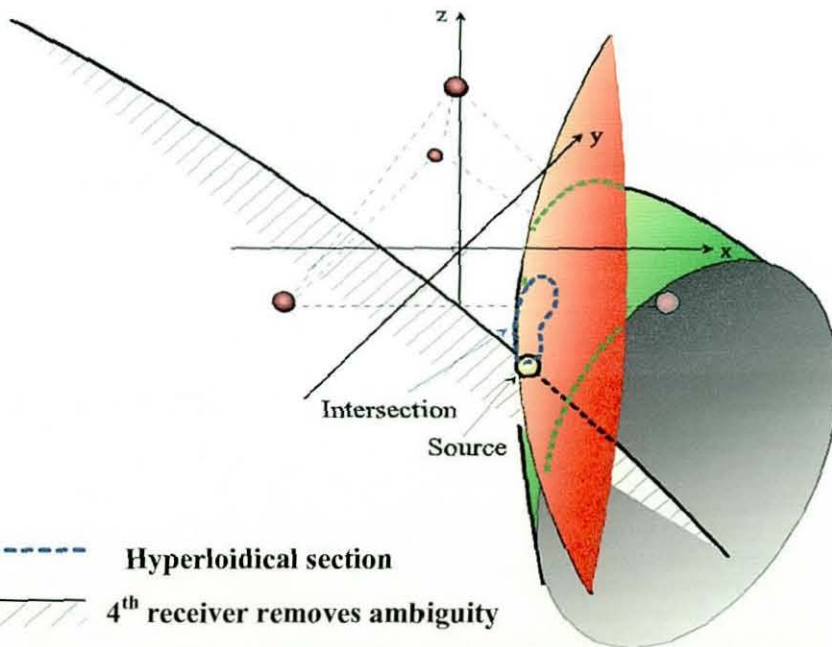
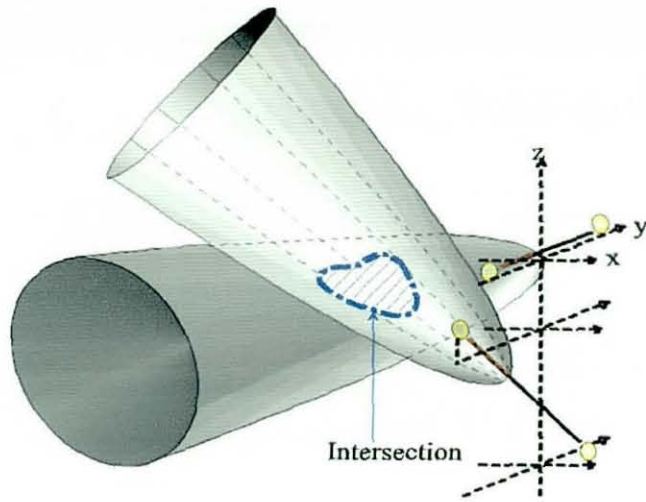


FIGURE 2.3-4 TRACKING ALGORITHMS IN THREE DIMENSIONS WITH AN UNKNOWN ACOUSTIC FLIGHT TIME – HYPERBOLOIDICAL, EACH PAIR OF HYPERBOLOIDS PRODUCES A RING WHOSE INTERSECTION GIVES THE SOLUTION

Subtracting (2-30) from (2-28)

$$\sqrt{x^2 + (y - y_2)^2 + (z - z_2)^2} = \frac{-2xx_4 + 2y(y_2 - y_4) + 2z(z_2 - z_4) + x_4^2 - y_2^2 + y_4^2 - z_2^2 + z_4^2 - c^2 \Delta t_{42}^2}{2c \Delta t_{42}} \quad (2-33)$$

Equating these and making the substitution

$$K_1 = \frac{\Delta t_{12}}{\Delta t_{32}} \quad K_2 = \frac{\Delta t_{12}}{\Delta t_{42}} \quad K_3 = \frac{\Delta t_{32}}{\Delta t_{42}}$$

yields y as a function of x and z

$$y = \alpha x + \beta z + \varphi \quad (2-34)$$

$$y = \gamma x + \xi z + \psi \quad (2-35)$$

$$y = \varepsilon x + \sigma z + \mu \quad (2-36)$$

where

$$\alpha = -\frac{K_1 x_3}{(y_2 - y_1) - K_1 (y_2 - y_3)} \quad (2-37) \quad \beta = \frac{K_1 (z_2 - z_3) - (z_2 - z_1)}{(y_2 - y_1) - K_1 (y_2 - y_3)} \quad (2-38)$$

$$\varphi = \frac{K_1 (x_3^2 - y_2^2 + y_3^2 - z_2^2 + z_3^2 - c^2 \Delta t_{32}^2) - (y_1^2 - y_2^2 + z_1^2 - z_2^2 - c^2 \Delta t_{12}^2)}{2[(y_2 - y_1) - K_1 (y_2 - y_3)]} \quad (2-39)$$

$$\gamma = -\frac{K_2 x_4}{(y_2 - y_1) - K_2 (y_2 - y_4)} \quad (2-40) \quad \xi = \frac{K_2 (z_2 - z_4) - (z_2 - z_1)}{(y_2 - y_1) - K_2 (y_2 - y_4)} \quad (2-41)$$

$$\psi = \frac{K_2 (x_4^2 - y_2^2 + y_4^2 - z_2^2 + z_4^2 - c^2 \Delta t_{42}^2) - (y_1^2 - y_2^2 + z_1^2 - z_2^2 - c^2 \Delta t_{12}^2)}{2[(y_2 - y_1) - K_2 (y_2 - y_4)]} \quad (2-42)$$

$$\varepsilon = \frac{(-K_3 x_4 + x_3)}{(y_2 - y_3) - K_3(y_2 - y_4)} \quad (2-43)$$

$$\sigma = \frac{K_3(z_2 - z_4) - (z_2 - z_3)}{(y_2 - y_3) - K_3(y_2 - y_4)} \quad (2-44)$$

$$\mu = \frac{K_3(x_4^2 - y_2^2 + y_4^2 - z_2^2 + z_4^2 - c^2 \Delta t_{42}^2) - (x_3^2 - y_2^2 + y_3^2 - z_2^2 + z_3^2 - c^2 \Delta t_{32}^2)}{2[(y_2 - y_3) - K_3(y_2 - y_4)]}$$

(2-45)

Equating (2-34) and (2-35) gives:

$$x = \frac{(\psi - \varphi) + z(\xi - \beta)}{\alpha - \gamma} \quad (2-46)$$

Substituting this into (2-36) gives z as a function of y

$$z = \left[\frac{\alpha - \gamma}{\varepsilon(\xi - \beta) + \sigma(\alpha - \gamma)} \right] y + \frac{\mu(\alpha - \gamma) - \varepsilon(\psi - \varphi)}{\varepsilon(\xi - \beta) + \sigma(\alpha - \gamma)} \quad (2-47)$$

$$\text{in the form } z = Gy + W \quad (2-48)$$

Similarly from (2-46) and (2-36) we obtain

$$x = \left[\frac{\xi - \beta}{\varepsilon(\xi - \beta) + \sigma(\alpha - \gamma)} \right] y + \frac{\sigma(\psi - \varphi) - \mu(\xi - \beta)}{\varepsilon(\xi - \beta) + \sigma(\alpha - \gamma)} \quad (2-49)$$

$$\text{which is in the form } x = Ty + S \quad (2-50)$$

Knowing x and z in terms of y we can substitute equations (2-48) and (2-50) into (2-31) giving a quadratic in y

$$Ay^2 + By + C = 0 \quad (2-51)$$

where

$$A = G^2 + 1 + T^2 - \frac{[G(z_2 - z_1) + (y_2 - y_1)]^2}{c^2 \Delta t_{12}^2} \quad (2-52)$$

$$B = 2G(W - z_2) - 2y_2 + 2TS - \frac{[G(z_2 - z_1) + (y_2 - y_1)] \cdot [2W(z_2 - z_1) + y_1^2 - y_2^2 + z_1^2 - z_2^2 - c^2 \Delta t_{12}^2]}{c^2 \Delta t_{12}^2} \quad (2-53)$$

$$C = (W - z_2)^2 + y_2^2 + S^2 - \frac{[2W(z_2 - z_1) + y_1^2 - y_2^2 + z_1^2 - z_2^2 - c^2 \Delta t_{12}^2]^2}{4c^2 \Delta t_{12}^2} \quad (2-54)$$

Enough information is now available to calculate the co-ordinates in terms of x, y and z.

Both the two- and three-dimensional equation sets produce some dual solutions, some of which can be eliminated simply using the original timing information, others are equally valid and rely on the user's intuition. The equation set contains a number of singularities and fails in a number of cases, usually due to a divide-by-zero operation caused by two main factors:

When a time difference Δt is zero, i.e. if the source is orthogonal to the centre line of a pair of receivers. In software, ignoring this case or biasing the solution slightly so that this case does not arise can eliminate this.

If the array is two-dimensional, this case can be ignored if the array is fixed. If it is not fixed, or a flat array is specifically needed, a new set of equations must be generated, as shown in section 2.3.2

This algorithms set is fully modelled and simulated in Chapter 3, where the sensitive areas are plotted.

2.3.2 ABSOLUTE METHOD FOR A FLAT ARRAY (METHOD 2)

The solution described in section 2.3.1 fails in certain situations. If the four receivers all fall on one plane, (2-38), (2-41) and (2-44) generating a value for ξ , β and σ relies on subtracting the z values of pairs of hydrophones, i.e. $(z_2 - z_4) - (z_2 - z_1)$ which, since all the z -values are the same, results in zero, which in turn is a divisor in equation 2-47 and 2-49 for z and x . Theoretically, it is possible to get information of the third dimension from a two-dimensional array in three-dimensional space. There is, however, a single ambiguity, resulting in the mathematics being incapable of detecting if the source is above or below the plane of the array. Hyperboloids formed around each pair of receivers will still intersect in three-dimensional space. To calculate a general solution for this specific case is extremely complex and lengthy due to the expression having two solutions for each pair of receivers. In certain cases the solution is greatly simplified.[9]

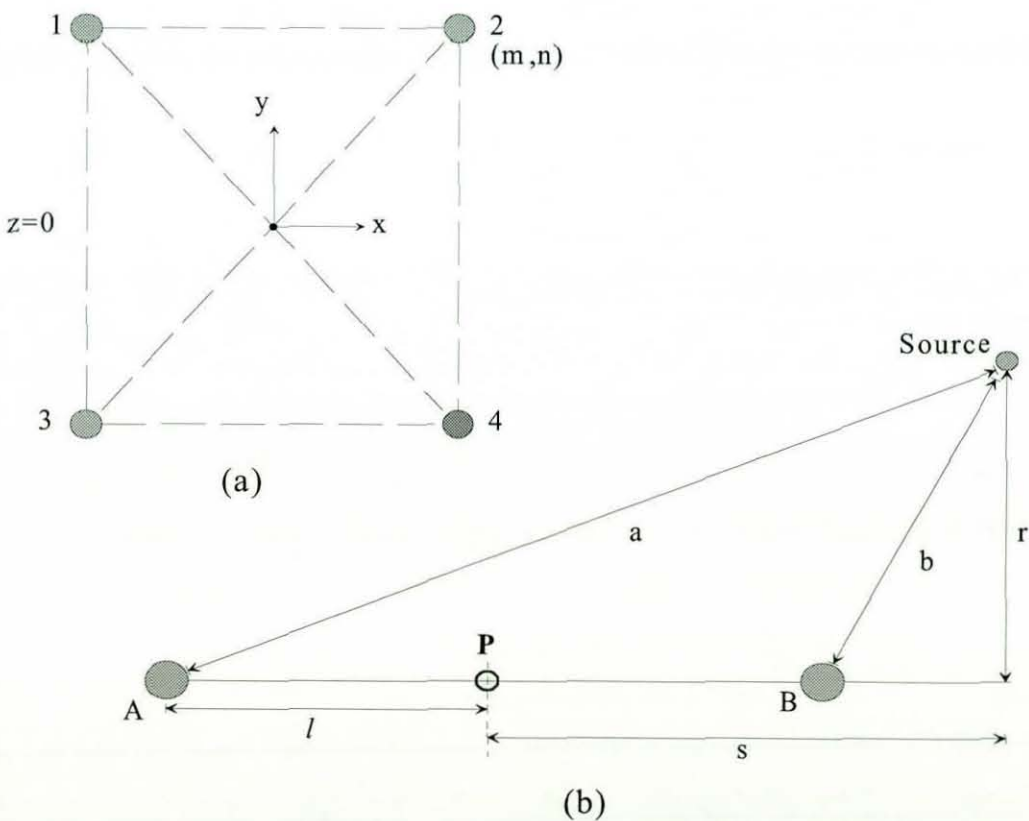


FIGURE 2.3.-5 (A) ARRAY CONFIGURATION FOR RECTANGULAR FLAT ARRAY
 (B) DIMENSIONS FOR GENERAL SOLUTION

Taking the case illustrated in Figure 2.3-5a and the dimensions shown in Figure 2.3-5b it can be shown (similar to equation (2-14)) that:

If $d = a - b$

$$4ls - d^2 = 2d \left((s-l)^2 + r^2 \right)^{\frac{1}{2}} \quad (2-55)$$

This formula uses to its advantage the fact that $c > 0, c \geq |d|, |s| \geq |d|$ and $\text{sign}(s) \equiv \text{sign}(d)$. This allows (2-55) to be restated as:

$$\frac{4ls - d^2}{4d} = 2d \left| \left((s-l)^2 + r^2 \right)^{\frac{1}{2}} \right| \quad (2-56)$$

Equation (2-55) is therefore adopted as the description of the locus.

As there is some redundancy in the receiver configuration shown, we choose pairs of receivers aligned with either the x or y axes for simplicity. Applying equation (2-56) yields the following four equations.

$$\frac{4mx - d_{12}^2}{2d_{12}} = \left| \left((x-m)^2 + (y-n)^2 + z^2 \right)^{\frac{1}{2}} \right| \quad (2-57)$$

$$\frac{4ny - d_{42}^2}{2d_{42}} = \left| \left((y-n)^2 + (x-m)^2 + z^2 \right)^{\frac{1}{2}} \right| \quad (2-58)$$

$$\frac{4mx - d_{34}^2}{2d_{34}} = \left| \left((x-m)^2 + (y-n)^2 + z^2 \right)^{\frac{1}{2}} \right| \quad (2-59)$$

$$\frac{4ny - d_{31}^2}{2d_{31}} = \left| \left((y-n)^2 + (x+m)^2 + z^2 \right)^{\frac{1}{2}} \right| \quad (2-60)$$

The right hand sides of equations 2-57 and 2-58 are similar. Combining their left hand sides produces:

$$x = \frac{d_{12}(d_{12}d_{42} + 4ny - d_{42}^2)}{4md_{42}} \quad (2-61)$$

Equations (2-59) and (2-60) cannot be directly combined as in (2-61) as their right hand sides are not similar in this case. If, however, one considers the right hand sides of these equations, they can be seen to represent the distance from the source to receivers four and one respectively.

Thus, from equation (2-58)

$$\begin{aligned} \frac{4mx - d_{34}^2}{2d_{34}} &= \text{distance from source to receiver 4} = \text{distance from source to } 2 + d_{42} \\ &= \left| \left((x-m)^2 + (y-n)^2 + z^2 \right)^{\frac{1}{2}} \right| + d_{42} \end{aligned} \quad (2-62)$$

and from equation (2-60)

$$\begin{aligned} \frac{4ny - d_{31}^2}{2d_{31}} &= \text{distance from source to receiver 1} = \text{distance from source to } 2 + d_{12} \\ &= \left| \left((x-m)^2 + (y-n)^2 + z^2 \right)^{\frac{1}{2}} \right| + d_{12} \end{aligned} \quad (2-63)$$

Combining equations (2-62) and (2-63), the following equation is obtained

$$x = \frac{d_{34}}{4m} \left(d_{34} + 2d_{42} + \frac{1}{d_{31}} (4ny - d_{31}^2 - 2d_{31}d_{12}) \right) \quad (2-64)$$

Combining equations (2-61) and (2-64) produces the following expressions for x and y

$$x = \frac{d_{12}d_{34}(d_{34}d_{31} - d_{12}d_{42} + 2d_{31}d_{42} - d_{31}^2 - 2d_{31}d_{12} + d_{42}^2)}{4m(d_{31}d_{12} - d_{42}d_{34})} \quad (2-65)$$

$$y = \frac{d_{31}d_{42}(d_{12}d_{42} - d_{34}d_{31} + 2d_{42}d_{34} - d_{12}^2 - 2d_{12}d_{34} + d_{34}^2)}{4n(d_{31}d_{12} - d_{42}d_{34})} \quad (2-66)$$

Substituting equations (2-65) and (2-66) back into (2-57) provides the following expression for the magnitude of z;

$$|z| = \left[\left(\frac{4mx - d_{12}^2}{2d_{12}} \right)^2 - (x - m)^2 - (y - n)^2 \right]^{\frac{1}{2}} \quad (2-67)$$

Limitations and a full simulation of this algorithm can be found in Chapter 3. This formula is limited in that it relies on the receivers being fixed in a particular configuration. If they are not in this configuration the simplifications made are invalid and the method fails. This method relies on the array being rectangular, which in practice is difficult to achieve if the array is not fixed. A general solution has not yet been found.

2.4 INACCURACIES IN MEASUREMENTS

Both methods described in section 2.3 lead to finding a position in terms of the inter-receiver timing information and receiver position. Both algorithms are imperfect, in that a single solution cannot be found or singularities result in no solution. This may be due to timing differences being zero, or pairs of timings being equal. In practice, errors occur in the measurements that result in the hyperbolae not quite meeting in a single point but in a zone around the actual point, as shown in Figure 2.4-1.

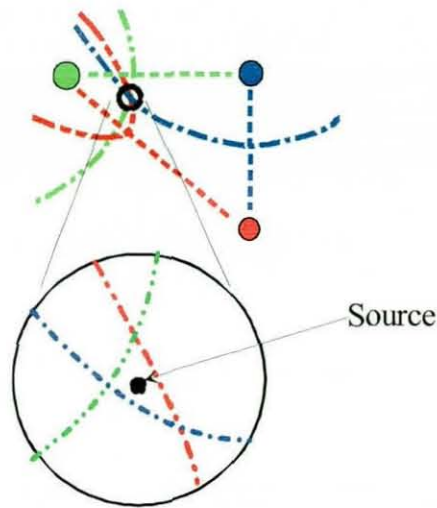


FIGURE 2.4-1 EFFECT OF TIMING INNACURACIES RESULTING IN NO ABSOLUTE SOLUTION

This means there will probably be an absolute solution very infrequently. To take this into account mathematical techniques such as averaging, centre of mass or least squares fit may be utilised, which effectively find the nearest acceptable solution to all the individual equations. In the case of the algorithms described in section 2.3.2 one method of performing the average is to find the centre of mass. This effectively allows weightings to be placed on the results from each pair of receivers, depending on confidence of each pair's accuracy, and will then find the point with the minimum distance to all the solutions.

To implement this, the axes are changed in the algorithm such that four readings are taken. The error from any particular receiver pair will result in the point in a slightly different place for each set of axes. The weighted mean of all the points can then be found and taken to be the answer. This method of finding the mean can also be applied to the method described in section 2.3.1. In this case each set of x- and y-axes are not at right angles to each other, but positioned in parallel and orthogonal to each pair of receivers. It is also possible that an extra receiver will eliminate some of the singularities, or improve the accuracy of the system with a source in the sensitive positions.

2.4.1 TRACKING USING EXCESS RECEIVERS (METHODS 5 AND 6)

Section 2.3 showed how sets of spherical equations for each pair of receivers could be subtracted to remove the absolute timing information, thus creating a hyperbolic equation set, which with manipulation can produce the position of the source. Using this method three-dimensional tracking can be accomplished with the use of four receivers. If, instead of manipulating the equations to remove the unknown range/absolute timing information of the source, the equations are linearised with the range information still included, a set of three simultaneous equations can be created for a 2-dimensional situation or four equations for the 3-dimensional case (the extra equation being for the timing variable). To create these linear equations an extra receiver is required such that time differences can be used, i.e. each pair of receivers produces an equation in the set. The equation set can be solved by applying standard matrix methods[10].

2.4.1.1 LINEARISING THE EQUATIONS

Defining the situation:

$r_1, r_2, r_3, \dots, r_n$ Position vectors of the receiving array

$\tau_1, \tau_2, \tau_3, \dots, \tau_n$ Relative arrival time of the signal at the receivers, where $\tau_1 = 0$

c Speed of sound in the medium

s Source position vector

T_1 Time of travel from the source to the first receiver at r_1

The time taken for the signal to arrive from the source to the first receiver can be specified (using Pythagoras) as

$$(S_x - r_{1x})^2 + (S_y - r_{1y})^2 = cT_1^2 \quad (2-68)$$

which is in the form

$$Ax^2 + By^2 = R^2 \quad (2-69)$$

i.e. the equation of a circle. This can also be written as:

$$\|s - r_n\|^2 = (cT_1)^2 \quad (2-70)$$

and for subsequent receivers:

$$\|s - r_n\|^2 = c^2(T_1 + \tau_n)^2 \quad (2-71)$$

If we now subtract (2-70) from each of the others as in section 3.2.1 we get

$$\|s - r_n\|^2 - \|s - r_1\|^2 = c^2(T_1 + \tau_n)^2 - c^2T_1^2 \quad (2-72)$$

which can be converted into a linear form (in two dimensions) as follows

$$\left([s - r_n]_x^2 + [s - r_n]_y^2 \right) - \left([s - r_1]_x^2 + [s - r_1]_y^2 \right) = c^2(T_1^2 + 2\tau_n T_1 + \tau_n^2 - T_1^2) \quad (2-73)$$

which in terms of x and y yields

$$\left[(s - r_n)^2 + (s - r_1)^2 \right]_x + \left[(s - r_n)^2 + (s - r_1)^2 \right]_y = c^2(2\tau_n T_1 + \tau_n^2) \quad (2-74)$$

This is the equation of a hyperbola in a slightly different form from (2-16). We can further manipulate (2-74) to give

$$[2sr_1 - 2sr_n]_x + [2sr_1 - 2sr_n]_y + [r_n]_x^2 + [r_n]_y^2 - [r_1]_x^2 - [r_1]_y^2 = c^2(2\tau_n T_1 + \tau_n^2) \quad (2-75)$$

and

$$2s \cdot (r_1 - r_n) - 2c^2 \tau_n T_1 = \|r_1\|^2 - \|r_n\|^2 + c^2 \tau_n^2 \quad (2-76)$$

This is the general form for the parabola. However, it still contains T_1 , the time of travel from source to receiver, which must be eliminated or calculated. We may now re-write the problem in a linear matrix form

$$\begin{pmatrix} 2[r_1 - r_2]_x & 2[r_1 - r_2]_y & -2c^2 \tau_2 \\ 2[r_1 - r_3]_x & 2[r_1 - r_3]_y & -2c^2 \tau_3 \\ \dots & \dots & \dots \\ \dots & \dots & \dots \\ 2[r_1 - r_{n-1}]_x & 2[r_1 - r_{n-1}]_y & -2c^2 \tau_{n-1} \\ 2[r_1 - r_n]_x & 2[r_1 - r_n]_y & -2c^2 \tau_n \end{pmatrix} \cdot \begin{pmatrix} [s]_x \\ [s]_y \\ T_1 \end{pmatrix} = \begin{pmatrix} \|r_1\|^2 - \|r_2\|^2 + c^2 \tau_2^2 \\ \|r_1\|^2 - \|r_3\|^2 + c^2 \tau_3^2 \\ \dots \\ \dots \\ \|r_1\|^2 - \|r_{n-1}\|^2 + c^2 \tau_{n-1}^2 \\ \|r_1\|^2 - \|r_n\|^2 + c^2 \tau_n^2 \end{pmatrix} \quad (2-77)$$

Which is in the form $\mathbf{A} \cdot \mathbf{m} = \mathbf{x}$. The inverse of matrix \mathbf{A} can be found using standard matrix techniques and thus the equations can be solved as $\mathbf{m} = \mathbf{A}^{-1} \cdot \mathbf{x}$.

2.4.1.2 LEAST SQUARE ERRORS

In practice, timing errors and singularities will result in exact solutions occurring rarely. The matrix form of linear equations allows a number of techniques to be applied in the solution of the equation set. One such method, Singular Value Decomposition (SVD) solves sets of simultaneous equations and also allows the user or software to change some parameters such that singularities can be compensated for and a form of least squares error reduction can be applied. This method is, as the title suggests, a method of decomposing a matrix that contains singularities, i.e. in certain areas there are infinite solutions, as is the case in this circumstance.

SVD can be stated as [11]: Any $M \times N$ matrix \mathbf{A} , whose number of rows M is greater or equal to its number of columns N , can be written as the product of an $M \times N$ column-orthogonal matrix \mathbf{U} , an $N \times N$ diagonal matrix \mathbf{W} with positive or zero elements, and a transpose of an $N \times N$ orthogonal matrix \mathbf{V} , as follows:

$$\begin{pmatrix} A \end{pmatrix} = \begin{pmatrix} U \end{pmatrix} \cdot \begin{pmatrix} w_1 \\ w_2 \\ \dots \\ w_N \end{pmatrix} \cdot \begin{pmatrix} V^T \end{pmatrix} \quad (2-78)$$

By replacing w_N with $1/w_N$ the inverse of A can be calculated

$$\mathbf{A}^{-1} = \mathbf{U} \cdot [\text{diag}(1/w_j)] \cdot \mathbf{V}^T \quad (2-79)$$

If a singularity occurs, i.e. the lines do not meet in a single spot, w_j values are zero, therefore $1/w_j$ are infinite. The method of SVD replaces the infinity with zero, thus effectively ignoring the parameter and allowing a least squares fit of the other points. If the matrix \mathbf{A} produces a w_j that is non-zero but very small the matrix is ill-conditioned, the $1/w$'s will approach the limit of the computer's floating point precision. In this case, replacing the $1/w$ with zero will allow the method to work; the value is probably produced by rounding errors. This will in effect ignore the singularity and take the shortest solution vector, i.e. the nearest point where an intercept occurs. In this case, the corresponding values of \mathbf{V} form a null-space of the equation, i.e. $\mathbf{A} \cdot \mathbf{m} = 0$, and so can be used to form a set of equations that can be added as linear combinations on to a solution for the original equation to span the solution space.

The method can only give a single solution when there are as many unknowns as equations, i.e. in the two-dimensional case, three unknowns (x , y , T) and three equations (made up of subtracting each receiver from the reference receiver) and therefore four receivers. It is possible to use more receivers, the only difference in this over-determined case being the shape of the matrices and the order.

If the matrix is under-determined, as would be expected, a set of solutions is produced.

This method, although over-determined, is versatile and practical and with use of the SVD algorithm, calculations can be made quickly over the whole solution space.

2.4.2 TABULAR METHOD (METHOD 4)

With the advent of faster computers and readily available memory all at a lower cost than ever before, a more basic method of tracking has become feasible. The method works by creating a large array where each element corresponds to a point in space around the receivers. Each element of this array holds a number of parameters, each relating to a time difference between two receivers, i.e. if there are four hydrophones there will be six time differences per element. For a given set of time differences, the computer searches for the corresponding element, which can be translated to a position in space. In theory this method is simple, but the limitations lie in the size of the space to be monitored and the speed of the computer in searching the array. For a real time system the search time can be greatly reduced by using sorting techniques. Instead of generating and searching the spatial array, a set of tables called bins is generated for each receiver pair. A bin contains all the possible positions for a particular time difference on that receiver pair. Effectively, this means storing all the positions in the spatial array of the hyperbola for that time difference. Bins are generated for each possible time difference. When the time differences are observed, the bins for each received time difference are compared and the positions that are present in all the time bins are the correct solutions. This method vastly reduces the amount of data to be sorted.

This method does not suffer from most of the ambiguities generated by the mathematical methods. It does, however, suffer from errors due to quantisation. Firstly, if the time accuracies are not exactly the same as those recorded, then a solution will not be found. This is easy to overcome by creating a zone around each point in space in which the closest point is used. If the time differences are not accurate enough a number of solutions will be possible, reducing the accuracy of the predicted source. If the quantisation of space is too fine in comparison to the time difference accuracy, a number of points will be detected. There is therefore an optimum spatial array size related to the

timing accuracy, but unfortunately this is not linear. A time difference may correspond to a single element near the array, but as the source moves away the timing accuracy limitation means that the surface of the hyperbola becomes thicker and so inaccuracies

are greater at greater ranges. Figure 2.4-2 shows the error becoming larger in the particular areas. A full analysis can be seen in Chapter 3. In fact, by sorting by time differences rather than spatial positions the array becomes non-linear and each spatial array element changes in size and shape.

This method is time consuming in the set-up stage, i.e. when the bins are generated, but once generated a solution can be reached very quickly. If a dynamic array is used the system will need to be recalibrated at regular intervals, depending on the movement of the array. Calculation of the source position is quick in any configuration, unlike the mathematical solutions that may need to change algorithm depending on the configuration. This method may also hold advantages in environments with a varying sound velocity profile. If the velocity profile is known before the table generation stage it can be compensated for in generation and then ignored at any later stage.

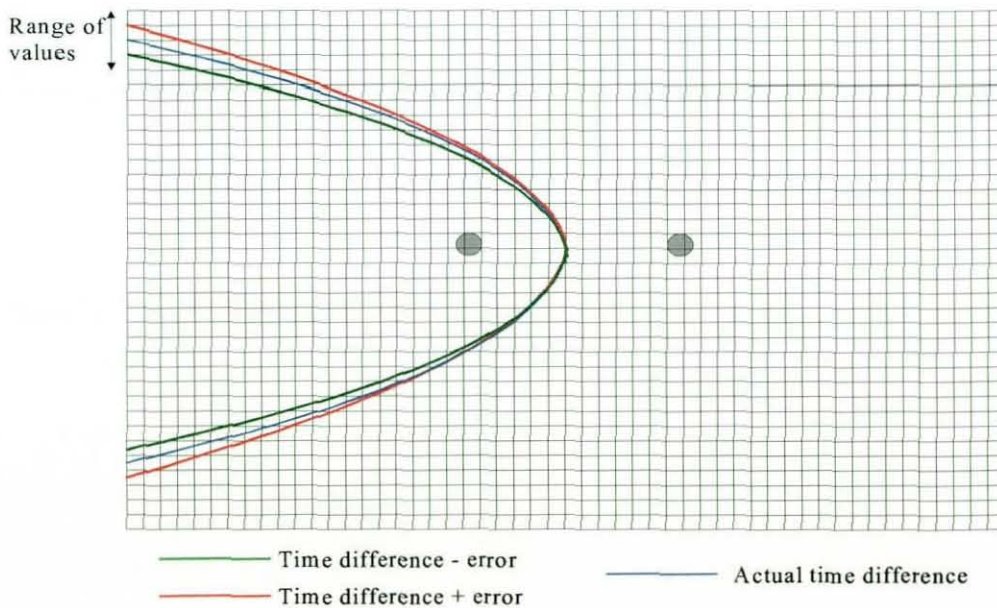


FIGURE 2.4-2 ERROR MARGIN DUE TO TIMING ACCURACY

$$F = c \times t_{rev2} \quad (2-84)$$

Using the cosine rule:

$$\cos \theta_1 = \frac{E^2 + C^2 - (C + D)^2}{2EC} \quad (2-85)$$

and

$$\cos \theta_2 = -\cos \theta_1 = \frac{G^2 + C^2 - (C + F)^2}{2GC} \quad (2-86)$$

Equating (2-86) and (2-85) gives:

$$C = \frac{G^2 E - F^2 E + E^2 G - D^2 G}{2(GD + EF)} \quad (2-87)$$

and

$$\theta_1 = \cos^{-1} \left(\frac{4A^2 - 2CD - D^2}{4AC} \right) \quad (2-88)$$

In this particular case it is possible to track in three-dimensional space with just three receivers. As range is known, the circular two-dimensional tracking algorithms shown in Section 2.2 can be utilised to find the position of the source in two-dimensional space. The depth information can then be used for the third dimension, but there are problems with this method however. The method relies on reverberations from both the surface and the seabed, and fails if either is not present. In some cases the reverberations may be very close to the direct signal, and this is particularly true if the receiver is close to the surface or the bottom. In this case it would be simpler to use a third or fourth reverberation, if present, as shown in Figure 2.5-2. In this case the algorithm must be modified, and a general solution can be reached.

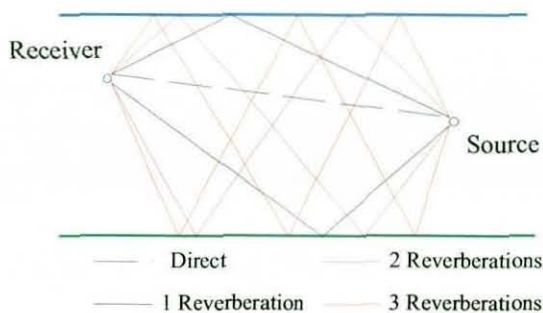


FIGURE 2.5-2 DETECTION OF RECEIVED SIGNALS DUE TO DIRECT, 1, 2 AND 3 REVERBERATIONS (7 SIGNALS IN ALL)

If we plot the rays as in Figure 2.5-1 but include the two and three reverberation case as in Figure 2.5-3 we can see that the main algorithm is still valid, but the values for E and G change.

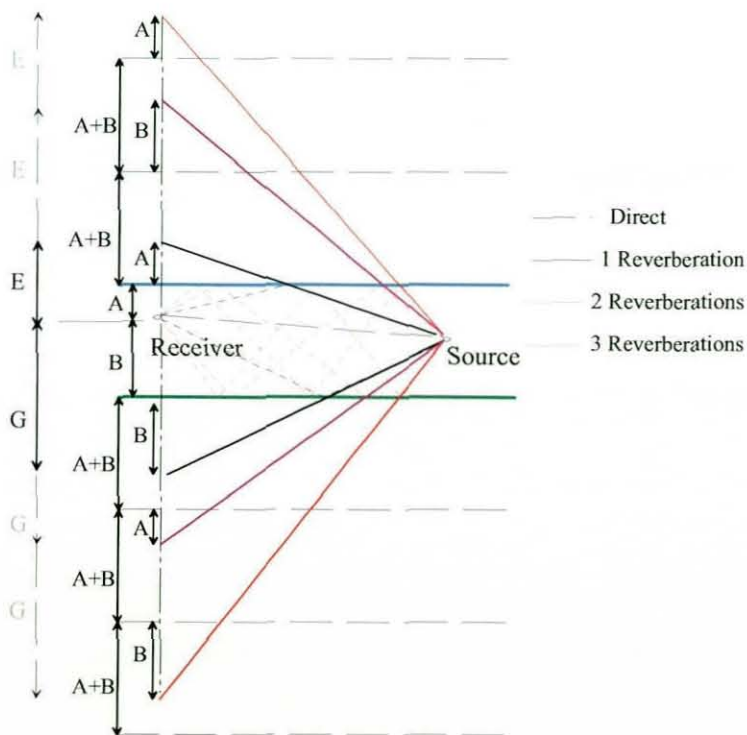


FIGURE 2.5-3 RAY PLOT OF THE REVERBERATION PAIRS FOR 1, 2 AND 3 REVERBERATIONS

In this case we can replace E and G in (2-87) with the value of A and B for the particular reverberation measured. Considering pairs of measurements where the direct signal is considered as r_0 the first surface reverberation as r_1 and the first bottom reverberation as r_2 then the values for E and G can be calculated as follows:

$$\text{For } r_{n \rightarrow \text{odd}} \Rightarrow E_n = (n+1)A + (n-1)B \quad (2-89)$$

$$G = (n-1)A + (n+1)B \quad (2-90)$$

$$\text{For } r_{n \rightarrow \text{even}} \Rightarrow E_n = G = nA + nB \quad (2-91)$$

It is possible that it may be useful to use two surface reverberations and ignore the adjacent bottom first reverberation, i.e. r_1 and r_3 . The geometry of the situation allows for this and G can be substituted by an E from a different reverberation.

This reverberation method provides a useful tool when the number of receivers is limited, but it does have drawbacks. It relies on a clear resolution of the reverberations, which are usually achieved by viewing the signal in the frequency domain in the form of a spectrogram. Once the initial direct signal is detected the time differences to the reverberations are measured. It is necessary to identify whether the reverberation is from the surface or the bottom. This can be achieved by observing the relative phases of the direct signal and the reverberation signal. If the signal has reflected from the surface it will be phase-inverted. If this cannot be measured (if the signal is a continuous wave it may be difficult to determine phase) it must be assumed there are two solutions, calculated by swapping the values for D and F. It is sometimes possible to discern which solution is correct if further information is available.

The need for human intervention in the identification process makes the technique long-winded and laborious, especially if three hydrophones are used to provide exact position information. The largest errors are derived from inaccuracies in timing information between the direct and reverberated signals (analysed in Chapter 3). It is possible to

automate this system, with the use of pattern recognition techniques, and correlation to find the reverberations, but this is outside the scope of the project.

2.6 COMPARATIVE ANALYSIS

Theoretically, each of the five sets of algorithms has advantages over the others. The method described in sections 2.3.1 and 2.4.1 require complex calculations, but are robust to changes in the receiver separations. The method described in section 2.3.2 relies heavily on the array being fixed in a rectangular formation. This method is capable of measuring a position in three-dimensional space using an array spanning only two dimensions. The method, described in section 2.3.2, also includes a crude form of error reduction from errors caused by timing inaccuracies. This may prove critical in a practical system for which perfect measurements are unrealistic. In theory hyperbolic systems behave very well in long baseline cases where the source is inside, or near, the array. As the source moves outside the array the error margin increases. Spherical systems suffer from a similar problem but the error is smaller. This is due to the effect of a timing error on the accuracy. Inside the array the loci of the hyperboloids or spheres cross each other at a large angle, often approaching a right angle. Outside the array the angles become smaller and decrease faster with the hyperboloids than with the spheres. This small angle effectively means that a small error in timing will move the predicted position of the source by a large distance. The method described in section 2.4.1 uses an efficient method of calculating the nearest position when errors in the system or limitations of the system dictate that no unique answer exists. This method in itself has disadvantages in that it requires an extra receiver channel, and like section 2.3.2, also requires a receiver in the third dimension. The reverberation method described in section 2.5.1 has been successfully used in situations where only one or two receivers are available. It relies on reverberations being present and to be accurate in depth, it also depends on knowledge of which reverberations are present.

Depending on the circumstances of use, any of the systems can be used, and at this stage none appear better than the others. To decide further on which algorithm to use in the

various case studies discussed in Chapter 5 it is necessary to model the algorithms to observe their response to the likely error conditions.

2.7 LIMITATIONS AND PARAMETERS FOR THE SYSTEM

This chapter has introduced a number of parameters that affect the configuration of a passive tracking system. These are placed in the Table 2-2 below, and where possible, values for the parameters are inserted from the theoretical situation described in the previous two chapters.

As can be seen from the table, a number of parameters cannot be set purely from theory or recommendation; instead simulation should provide these values, and the results from which will obviate the need for specific types of equipment or variable settings.

Parameter	Value	Dependant upon	Reference
Array size Max, Min	0.1m – 4m (preferably flat)	Species, Mounting	1.7
Range Max, Min	3m – 500m	Species, Received frequency, SL and Signal/noise & trawl size	2.1.1
Array Shape	Simulation	Mounting, Algorithm	3.1.3.4
Array Size	Simulation	Species, Sample rate	3.4.x.1
Sample rate	Simulation	Array size, Mounting	3.3.x.2 3.4.x.2
Hydrophone type	Simulation	Mounting,	-
Detection Frequency	40kHz	Mounting, Array size, Species	1.2.6
Algorithm	Simulation	Mounting	3.8
Array Type	Simulation	Algorithm, hydrophones	3.6

TABLE 2-2 SHOWING THE PARAMETERS SET BY THEORY.

2.8 References in Chapter 2

- [1] W.W.L. Au, *The sonar of dolphins*, Springer-Verlag, 1993.
- [2] W.W.L. Au, Echolocation signals of the Atlantic bottlenose dolphin (*Tursiops Truncatis*) in open waters. In: *Animal sonar systems*, eds. G.B. Busnel and J.F. Fish. London: Plenum press, 1980, pp. 251-282.
- [3] Rasmussen, Miller, and Au, The sounds and calculated source levels from the whitebeaked dolphin recorded in Islandic waters. eds. P. Evans, J.A. Raga, and L.J. Cruz. *European Research on Cetaceans*. vol 13, no. 1, 1999. European Cetacean Society, Proc. 13th Ann. Conf. ECS, Valencia Spain.
- [4] A.D. Goodson, A narrow band bio-sonar: Investigating echolocation in the harbour porpoise, *Phocoena phocoena*, *Proc Inst. of Acoustics*, Vol 19, no. 9, pp. 19-28, 1997
- [5] Y. Hatekeyama and H. Soeda, Studies on echolocation of porpoises taken in salmon gillnet fisheries. Sensory abilities of cetaceans, laboratory and field evidence, pp. 269-281, 1990
- [6] V.S. Gurevich, Echolocation discrimination of geometric figures in the dolphin, *Delphinus delphis*, *Vestnik Moskovskogo Universiteta, Biologia*. Vol 3, pp 109-12, Pochovedeniye. Moscow, 1969
- [7] T.R. Stockton and M.W. McLennan, Acoustic position measurement, an overview, *Proc. 7th Ann. Offshore Technol. Conf.*, Houston 1, pp. 255-264, 1975.
- [8] P.A. Hardman and B. Woodward, Underwater position fixing by diver operated acoustic telemetry system, *Acustica*, Vol. 55, pp 34-44, 1984.
- [9] Hay R. and Connelly P., Internal report . Passive Tracking using a flat array. Dept of Elec Eng. Loughborough (unpublished).
- [10] J.L. Spiesberger and K.M. Fristrup, Passive localization of calling animals and sensing of their acoustiv environment using acoustic tomography, *The American Naturalist*, Vol 135, pp 107-153, 1990, 0003-0147.
- [11] W.H. Press, B.P. Flannery, S.A. Teukolsky, and W.T. Vetterling, *Numerical Recipes*, Cambridge: Cambridge University Press, 1986, pp. 52-64.

CHAPTER 3

SIMULATION

The aim of this chapter is to demonstrate the algorithms presented in Chapter 2 and perform error analysis on each to find sensitivities to change in its parameters. Once these are found the design process can continue, and the sensitive areas can be marked or eliminated by other methods. From this analysis it should be possible to make a decision as to the most appropriate algorithm for any particular tracking situation.

3.1 ERROR ANALYSIS

To exhaustively test all the algorithms for all situations is long-winded and thought unnecessary for this project. Instead the main error contributors are considered. [1]:

- a) Slant range errors due to
 - i) Environmental errors, i.e. variations in velocity of sound due to temperature, salinity and pressure;
 - ii) Electronic errors, recognition and response time delays;
 - iii) Residual timing errors, caused by phase shifts in the electronics or random timing errors due to noise;
 - iv) Curvilinear acoustic ray paths;
 - v) Image interference due to interference.
- b) Baseline errors due to errors in initial calibration, i.e. position of array.
- c) Multiplicative errors for speed of sound in slant-range measurements.
- d) Square law errors from quadratic equations.
- e) Transducer motion during reception.

A number of these errors will be constant and predictable (e.g. residual timing errors, baseline errors due to calibration and algorithmic square law errors), and therefore if quantified for a particular system they can be compensated for. Other errors have upper limits set by design (e.g. a-ii and e). The other errors tend to be random, but parameters

defining the likely limits can be set for these and simulations performed for worst-case situations. The analysis will be performed in the following stages:

3.1.1 VERIFICATION OF THE ALGORITHM BEING TESTED

For this analysis a spatial array will be created. For each position in the array the correct timings will be calculated assuming the source is in that spatial position. The algorithms will then be made to calculate the position for each set of timing information. This will show any errors or duality in the algorithms. To display this information in a format that is easy to understand, space will be sliced into layers, and the layers representing the extremes will be plotted together with the zero z co-ordinate slice (effectively the two-dimensional case).

3.1.2 TIMING ERRORS

Small timing errors will then be introduced, and errors in output will be analysed. This analysis will give an idea of areas sensitive to the algorithm, and also an idea of the necessary sampling speed for the system for any given accuracy requirement.

3.1.3 RECEIVER POSITION ANALYSIS

A range of receiver positions will be tested to see how array configuration affects tracking accuracy. Small errors in these positions will also be introduced to see the effect of inaccurate calibrations.

3.1.4 VELOCITY PROFILE VARIATIONS

Until now a constant velocity profile has been considered, but in practice this is never the case. Acoustic velocity will vary with depth and in some parts of the water column it is possible to predict the velocity, although near the surface this is often not the case. Variations in temperature and salinity tend to make the velocity vary in quite a short time period. Figure 3.1-1 shows the three profiles that will be simulated to see the effect of the errors generated. The fourth profile is a constant velocity profile included to show a baseline for the simulation method.

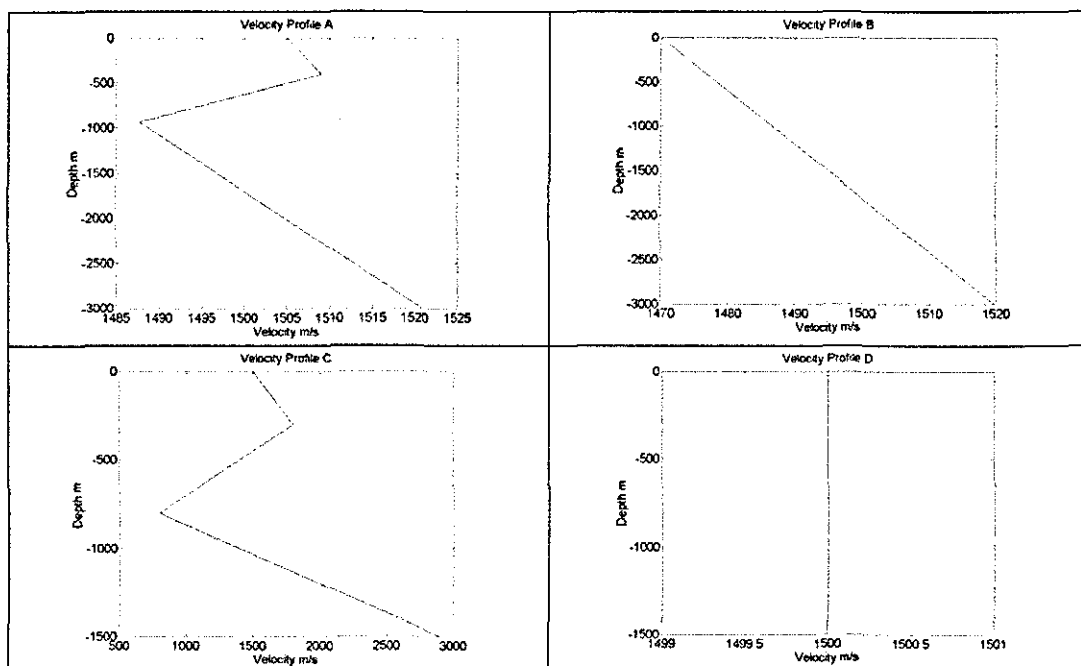


FIGURE 3.1-1 VELOCITY PROFILES CONSIDERED IN SIMULATIONS A) TYPICAL OCEAN, B) STABLE DUE TO PRESSURE, C) EXTREME, D) CONSTANT.

Analysis of each of these profiles will be performed by calculating the ray-path from source to the receiver through the water column. The time difference between the time of flight from source to receiver in the constant velocity case and that with the profile will be calculated. The errors in position can then be calculated.

For each algorithm considered in the previous chapter each of the reported analyses (3.1.1-3.1.4) will be performed allowing comparative analysis. So as not to make this chapter too long many of the results have been placed in Appendix B and only those showing the trends have been included here.

3.2 ACTIVE TRACKING ALGORITHMS

The simulation of these algorithms is outside the scope of the thesis. Simulations of these algorithms can be found in the literature, notably [1].

3.3 DIRECTLY-SOLVED PASSIVE TRACKING ALGORITHMS

3.3.1 ABSOLUTE METHOD – LIMITED RECEIVER POSITIONING (METHOD 1)

The full algorithm simulated in this section can be found in section 2.3.1 and results in the following terms.

$$Ay^2 + By + C = 0 \quad (\text{from 2-51})$$

$$x = \left[\frac{\xi - \beta}{\varepsilon(\xi - \beta) + \sigma(\alpha - \gamma)} \right] y + \frac{\sigma(\psi - \varphi) - \mu(\xi - \beta)}{\varepsilon(\xi - \beta) + \sigma(\alpha - \gamma)} \quad (\text{from 2-49})$$

and

$$z = \left[\frac{\alpha - \gamma}{\varepsilon(\xi - \beta) + \sigma(\alpha - \gamma)} \right] y + \frac{\mu(\alpha - \gamma) - \varepsilon(\psi - \varphi)}{\varepsilon(\xi - \beta) + \sigma(\alpha - \gamma)} \quad (\text{from 2-47})$$

where the symbols are defined in section 2.3.1.

From these results the predicted positions of the source can be calculated.

3.3.1.1 NO ERROR SIMULATION

If the signal is generated, the difference between the actual position and the estimated position can be calculated, and a plot of the errors in space can be plotted.

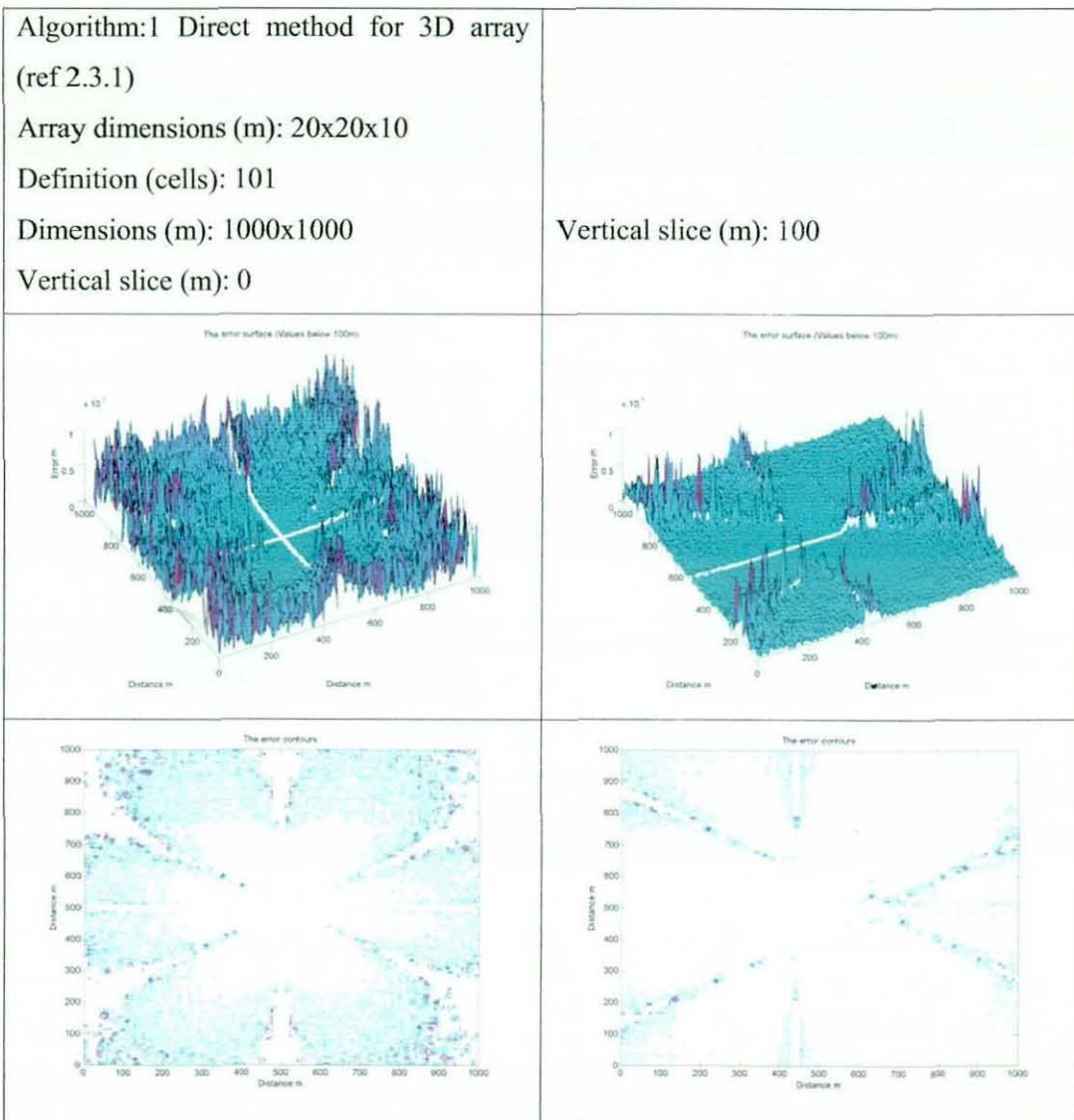


FIGURE 3.3-1A ERRORS IN ALGORITHM 1 DUE TO COMPUTER LIMITATIONS IN A 20M ARRAY

Figure 3.3-1A shows the errors over a space of a square km. The maximum errors in this case are in the region of 10^{-9} , although the white areas on the diagonals do rise to 10^{-6} before they become ambiguities. An ambiguity can be seen in the 0m section along the line perpendicular and orthogonal to the receivers, which are placed in the middle of the surface in a tetrahedron configuration. Each of these lines is actually a plane along one of the surfaces of the tetrahedron. The 100m section shows a distinct triangle in the centre where the ambiguity planes have moved farther apart.

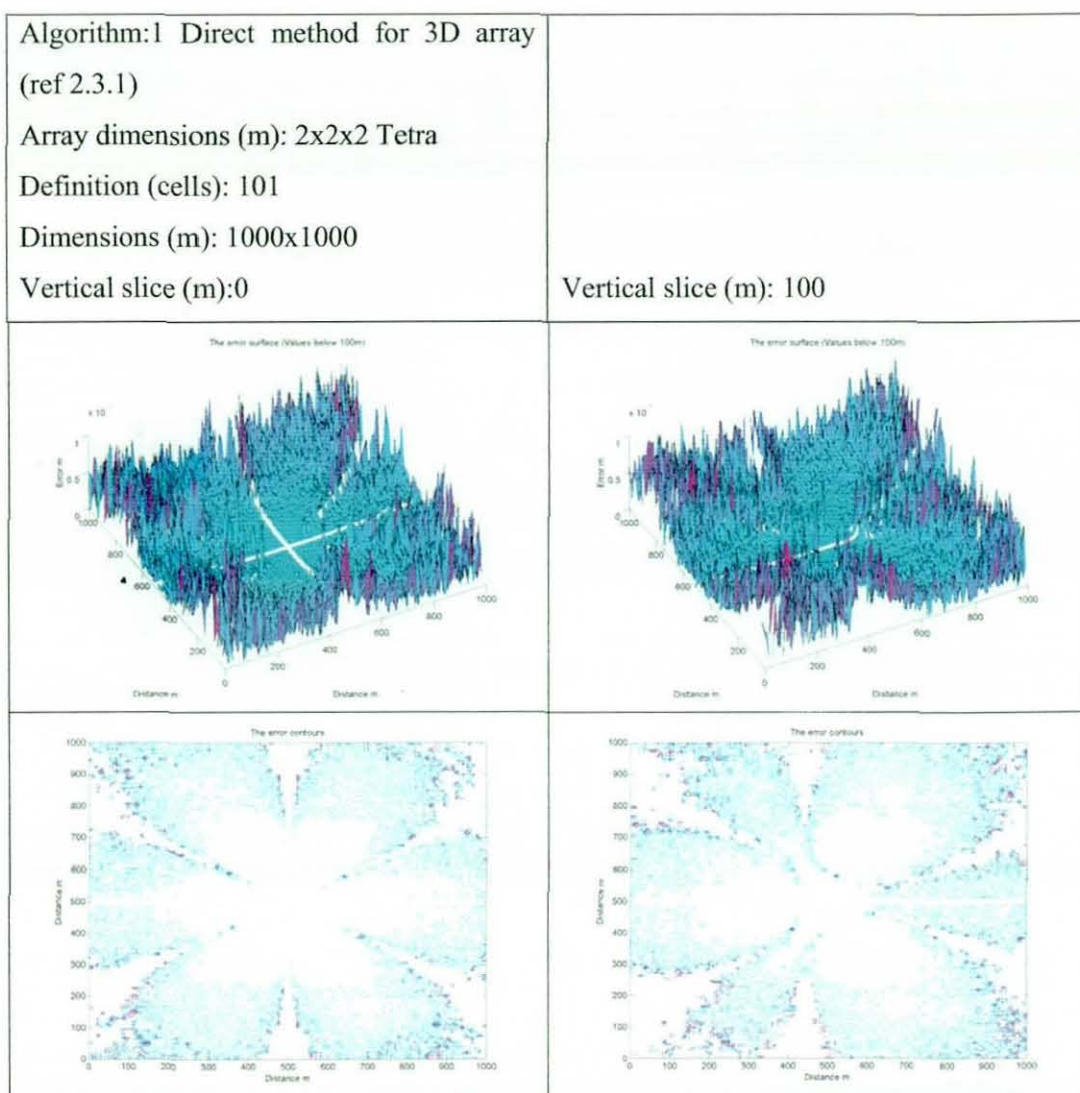


FIGURE 3.3-1B ERRORS IN ALGORITHM 1 DUE TO COMPUTER LIMITATIONS FOR A 2M ARRAY

These diagrams serve to prove the algorithm is working and the limitations due to the algorithm, the PC and software simulation. In effect, this is the best we can expect from the algorithm.

To check the effect of different sizes of receiver spacing the spacing is altered and we again perform a baseline simulation (Figure 3.3-1B). In this case we should expect to see a similar pattern of ambiguities and the error will be increased. As expected, Figure 3.3.1B shows a similar ambiguity pattern and the maximum error is 10^{-7} , a factor of 10

different from the 20m-spaced array. The 100m section shows three distinct lobes forming. If we now decrease the array further we should observe a similar trend (Figure 3.3-1C).

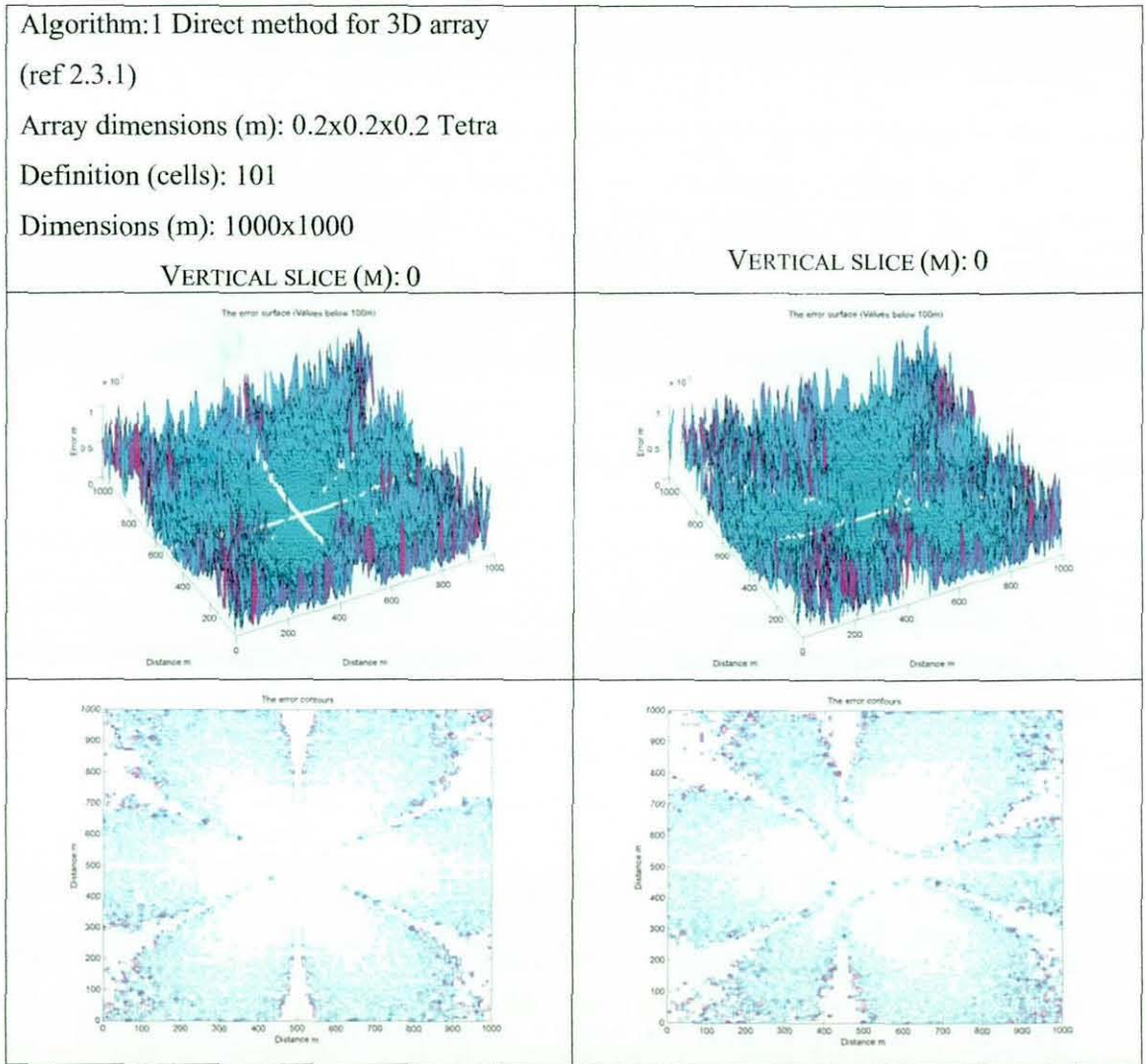


FIGURE 3.3-1C ERRORS IN ALGORITHM 1 DUE TO COMPUTER LIMITATIONS, 0.2M ARRAY

Again as expected, the maximum error is 10^{-5} and in the 100m section the ambiguous areas are larger. These simulations contain no element of frequency, so the lobe behaviour is not connected to phased array theory, but is a true feature of the algorithm.

To create a more realistic impression of the performance of the algorithm, it is necessary to adjust the parameters thought to have the largest effect on its output. These are adjusted one at a time to see the effect.

3.3.1.2 TIMING ERROR

The most likely parameter to have a significant effect on the algorithm is the timing errors. These errors are most likely to be caused by time quantisation, i.e. sample rates of the data collection systems. If a system collects data at a rate of 1kHz, the maximum timing accuracy will be 1ms. The simulations in Figures 3.3-2 A-D show the positional error caused by sample rates of 100MHz, 10 MHz and 100 kHz in spatial slices around the array corresponding to relative depths of 0m and 100m.

Figure 3.3-2A shows the best case for a 2m array (other array sizes can be found in Appendix B3). Here a sampling rate of 100MHz has been used, giving a maximum definition of $\pm 0.005\mu\text{s}$

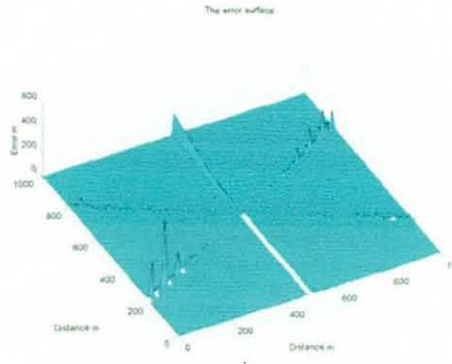
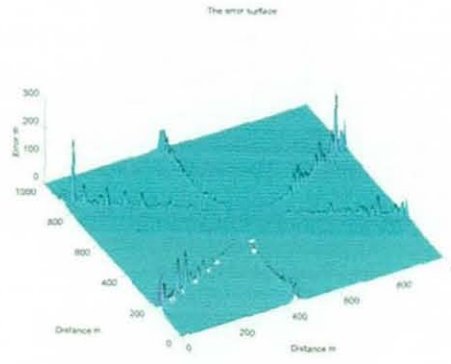
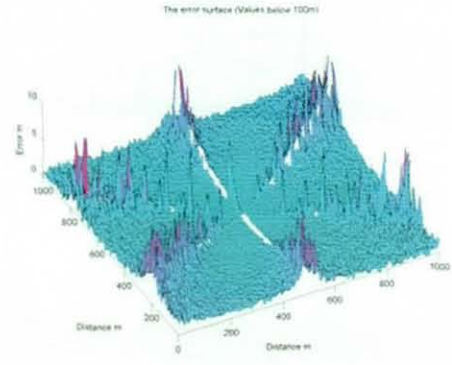
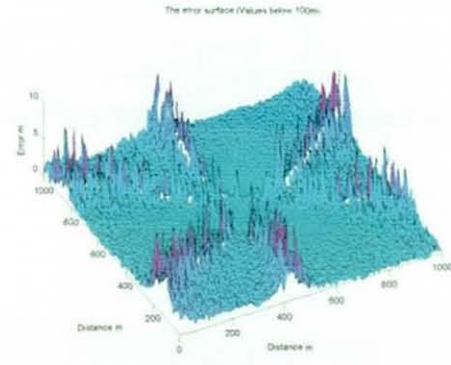
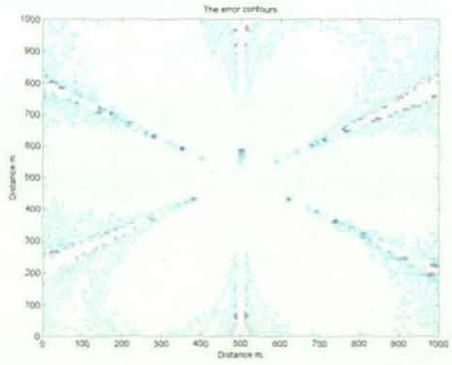
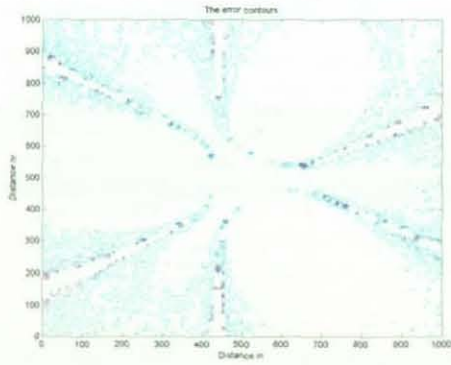
<p>Algorithm: 1 Direct method for 3D array (ref 2.3.1)</p> <p>Array dimensions (m): 2x2x1</p> <p>Definition (cells): 101</p> <p>Dimensions (m): 1000x1000</p> <p>Vertical slice (m): 0</p> <p>Timing error (μs): 0.001</p>	<p>Algorithm: 1 Direct method for 3D array (ref 2.3.1)</p> <p>Array dimensions (m): 2x2x1</p> <p>Definition (cells): 101</p> <p>Dimensions (m): 1000x1000</p> <p>Vertical slice (m): 100</p> <p>Timing error (μs): 0.001</p>
	
	
	

FIGURE 3.3-2A ERRORS IN ALGORITHM 1 (2M) DUE TO TIMING ERRORS, SAMPLING AT 100MHZ

The results of this simulation (Figure 3.3-2A) look similar to those of Figure 3.3-1A, but the maximum errors are larger, typically 0.5m at 500m (getting larger near the ambiguities). In this case the x-axis ambiguity is not obvious, possibly due to quantisation of the simulation. If we now decrease the sampling rate by a factor of 10 to 10MHz ($\pm 0.05\mu\text{s}$) we get Figure 3.3-2B.

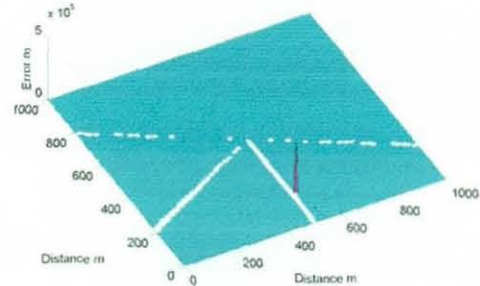
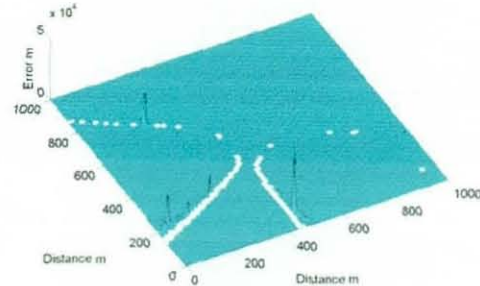
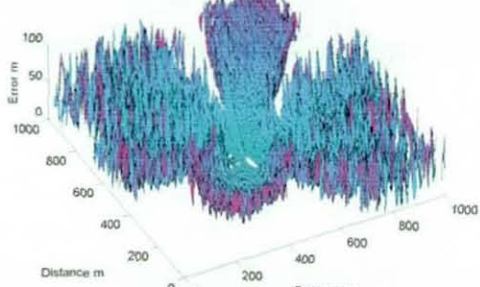
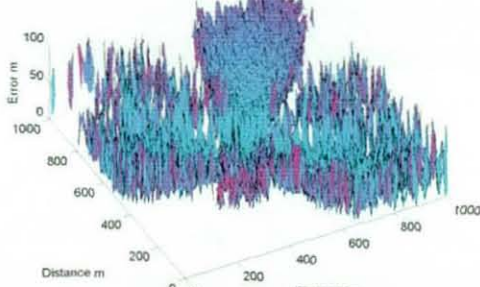
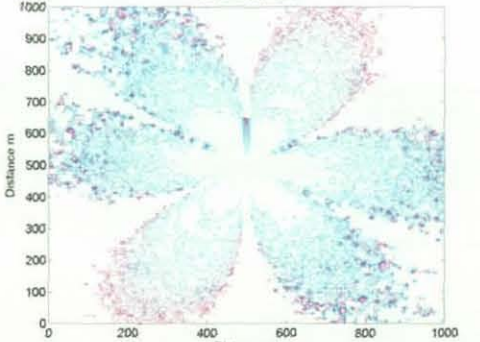
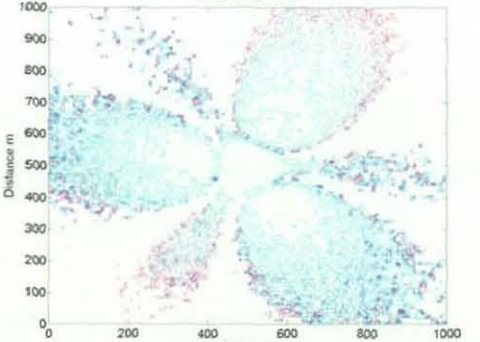
<p>Algorithm:1 Direct method for 3D array (ref 2.3.1)</p> <p>Array dimensions (m): 2x2x1</p> <p>Definition (cells): 101</p> <p>Dimensions (m): 1000x1000</p> <p>Vertical slice (m): 0</p> <p>Timing error (μs): 0.10</p>	<p>Algorithm:1 Direct method for 3D array (ref 2.3.1)</p> <p>Array dimensions (m): 2x2x1</p> <p>Definition (cells): 101</p> <p>Dimensions (m): 1000x1000</p> <p>Vertical slice (m): 100</p> <p>Timing error (μs): 0.10</p>
<p>The error surface</p> 	<p>The error surface</p> 
<p>The error surface (Values below 100m)</p> 	<p>The error surface (Values below 100m)</p> 
<p>The error contours</p> 	<p>The error contours</p> 

FIGURE 3.3-2B ERRORS IN ALGORITHM 1 (2M) DUE TO TIMING ERRORS, SAMPLING AT 10MHZ

As can be seen the error has risen by a factor of 100 and the ambiguities (defined in this case as errors greater than 100m) have grown. Again, decreasing the sampling frequency to 100kHz ($\pm 5\mu\text{s}$) we get Figure 3.3-2C.

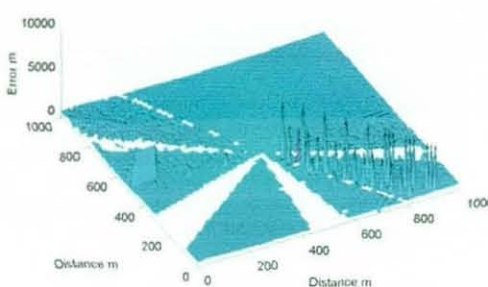
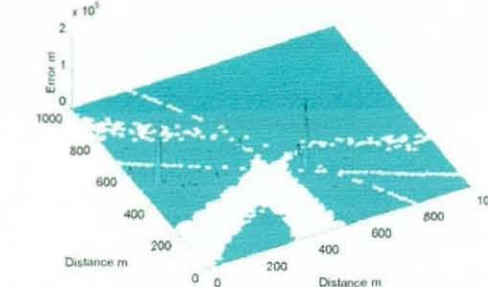
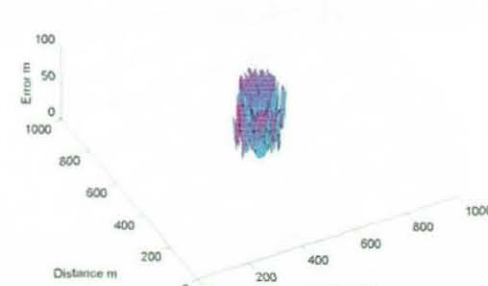
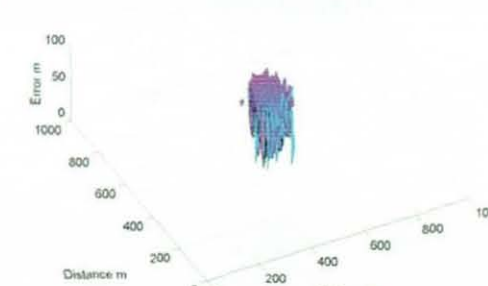
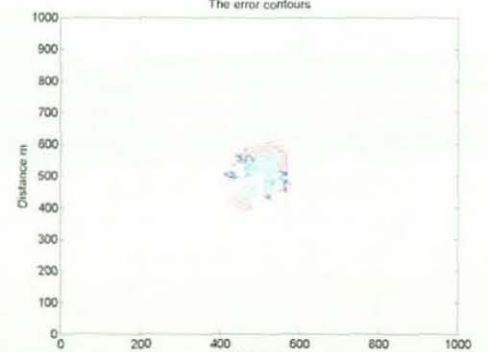
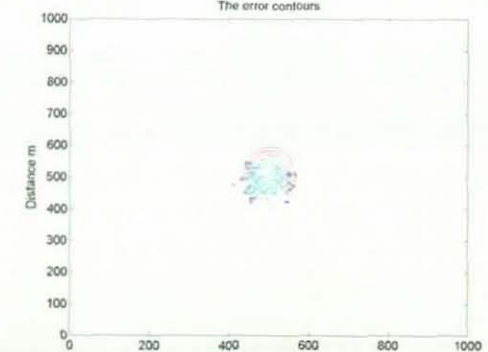
<p>Algorithm: 1 Direct method for 3D array (ref 2.3.1)</p> <p>Array dimensions (m): 2x2x1</p> <p>Definition (cells): 101</p> <p>Dimensions (m): 1000x1000</p> <p>Vertical slice (m): 0</p> <p>Timing error (μs): 10</p>	<p>Algorithm: 1 Direct method for 3D array (ref 2.3.1)</p> <p>Array dimensions (m): 2x2x1</p> <p>Definition (cells): 101</p> <p>Dimensions (m): 1000x1000</p> <p>Vertical slice (m): 100</p> <p>Timing error (μs): 10</p>
<p>The error surface</p> 	<p>The error surface</p> 
<p>The error surface (Values below 100m)</p> 	<p>The error surface (Values below 100m)</p> 
<p>The error contours</p> 	<p>The error contours</p> 

FIGURE 3.3-2C ERRORS IN ALGORITHM 1 (2M) DUE TO TIMING ERRORS SAMPLING AT 100 KHz
Chapter 3 Simulation Page 88

This time the error has risen so much that the resultant solutions are too much in error to use. This implies the accuracy of the algorithm with sampling frequency is exponential, as found in previous simulations of this algorithm [2].

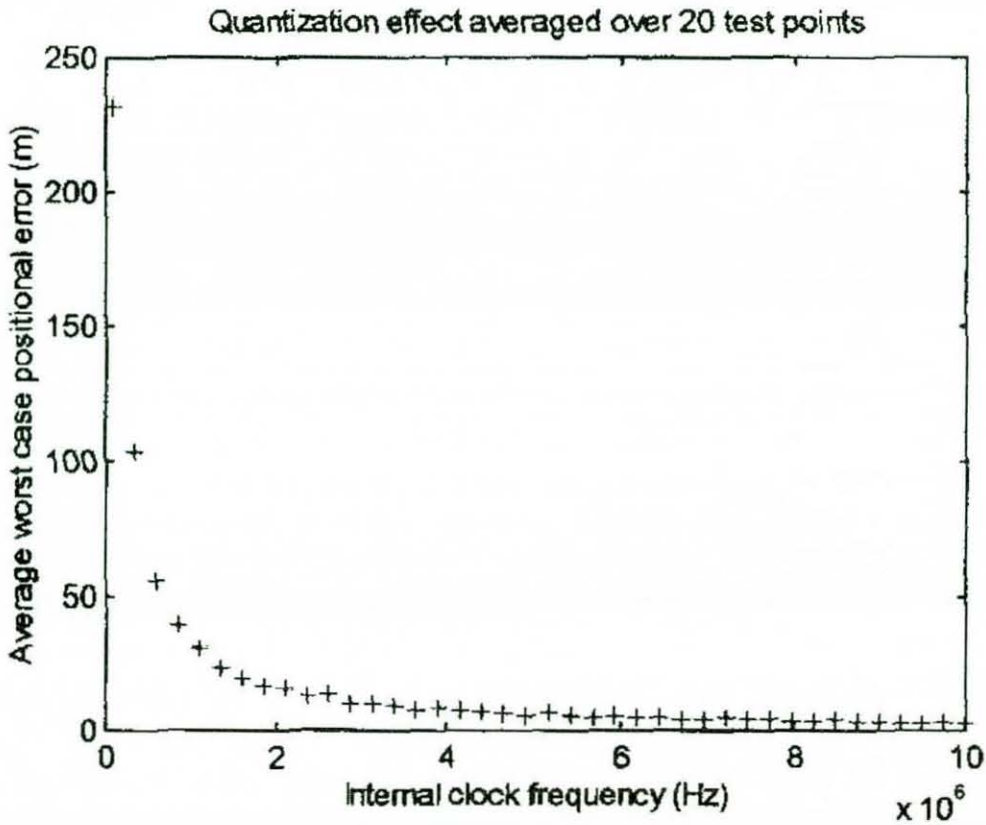


FIGURE 3.3-3 AVERAGE WORST-CASE POSITIONAL ERROR USING A 3M HYDROPHONE ARRAY AT RANGES 1-200M [2]

3.3.1.3 RECEIVER POSITIONAL ERRORS

Another factor likely to have an effect is the positional error of the receivers, since the algorithm relies on an accurate knowledge of their positions. The resulting computed errors are shown in Figures 3.3-4A to 3.3-4C.

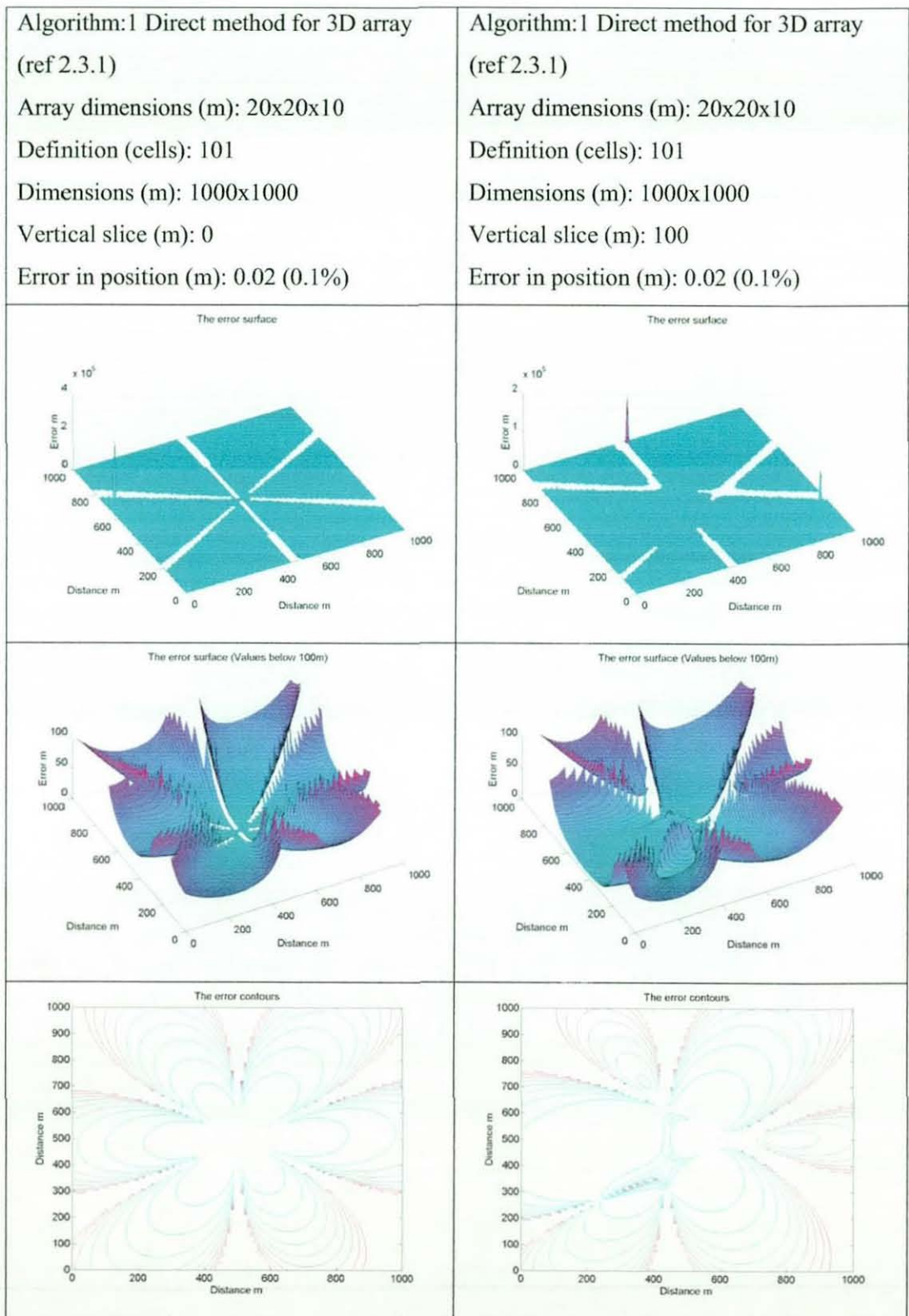


FIGURE 3.3-4A ERRORS CAUSED BY 0.1% ERROR IN RECEIVER POSITION WITH 20M ARRAY

Figure 3.3-4A shows the familiar ambiguities, but there is now an obvious error due to the positional error of the receivers. In this case all the receivers have been moved by a similar amount such that there is no exaggeration in any particular direction as would be seen if only one receiver were to be moved. Even at this small error margin (0.1%) the error is large, showing that the algorithm is sensitive to this kind of error. If we now increase the error we would expect the ambiguities to quickly grow (Figure 3.3-4B).

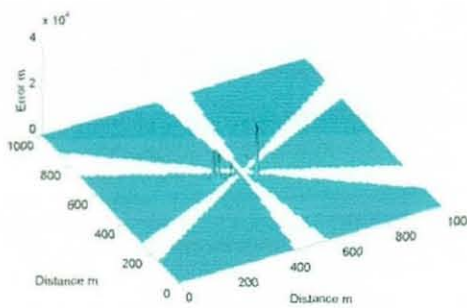
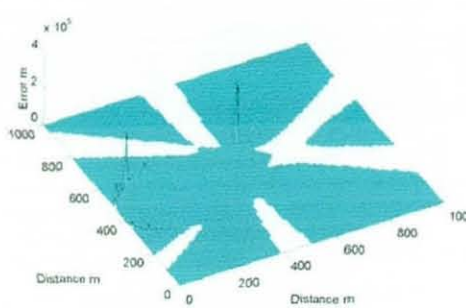
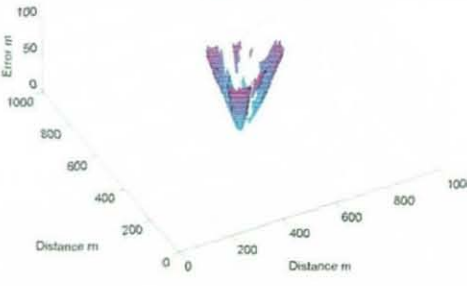
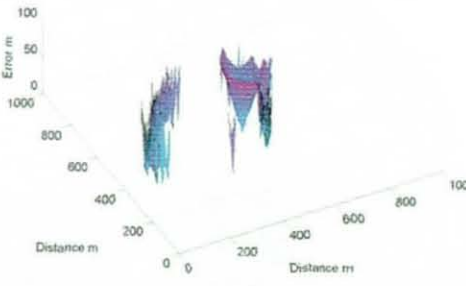
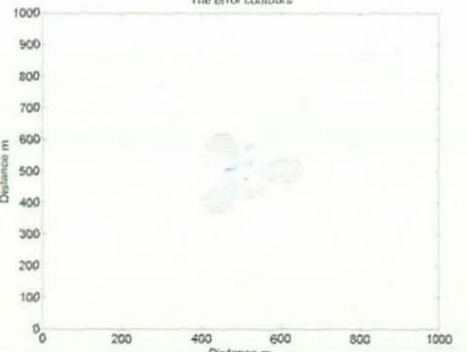
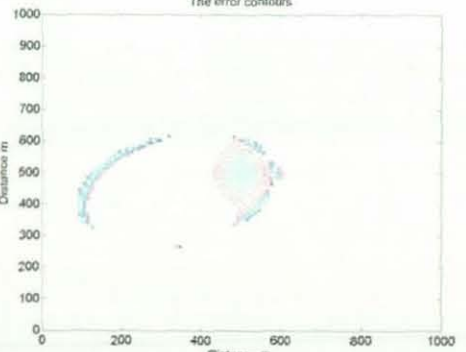
<p>Algorithm: 1 Direct method for 3D array (ref 2.3.1)</p> <p>Array dimensions (m): 2x2x1</p> <p>Definition (cells): 101</p> <p>Dimensions (m): 1000x1000</p> <p>Vertical slice (m): 0</p> <p>Error in Position (m): 0.02 (1%)</p>	<p>Algorithm: 1 Direct method for 3D array (ref 2.3.1)</p> <p>Array dimensions (m): 2x2x1</p> <p>Definition (cells): 101</p> <p>Dimensions (m): 1000x1000</p> <p>Vertical slice (m): 100</p> <p>Error in position (m): 0.02 (1%)</p>
<p>The error surface</p> 	<p>The error surface</p> 
<p>The error surface (Values below 100m)</p> 	<p>The error surface (Values below 100m)</p> 
<p>The error contours</p> 	<p>The error contours</p> 

FIGURE 3.3-4B ERRORS CAUSED BY 1% ERROR IN RECEIVER POSITION WITH 2M ARRAY
 Chapter 3 Simulation Page 92

Figure 3.3-4B shows, as expected, errors that quickly rise to over 100m, serving to prove that this algorithm is extremely sensitive to positional errors. Further increasing this error may seem pointless but is included to show that this is a real trend.

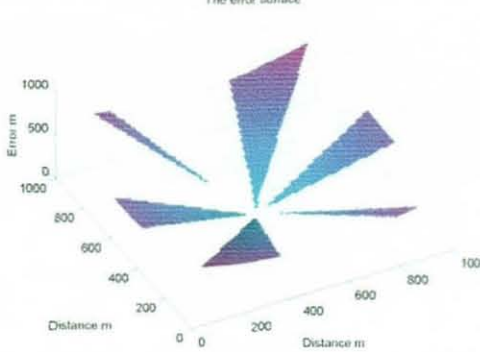
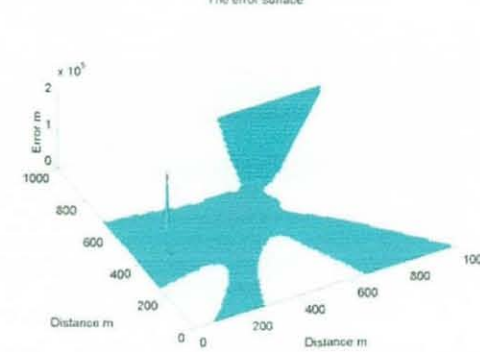
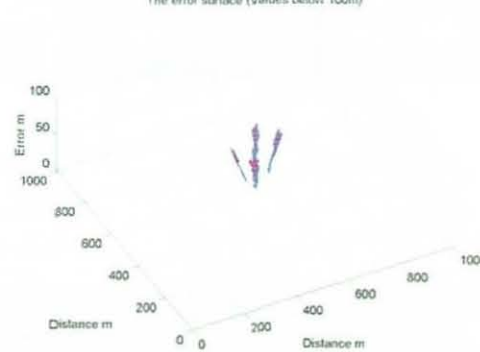
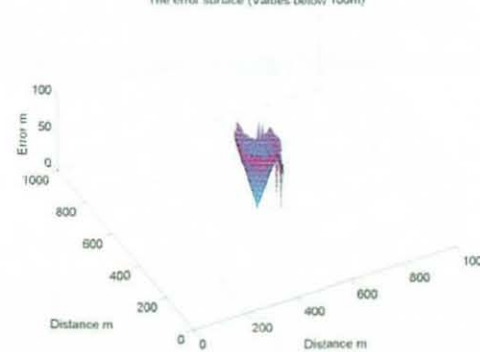
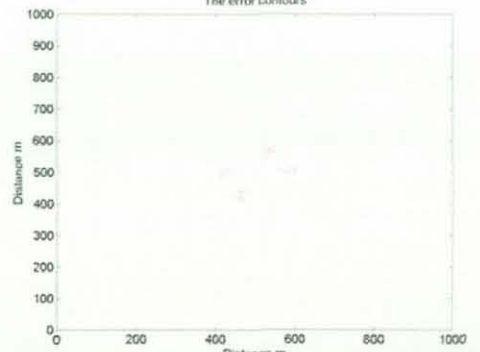
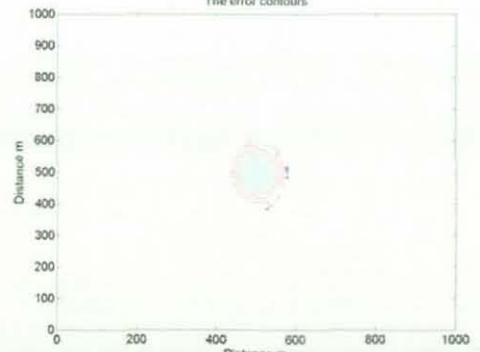
<p>Algorithm: 1 Direct method for 3D array (ref 2.3.1)</p> <p>Array dimensions (m): 2x2x1</p> <p>Definition (cells): 101</p> <p>Dimensions (m): 1000x1000</p> <p>Vertical slice (m): 0</p> <p>Error in Position (m): 0.2 (10%)</p>	<p>Algorithm: 1 Direct method for 3D array (ref 2.3.1)</p> <p>Array dimensions (m): 2x2x1</p> <p>Definition (cells): 101</p> <p>Dimensions (m): 1000x1000</p> <p>Vertical slice (m): 100</p> <p>Error in Position (m): 0.2 (10%)</p>
<p>The error surface</p> 	<p>The error surface</p> 
<p>The error surface (Values below 100m)</p> 	<p>The error surface (Values below 100m)</p> 
<p>The error contours</p> 	<p>The error contours</p> 

FIGURE 3.3-4C ERRORS CAUSED BY 10% ERROR IN RECEIVER POSITION WITH 2M ARRAY

3.3.1.4 ERRORS DUE TO THE VELOCITY PROFILE

If the array is close to the surface and tracking a source some distance below, or vice versa, the change in the velocity of sound in the water cause the errors shown in Figure 3.3-5 A-D.

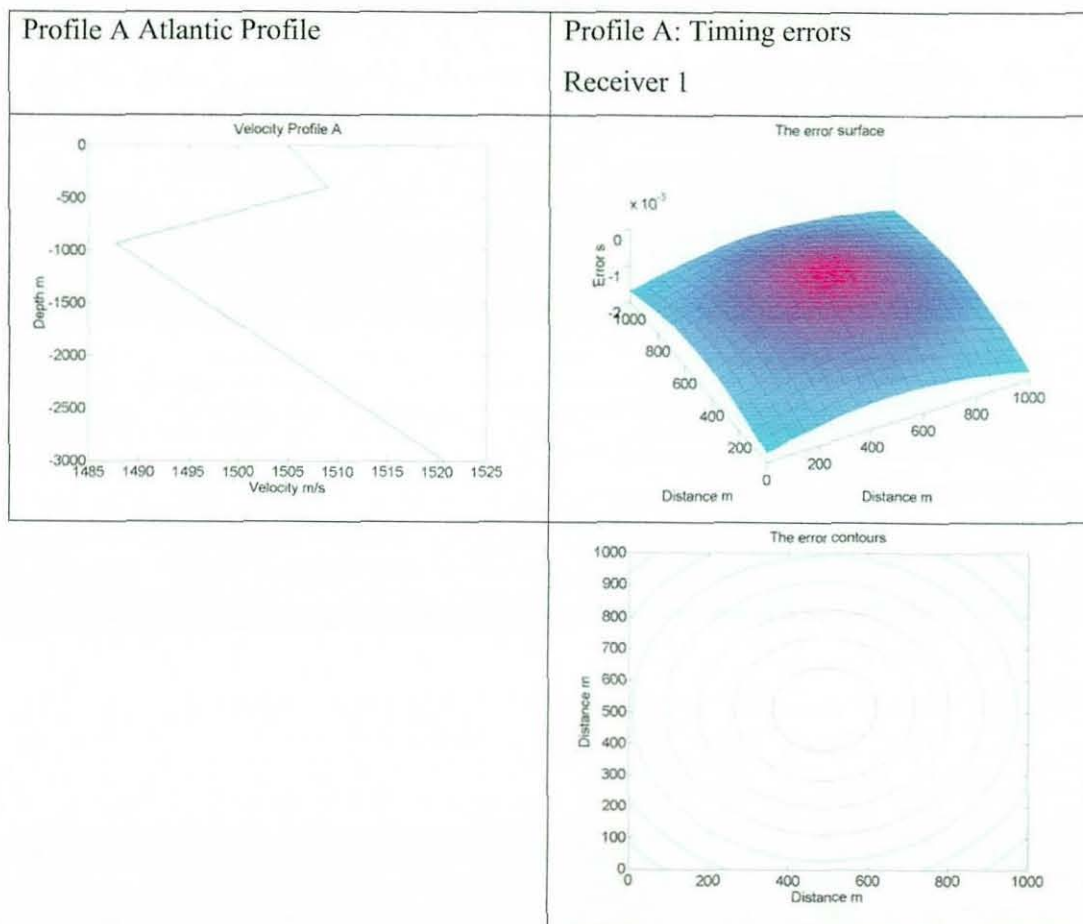


FIGURE 3.3-5A ERRORS CAUSED BY CHANGES IN SOUND VELOCITY THROUGH THE WATER COLUMN, PROFILE A

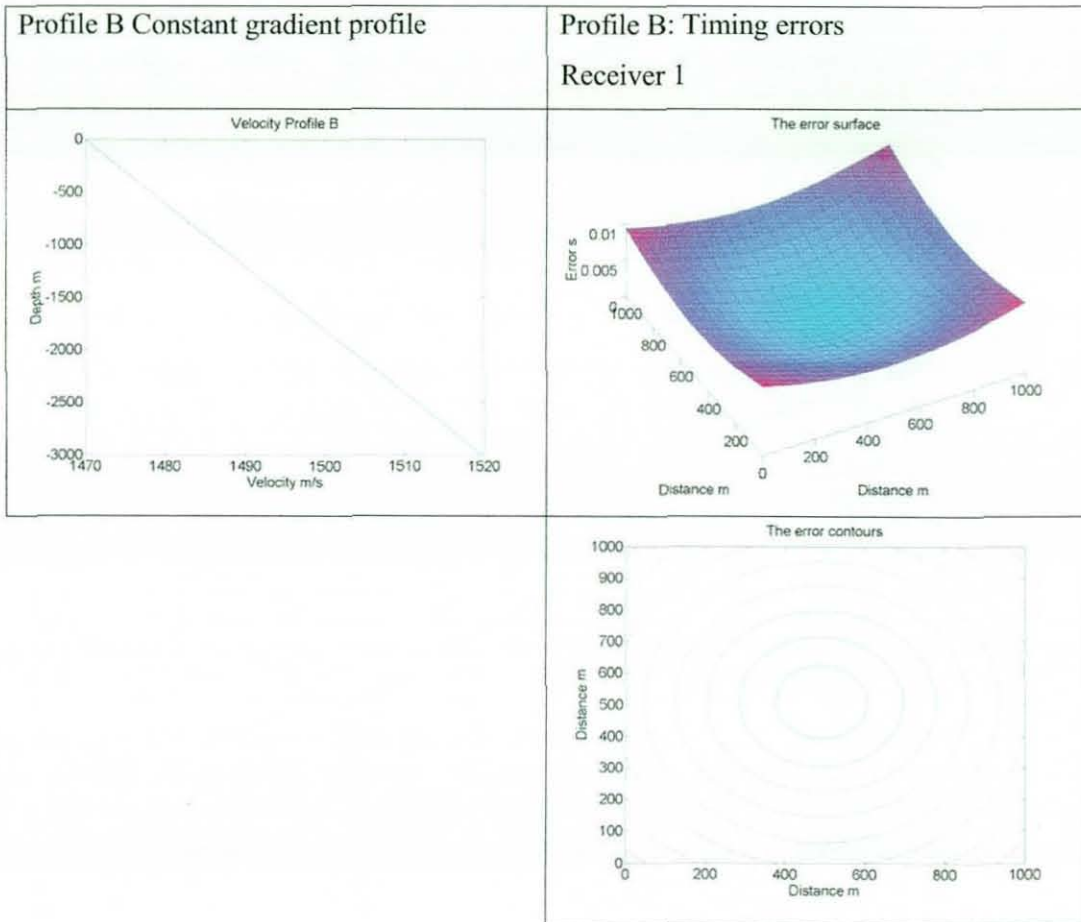


FIGURE 3.3-5B ERRORS CAUSED BY CHANGES IN SOUND VELOCITY THROUGH THE WATER COLUMN, PROFILE B

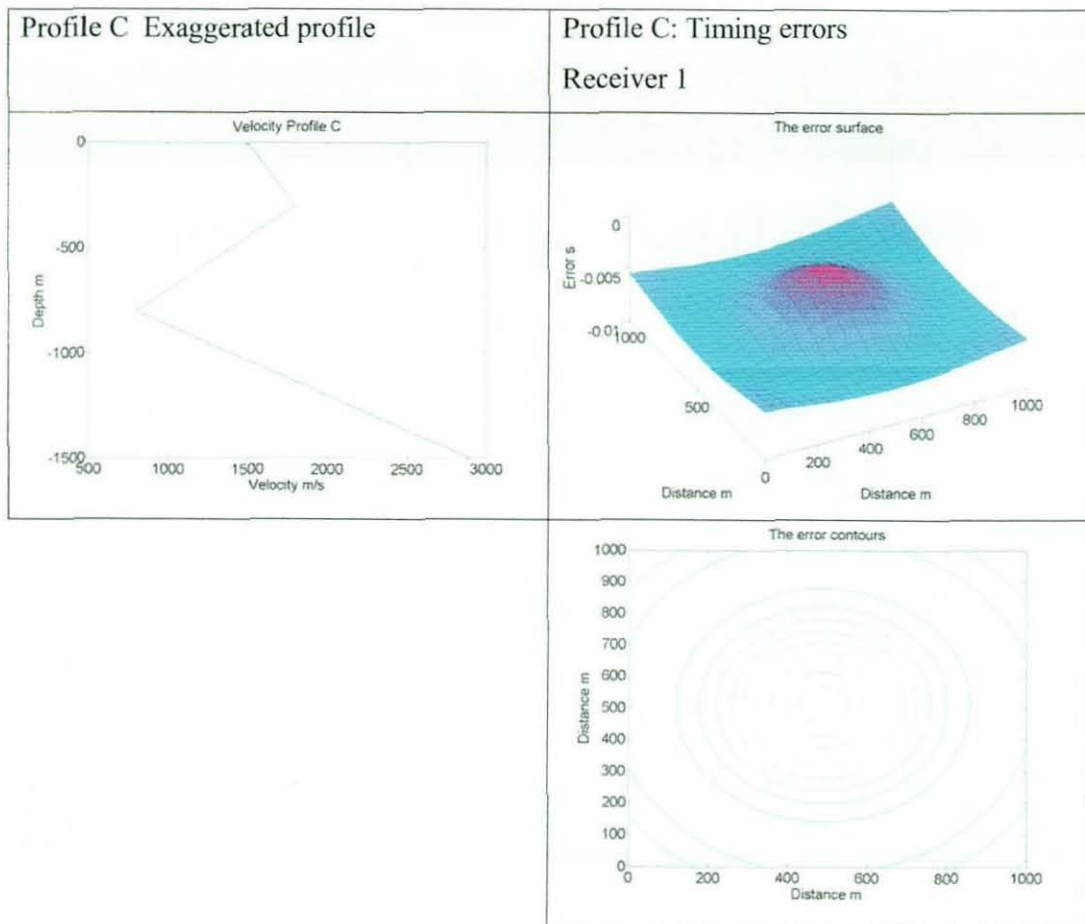


FIGURE 3.3-5C ERRORS CAUSED BY CHANGES IN SOUND VELOCITY THROUGH THE WATER COLUMN, PROFILE C

To prove that the algorithms calculating these errors are correct a constant velocity profile is presented to the simulation. The errors resulting show the limit of the computers calculations.

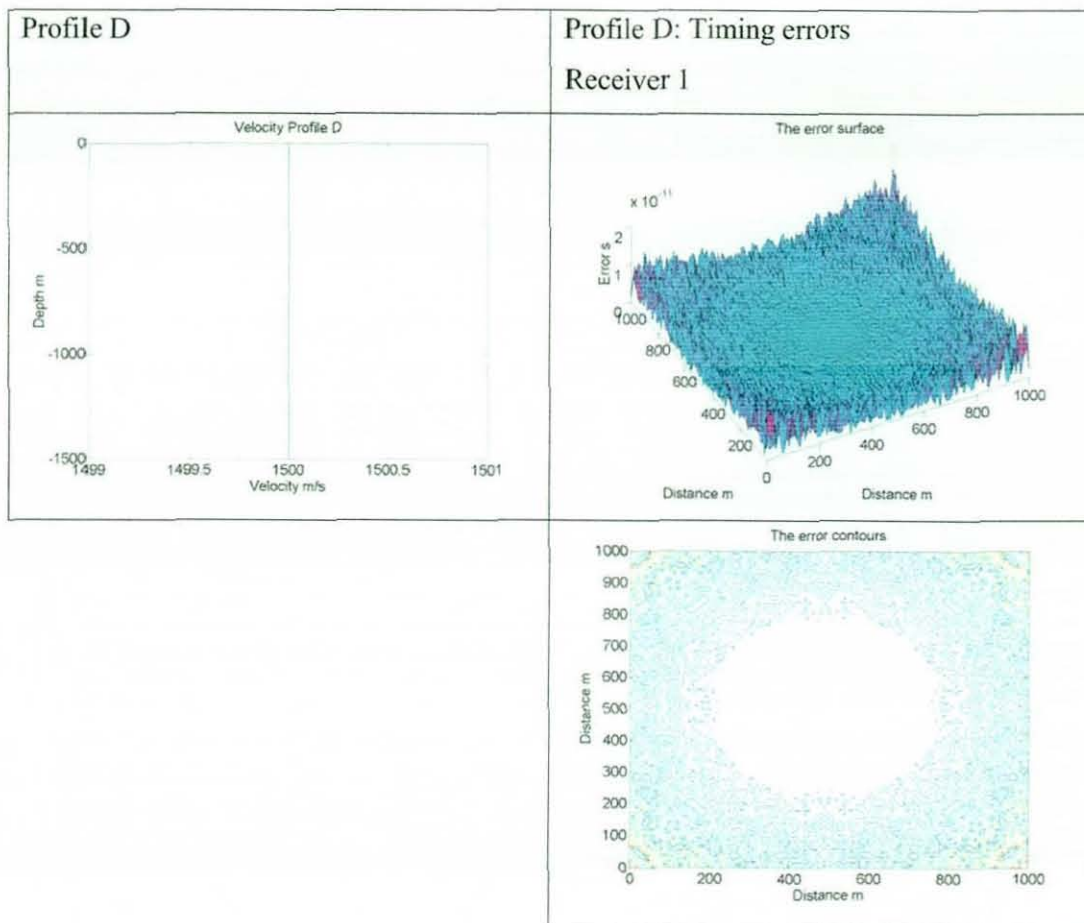


FIGURE 3.3-5D ERRORS CAUSED BY CHANGES IN SOUND VELOCITY THROUGH THE WATER COLUMN, PROFILE D

The values given by these simulations can be used in collaboration with the simulations for time and positional errors to give the error factors. To demonstrate the effect of these errors, an algorithm has been chosen and simulated with these errors incorporated. Algorithm 2 was chosen and the results of the velocity profile simulation can be seen in section 3.3.2.4.

3.3.2 ABSOLUTE METHOD FOR A FLAT ARRAYS (METHOD2)

As shown in section 2.3.2 the position of a source with respect to a symmetrical flat array can be calculated using the following equations.

$$x = \frac{d_{12}d_{34}(d_{34}d_{31} - d_{12}d_{42} + 2d_{31}d_{42} - d_{31}^2 - 2d_{31}d_{12} + d_{42}^2)}{4m(d_{31}d_{12} - d_{42}d_{34})} \quad (\text{from 2-65})$$

$$y = \frac{d_{31}d_{42}(d_{12}d_{42} - d_{34}d_{31} + 2d_{42}d_{34} - d_{12}^2 - 2d_{12}d_{34} + d_{34}^2)}{4n(d_{31}d_{12} - d_{42}d_{34})} \quad (\text{from 2-66})$$

and

$$|z| = \left[\left(\frac{4mx - d_{12}^2}{2d_{12}} \right)^2 - (x - m)^2 - (y - n)^2 \right]^{\frac{1}{2}} \quad (\text{from 2-67})$$

Again we will simulate the algorithm, inserting errors for timing, position and velocity profile.

3.3.2.1 NO ERRORS

With no errors in the parameters other than the limitation of the processor a positional error plot can be calculated. Figure 3.3-6A shows the positional errors for this algorithm when the receivers are placed in a single plane. The errors are in the region 10^{-9} and the x- and y-axis ambiguities can be clearly observed. In this case, the errors are due to time differences equating to zero, causing the equation set to fail.

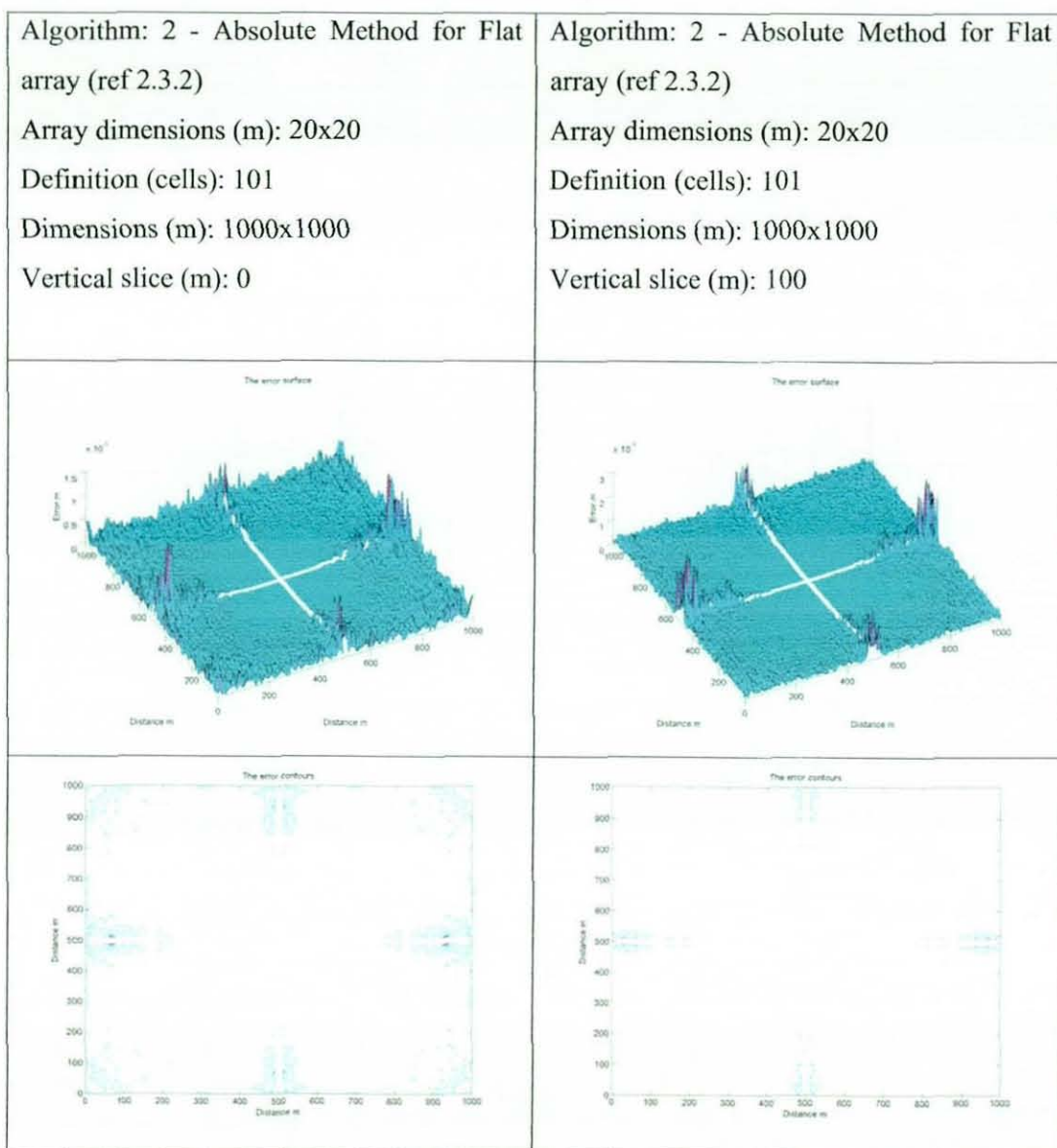


FIGURE 3.3-6A ERRORS IN ALGORITHM 2 DUE TO COMPUTER LIMITATIONS, 20M ARRAY
 If we now reduce the size of the array by a factor of 10 we get maximum errors in the region of 10^{-7} .

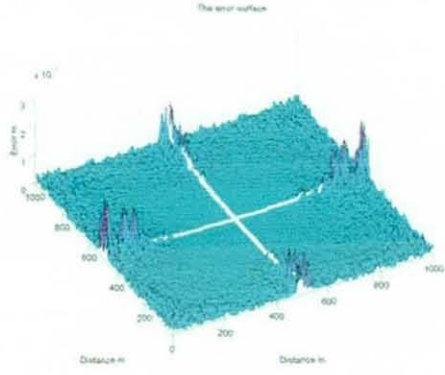
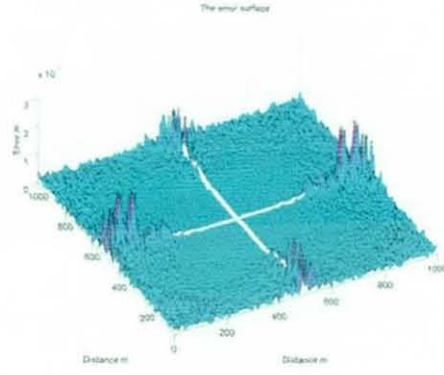
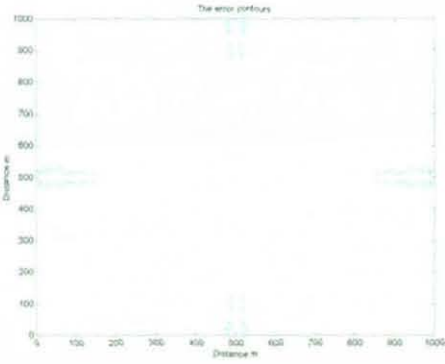
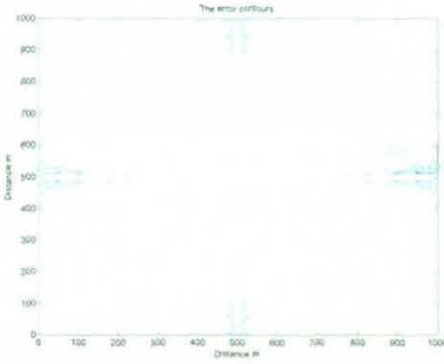
<p>Algorithm: 2 - Absolute Method for Flat array (ref 2.3.2)</p> <p>Array dimensions (m): 2x2x1</p> <p>Definition (cells): 101</p> <p>Dimensions (m): 1000x1000</p> <p>Vertical slice (m): 0</p>	<p>Algorithm: 2 - Absolute Method for Flat array (ref 2.3.2)</p> <p>Array dimensions (m): 2x2x1</p> <p>Definition (cells): 101</p> <p>Dimensions (m): 1000x1000</p> <p>Vertical slice (m): 100</p>
	
	

FIGURE 3.3-6B ERRORS IN ALGORITHM 2 DUE TO COMPUTER LIMITATIONS, 2M ARRAY

The shape of the error surface, as would be expected, is symmetrical about the four receivers, and the middle area out to a radius of 200m shows very little effect. Further reducing the array size by a factor of 10 has no effect on the error surface, but the maximum error increases to 10^{-5} . As there is no receiver out of the plane, the error surface pattern is very similar for the 100m section.

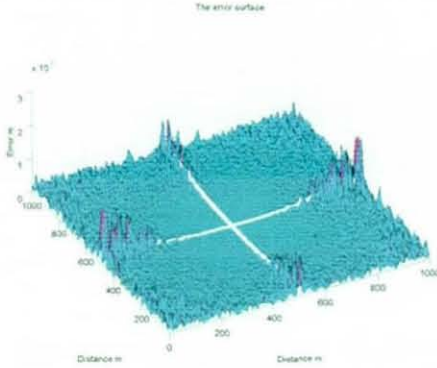
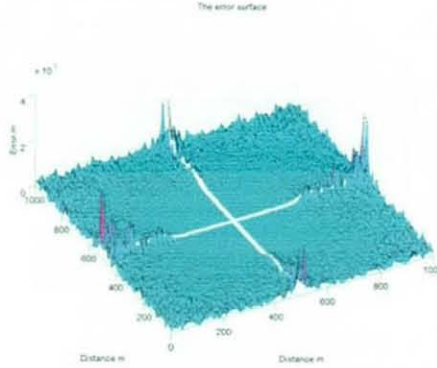
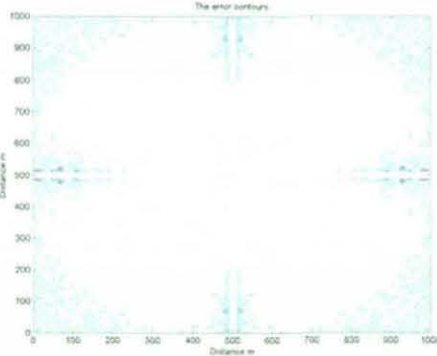
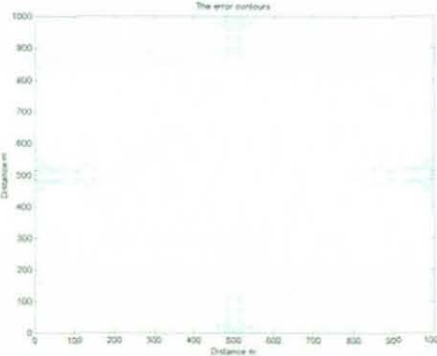
<p>Algorithm: 2 - Absolute Method for Flat array (ref 2.3.2)</p> <p>Array dimensions (m): 0.2x0.2x0.1</p> <p>Definition (cells): 101</p> <p>Dimensions (m): 1000x1000</p> <p>Vertical slice (m): 0</p>	<p>Algorithm: 2 - Absolute Method for Flat array (ref 2.3.2)</p> <p>Array dimensions (m): 0.2x0.2x0.1</p> <p>Definition (cells): 101</p> <p>Dimensions (m): 1000x1000</p> <p>Vertical slice (m): 100</p>
 <p>The error surface plot shows a 3D surface of error values over a 1000m x 1000m distance. The vertical axis is labeled 'Error' with a multiplier of $\times 10^{-1}$ and ranges from 0 to 3. The surface is highly irregular and noisy, with a maximum error value of approximately 3.0.</p>	 <p>The error surface plot shows a 3D surface of error values over a 1000m x 1000m distance. The vertical axis is labeled 'Error' with a multiplier of $\times 10^{-1}$ and ranges from 0 to 4. The surface is highly irregular and noisy, with a maximum error value of approximately 4.0.</p>
 <p>The error contours plot shows a 2D contour map of error values over a 1000m x 1000m distance. The vertical axis is labeled 'Distance m' and ranges from 0 to 1000. The horizontal axis is labeled 'Distance m' and ranges from 0 to 1000. The plot shows a dense field of light blue contours, indicating high error values across the entire area.</p>	 <p>The error contours plot shows a 2D contour map of error values over a 1000m x 1000m distance. The vertical axis is labeled 'Distance m' and ranges from 0 to 1000. The horizontal axis is labeled 'Distance m' and ranges from 0 to 1000. The plot shows a sparse field of light blue contours, indicating significantly lower error values compared to the 0m vertical slice.</p>

FIGURE 3.3-6C ERRORS IN ALGORITHM 2 DUE TO COMPUTER LIMITATIONS, 0.2M ARRAY

In summary, the size of the array seems to have little effect on the shape of the error surface, but has a factor of at least ten times the change in size in accuracy.

3.3.2.2 TIMING ERRORS

Again, errors are introduced to the parameters of the algorithm. To allow comparison the same errors are introduced as in section 3.3.1, starting with 100MHz

Algorithm: 2 - Absolute Method for Flat array (ref 2.3.2)

Array dimensions (m): 2x2x1

Definition (cells): 101

Dimensions (m): 1000x1000

Vertical slice (m): 0

Timing error (μ s): 0.001

Algorithm: 2 - Absolute Method for Flat array (ref 2.3.2)

Array dimensions (m): 2x2x1

Definition (cells): 101

Dimensions (m): 1000x1000

Vertical slice (m): 100

Timing error (μ s): 0.001

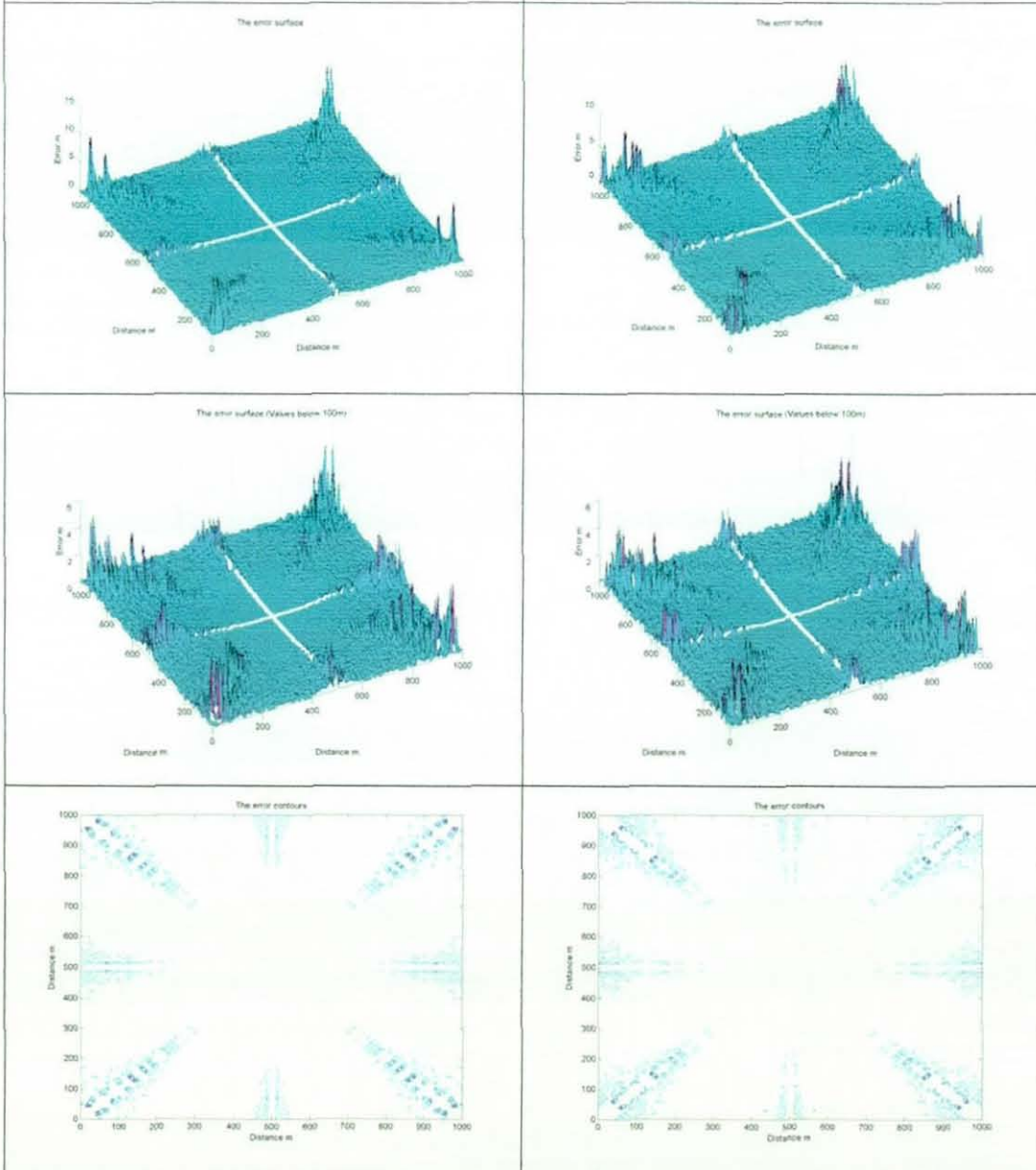


FIGURE 3.3-7A ERRORS IN ALGORITHM 2 (2M) DUE TO TIMING ERRORS, SAMPLING AT 100MHZ

Figure 3.3-7A shows a further ambiguity on the diagonals, which would be expected as this gives a time difference of zero on the diagonal pairs. The maximum error is in the region of 5m, although at the extremes this is in the region of 15m. Reducing the sampling rate to 10MHz gives Figure 3.3-7B. Here the error can be seen to be larger by a factor of 10, with the maximum error being approximately 50m at 500m. The diagonal ambiguities (set to be limited at 100m) are also much larger. Reducing the sample rate to 100kHz (Figure 3.3-7C) shows further increases in the error margin, to such effect that the ambiguous areas become dominant.

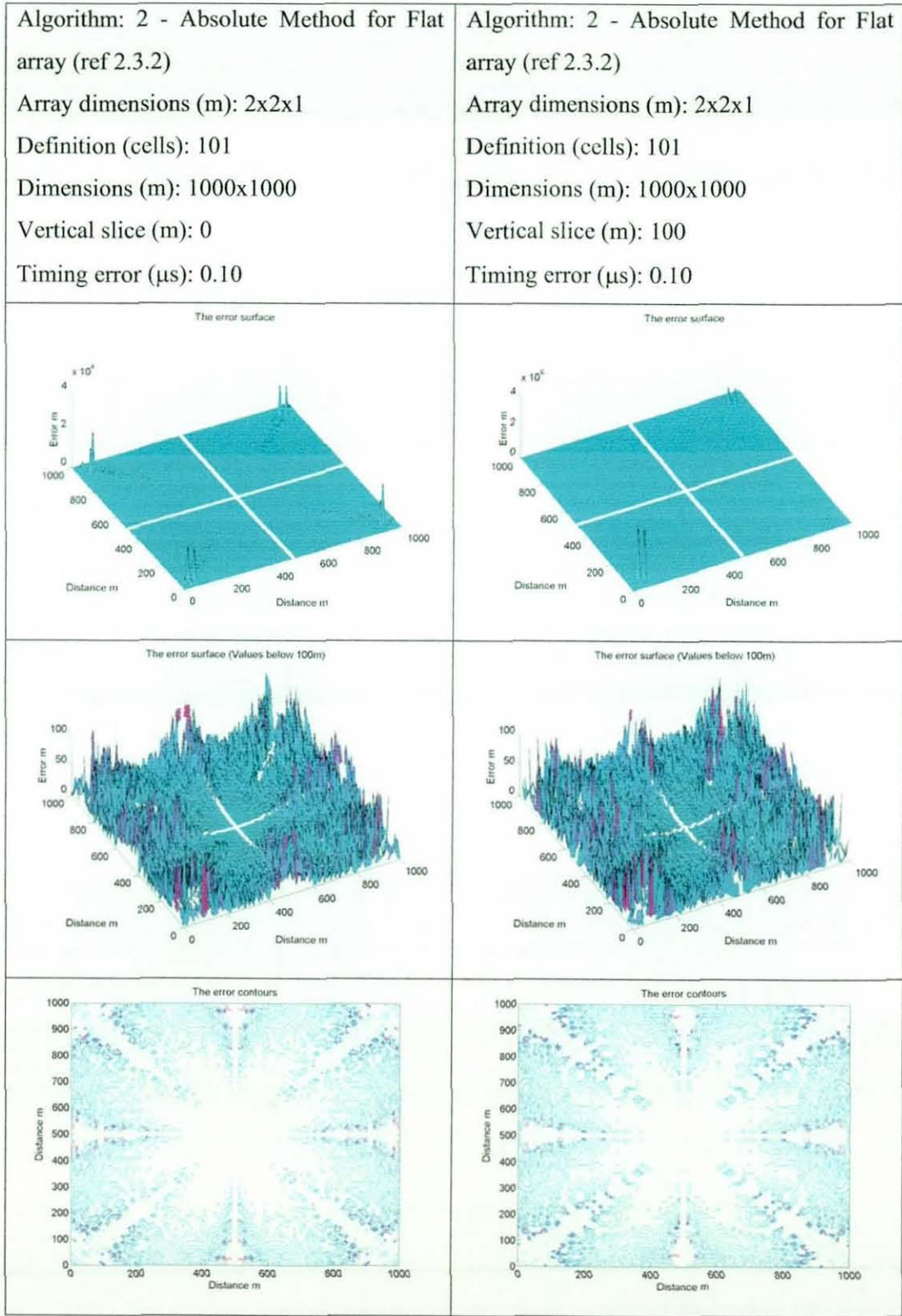


FIGURE 3.3-7B ERRORS IN ALGORITHM 2 (2M) DUE TO TIMING ERRORS, SAMPLING AT 10MHZ
 Chapter 3 Simulation Page 105

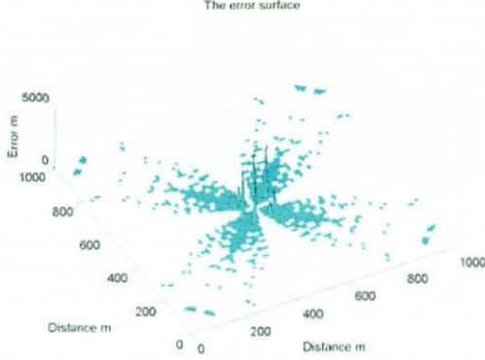
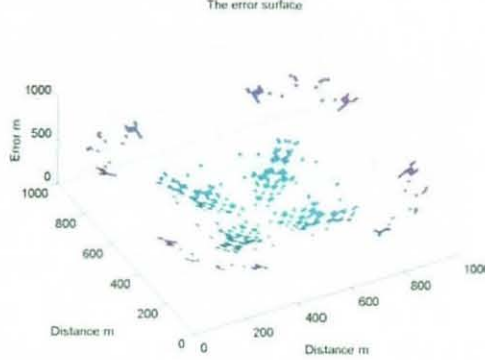
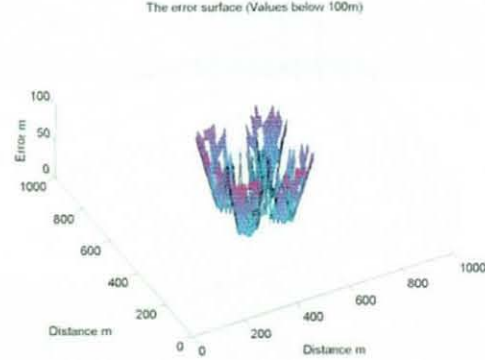
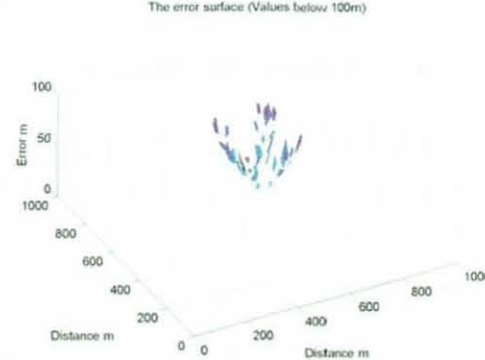
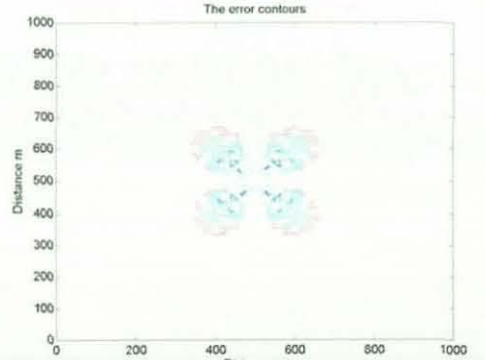
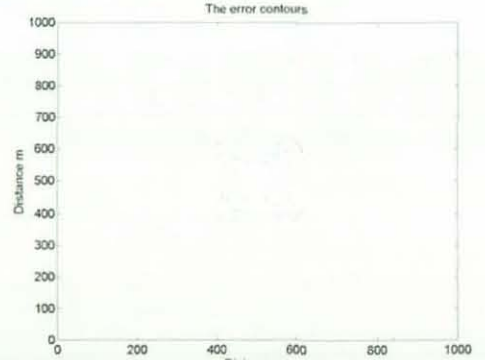
<p>Algorithm: 2 - Absolute Method for Flat array (ref 2.3.2)</p> <p>Array dimensions (m): 2x2x1</p> <p>Definition (cells): 101</p> <p>Dimensions (m): 1000x1000</p> <p>Vertical slice (m): 0</p> <p>Timing error (μs): 10</p>	<p>Algorithm: 2 - Absolute Method for Flat array (ref 2.3.2)</p> <p>Array dimensions (m): 2x2x1</p> <p>Definition (cells): 101</p> <p>Dimensions (m): 1000x1000</p> <p>Vertical slice (m): 100</p> <p>Timing error (μs): 10</p>
	
	
	

FIGURE 3.3-7C ERRORS IN ALGORITHM 2 (2M) DUE TO TIMING ERRORS, SAMPLING AT 100KHZ

3.3.2.3 RECEIVER POSITIONAL ERRORS

It is assumed that inserting an error in one receiver position will produce maximum error with this algorithm, as this will remove the symmetry upon which the algorithm is based. Placing an error comparable to those in section 3.3.1 (0.1%-10%) gives Figures 3.3-8A to 3.3-8C.

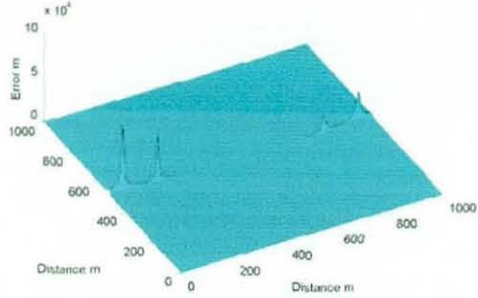
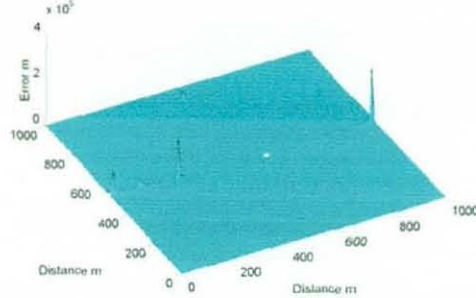
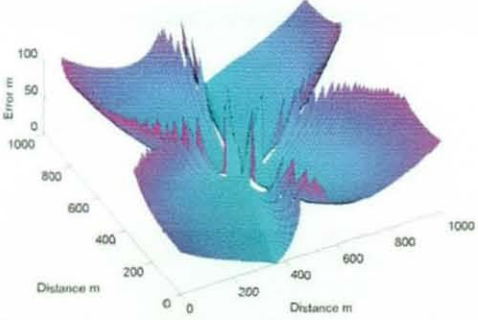
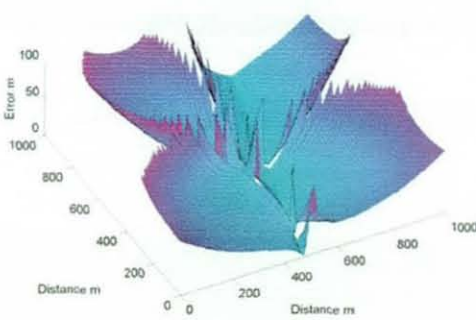
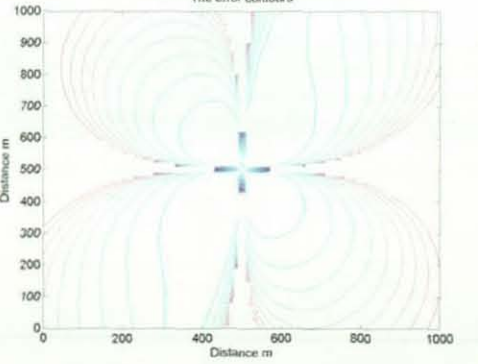
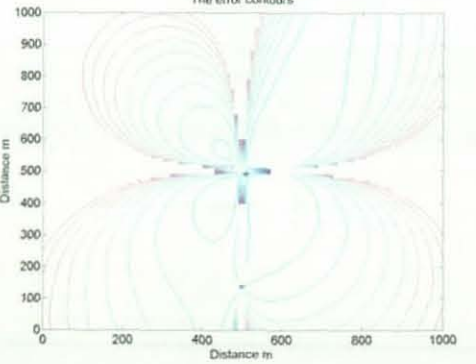
<p>Algorithm: 2 - Absolute Method for Flat array (ref 2.3.2)</p> <p>Array dimensions (m): 20x20</p> <p>Definition (cells): 101</p> <p>Dimensions (m): 1000x1000</p> <p>Vertical slice (m): 0</p> <p>Error in position (m): 0.02 (0.1%)</p>	<p>Algorithm: 2 - Absolute Method for Flat array (ref 2.3.2)</p> <p>Array dimensions (m): 20x20</p> <p>Definition (cells): 101</p> <p>Dimensions (m): 1000x1000</p> <p>Vertical slice (m): 100</p> <p>Error in position (m): 0.02 (0.1%)</p>
<p>The error surface</p> 	<p>The error surface</p> 
<p>The error surface (Values below 100m)</p> 	<p>The error surface (Values below 100m)</p> 
<p>The error contours</p> 	<p>The error contours</p> 

FIGURE 3.3-8A ERRORS CAUSED BY 0.1% ERROR IN RECEIVER POSITION WITH 20M ARRAY

Figure 3.3-8A shows the accuracy around the receiver in error reducing fastest (top left side of the diagrams). It can be expected that this will continue as the error is increased.

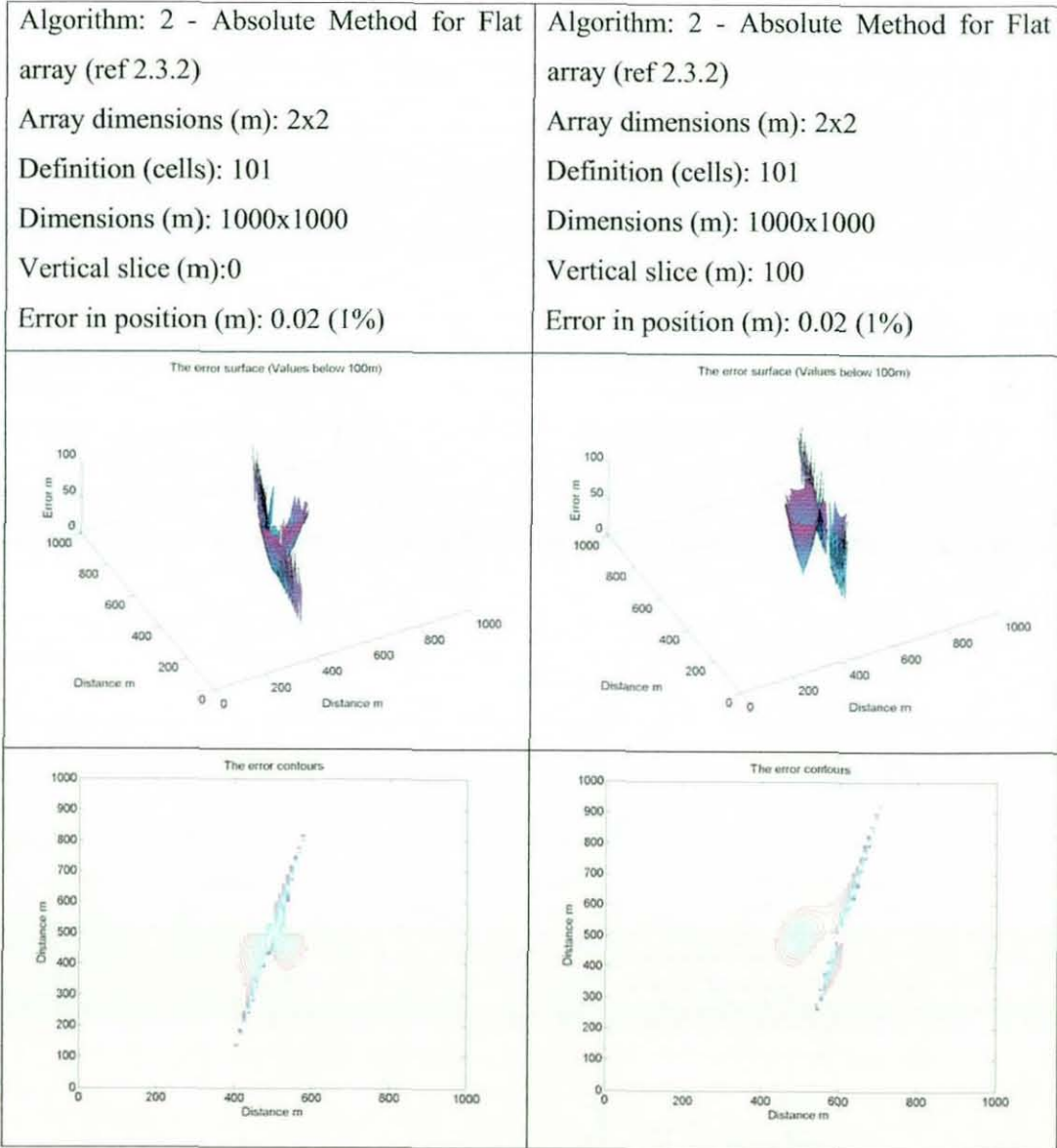


FIGURE 3.3-8B ERRORS CAUSED BY 1% ERROR IN RECEIVER POSITION WITH 2M ARRAY

Figure 3.3-8B clearly shows that a small movement in the position of one of the receivers results in almost total collapse of the algorithm. This implies that the method needs a fixed array or frequent re-calibration. If the error is extended further to 10% we can see (Figure 3.3-8C) that the algorithm has failed and the positions are unusable.

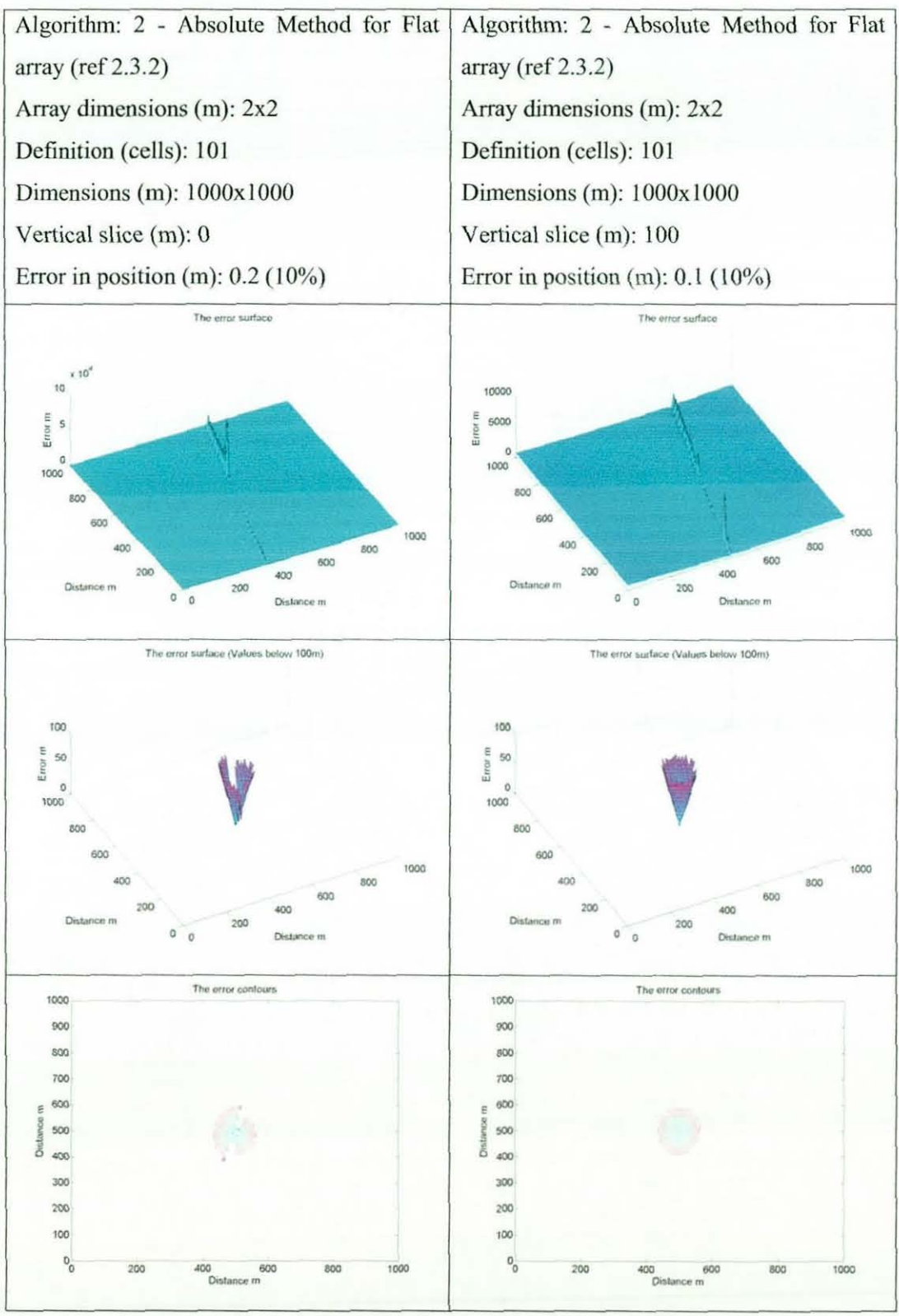


FIGURE 3.3-8C ERRORS CAUSED BY 10% ERROR IN RECEIVER POSITION WITH 2M ARRAY

3.3.2.4 ERRORS DUE TO THE VELOCITY PROFILE

The errors due to velocity profiles were demonstrated in section 3.3.1.4. To demonstrate the effect on a typical algorithm, the values have been entered into this algorithm and the results are shown in Figures 3.3-9A-F

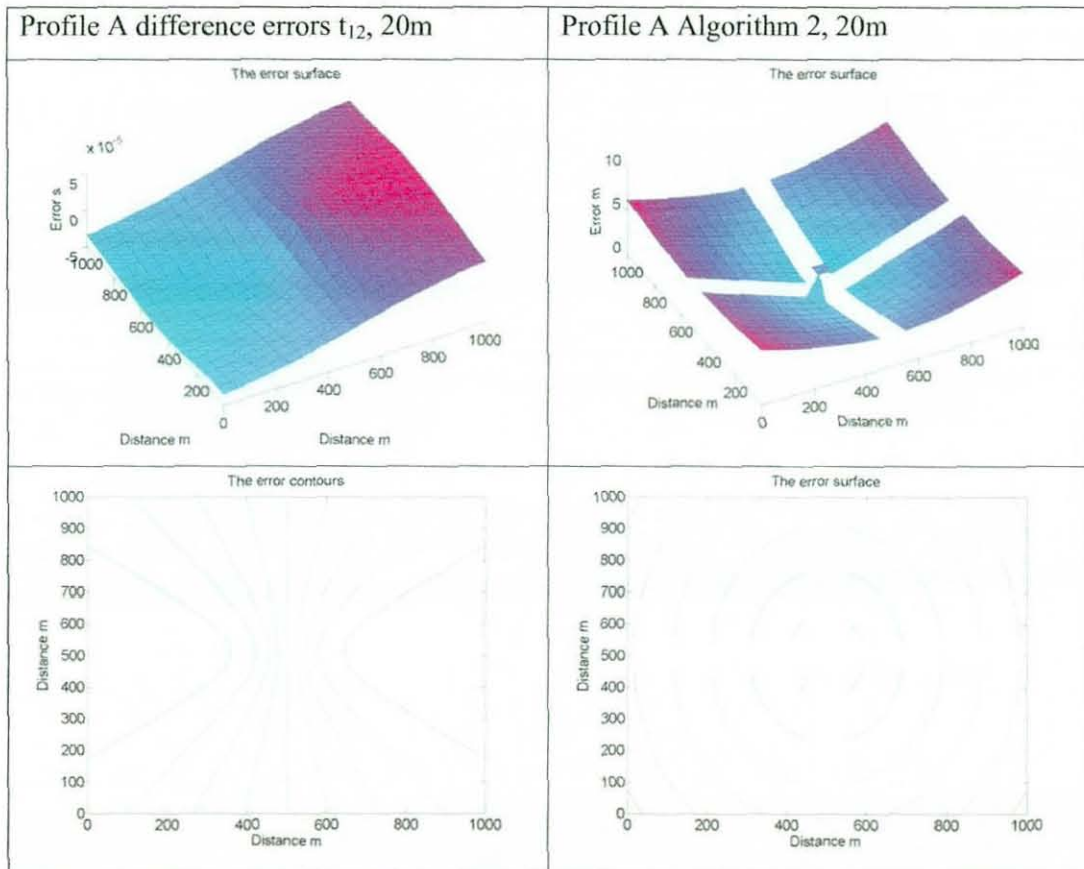


FIGURE 3.3-9A TIMING ERRORS INSERTED DUE TO VELOCITY PROFILE A (MID-ATLANTIC) WITH A 20M ARRAY

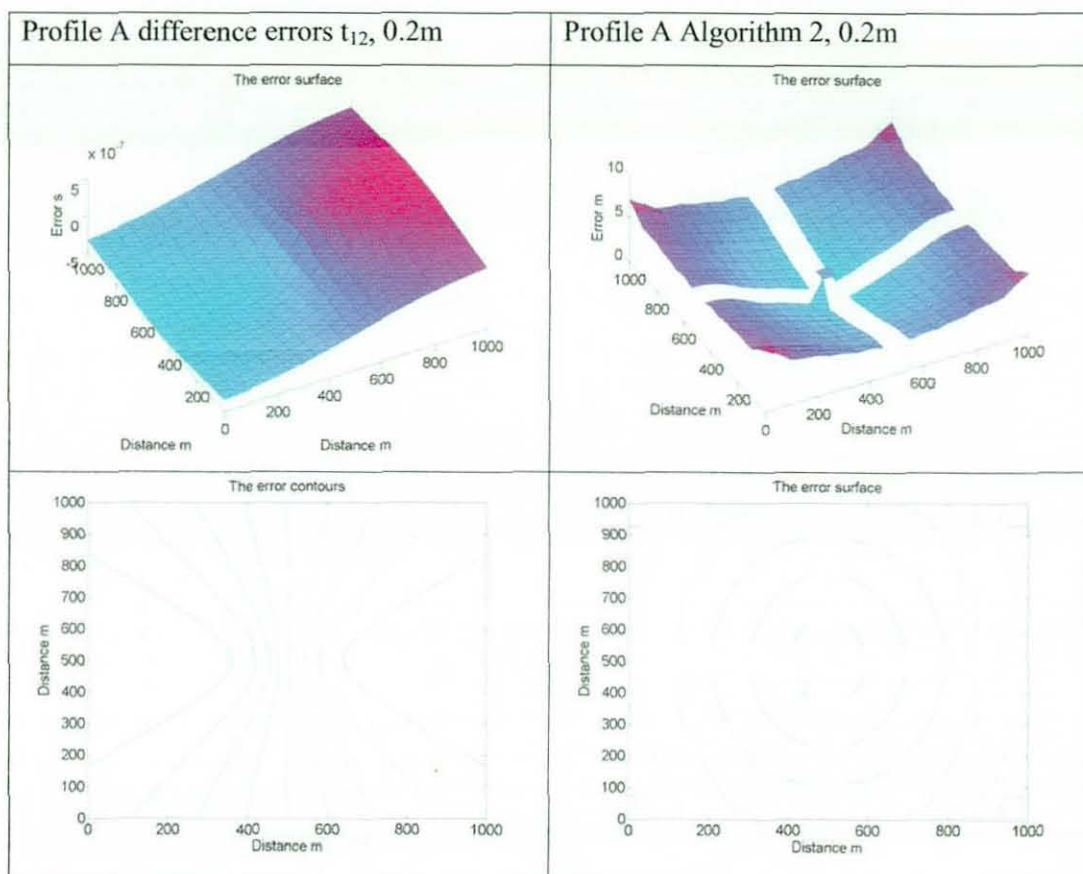


FIGURE 3.3-9B TIMING ERRORS INSERTED DUE TO VELOCITY PROFILE A (MID-ATLANTIC) WITH A 0.2M ARRAY

Figures 3.3-9A and B for Profile A show a typical oceanic depth velocity profile and the errors due to the bending of the sound waves. Both A and B show the same errors although A appears to be slightly less stable.

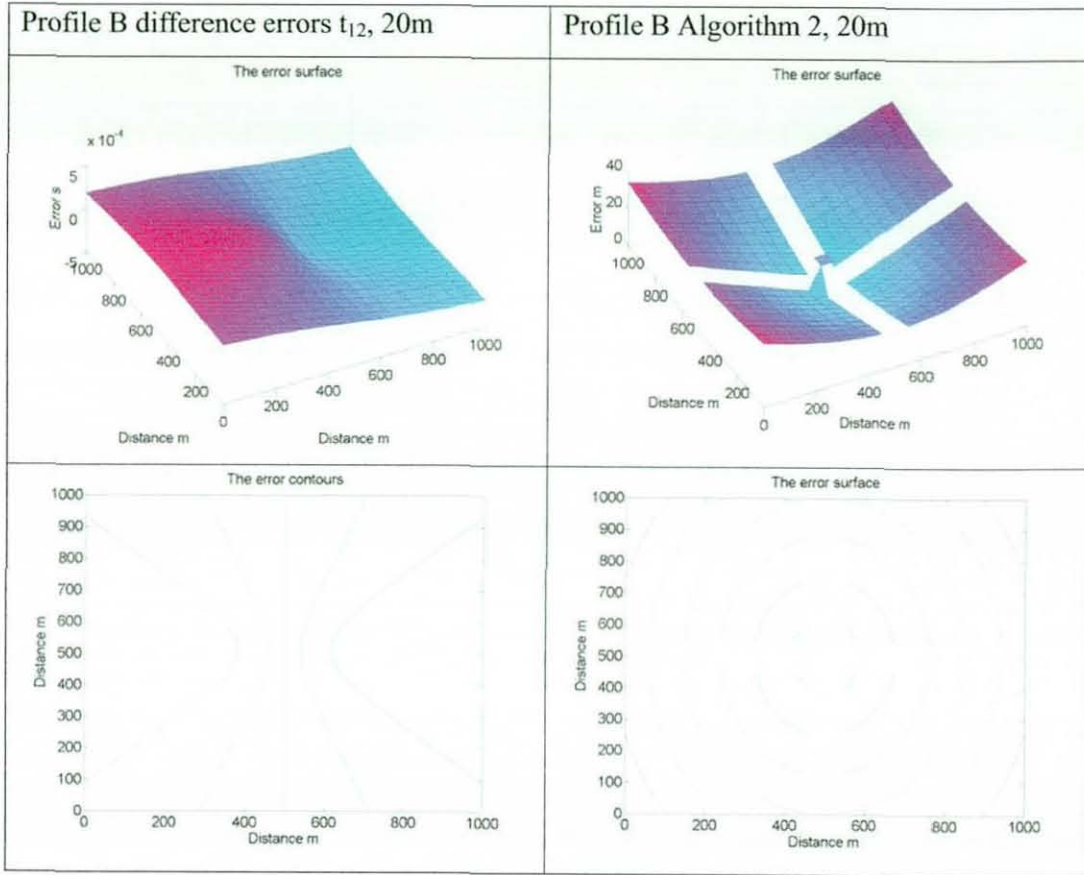


FIGURE 3.3-9C TIMING ERRORS INSERTED DUE TO VELOCITY PROFILE B (PRESSURE VARYING WITH DEPTH) WITH A 20M ARRAY

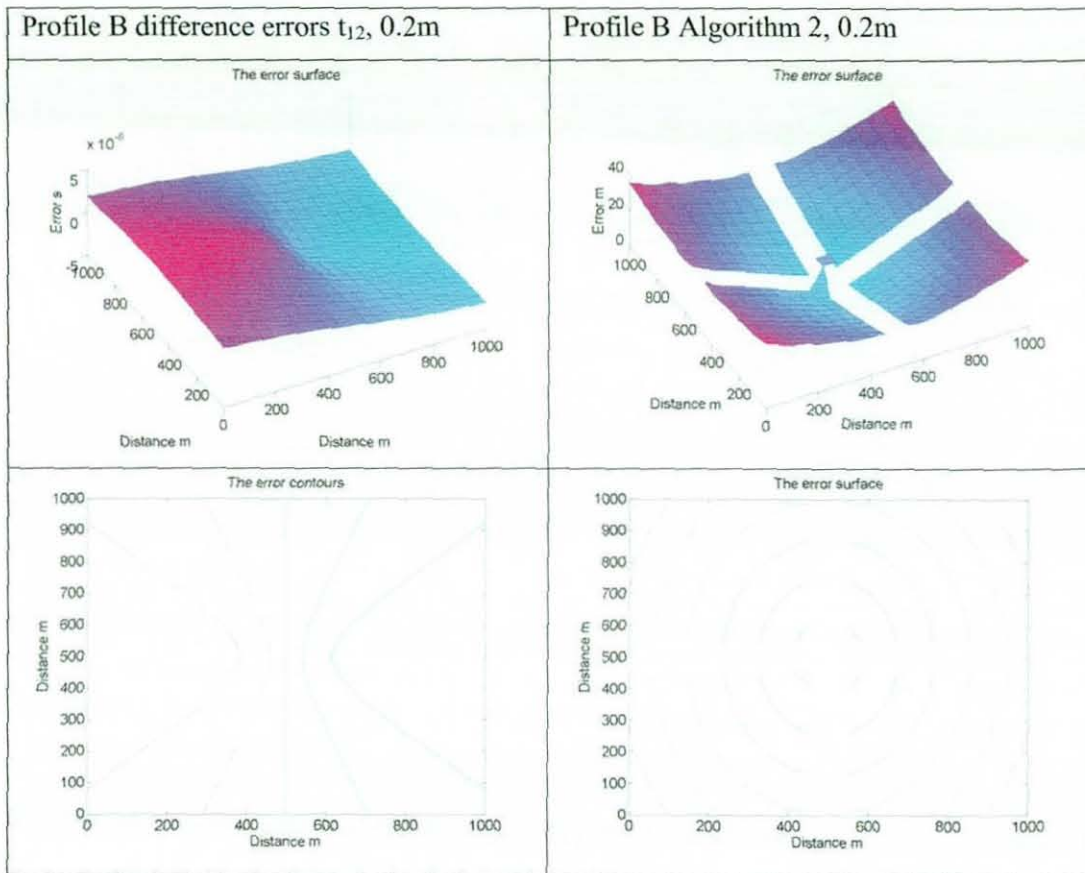


FIGURE 3.3-9D TIMING ERRORS INSERTED DUE TO VELOCITY PROFILE B (PRESSURE VARYING WITH DEPTH) WITH A 0.2M ARRAY

Figures 3.3-9 C and D for Profile B show the effects of a profile affected only by changes in pressure due to depth. The pressure gradient is extrapolated from the stable pressure change in the deep ocean. One rather odd thing with this simulation is that the maximum error is actually larger for this situation than in at typical oceanic profile.

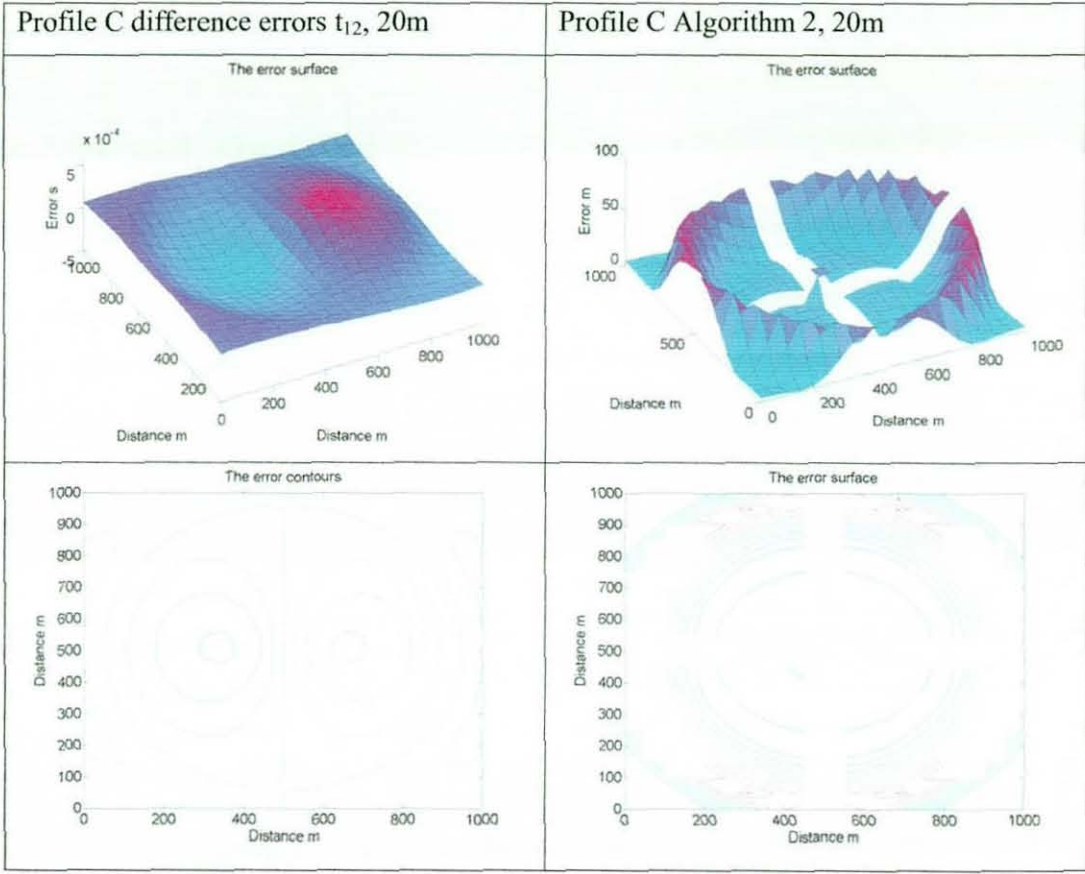


FIGURE 3.3-9E TIMING ERRORS INSERTED DUE TO VELOCITY PROFILE C (EXTREME) WITH A 20M ARRAY

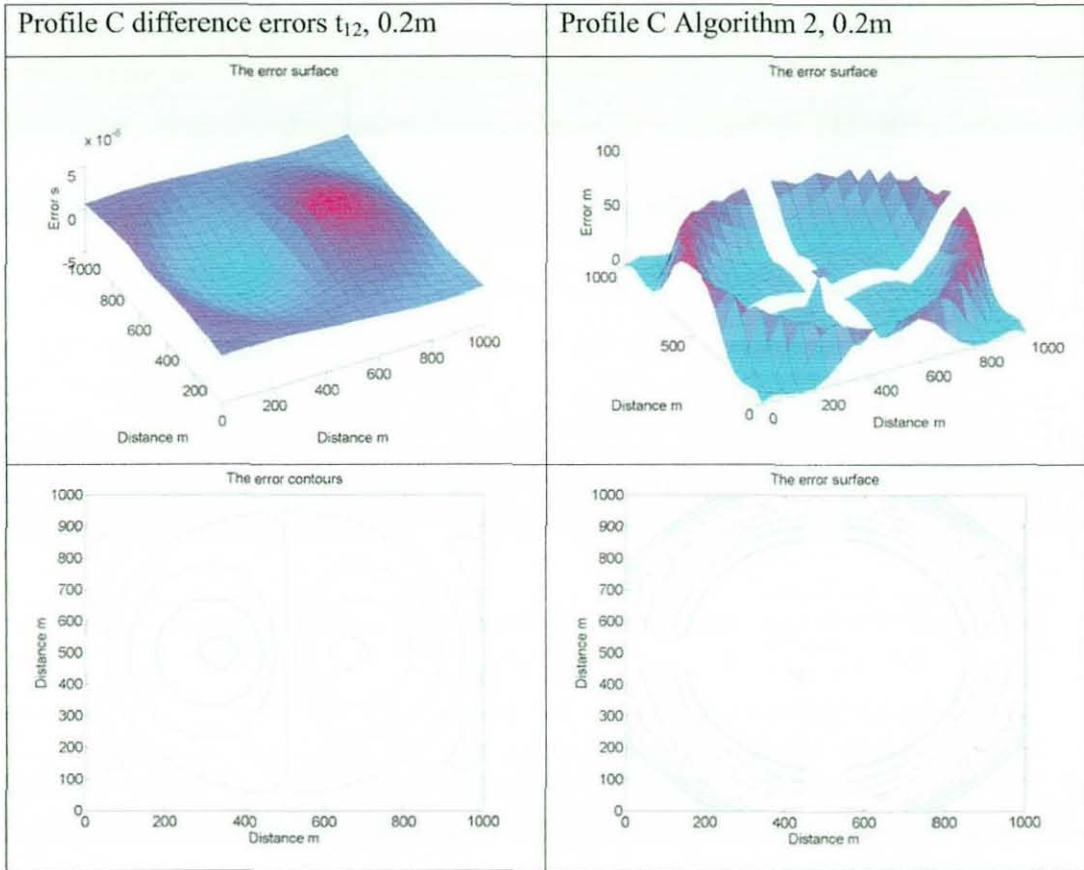


FIGURE 3.3-9F TIMING ERRORS INSERTED DUE TO VELOCITY PROFILE C (EXTREME) WITH A 0.2M ARRAY

Figures 3.3-9 E and F for Profile C show a greatly exaggerated profile, which is unrealistic but serves to show the extent of the errors induced by velocity profile error.

Finally, to provide a baseline for the method used in this simulation, Profile D is used to show that errors are of a similar order to those in the previous baselines.

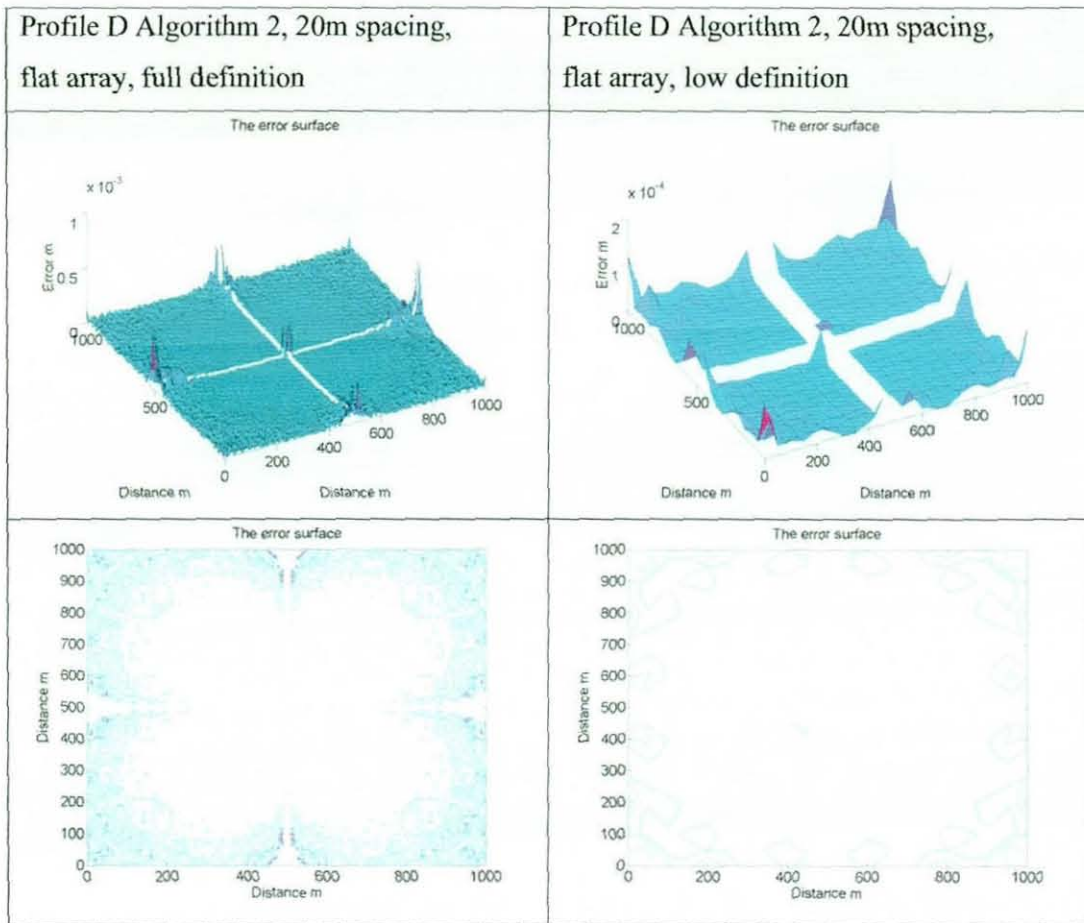


FIGURE 3.3-10 TIMING ERRORS INSERTED DUE TO VELOCITY PROFILE D (CONSTANT) WITH A 20M ARRAY

The simulation shown in Figure 3.3-10 gives a maximum error in the region 10^{-3} , which is much larger than the previous baselines but is still within acceptable limits. The error is a result of quantisation errors induced in the generation of the error times (1m quantisation in the velocity profile).

3.4 COMPENSATING PASSIVE TRACKING ALGORITHMS

The method simulated in this section is more robust and compensates for some of the parameters being adjusted in simulation. In particular it is designed to reduce the number and size of the ambiguities. Two methods have been simulated, although only the SVD method is reported here. Full results can be found in Appendix B.

3.4.1 MATRIX-SOLVED DIFFERENTIAL EQUATIONS USING SINGULAR VALUE DECOMPOSITION METHOD

The formula for this method is too complex to be summarised here (a full explanation is presented in section 2.3.2), but it is basically

$$\mathbf{m}=\mathbf{A}^{-1}.\mathbf{x}$$

where \mathbf{m} is the positional matrix, and \mathbf{A} and \mathbf{x} describe the linearised matrix of simultaneous equations for the hyperbolae. This method compensates for any singularities, and unlike the other methods, it should – theoretically - not fail, although it can still give large errors.

3.4.1.1 NO ERRORS

With no inserted errors we get error the plots shown in Figure 3.4-1A to E.

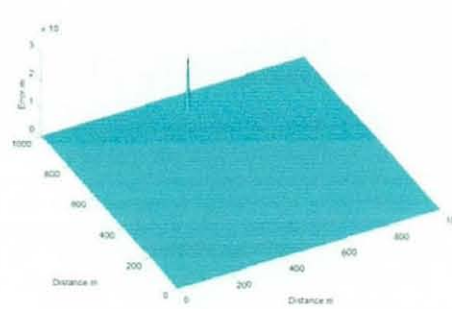
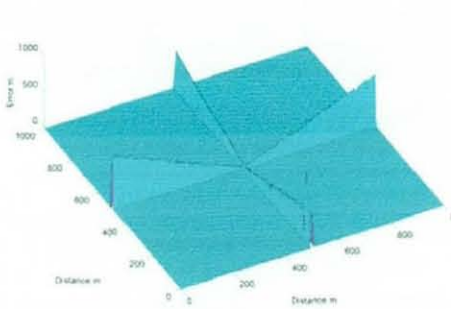
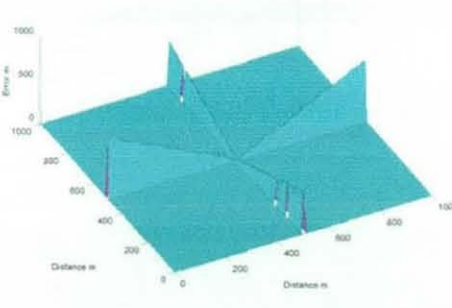
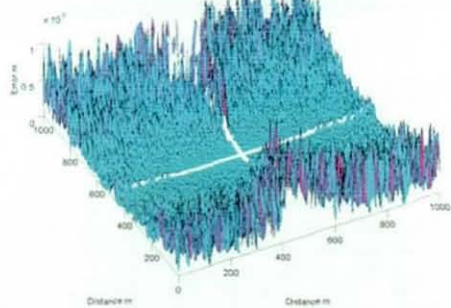
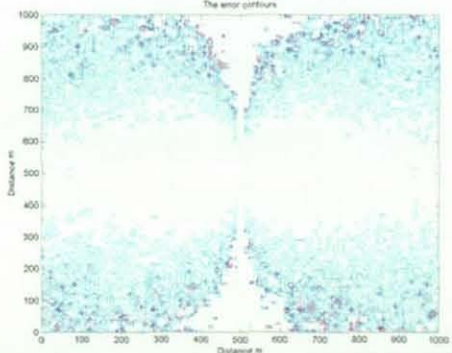
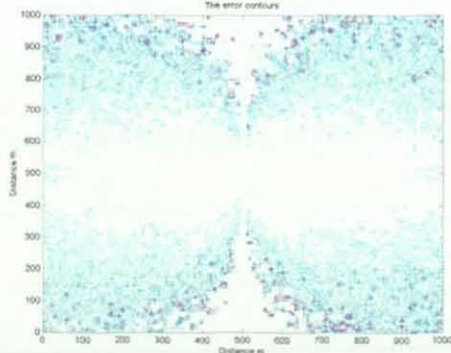
<p>Algorithm: 6 Matrix SVD Method (ref 2.4.1)</p> <p>Array dimensions (m): 20x20x10</p> <p>Definition (cells): 101</p> <p>Dimensions (m): 1000x1000</p> <p>Vertical slice (m): 0</p>	<p>Algorithm: 6 Matrix SVD Method (ref 2.4.1)</p> <p>Array dimensions (m): 20x20x10</p> <p>Definition (cells): 101</p> <p>Dimensions (m): 1000x1000</p> <p>Vertical slice (m): 100</p>
<p>The error surface</p> 	<p>The error surface</p> 
<p>The error surface (values below 100m)</p> 	<p>The error surface (values below 100m)</p> 
<p>The error contours</p> 	<p>The error contours</p> 

FIGURE 3.4-1A ERRORS IN ALGORITHM 2 DUE TO COMPUTER LIMITATIONS, 20M ARRAY
Chapter 3 Simulation Page 120

As stated, this method should have no ambiguities due to singularities; instead, a 'nearest solution' is found. The method does not perform miracles and as Figure 3.4-1A shows the solutions provided by the x- and y-ambiguities are far from ideal. The fact that there is a solution can prove to be very useful when it comes to implementation, as the error state will not cause a processor error. The maximum error of this algorithm is in the region of 10^{-8} , which is on a par with the other algorithms.

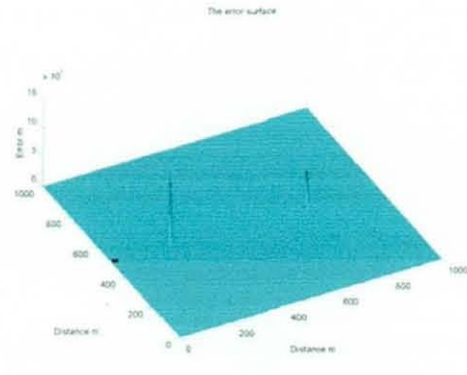
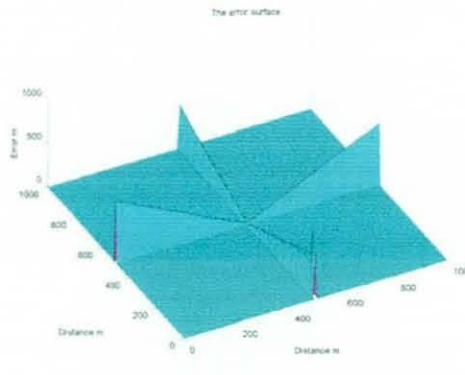
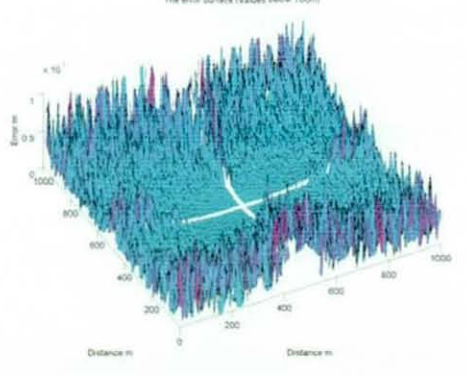
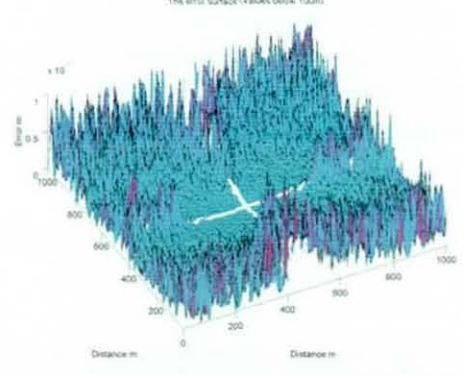
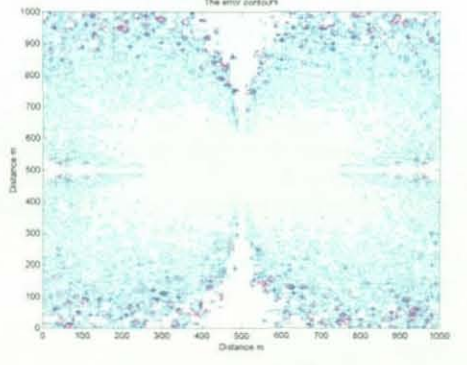
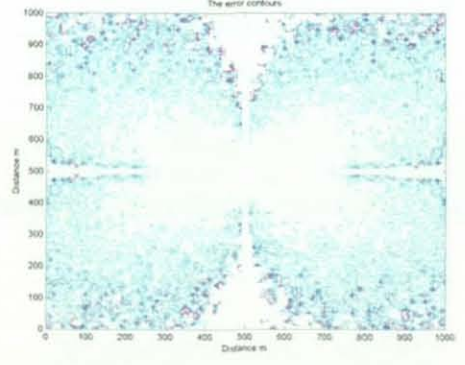
<p>Algorithm: 6 Matrix SVD Method (ref 2.4.1)</p> <p>Array dimensions (m): 2x2x1</p> <p>Definition (cells): 101</p> <p>Dimensions (m): 1000x1000</p> <p>Vertical slice (m): 0</p>	<p>Algorithm: 6 Matrix SVD Method (ref 2.4.1)</p> <p>Array dimensions (m): 2x2x1</p> <p>Definition (cells): 101</p> <p>Dimensions (m): 1000x1000</p> <p>Vertical slice (m): 100</p>
	
	
	

FIGURE 3.4-1B ERRORS IN ALGORITHM 2 DUE TO COMPUTER LIMITATIONS, 2M ARRAY

Algorithm: 6 Matrix SVD Method
(ref 2.4.1)

Array dimensions (m): 0.2x0.2x0.1

Definition (cells): 101

Dimensions (m): 1000x1000

Vertical slice (m): 0

Algorithm: 6

Array dimensions (m): 0.2x0.2x0.1

Definition (cells): 101

Dimensions (m): 1000x1000

Vertical slice (m): 100

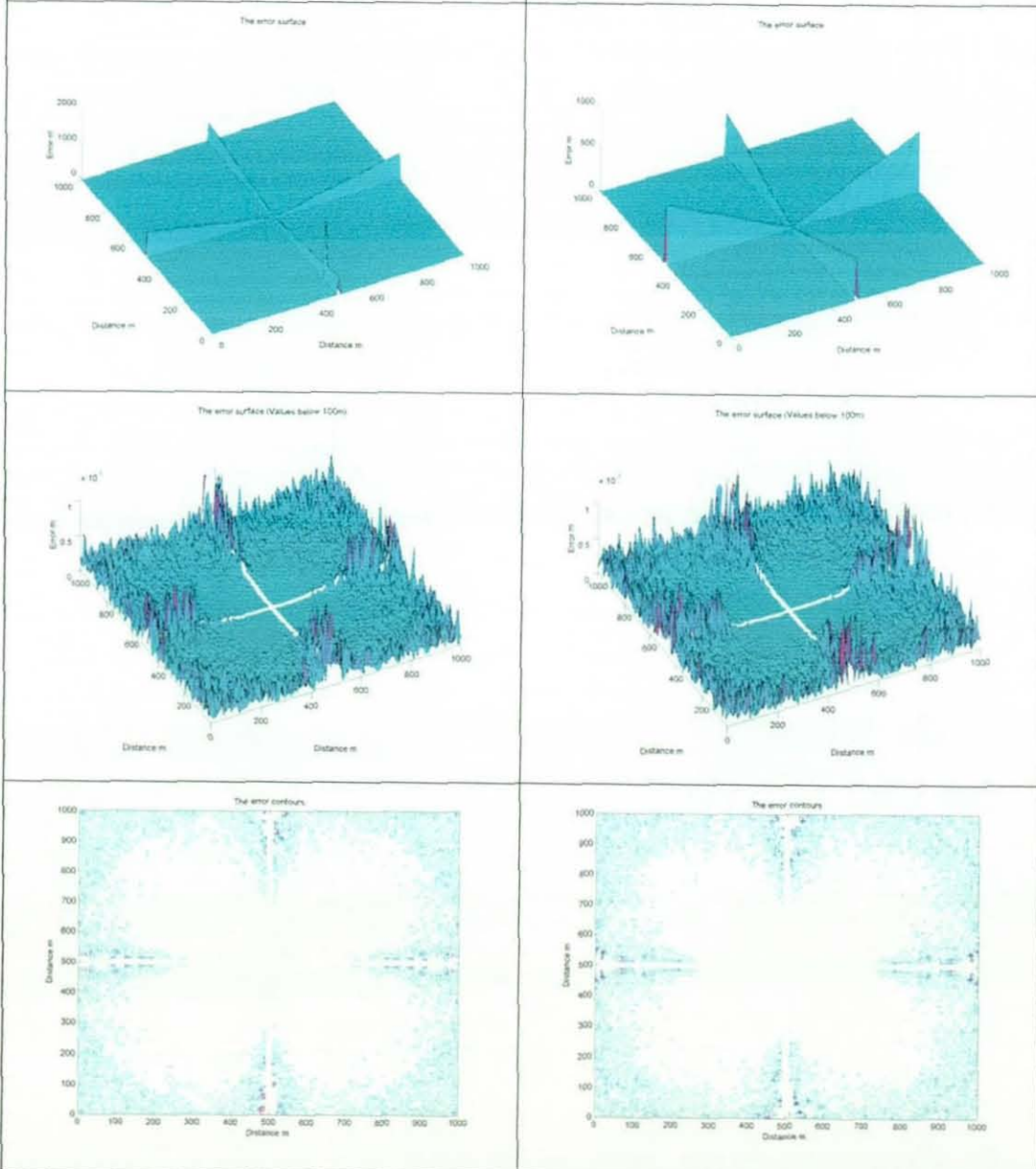


FIGURE 3.4-1C ERRORS IN ALGORITHM 2 DUE TO COMPUTER LIMITATIONS, 0.2M ARRAY

Figures 3.4-1A to C show a similar trend to the algorithms in sections 3.2 and 3.3, with the error increasing by a factor of approximately 100 as the array size is reduced by a factor of 10.

3.4.1.2 TIMING ERRORS

With timing errors inserted as in previous sections we also see similarities between the algorithms, as shown in Figures 3.4-2A-C.

Figure 3.4-2A shows similar behaviour to the other flat array algorithms with a maximum error of 1m at 100MHz. There is little difference at a distance of 100m out of the plane of the hydrophones.

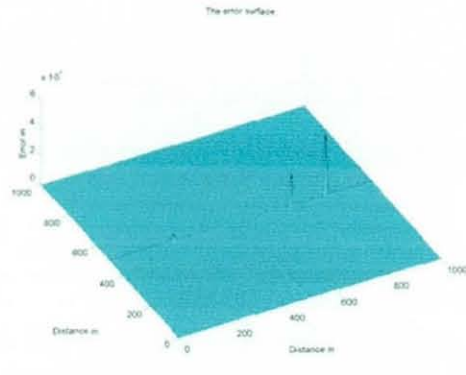
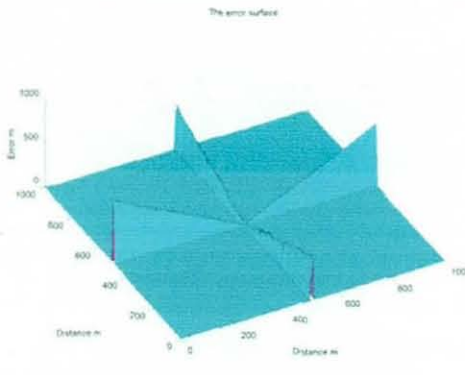
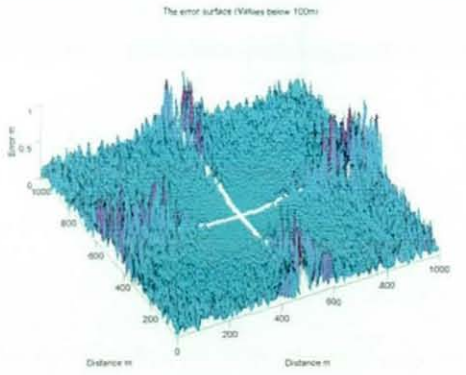
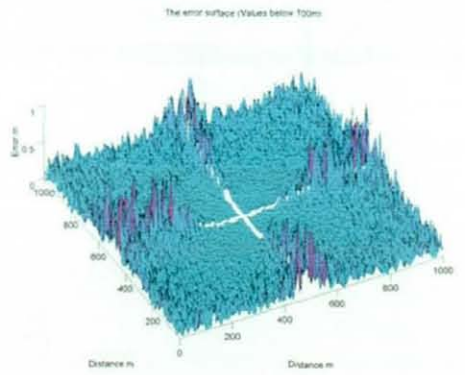
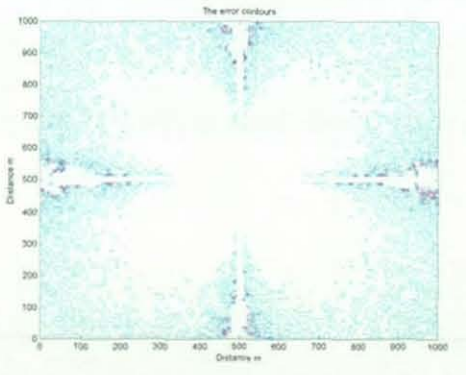
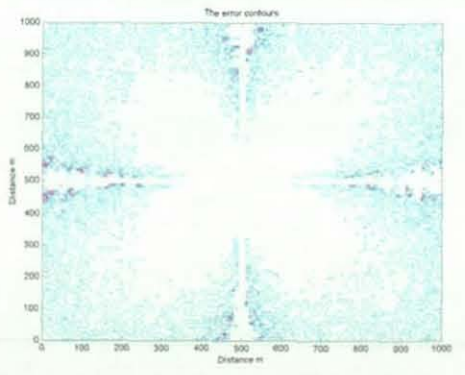
<p>Algorithm: 6 Matrix SVD Method (ref 2.4.1) Array dimensions (m): 2x2x1 Definition (cells): 101 Dimensions (m): 1000x1000 Vertical slice (m): 0 Timing error (μs): 0.001</p>	<p>Algorithm: 6 Matrix SVD Method (ref 2.4.1) Array dimensions (m): 2x2x1 Definition (cells): 101 Dimensions (m): 1000x1000 Vertical slice (m): 100 Timing error (μs): 0.001</p>
	
	
	

FIGURE 3.4-2A ERRORS IN ALGORITHM 2 (2M) DUE TO TIMING ERRORS, SAMPLING AT 100MHZ

With a 10MHz sampling rate (Figure 3.4-2B) the error is larger (10-100 times), but the ambiguities (over 100m error) are as before.

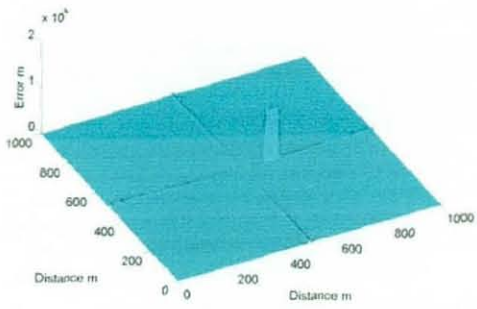
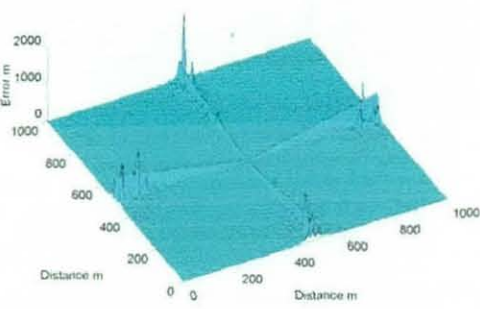
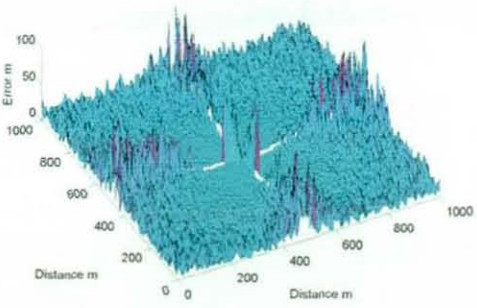
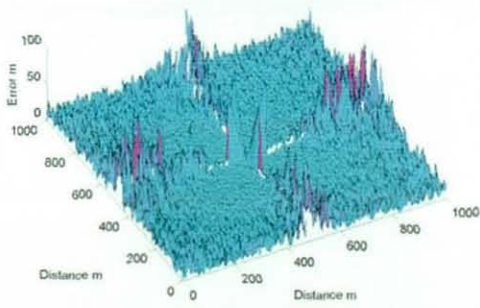
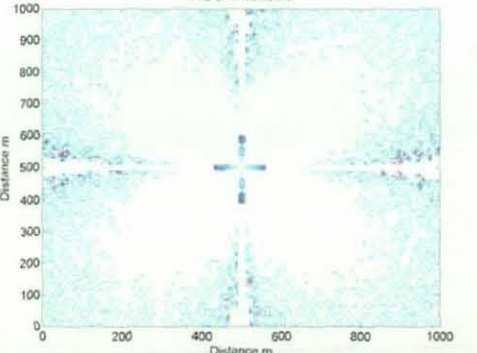
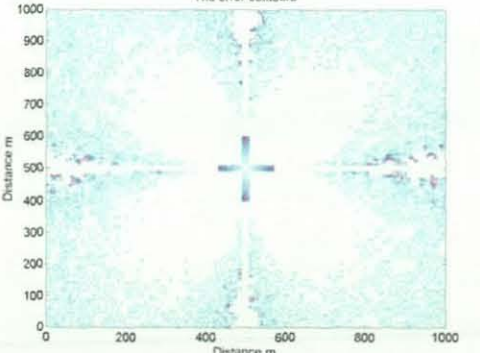
<p>Algorithm: 6 Matrix SVD Method (ref 2.4.1)</p> <p>Array dimensions (m): 2x2x1</p> <p>Definition (cells): 101</p> <p>Dimensions (m): 1000x1000</p> <p>Vertical slice (m): 0</p> <p>Timing error (μs): 0.10</p>	<p>Algorithm: 6 Matrix SVD Method (ref 2.4.1)</p> <p>Array dimensions (m): 2x2x1</p> <p>Definition (cells): 101</p> <p>Dimensions (m): 1000x1000</p> <p>Vertical slice (m): 100</p> <p>Timing error (μs): 0.10</p>
<p>The error surface</p> 	<p>The error surface</p> 
<p>The error surface (Values below 100m)</p> 	<p>The error surface (Values below 100m)</p> 
<p>The error contours</p> 	<p>The error contours</p> 

FIGURE 3.4-2B ERRORS IN ALGORITHM 2 (2M) DUE TO TIMING ERRORS, SAMPLING AT 10MHZ

If a sampling rate of 100kHz is now considered the workable area is again severely reduced and although the algorithm still functions the results are useless.

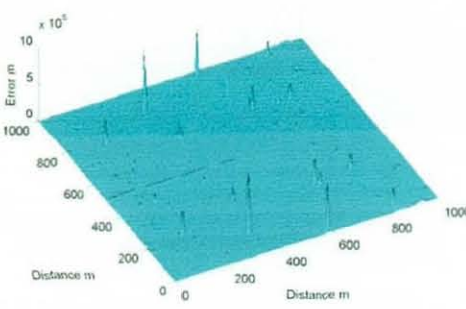
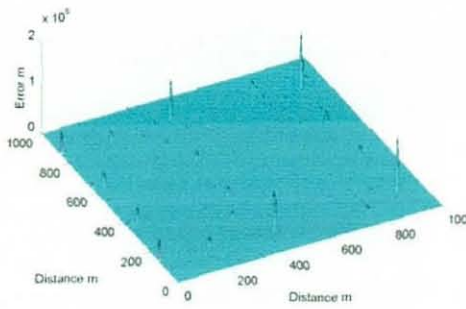
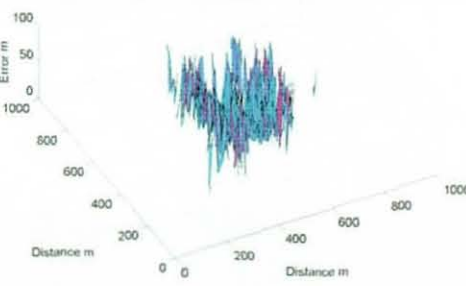
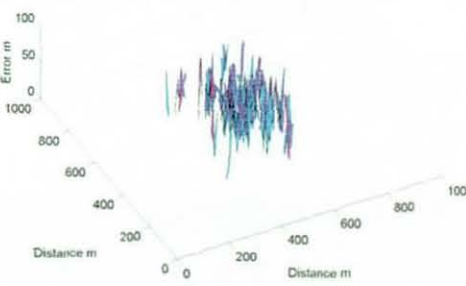
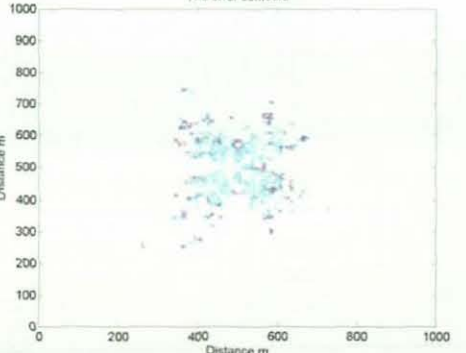
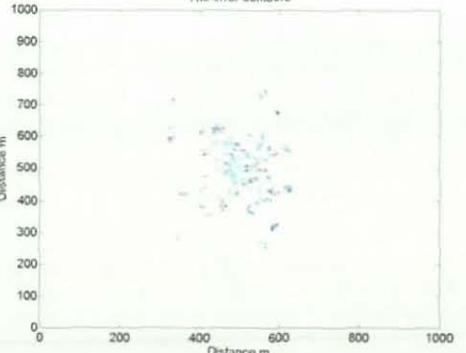
<p>Algorithm: 6 Matrix SVD Method (ref 2.4.1)</p> <p>Array dimensions (m): 2x2x1</p> <p>Definition (cells): 101</p> <p>Dimensions (m): 1000x1000</p> <p>Vertical slice (m): 0</p> <p>Timing error (μs): 10</p>	<p>Algorithm: 6 Matrix SVD Method (ref 2.4.1)</p> <p>Array dimensions (m): 2x2x1</p> <p>Definition (cells): 101</p> <p>Dimensions (m): 1000x1000</p> <p>Vertical slice (m): 100</p> <p>Timing error (μs): 10</p>
<p>The error surface</p> 	<p>The error surface</p> 
<p>The error surface (Values below 100m)</p> 	<p>The error surface (Values below 100m)</p> 
<p>The error contours</p> 	<p>The error contours</p> 

FIGURE 3.4-2C ERRORS IN ALGORITHM 2 (2M) DUE TO TIMING ERRORS, SAMPLING AT 100kHz

3.4.1.3 RECEIVER POSITIONAL ERRORS

Adjusting the position of one of the receivers to give an error we find once again that we have similar results to those for the other flat array algorithms. Figures 3.4-3A-C show that the algorithm is very sensitive to this form of error.

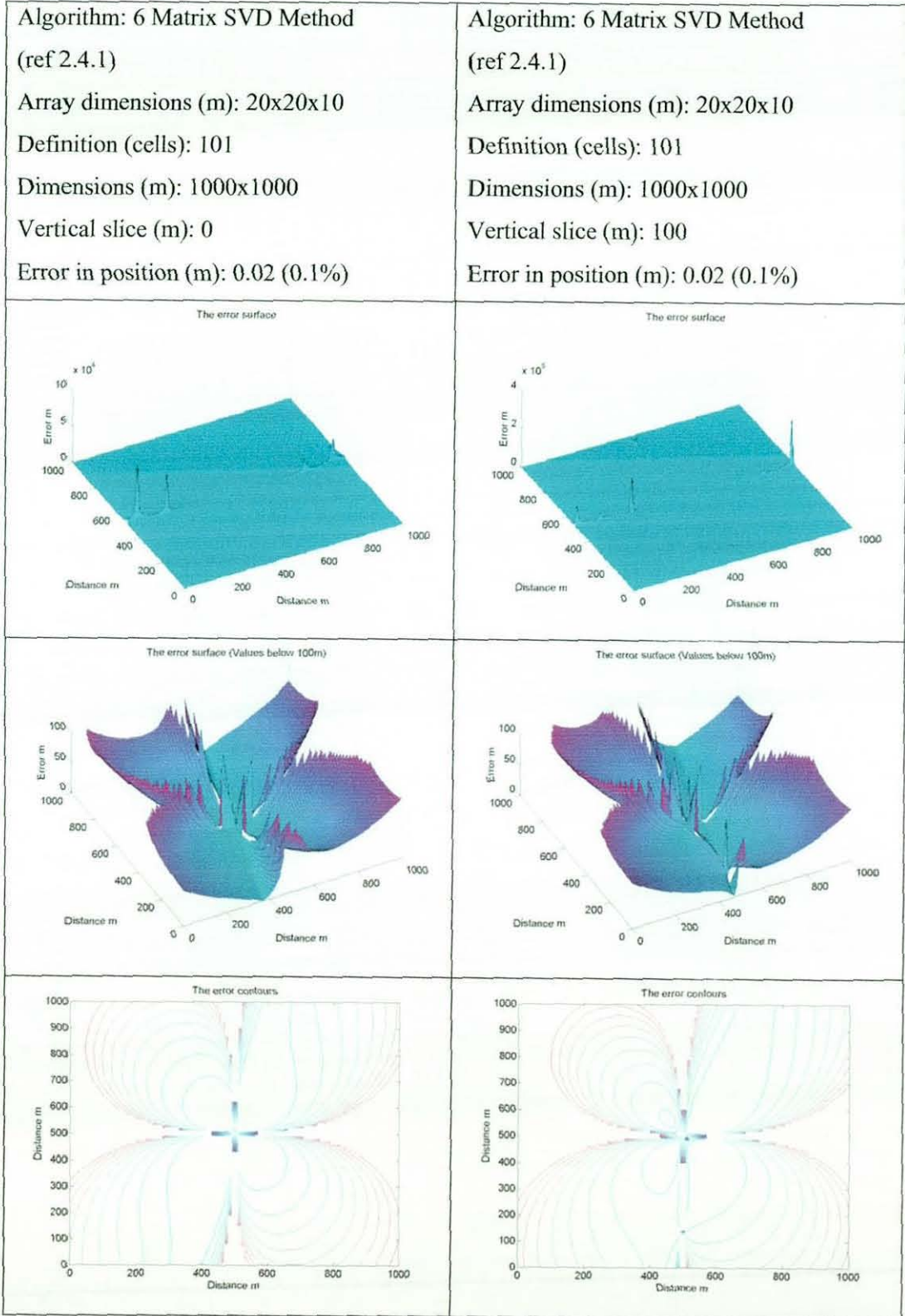


FIGURE 3.4-3A ERRORS CAUSED BY 0.1% ERROR IN RECEIVER POSITION WITH 20M ARRAY

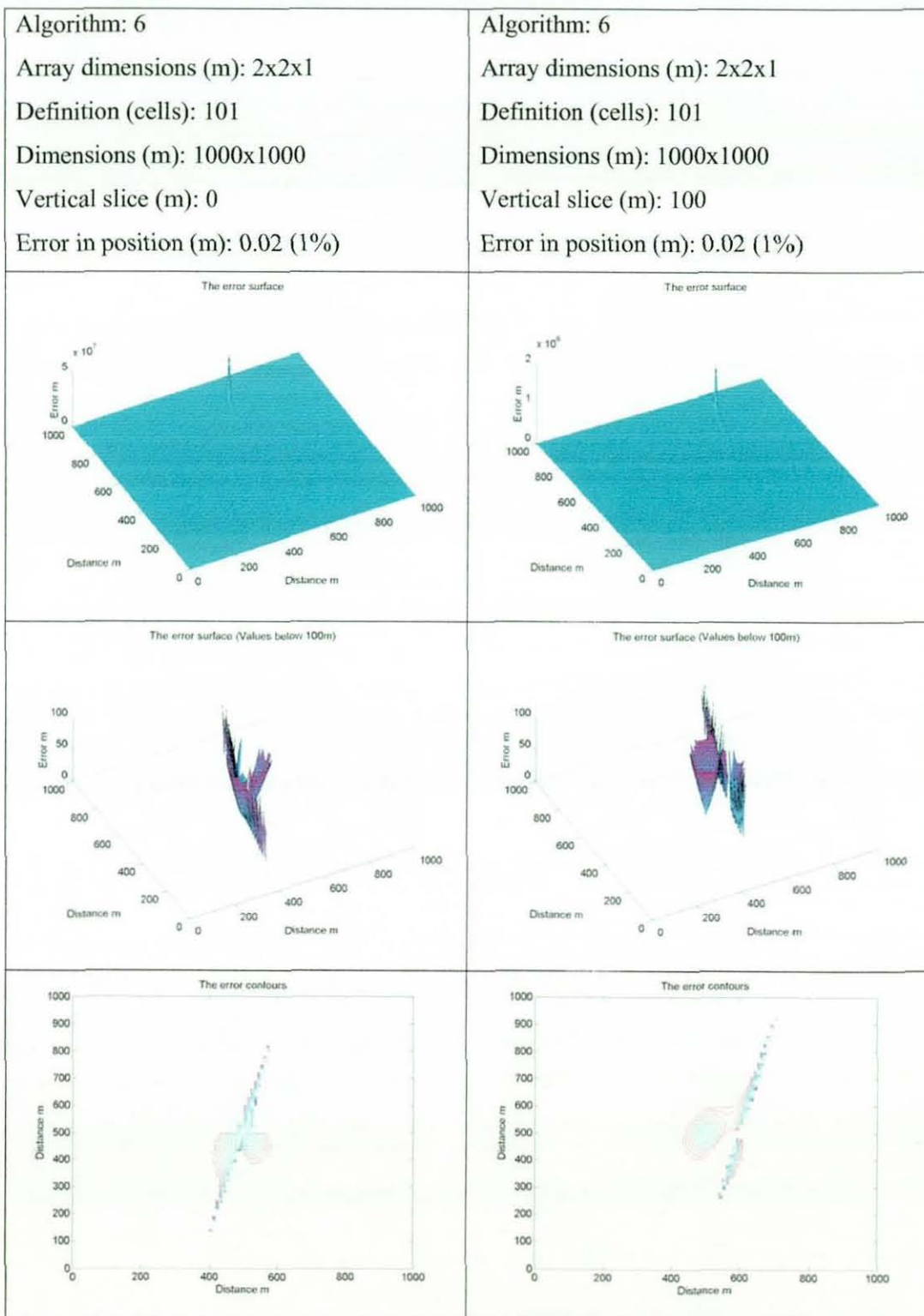


FIGURE 3.4-3B ERRORS CAUSED BY 1% ERROR IN RECEIVER POSITION WITH 2M ARRAY

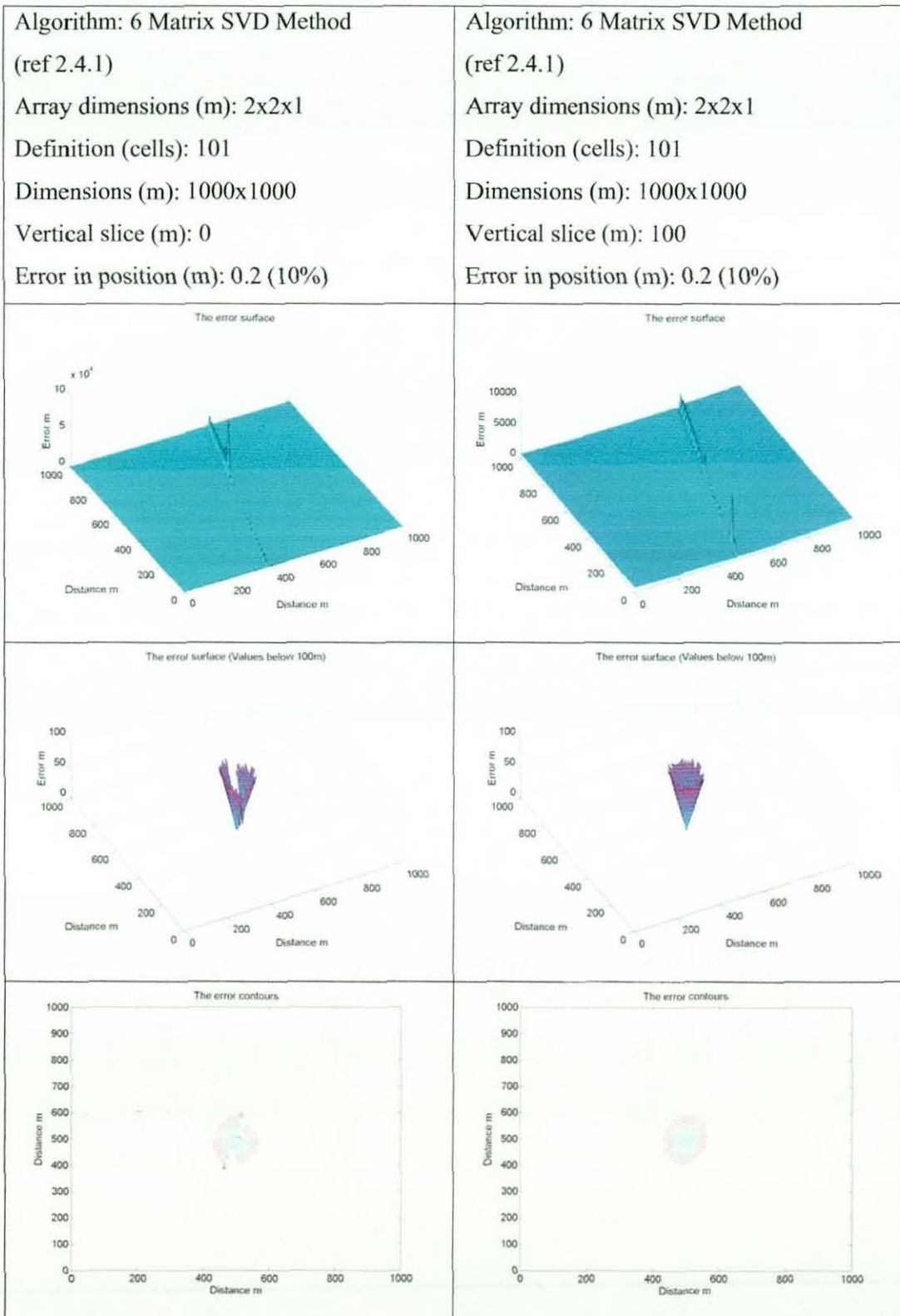


FIGURE 3.4-3C ERRORS CAUSED BY 10% ERROR IN RECEIVER POSITION WITH 2M ARRAY

3.4.2 TABULAR METHOD (METHOD 4)

3.4.2.1 NO ERRORS

This method can be split into two major sections, (a) the generation of a spatial array and sorting into timing bins, and (b) the determination of a position from received time differences.

a) Generation of the spatial table and sorting

Pythagorean mathematics can be applied for the determination of the time differences in the simple case. The physical distance between the elements in the initial table is defined by the worst-case situation of the timing differences. These occur orthogonal to the receiver pair at the greatest range, i.e. at the edge of the defined area with maximum x , y and z . The difference in timings between concurrent elements of the table in these areas defines the necessary inter-element range and hence the required table size. Once the table dimensions are known the time differences for each spatial element are calculated. The table is then sorted by timing. The size definition of the table also corresponds to a timing definition. For each receiver pair a set of bins is created, each with the minimum timing definition. The table is then sorted, and the receiver pair timing contained in the positional array is used as the bin in which the position (x , y , z) is placed. This method produces a large number of timing bins, each containing relatively few positions.

b) Determination of a position

To determine the position, the set of bins for the receiver pair is sorted. The bin nearest the received timing difference is taken; this is repeated for each pair of receivers, and the resulting bins are then compared for like solutions. If more than one solution is found, both are recorded; if none are found this may be due to the source being out of range or due to errors in timing, causing the position to be placed in one of the surrounding bins. This can be partly compensated for by considering groups of timing bins rather than individual bins, although this tends to generate multiple solutions. If plotted, these groups of positions describe the hyperbolae on which the source is positioned. Further processing of the data to find where the hyperbolae meet gives a more accurate position.

As stated, the major limitation of this method is the size of the initial table required. Changing the shape of each physical cell in the table may reduce the size. The greatest definition is required in orthogonal regions; if these are made smaller then the number of points can be reduced.

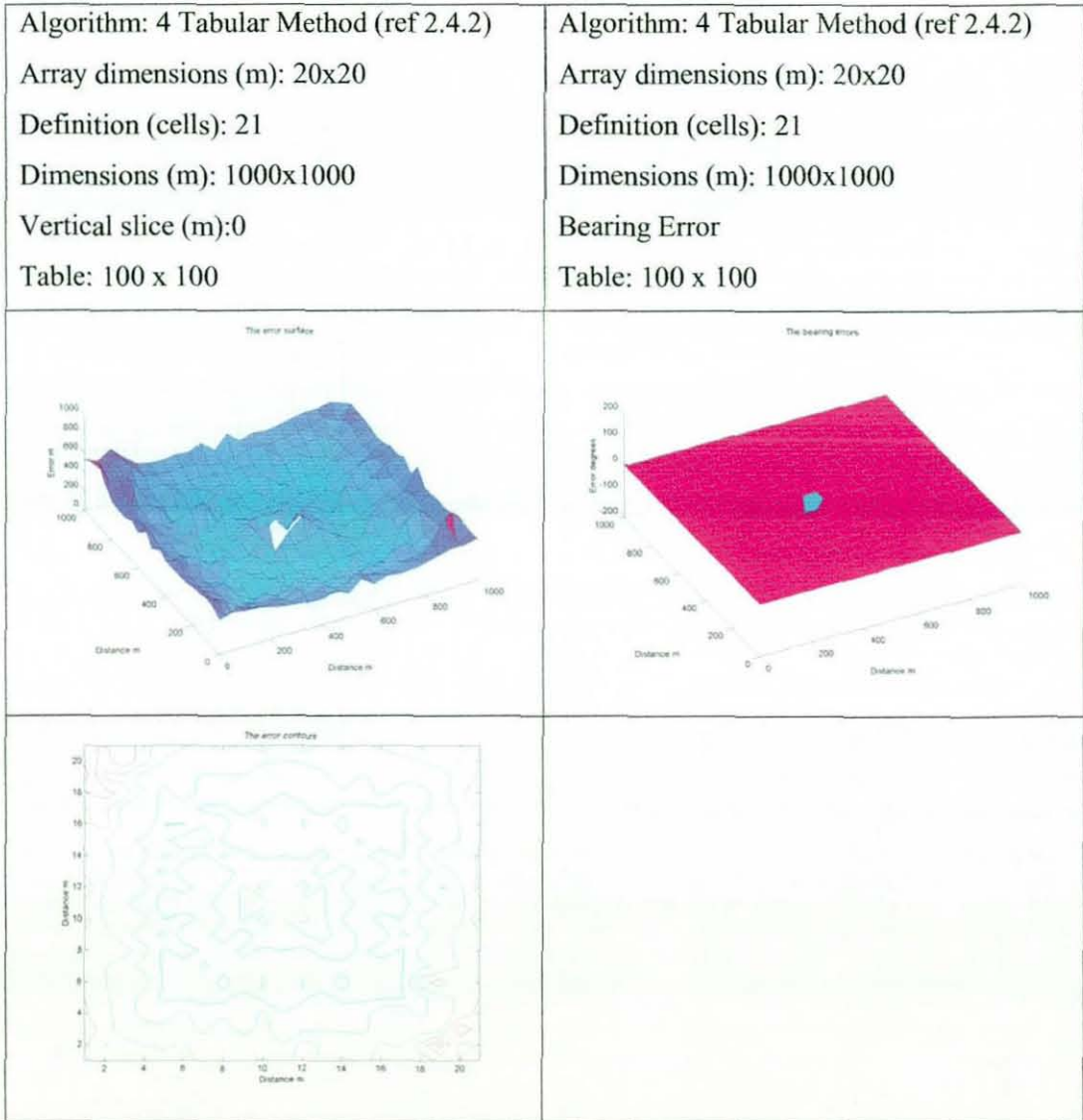


FIGURE 3.4-4A ERRORS IN ALGORITHM 2 DUE TO COMPUTER LIMITATIONS, 20M ARRAY

If a velocity profile is to be compensated for, the algorithm must be changed slightly. Instead of using Pythagoras to calculate the range, and hence the time, a model of the acoustic flight path must be used and the changes in velocity accounted for. This extra calculation increases the calculation time but does not effect the tracking time.

Figure 3.4-4A shows the error surface generated using this method with no error inserted. Errors are larger and dimensions above $\pm 200\text{m}$ are greatly in error. Figure 3.4-5B shows the effect of varying the array size. In terms of accuracy the method is of little use above 200m from the receiver array, but the figure in the top right shows the errors in bearing to the source. These are very low, in fact near zero except within the array. This means that the method can possibly be used for full tracking at low ranges and as a bearing at the greater ranges.

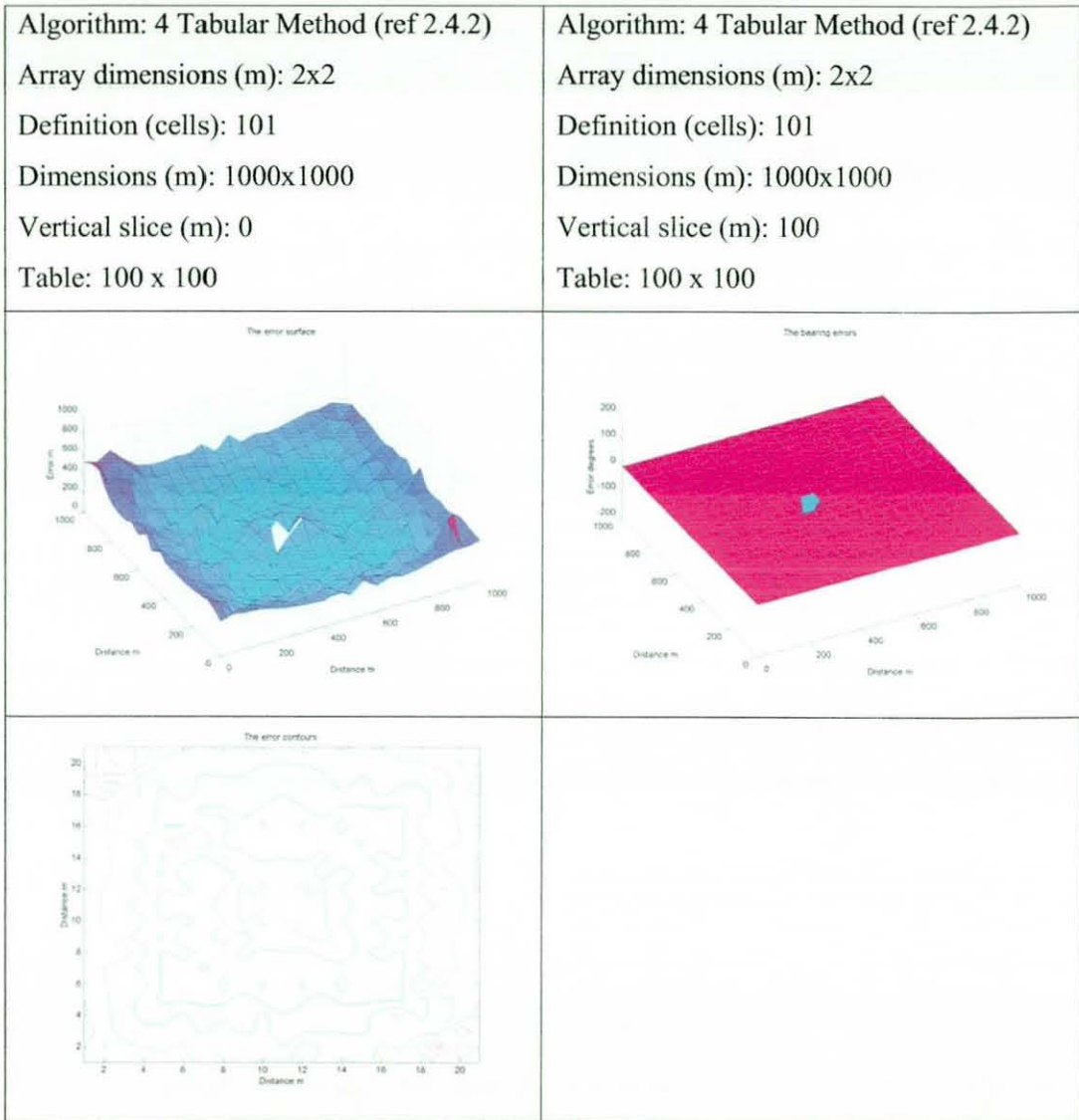


FIGURE 3.3-4B ERRORS IN ALGORITHM 2 DUE TO COMPUTER LIMITATIONS, 2M ARRAY

If we now reduce the array size to an ultra-short baseline and perform the same simulation we see very similar results in range and slightly more quantisation in the bearing (still within ± 2 degrees).

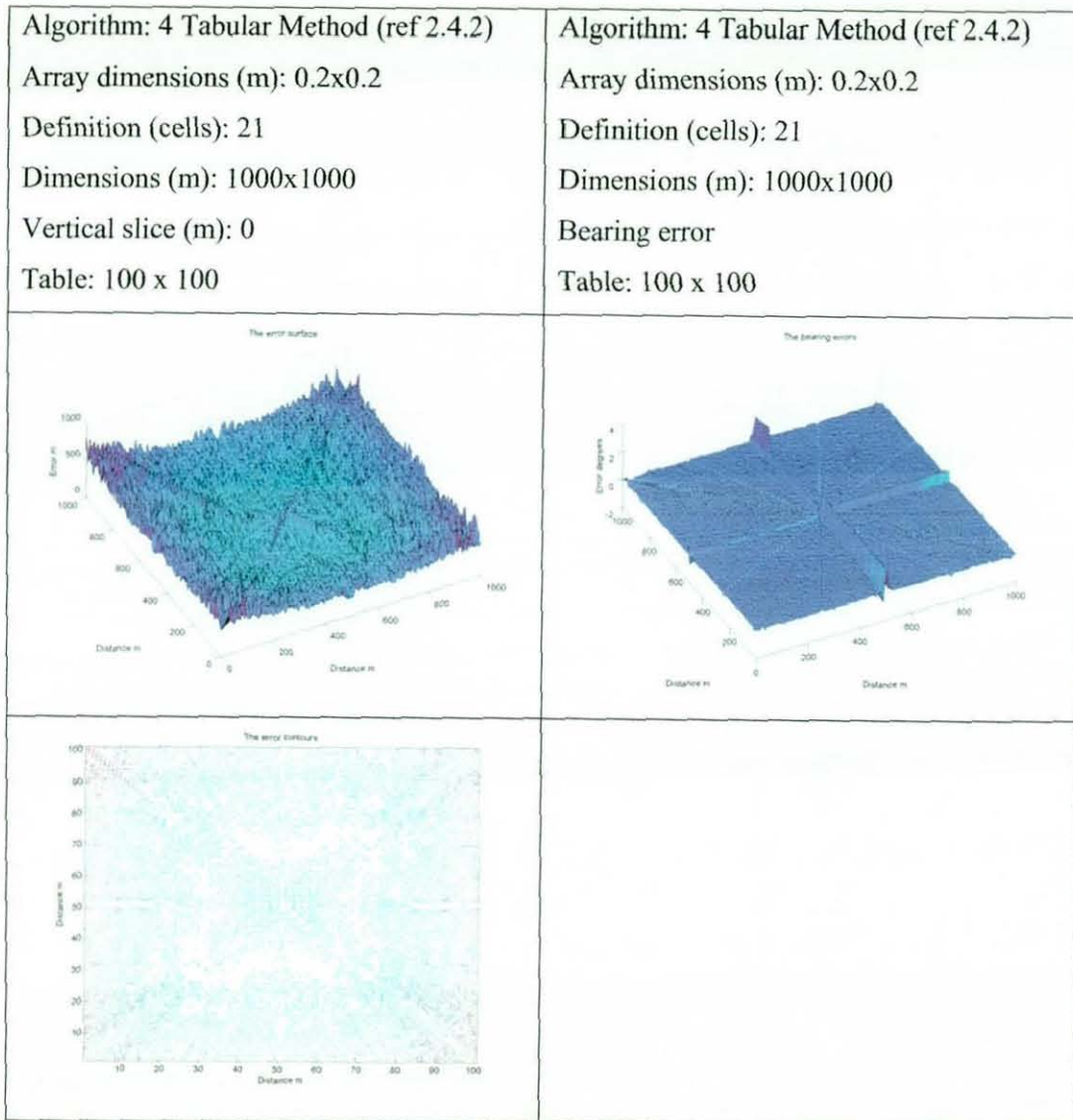


FIGURE 3.4-4C ERRORS IN ALGORITHM 2 DUE TO COMPUTER LIMITATIONS, 0.2M ARRAY

3.4.2.2 TIMING ERRORS

If we now introduce timing errors as before we see that instead of maximum positional errors the algorithm has problems finding some positions. This may be due to there being more than one correct solution and the wrong one being selected (although filters are added to remove such ambiguities). Figure 3.4-5 shows the worst case of a 100kHz sampling rate, demonstrating that the algorithm has problem areas, although bearing is still good except where other algorithms have been found to contain ambiguities.

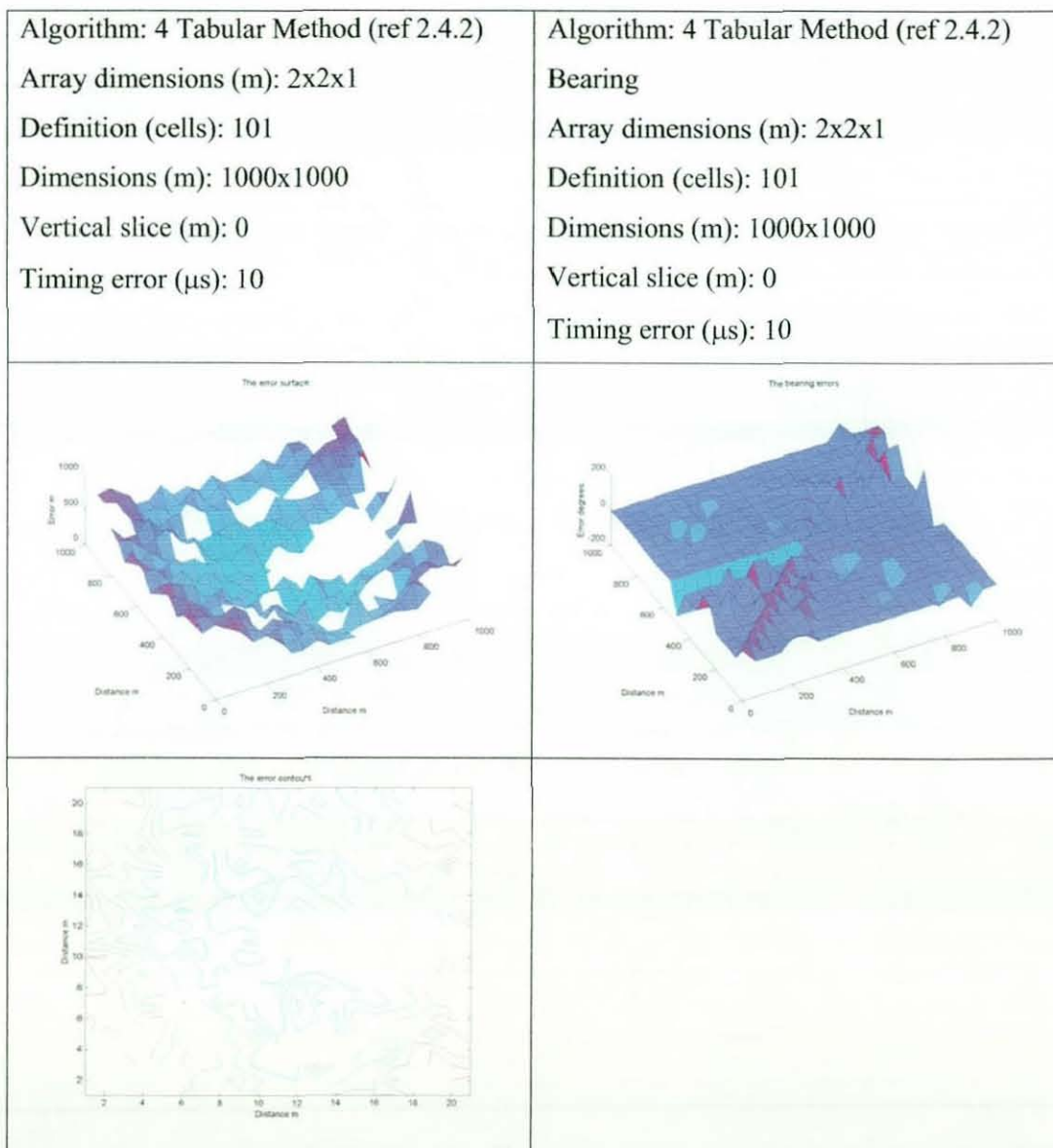


FIGURE 3.4-5 ERRORS IN ALGORITHM 2 (2M) DUE TO TIMING ERRORS, SAMPLING AT 100MHZ

3.4.2.3 RECEIVER POSITIONAL ERRORS

If receiver positional errors are introduced we find little effect with small errors (Figure 3.4-6A), but as we increase these (Figure 3.4-6B) we find some increase in the error surface, although little increase in the bearing simulation.

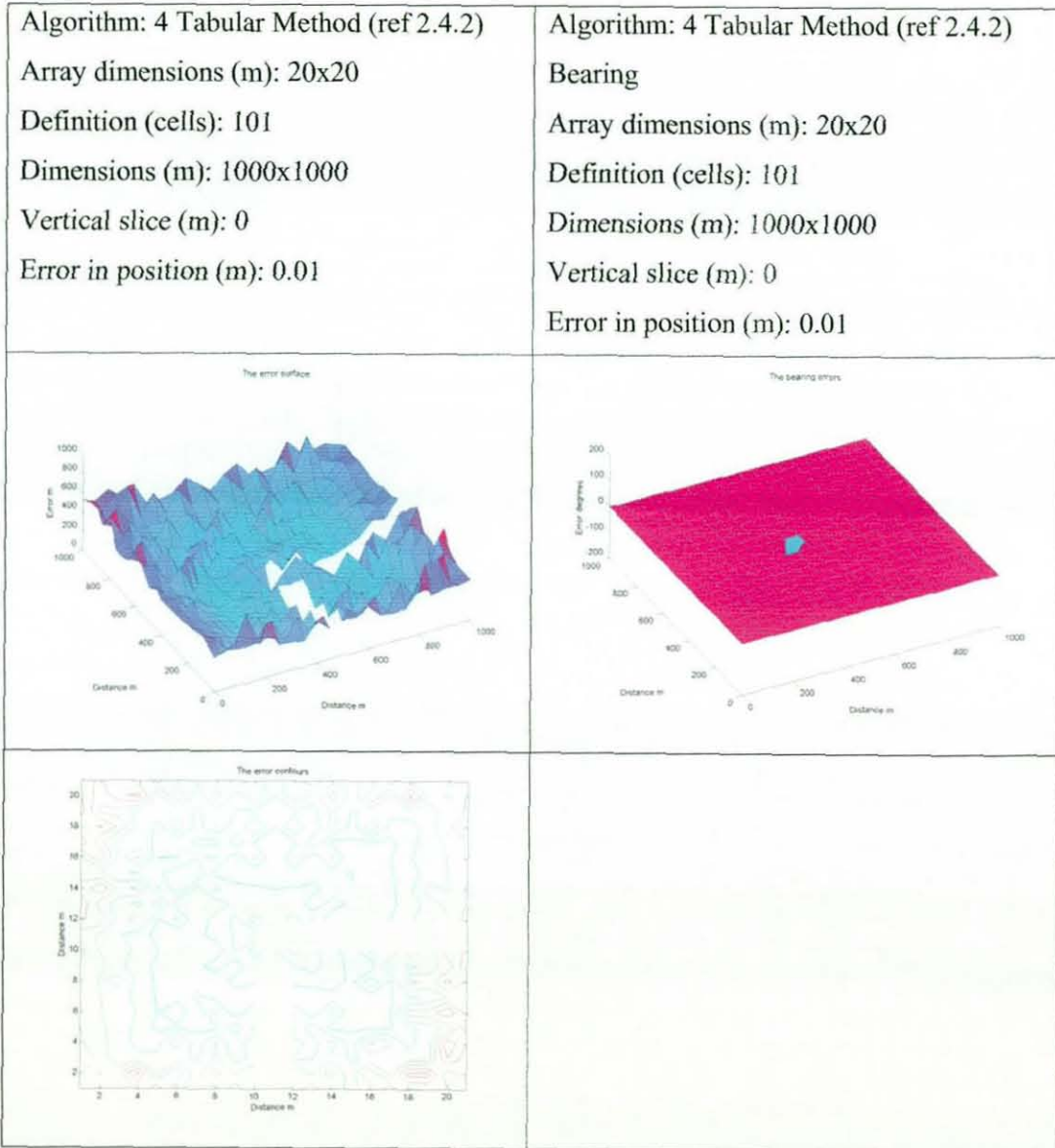


FIGURE 3.4-6A ERRORS CAUSED BY 0.1% ERROR IN RECEIVER POSITION WITH 20M ARRAY

Algorithm: 4 Tabular Method (ref 2.4.2)

Array dimensions (m): 2x2

Definition (cells): 101

Dimensions (m): 1000x1000

Vertical slice (m): 0

Error in Position (m): 0.1

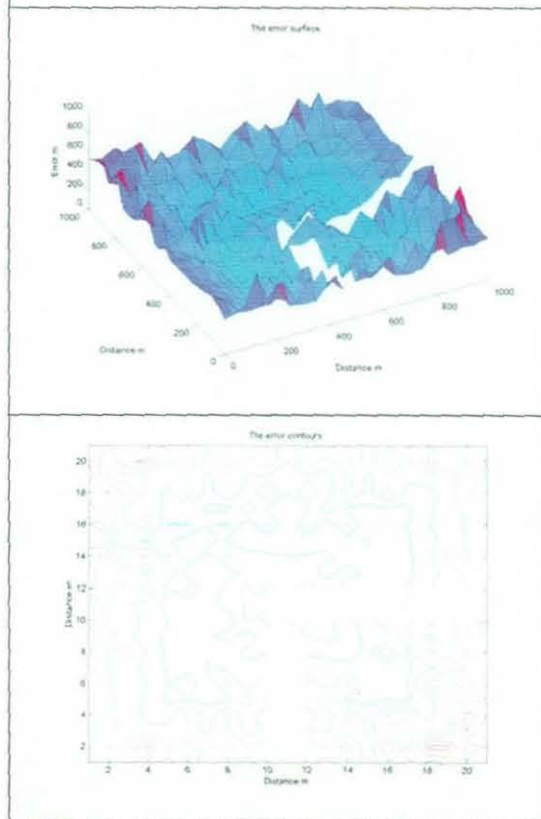


FIGURE 3.4-6B ERRORS CAUSED BY 1% ERROR IN RECEIVER POSITION WITH 2M ARRAY

In the worst case the bearing simulation (Figure 3.3-6C) shows virtually no increase in error (less than 1 degree). This serves to show that the method, although not very accurate in position, is still excellent at finding a bearing to the target.

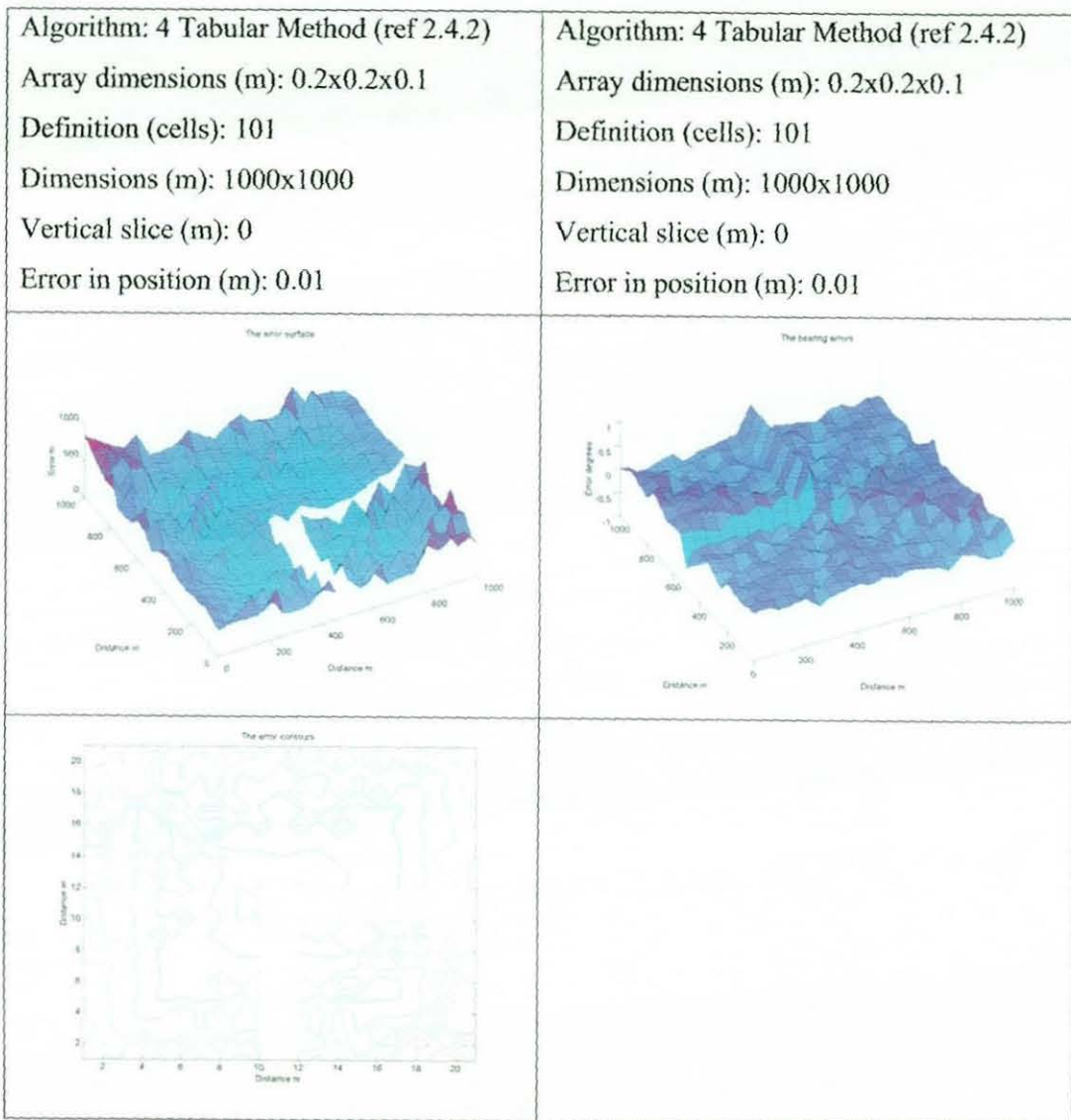


FIGURE 3.4-6C ERRORS CAUSED BY 10% ERROR IN RECEIVER POSITION WITH 2M ARRAY

3.5 OTHER TRACKING METHODS

3.5.1 THE REVERBERATION METHOD (METHOD 7)

Using the formulae in section 2.5.1

$$\theta_1 = \text{Cos}^{-1}\left(\frac{4A^2 - 2CD - D^2}{4AC}\right) \quad (\text{from 2-89})$$

and

$$C = \frac{G^2E - F^2E + E^2G - D^2G}{2(GD + EF)} \quad (\text{from 2-88})$$

we can get a range and depth of the source. By varying the timing accuracy and the velocity profile we can identify the errors caused.

3.5.1.1 NO ERRORS

As Figure 3.5-1 shows there is an error associated with this ranging method, in the range of 10^{-3} m. The graph shows the errors below the receiver, while those above the receiver are identical but mirrored.

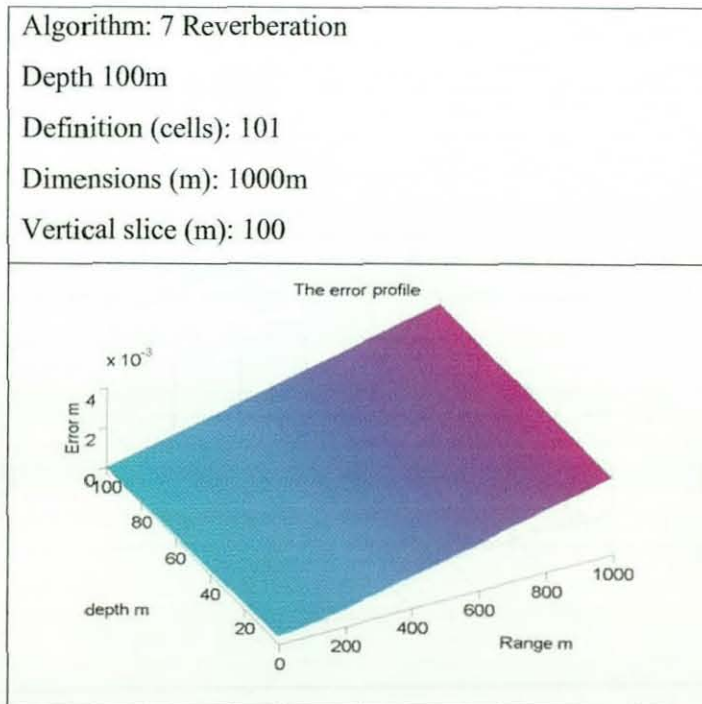


FIGURE 3.5-1 NO ERRORS

3.5.1.2 TIMING ERRORS

If we now insert a timing error in the simulation due to, for example, sampling rate or ray bending, we get Figure 3.5-2, which shows the errors due to timing definitions of 100 Hz and 1 kHz. These values are relevant, as this method relies on transforming to the frequency domain to identify the source and its reverberation, and tools to achieve better definition are rare.

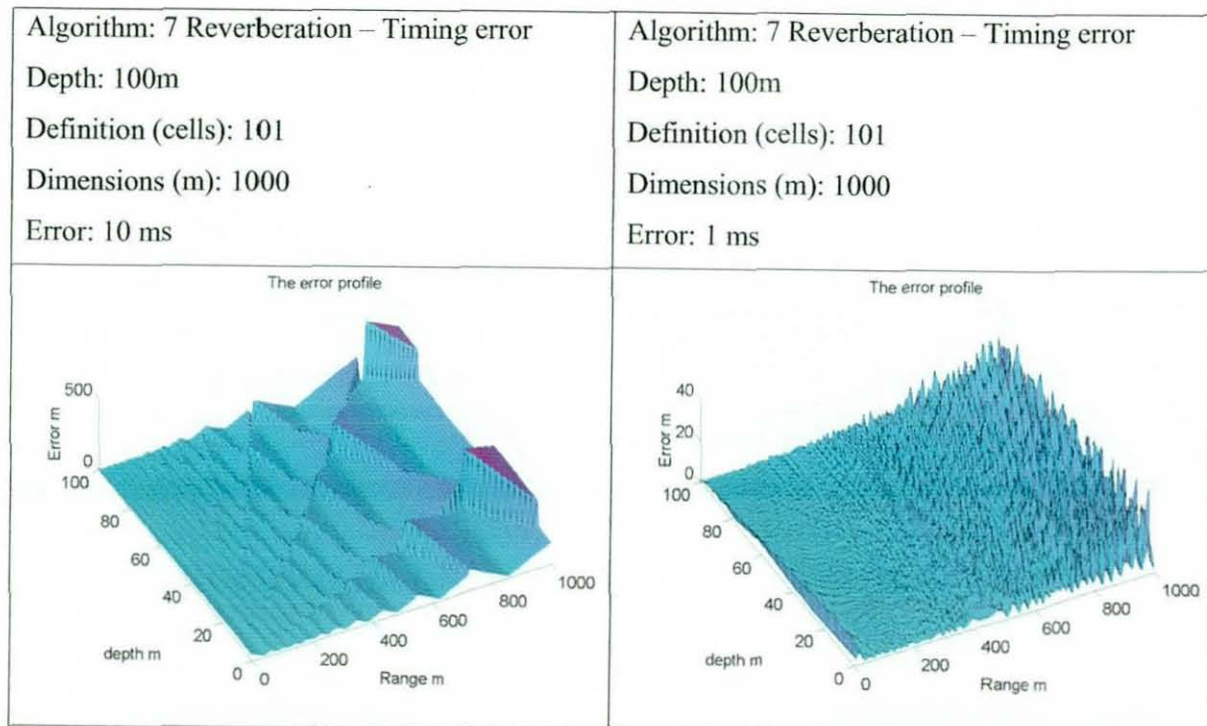


FIGURE 3.5-2 TIMING ERRORS

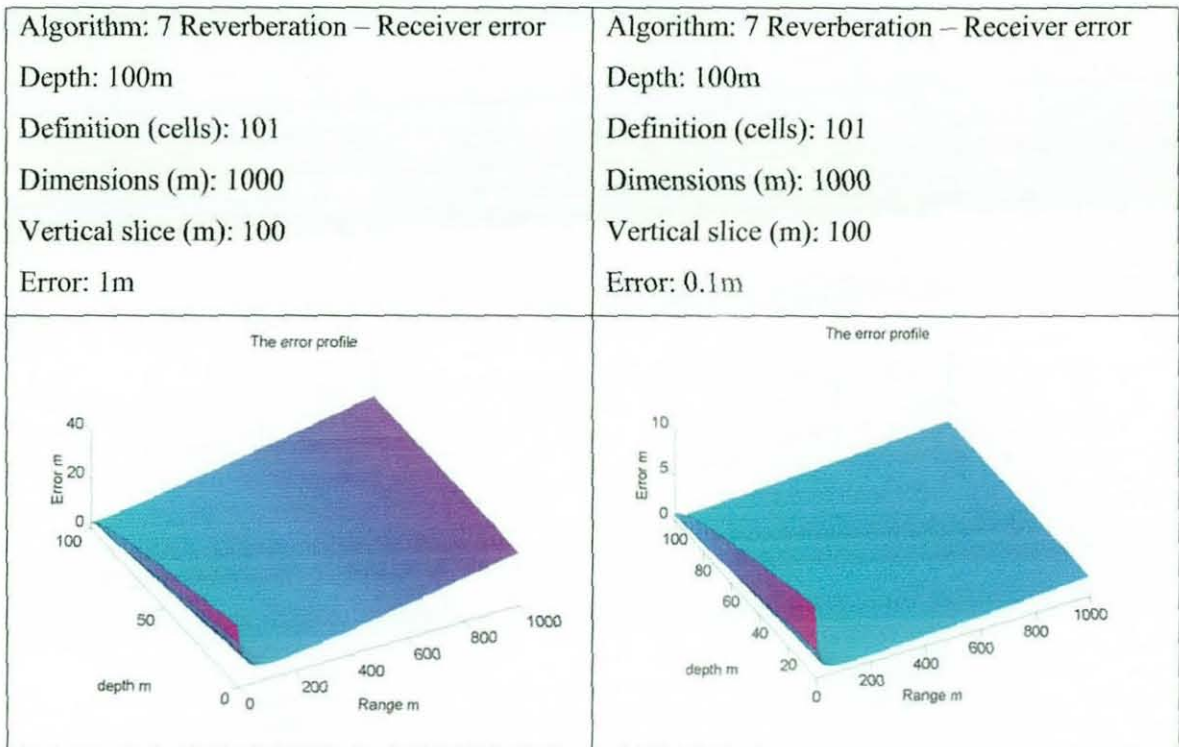


FIGURE 3.5-3 POSITIONAL ERRORS

3.5.2.2 POSITIONAL ERRORS IN THE VERTICAL

If we now place assume an incorrect vertical position of a transducer we get the results shown in Figure 3.5-3, showing that the algorithm is less sensitive to this form of error than timing errors. The major error is directly between the receiver and the sea-bed or surface.

3.6 COMPARATIVE ANALYSIS

The simulations shown in this chapter are the culmination of many simulations run with many of the parameters varied. There is not space, nor is it relevant, to show all the results here; however, some of the more interesting results from the algorithms are presented and some others are more extensively documented in Appendix B. The four algorithms presented all have advantages over the others and all are best suited for particular situations. Algorithm 1 is the only algorithm to use a three-dimensional array

and although algorithmically complex, it is reasonably easy to implement. The algorithm is reasonably robust to errors in position and timing error.

Summary of algorithms:

Algorithm	Description
1 Absolute method for 3D arrays	A direct method developed for use with tetrahedron arrays derived by subtracting spherical equations to remove time of flight
2 3D Absolute method for 2D rectangular arrays	A direct method for finding a target in three dimensions using a 2D square array.
3-4 Tabular methods	A two stage method, a calibration stage, calculates the possible timing differences, and sorts them by time. The second stage retrieves the most likely positions from the time differences
5-6 Excess receivers	A simultaneous equation method, using a matrix of equations for each hydrophone and solving them simultaneously using inversion methods (SVD)
7 Reverberation	A method of finding range and depth using a single hydrophone, relying on time differences between direct and reverberated signals

Algorithm 2 is very simple to implement but suffers badly from errors in position and is therefore best suited for fixed arrays such as boat-mounted systems; it also lacks direction information as to whether the source is above or below the array. If the array is mounted near the surface or near the bottom the information is not needed. Otherwise a further receiver is necessary; this must be placed out of the plane of the other receivers to detect the direction. This limitation is true of algorithm 6, which is robust if not accurate. The table method (Method 4) lacks in accuracy but can give very useful information at low sampling rates, and if combined with the reverberation method it can give accurate bearing and range, hence position, although at present only after post-processing.

The choice of algorithm is therefore difficult unless the application is known. If the system is fixed or needs to be flat, algorithms 2 and 6 are best unless the timing accuracy is severely limited, at which point algorithms 4 and 7 are suited. If the array cannot be fixed but must be flat, algorithm 4 and 7 are best. If the array is to be dynamic, algorithm 1 seems best.

3.7 RECOMMENDATIONS FOR FINAL SYSTEM

Ideal Parameter limits

Parameter	Value	Dependant upon
Array size Max, Min	20m-2m	Species, mounting
Range Max, Min	500m average	Species, received freq, SL and signal / noise ratio
Hydrophone Sensitivity	As high as possible	Sea state, noise, SL
Array Shape	Flat square, or tetrahedron	Mounting
Sample rate	>10MHz Update \leq 800Hz	Array size, mounting
Hydrophone type	Omni-directional	Mounting
Detection Frequency	30kHz – 120kHz	Mounting, Array size, species
Algorithm	Algorithms 1, 6	Array format
Array Type	Tetrahedron or Flat square	Algorithm, hydrophones

3.8 References in Chapter 3

- [1] Milne PH, *Underwater acoustic positioning systems*, London: E & F. N. Spon Ltd, 1983.
- [2] Coggrave CR, *Performance Analysis of 3D underwater tracking system using computer simulation techniques*, ed. Woodward B. *CETASEL 1*, pp. 41-41, Oct 1, 1996, Internal Report, Department of Electronic and Electrical Engineering, Loughborough University, UK.

Chapter 4

EXPERIMENTAL SYSTEMS

The aim of this chapter is to implement the theory discussed in the previous chapters by the use of electronic design and computer software. Two systems were developed and tested and some of the tracking strategies discussed in the previous chapter will be implemented in software to produce a full system capable of tracking impulsive acoustic signals.

The tracking system can be split into two main blocks, the data capture systems using mainly hardware or a combination of hardware and software, and the tracking algorithms and display, using PC-based software.

4.1 DATA CAPTURE SYSTEMS

Two methods of capturing the data were tried. The tracking algorithms rely on accurately measuring the timings between arrivals of impulsive signals on a number of channels. Being a passive system, the time of flight of a pulse is immaterial, the important information being the inter-pulse timing information. The timing accuracy required depends on the array size and the required tracking accuracy. The two methods designed provide a medium accuracy system (~500kHz bandwidth), and a very high accuracy system (20 MHz bandwidth). Both methods take into account the possibility of reverberation, which could possibly confuse the tracking algorithms.

4.1.1 FILTERED AMPLITUDE METHOD

The filtered amplitude method can provide timing accuracies in the worst case of up to $1 / 4f_0$, where f_0 is the frequency of the pulse or leading edge of the impulse. A typical value of a wide beamwidth dolphin click is approximately 40 kHz, so at this frequency the worst-case accuracy will be $\pm 6.25\mu\text{s}$.

4.1.1.1 PRINCIPLE

This method of data capture relies on timing the rising edge of the pulse. The signals

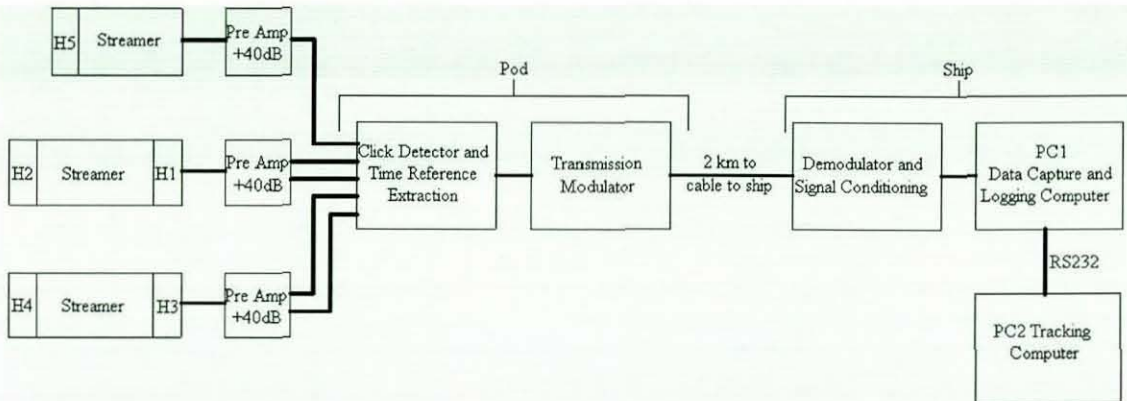


FIGURE 4.1-1 BLOCK DIAGRAM OF THE FILTERED AMPLITUDE METHOD

from the receivers are amplified and sharply filtered, and after removal of ambient noise the incoming signals are detected using a comparator. The output of the comparator is time-stamped and a monostable holds the output high for a fixed blanking period allowing any reverberations to pass undetected. When all channels have received a time stamp the times are subtracted and the resulting values are the inter-channel arrival times. Figure 4.1 shows a block diagram of the system.

4.1.1.2 METHOD

The filtered amplitude method has been implemented as a two-stage system. The first stage comprises the signal conditioning system. This takes the wideband signals from the receiver as an input, and outputs TTL pulses of which the leading edges provide the timing information of the incoming pulses. The second stage feeds the pulses (up to six in this implementation) into a PC via the parallel port, and calculates the inter-pulse timings by using the PC's clock. This timing data is transferred to a second PC for the algorithms to calculate a position.

The Signal conditioning section consists of four main blocks as shown in figure 4.1-2.

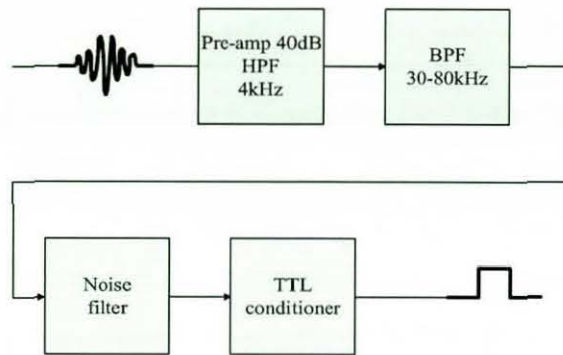


FIGURE 4.1-2 SIGNAL CONDITIONING HARDWARE

The pre-amplification section consists of filters and low noise pre-amplifiers. A gain of 40 dB is added to the signal and a single-pole high-pass filter is tuned to remove low frequency shipping and ambient noise. This circuitry is positioned close to the receiver transducer to reduce the likelihood of electromagnetic pick-up at the sensitive end of the system.

The signals from these preamplifiers then pass to an underwater pressure housing containing band pass filter sections designed to pass only the omni-directional part of the cetacean click. This removes any low frequency vocalisations of the cetacean and reduces the noise by allowing the system to work in one of the quieter areas of the noise spectrum. Phase shifts due to the filters can be ignored with this system as the signals and filters are identical, so that the time lag will be uniform across the channels. The likelihood of the received signal being that of the cetacean rather than any unwanted factors is now greatly increased and the signal timings can be measured.

To measure the ambient noise level, the signals from the filters are rectified and then

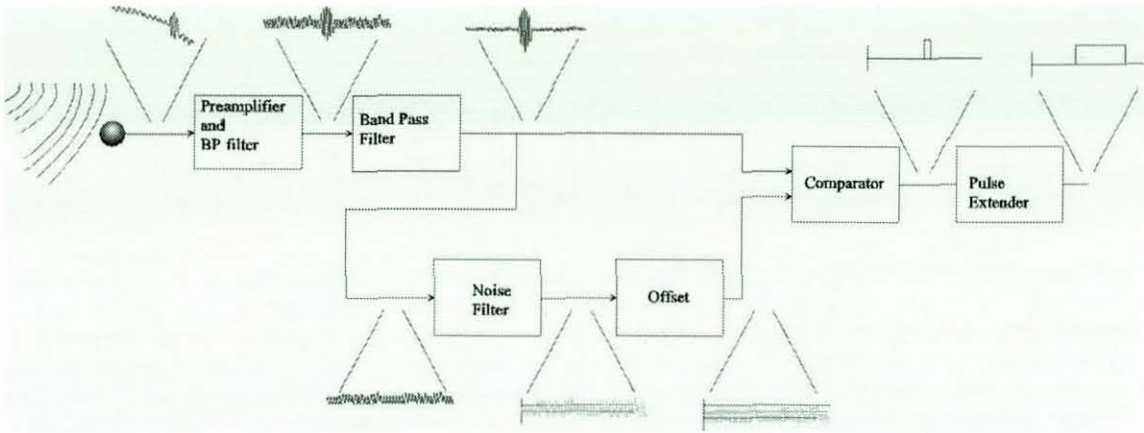


FIGURE 4.1-3 SIGNALS THROUGH THE CIRCUIT.

applied to a low-pass filter with a very long time constant. This averages the noise and provides a DC level. This DC level has an offset added as shown in Figure 4.1-3, to allow for perturbations, and this signal is then compared with the main filtered signal containing the cetacean echolocation clicks. The result of this comparator is a TTL pulse of a similar width to that of the click.

To remove the reverberations of the clicks, usually from the sea surface, sea-bed, or nearby objects, a blanking period is included after the comparator. This is achieved with a monostable, which effectively stretches the length of each received click to reduce multiple triggering by the same click.

Measurements of the inter-pulse times are performed by a dedicated PC at the surface (signal transmission techniques are discussed in section 4.3). This PC uses the system clock to time the arrivals of pulses at the pins of the parallel port. The code for this section removes any multi-tasking by the PC and dedicates the processor entirely to the timing process. The accuracy of the system depends on the speed of the parallel port, but is typically 5-10 μ s. Each time a pulse is detected, it is time stamped and dated and sent to the RS232 communications port of the PC. This sends the information to the main tracking computer without using the central processor.

4.1.1.3 LIMITATIONS

The major limitation of the system is the maximum achievable accuracy. The system was designed for a particular scenario (see section 5.1) where the limitations were acceptable; however, as the simulations show, a bandwidth of 500kHz does not yield acceptable error margins except with large array sizes (LBL). The system is neat in that it does not require complex processing underwater, but any adjustment of parameters within the underwater system is limited (i.e. filter bandwidth, noise-trigger offset). The accuracy of the time difference was imposed mainly by the method of pulse detection. The system relies on the detection of the first rising edge of the pulse at a particular threshold. If the amplitudes of the incoming signals are different (a very likely scenario), the level detector detects higher up the rising edge of the lower amplitude pulses. By ensuring all channels have a similar amplitude, therefore triggering at the same point of the rising edges of the pulses, the noise floor is also adjusted on each individual channel, which means they do not detect at the same point. A better method of detecting the pulse is therefore needed to increase accuracy.

4.1.1.4 TESTING

Testing the system was performed on the bench using a dolphin simulator package, with a PC to emulate a cetacean swimming in space and producing echolocation clicks at a pre-programmed rate. The timings were calculated for given array dimensions and the pulses were produced via the parallel port. The display of the simulator can be seen in figure 4.1-4. This allowed signals to be injected into the circuit at the output of the comparator to test the transmission system or directly into the timing computer PC1. The software also had the facility to send the RS232 message to the tracking computer PC2 to test just the algorithm stage. Further results of the system can be seen in Chapter 5.

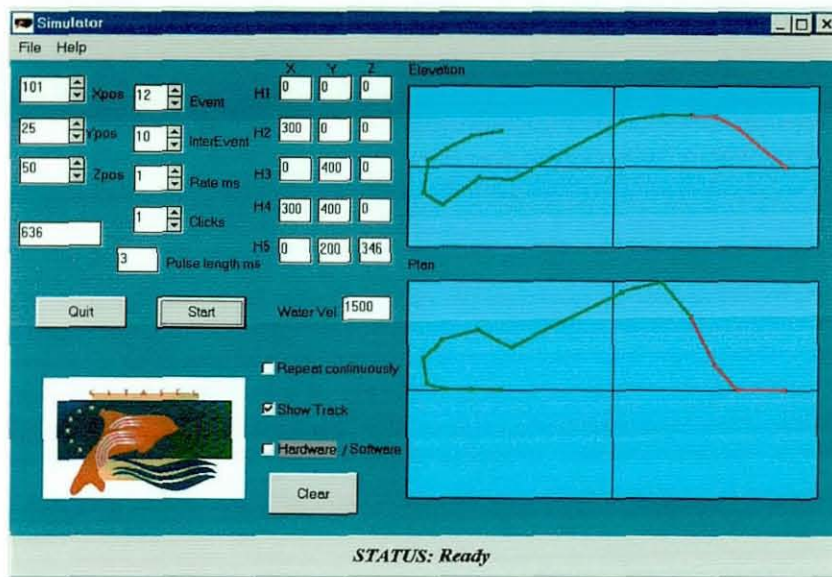


FIGURE 4.1-4 DISPLAY OF CETACEAN ECHOLOCATION CLICK EMULATOR

4.1.1.5 RECOMMENDATIONS

The process of designing and testing the system highlighted a number of limitations. The working environment imposed some limitations, as did the principle of operation. The system provided the greatest possible accuracy for the conditions imposed. The next stage in the development of the system was to remove some of the limiting factors and to redevelop the system with greater flexibility so that it is capable of running in a high definition mode in addition to the low frequency mode, as described. The system would benefit greatly from a capability to adjust the important parameters from the surface. Such parameters would be preamplifier gain, the break points of the filters and the level of the detection threshold on the comparator.

4.1.2 CORRELATION METHOD

To improve the previous system such that the recommendations of section 4.1.1.5 were taken into account a slightly different approach had to be taken. The first system was limited in time accuracy by the point of detection of the amplitude of the incoming signal. If instead the same cycle of the incoming signal were detected it is then possible to match the phase of the incoming signal relative to the other channels. In this case the time accuracy could then be vastly improved, and could in principle be

as accurate as the sample rate of the digitiser for the correlator. This section describes such a system using a correlation technique with a few short cuts.

4.1.2.1 PRINCIPLE

Signals arriving from the receivers are stored in memory as they arrive, the channels of data are then correlated with each other and the peak of the correlation is then detected as the time of arrival. The duration between these peaks is the inter-pulse timing required by the algorithms. To ensure the signals are similar enough to produce a good correlation, it is important that the same frequency component of the incoming signal is received. To achieve this, sharp band-pass filters are required.

4.1.2.2 METHOD

It was decided that this system would have as high an accuracy as was possible within

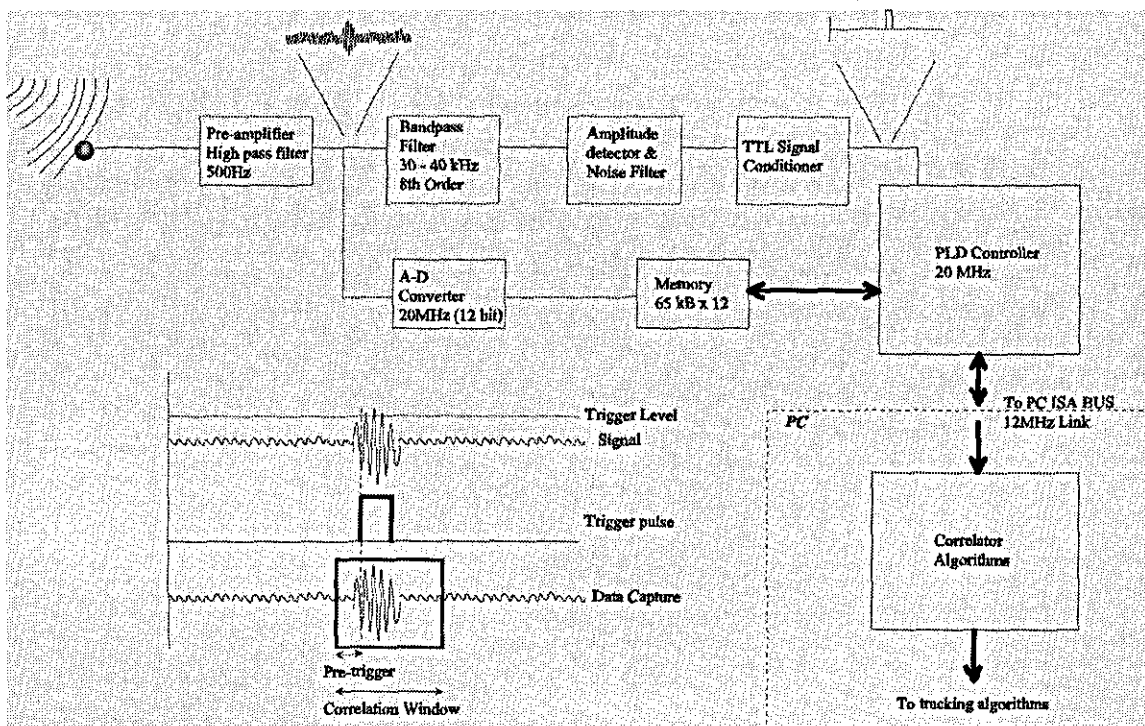


FIGURE 4.1-5 BLOCK DIAGRAM OF THE COMBINED CORRELATION/AMPLITUDE SYSTEM

the constraints of budget and technology. A 20 MHz sampling system was considered feasible. To achieve this high sample rate it is impossible to use most microprocessors. Instead a Field Programmable Gate Array (FPGA) or a Programmable Logic Device (PLD) was considered. These devices are capable of working at more than 100 MHz and although limited in functionality, they were considered to be capable of performing the tasks for this system. It was decided to use

a PC to perform the correlation process. However, to have a real time correlator for up to eight channels working at 20 MHz was considered unachievable. There is little point in correlating all the data arriving at the receiver if the desired part of the data can be detected, however coarsely, and is of a predictable length, as is the case with cetacean echolocation clicks. Instead the click can be detected using a filtered amplitude method, as described in section 4.1.1, and a window of data is captured at this time. The capture window has to be rolling, so that at the time of click detection, a pre-set window time can be generated before the amplitude trigger. This allows the whole click to be recorded and not just the section after the trigger. Performing this operation means the amplitude circuit records coarse timings that can be finely tuned by the correlation. Figure 4.1-5 shows how the signal is detected. If the system is working at 20 MHz sample rate, it looks for a pulse approximately 300 μ s in length at 40 kHz. As figure 4.1-5 shows, it is necessary to have the window larger than the pulse so as to catch the beginning of the pulse and to allow for errors created by the amplitude detection method. This means approximately 600 μ s of samples are recorded and correlated. This amounts to correlations of two channels, each with 12000 samples, which are achievable in near- real time.

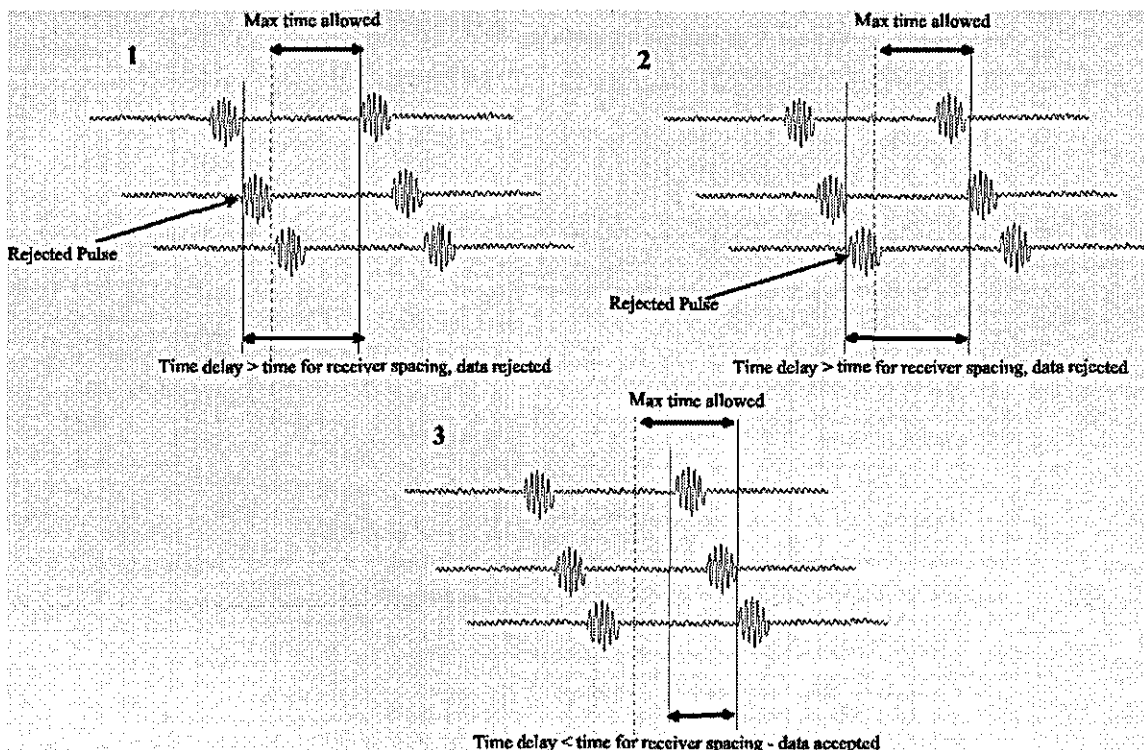


FIGURE 4.1-6 ROLLING WINDOW TO PREVENT MULTIPLE CLICK DETECTION

The hub of this system is the PLD controller, which serves as a form of processor with the task of organising data capture, capturing the trigger times, and keeping a log of which channels triggered at which time. It must also count the pulses such that it can indicate to the PC when a new data set is valid. Like the previous system a blanking period is required to prevent the system re-triggering on reverberations. In addition to this the system can be made to check each time as it arrives to check if the time period between the timings is feasible. If the time between the first and last arrival is greater than the greatest possible timing (due to receiver spacing), as shown in Figure 4.1-6, then the first arrival is removed and a new one recorded. This reduces the possibility of different pulses being received in the same capture window. The internal structure of the PLD contains four main blocks, each performing separate tasks and capable of running simultaneously. By allowing simultaneous operations, the speed of operation can be increased, the only limitations being safeguards to prevent simultaneous access to the controller peripherals such as the memory and the PC ISA bus. Figure 4.1-7 shows a block diagram containing the inner structure of the PLD.

The housekeeping of the controller gives the user greater control of such things as gain and filter characteristics. Gain adjustment is achieved with the use of digital potentiometers. Wiper values can be programmed directly into the potentiometer giving different gain values as required. The software can therefore perform the function of an automatic gain control by monitoring the incoming signal. The filter characteristics can be adjusted using a serial link to the controller. It is then possible to change the passband of the band-pass filter by software control. This is particularly useful for the diver tracking implementation of the system, as the variable filter band allows multiple pingers to be operational simultaneously, each operating at a different frequency. The users can then select which pinger they wish to track.

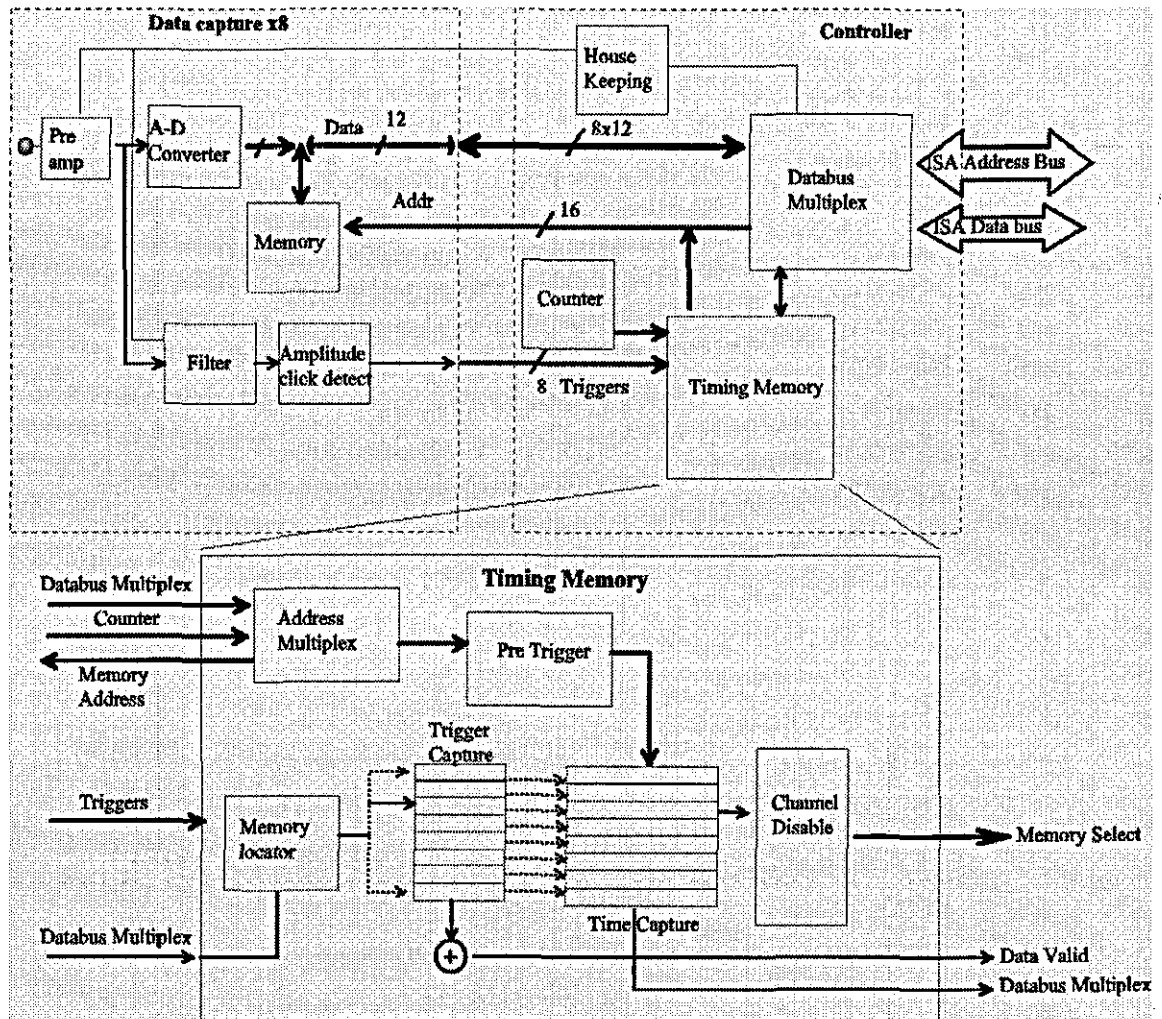


FIGURE 4.1-7 BLOCK DIAGRAM INCLUDING THE INNER STRUCTURE OF THE PLD

4.1.2.3 LIMITATIONS

This system is much more robust than the first system; however, the coding method is limited in its multiple pinger mode. The variable filter is 4th-order and the number of pingers is limited by the useable bandwidth and by the bandwidth needed for each pinger. The system is also limited in the repetition rate in real-time mode. Transfer of the data to the PC takes some time approximately 10ms per channel, but more significant is the time taken to perform a correlation in software. The implementation of a DSP capable of performing the real time correlations would improve the speed, but would also significantly increase the cost of the system.

4.1.2.4 TESTING

Testing procedures are as follows:

- a) Test the circuits by injecting a dolphin-like click. Test that the times are accurate and that parameters can be changed in the circuit.
- b) Tank test one channel of the system, and check that the data correlates and that the software controls the hardware adequately.
- c) Tank test four channels of the system. A source is accurately placed in the tank and a dolphin like click is emitted into the water. Four accurately placed receivers collect the data and store. The stored information can then be correlated and compared with the true value.

The hardware, once tested, is interfaced with the tracking algorithms and the complete system can then be tested.

4.2 TRACKING SOFTWARE

The software is written in Pascal in the Delphi environment. It is Windows-based and uses the multi-tasking properties of Windows 95+ to perform multiple operations simultaneously where necessary. Two versions of the software have been created. The first uses solely the array method, whereas the second is primarily to capture data for post processing, but is also capable of all the near-real time methods discussed.

4.2.1 ARRAY METHOD

This software is designed to operate with the low definition data capture system. The look-up table system described in section 2.4.2 was coded under Microsoft Windows 95 using a mixture of Borland Delphi 2 (Pascal) and C++. The code was later transposed to Borland C++ Builder. By the use of threads, these packages offer multi-tasking, allowing a number of processes to be performed simultaneously. This feature is essential for the tracking system due to the necessity of calibrating and tracking in real-time. Although Delphi 2 is a user-friendly package allowing object-orientated software to be developed under Windows, its complexity tends to slow the software, so for this application a large amount of the background processing was coded in C++ and Assembly language.

The software has four main processes running continuously. These processes calibrate the system, run the tracking algorithm, read the information from the serial

port (data from the data-logging computer), and run the clock, which becomes complicated due to the speed restrictions of the PC. Data arrives from the array in real time and all data needs to be displayed; at the maximum click rate of the system this can mean up to 667 clicks per second on all five channels. If this happens at the same time as the calibration, the machine may be unable to process the data in real time. To allow for this, the system has two clocks, one showing real time, the other showing the time of the data. If the data is too fast, this clock slows to match the time-stamps on the data. This clock then runs in real time, and clocks out the received data at the correct track time, i.e. if the clock slows due to a data overload, and then falls to an acceptable rate, the clock stays in time but 'slow'. The software also contains a 'fall back' mode, which is only capable of producing crude vectors to the source. This works by placing the received click differences in coarse bands and giving sectors for the source location. At worst, this supplies 16 sectors, and as the confidence in the accuracy of the time differences grows so do the number of sectors. The following sections explain the logical flow of each of the main threads:

Channel no.	Date	Time hh:mm:ss	μ s
-------------	------	---------------	---------

FIGURE 4.2-1 SINGLE CLICK TIMING MESSAGE

(a) *Data-capture thread.* The data-logging PC receives two main pieces of information, clicks from the five hydrophones, and calibration data from the calibration controller hardware. The data from each channel is processed in the data-logger and is passed in the format shown in Figure 4.2-1. The normal data is stored in a large rolling buffer, which can be accessed by the other threads. When the buffer is full the data overwrites; however by that stage the data should have been used and so this has no effect. If calibration data is received it is passed in the same format but an extra channel (number 6) is used to indicate the special nature of the data, which is placed in a separate buffer and handled when the calibrator becomes available.

(b) *Calibration / sort thread.* Calibration of the array may happen at any time, depending on the stability of the array. The calibration is initiated by the hardware and always follows the same procedure, shown in Fig. 4.2-2. Each time a calibration

ping is transmitted the start-of-pulse time is transmitted and converted to a time / date stamp by the data-logging PC. A header is inserted, indicating that the data is calibration data. The next five pieces of data are the timings from the five hydrophones. Each one is given a header with its channel number and then the time information is passed. This happens three times, as each pinger is activated. The software performs some basic checks on data validity, and then begins the main calibration routine. Figure 4.2-3 shows the logical process of array calibration.

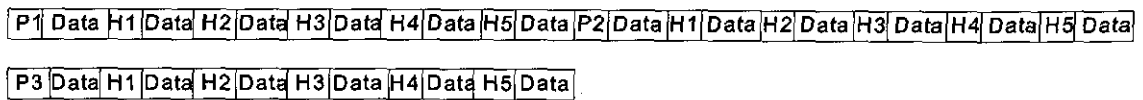


FIGURE 4.2-2 CALIBRATION PROCEDURE

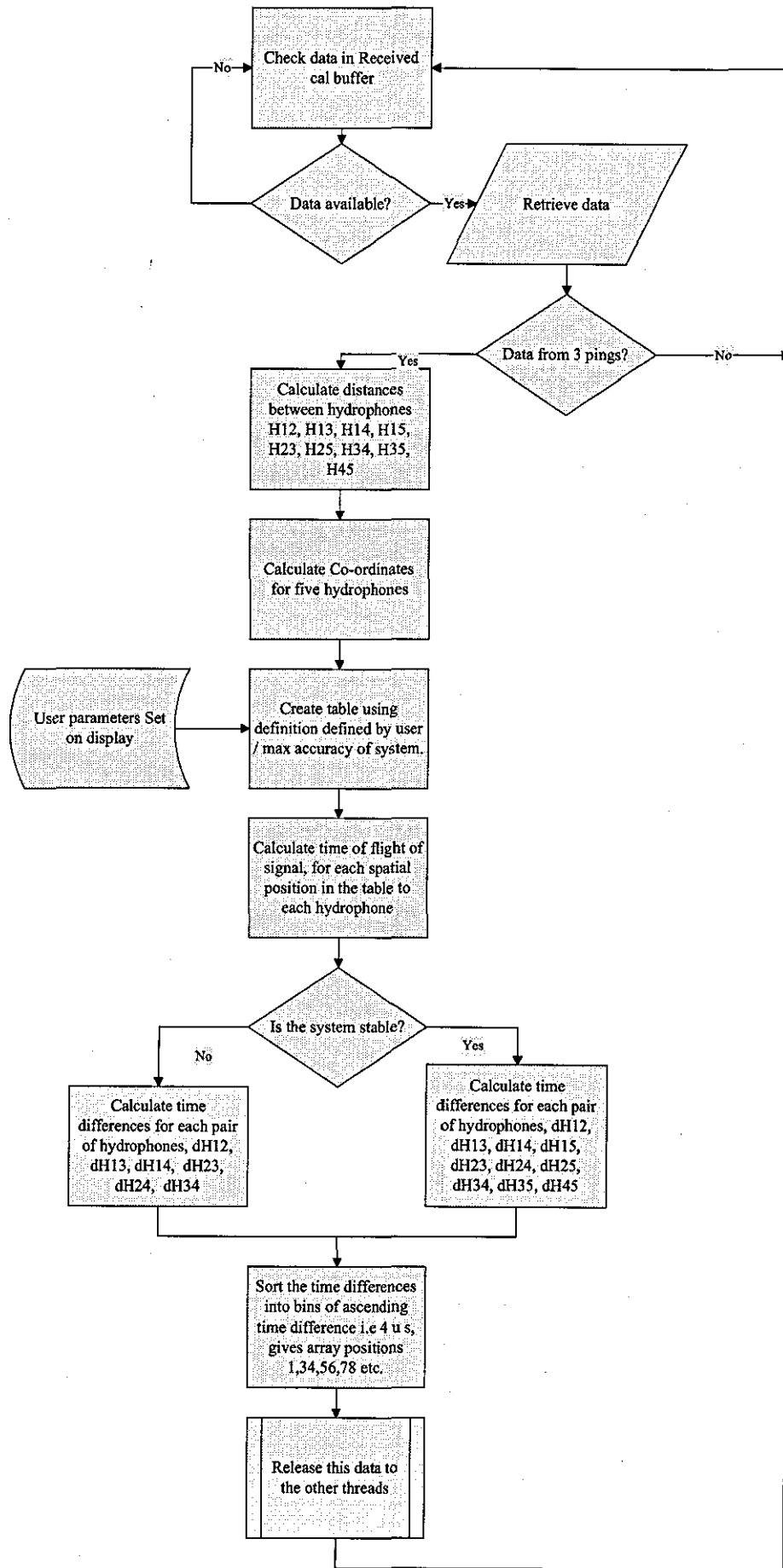


FIGURE 4.2-3 LOGICAL CALIBRATION PROCESS

The timing data arriving in the calibration receiver buffer can easily be converted to distances between the different sets of hydrophones. These distances are then converted into three-dimensional co-ordinates in x,y,z, with hydrophone 1 as the datum point. From this information the new look-up table can be generated. Pre-set information by the user determines the size of the space around the tracking array to be scanned. The accuracy of the timings defines the maximum definition of the look-up table. A user-defined accuracy is used to predict the number of zones available. For each of these zones the distance to each hydrophone is calculated using three-dimensional trigonometry from the times of flight, which are calculated using an assumed velocity of propagation. The difference between each of the hydrophone signal arrival times is then calculated. Six values result (ten if H5 is used) for each spatial position on the table. For speed in the tracking thread, these values are sorted into timings. Each timing band (i.e. if accuracy is $1 \mu s$ then the bands are separated with $1 \mu s$ spacings), named a "bin", contains all the possible positions for that hydrophone at that time. Effectively, each bin describes a paraboloid for that particular time difference.

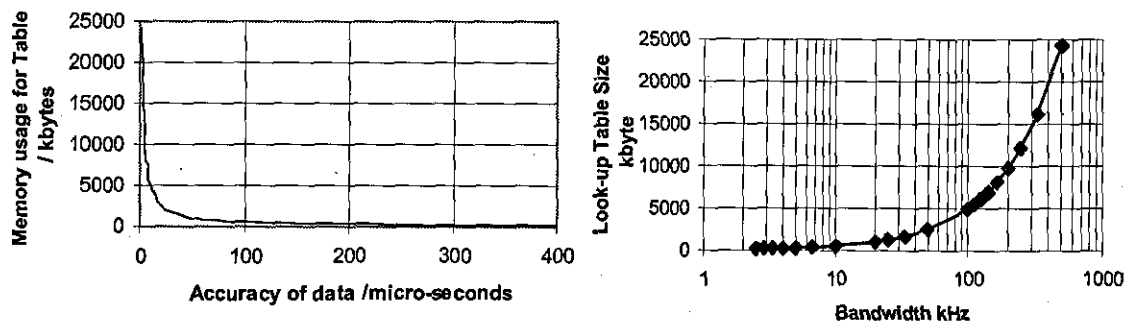


FIGURE 4.2-4 MEMORY VS ACCURACY OF DATA

A two-table system is used throughout operation. On initial start-up the first table is generated from approximate values. Once calibration data has been generated, this table is made available to the tracking thread, and the old one is replaced by the next calibration. Figure 4.2-4 shows the amount of memory required for the look-up table, using all five hydrophones to generate the table as the accuracy of the incoming data varies.

(c) *Tracking thread.* The main calculations are performed during calibration. The tracking procedure is quite short, which is ideal for real-time performance. Figure 4.2-5 shows the flow diagram for this thread.

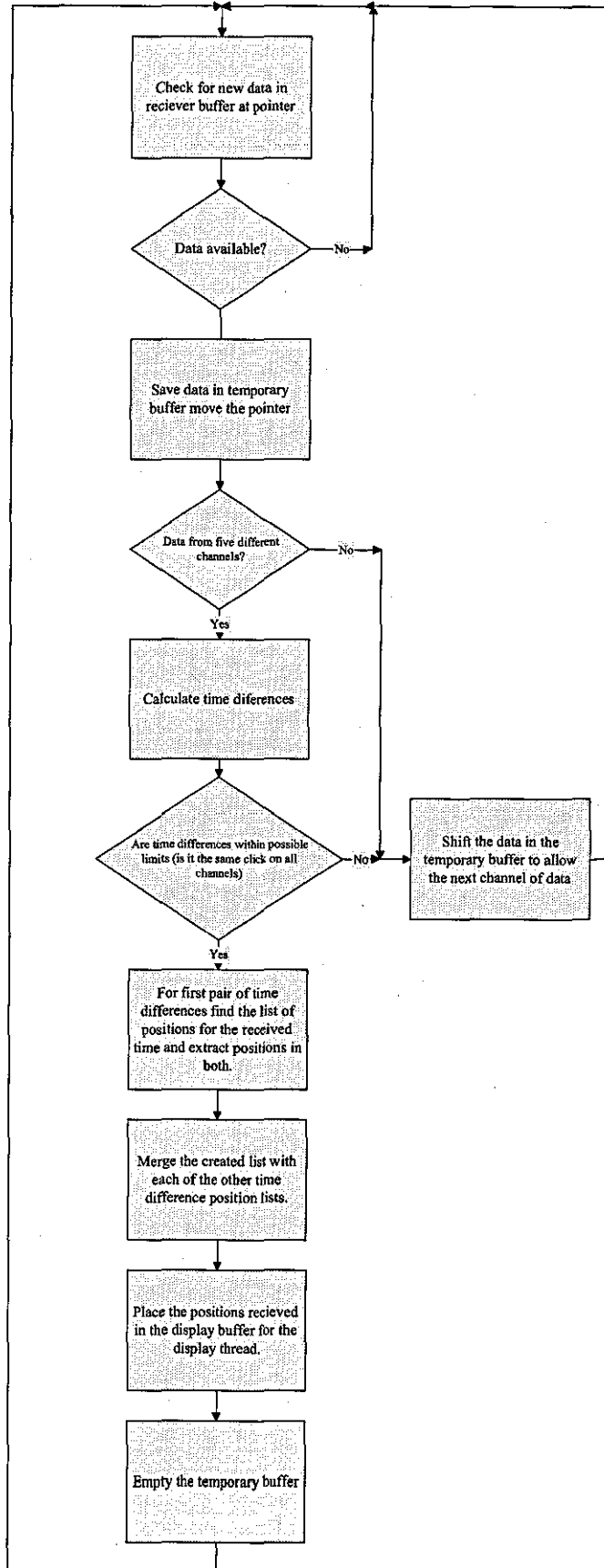


FIGURE 4.2-5 CALIBRATION FLOW

The system performs validity checks on the data as it arrives. It then takes the first pair of time differences and compares the appropriate time bins. The positions present in both bins represent the intersection of the paraboloid surfaces for those three hydrophones. This may result in a large number of positions depending on the accuracy of the timings. This table is then compared with the next set of time difference and the intersections are again found. This process is repeated for the six time differences, or ten time differences if the fifth hydrophone is used. The resulting position or positions are centred on the area from which the echolocation click emanated. This position is translated from a look-up table address to the x,y,z coordinates and is placed in the position buffer for the display thread and logged. As the accuracy of the timing data is reduced the number of locations increases, but the position of these points tends to follow a vector towards the source.

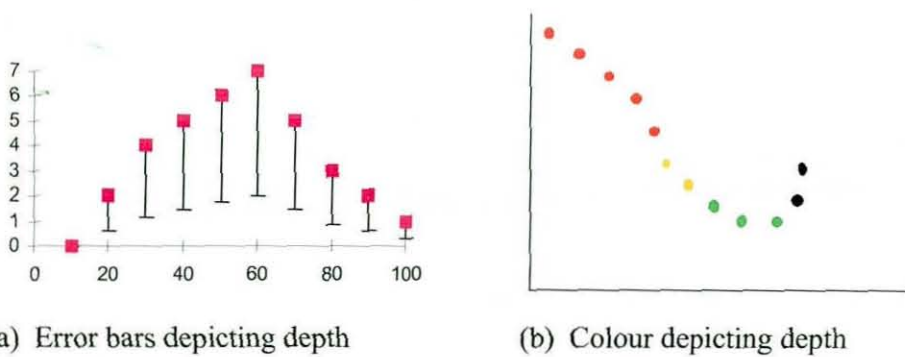


FIGURE 4.2-6 DISPLAY METHODS

(d) *Display thread.* There are various methods of displaying three-dimensional information on a two-dimensional screen, as shown in Figure 4.2-6. These include the use of pseudo-three-dimensional graphics, i.e. size and diagonal displacement, or the use of colour or error bars to show the third dimension. Other methods include splitting the third dimension from the other two, i.e. plan and elevation, or by the use of high technology methods such as virtual reality and stereo vision or colour / polaroid glasses.

As the system is designed as an analysis tool it is important to be able to detect ranges accurately. This rules out all these methods except the simple plan / elevation method. The display thread adopts this method, and displays each source as a dot or vector on a scaleable background. Other parameters needed from the user are entered in a page-sized section, which temporarily becomes unavailable when the system is in use. Figure 4.2-7 shows the display. The system regularly monitors the position buffer generated by the tracking thread. The information is synchronised with the track time and clocks out the information to the display by a time-stamp on the data. In this way everything happens in pseudo-real time. The display also shows the status of the system, including time between calibrations and distances between hydrophones.

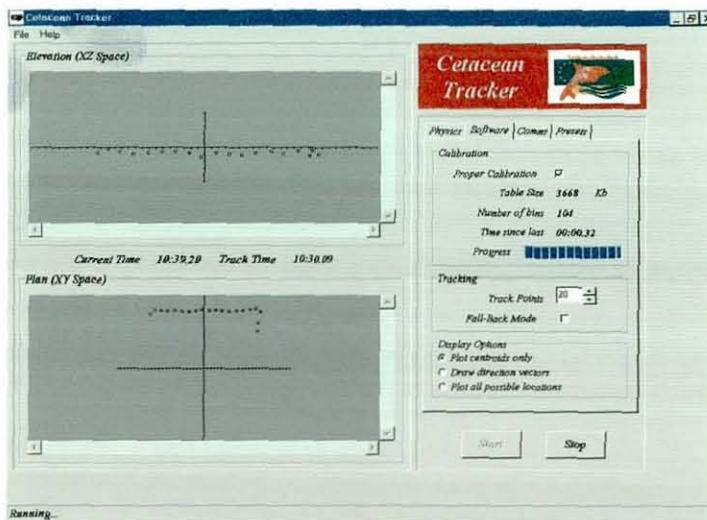


FIGURE 4.2-7 DISPLAY

4.2.2 HIGH DEFINITION SYSTEM SOFTWARE

This software, designed to run with the high definition system, is programmed under Windows 95, using Pascal and Delphi, and uses multi-tasking to perform the various tasks simultaneously as required. The threads running on this software depend on which algorithm is in use. In continuous use are the threads for correlation, data transfer, and the system control, the data logging and display. This software is not fully developed and for most results so far the data has been post processed using MatLab; however, it is a simple task to implement most algorithms directly into the software to provide a near real-time track. Time limitations have prevented this.

4.2.2.1 TIME DIFFERENCE EXTRACTION

The system described in section 4.2.1 uses the amplitude of the arriving pulses to determine the time of arrival and hence the time differences. By sampling the whole signal it is possible to do direct signal comparisons and hence use correlation to find a more exact time difference. Correlations have been calculated using standard FFT techniques. Each echolocation click is estimated to be 3-600 μ s long, which if sampled at 20 MHz gives 12000 data points. Cross-correlation of four of these (three correlations) in MatLab takes a number of seconds. Encoding these directly into the Pascal software or using machine code greatly reduces this time period. To ensure that optimal use is made of the sampled data, several real data points have been processed manually using MatLab and extra stages have been added to the time extraction process.

The time differences are extracted in the following stages:

- a) The incoming signal is band-pass filtered to the expected range (Figure 4.2-8A).
- b) Using a low-pass filter the noise level of the channel is detected.
- c) An offset is added to the noise value and when this value is crossed, this is deemed to be the start of the incoming click.(Figure 4.2-8B&C green/light blue).
- d) When a signal is detected a preset time sample is recorded (with a pre-trigger), i.e. 12000 samples.
- e) This signal is sent to the PC together with the same time period of memory from the other channels.
- f) The pairs of signals are cross-correlated to give a time difference.

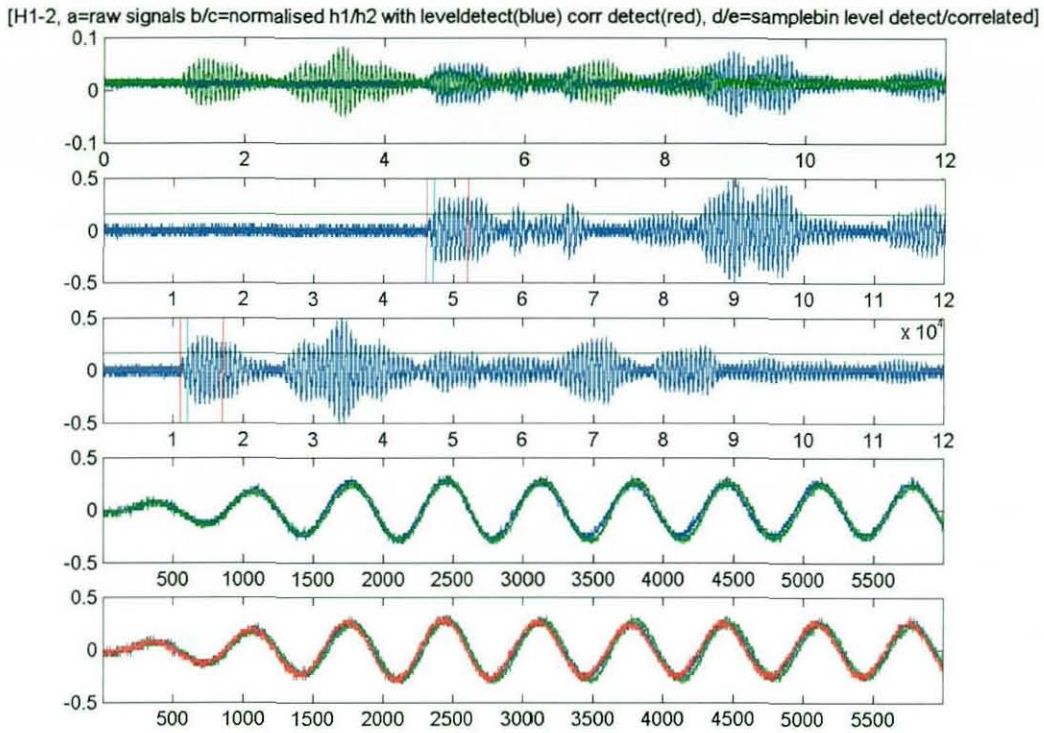


FIGURE 4.2-8 PROCESSING STAGES:

- (A) BOTH RAW SIGNALS,
- (B) RX1 WITH CALCULATED DETECTION LEVEL (GREEN), DETECTED PULSE TIME (BLUE), AND THE CORRELATION BIN (RED)
- (C) AS FOR (B) FOR RX2
- (D) AMPLITUDE DETECTED SIGNALS OVERLAID (BLUE AND GREEN)
- (E) AMPLITUDE SIGNALS AND CORRELATION-DETECTED SIGNAL (GREEN AND RED)

Problems may occur if the signals have some interference, the peak correlation may not correspond to the correct cycle of the signal. In Figure 4.2-9A the peak should be in the middle of the correlation but is actually one cycle later. In this case the correlation is rectified and low pass filtered to give an envelope of the signal. The peak of this signal is then more likely to be close to the actual peak cycle of the original correlation. This peak is then used instead.

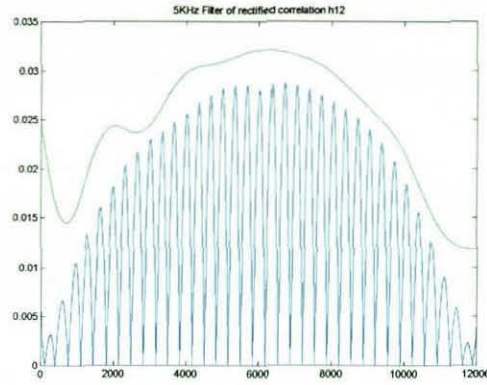


FIGURE 4.2-9B: RECTIFIED AND FILTERED CORRELATION

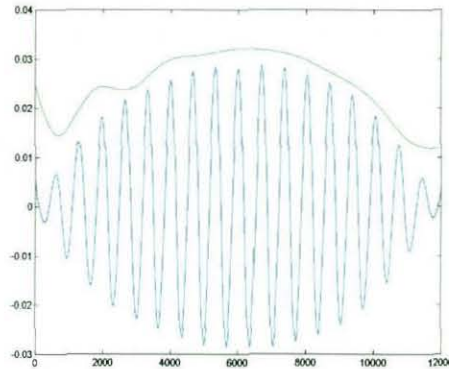


FIGURE 4.2-9A: CORRELATION WHERE MAXIMUM CORRELATION IS ON INCORRECT CYCLE

- g) To ensure full utilisation of the sample rate the peak correlation cycle (Figure 4.2-10A) is then re-correlated with a half sine wave of the same length (Figure 4.2-10B) to find the centre of the peak. It is therefore possible to re-sample the correlation to give an interpolation of this signal to increase the accuracy by a factor of two.

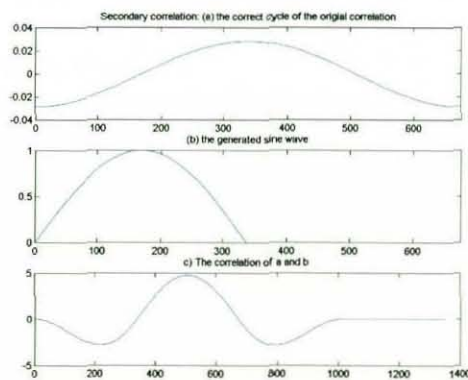


FIGURE 4.2-10 SECONDARY CORRELATION TO GET INTERPOLATED CORRELATION PEAK

- h) The time of this peak is the time difference between the channels as shown in Figure 4.2-8E (green and red).

4.2.2.2 DATA TRANSFER

As described in section 4.1.2.2 the system consists of two data capture sub-systems. The first sub-system, as described in the previous system, detects the voltage level of the envelope of the pulse, and when this exceeds a predetermined point the time is recorded. Once the signal is captured on all channels the PC downloads these channel numbers and the corresponding times. Each of these is 18 bits long and takes virtually no time to download (0.18ms).

The second sub-system consists of a user-definable length circular buffer with a maximum of 65536 data points (3.3 ms). When a click is detected, this buffer is filled with the click data and a user-definable number of data points before the trigger (pre-trigger) is enabled. When the buffers are full for each channel, the PC uploads this data. Data is transferred from the tracker memory directly via the PC ISA bus, allowing data to be transferred at rates of up to 100kbit/s.

4.2.2.3 SYSTEM CONTROL

The system has shared control of the tracking system, and in data capture mode the system itself controls the data capture and timing processes. When the required number of pulses has arrived the system indicates the presence of new data to the PC using an interrupt. The PC then takes control and downloads the times and channel numbers. It then checks if first and last arrival times are possible. This relies on the user programming the largest spacing between receivers (usually the diagonal). If the time difference is too great this indicates the system has not detected the same pulse on all the channels. This could indicate that the end of the previous pulse may have been detected, that noise is interfering with the triggering, or that there is more than one pulse in the water. In this case the PC wipes the first pulse from memory and instructs the system to continue capturing. This is repeated until a valid pulse occurs. At this stage the PC downloads the memory, and processes the data. As the capture stops whenever the correct number of pulses occurs, the system cannot rely on the pre-trigger if a false click has occurred. If this happens more than one time the system resets and start collecting anew.

4.2.2.4 DATA LOGGING

Data is stored in binary format, which when full data sets are stored amounts to approximately 150 kilobits per click. Memory is stored initially to RAM and then to

hard disk when approved. If correlation is performed in software this quantity of data is vastly reduced, since only the time differences and the collection time need to be stored.

4.2.2.5 DISPLAY

The data capture system display is very efficient. Since there is little to be displayed, only status and the control parameters are permanently on the screen, together with the control buttons. The software contains a display option allowing a user-defined number of points to be viewed on screen.

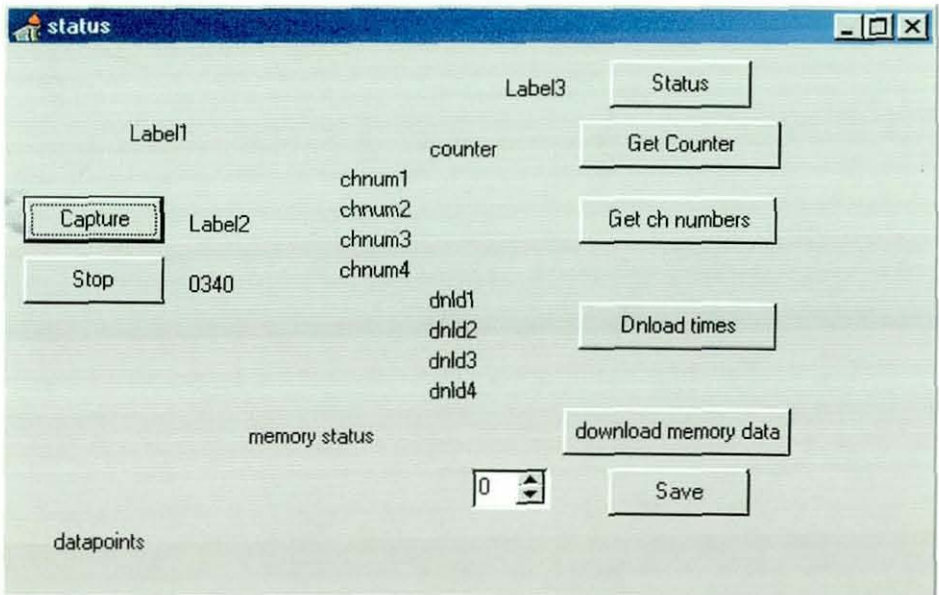


FIGURE 4.2-11 BASIC DATA CAPTURE SOFTWARE SHOWING ONLY STATUS INFORMATION

The user can also display the position of the ping with respect to the array in the xy, xz co-ordinate system when the tracking algorithms are used in real time. Figure 4.2-11 shows the basic data capture system software display that enables the user to capture and downloading of data but without displaying the data itself.

Figure 4.2-12 shows the more elaborate software that incorporates displays for the raw data and the window control algorithms, as well as the tracking algorithms.

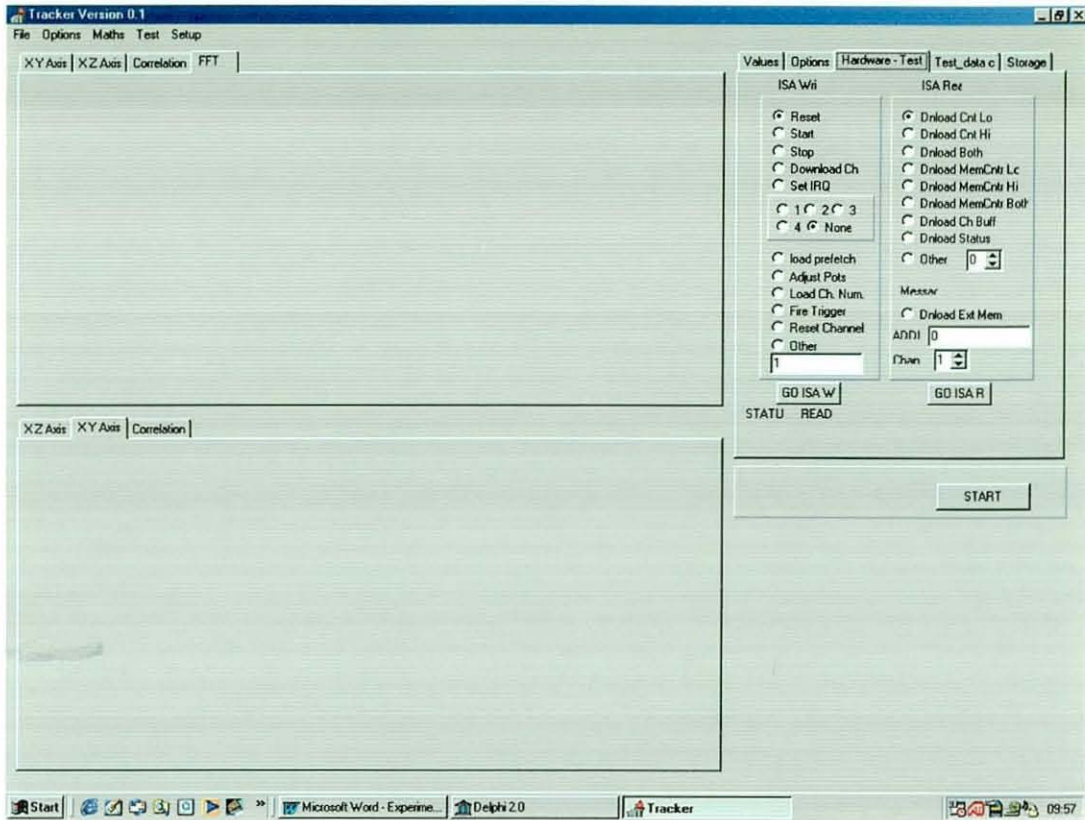


FIGURE 4.2-12 FULL TRACKING SOFTWARE.

For pure demonstration of the system functionality and display of individual points it was considered sufficient to plot the positions of pings in two dimensions using MatLab. In this case a reference can be included showing the true position of the source and hyperbola can be shown indicating the possible positions for each time difference. In this case the output will be as in Figure 4.2-13

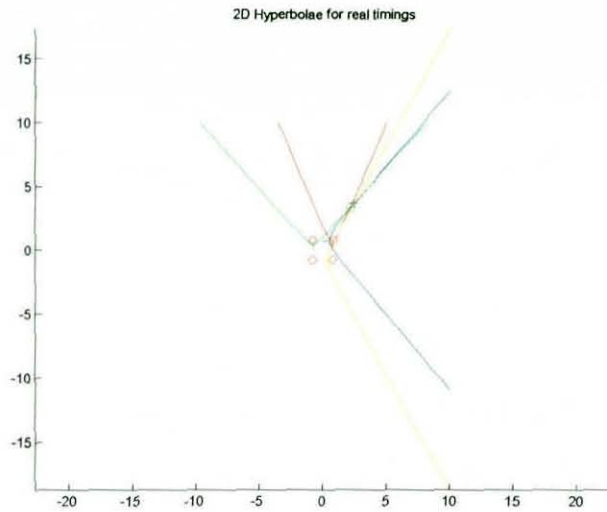


FIGURE 4.2-13 SPATIAL PLOT OF AN AREA WITH RECEIVERS (RED RINGS), ACTUAL POSITION (GREEN RING) AND THE PREDICTED POSITION (BLUE CROSS)

4.2.2.6 ALGORITHMS

Three of the algorithms discussed in Chapter 2 and simulated in Chapter 3 are implemented for this system. Choice of algorithm depends on the array configuration in use.

4.2.3 LIMITATIONS

The development of these systems has occurred over a period of eight years and has been an evolutionary process. The initial data capture system described in section 4.1.1 was developed under considerable time pressure in parallel with the processing algorithms. This led to the system not being optimum for the situation. When time pressure reduced, the system was reviewed and its faults were highlighted. The principal faults were the limitation in bandwidth and hence in tracking accuracy. The work situation for this technology was extremely harsh and the streamer solution showed weaknesses when the trawl entangled. Armoured cables were introduced, but cable stretching resulted in frequent faults.

Noise from the trawl itself often caused false triggering and this was near impossible to eliminate. As a result very few results exist from this system, partly due to lack of cetaceans (thirteen weeks of sea time resulted in less than two hours of data).

The second system was designed chiefly to prove the algorithms. It relies on accurate positioning of the receivers and the array being reasonably near the PC. It is primarily designed as a prototype, not for production. The tracking system suffers from noise problems due to poor layout. This in turn reduces the effect of a high sample rate again reducing the accuracy. Professional production of a second generation of this system will increase the accuracy of the results. Further development of the system control and filters to reduce the amount of false information is possible without major hardware changes.

Time restrictions have limited the amount of water testing this system has received, however bench tests and tank tests show its capability, and data collection using other data capture systems helps to show its potential.

4.3 OTHER CONSIDERATIONS

Various other considerations need to be taken in the production of a working system, all of which is not documented here. Some of the more important ones are as follows:

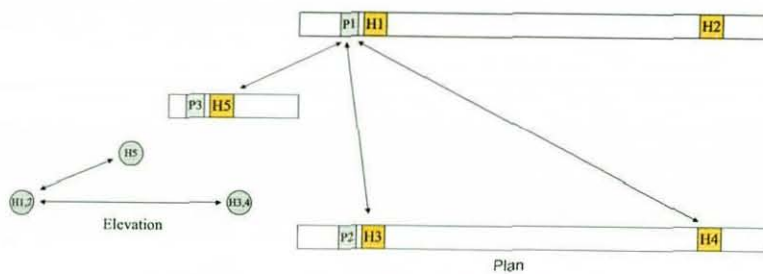
4.3.1 CALIBRATION

As mentioned in section 4.2.1 the implementation of the low-accuracy system included a dynamic array. This consisted of two streamers made to fly side by side, with a single hydrophone slightly above one of the streamers. These streamers were made to be stable in non-turbulent water flow conditions; however, a small amount of movement was expected. As simulations showed, a small movement in the receivers of such a system can result in significant changes in the calculated position of the source. It is therefore necessary to measure the locations of the hydrophones and continue doing this throughout tracking operations. Algorithms were developed to calculate these positions using a low powered acoustic source enclosed in each streamer.

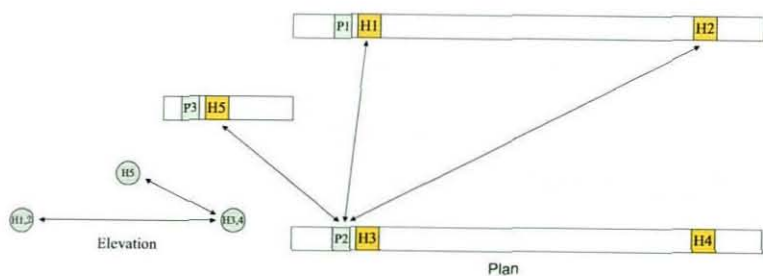
Click generation hardware: To provide a means of calibration, a click generator / pinger is placed in each streamer. Each time these are activated in turn, a simulated dolphin click is generated at 40 kHz that should be detected by all five hydrophones. Since the position of the source is known in relation to one of the transducers (the

pinger is within 5cm), the exact time of transmission is known and by taking the time of arrival at the other four hydrophones, the distance from the source to each hydrophone can be calculated. This cycle repeats for each of the streamers, and so the ranges shown in Figure 4.3-1 are known. From this information the angles between the hydrophones can be calculated, allowing the co-ordinates of each hydrophone relative to the others to be calculated. The control of the pingers (when to generate a ping, and for how long) is taken by a PAL in the main pressure housing. This also transmits similar information to the surface via a sixth channel, allowing the PC to accurately calculate the time of flight to each hydrophone.

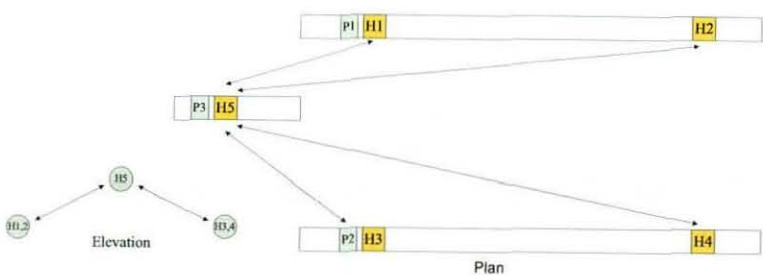
As Figure 4.3-1 shows, by activating each individual pinger at a known time, distances between each hydrophone and the pingers can be determined. As these pingers are fixed relative to at least one hydrophone, the distance between the hydrophones can be calculated using trigonometry.



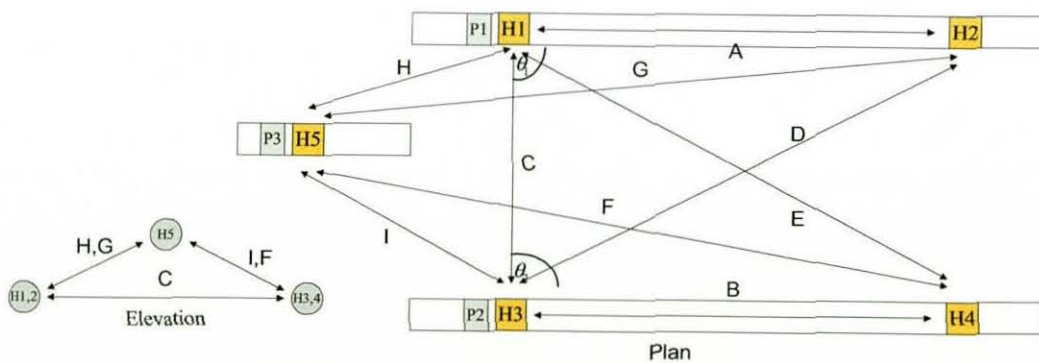
(a) Distances available from pinger 1



(b) Distances available from pinger 2



(c) Distances available from pinger 3



(d) Distances available from all 3 pingers

FIGURE 4.3-1 CALCULATION OF DISTANCES BETWEEN HYDROPHONES

From these distances the exact co-ordinates of each hydrophone can be calculated as follows:

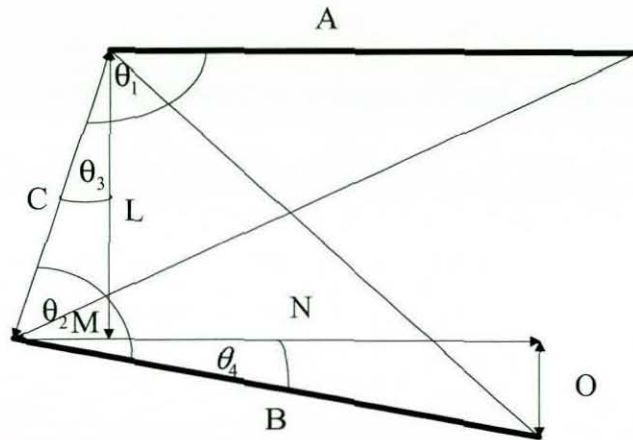


FIGURE 4.3-2 THE NON-PARALLEL CASE.

θ_1, θ_2 can be determined by the cosine rule.

Assuming a non-parallel case, shown in Figure 4.3-2, and taking the coordinates of hydrophone 1 as the reference datum, we have:

$$\theta_3 = \theta_1 - 90$$

$$L = C \cos \theta_3$$

$$M = C \sin \theta_3$$

$$\theta_4 = \theta_2 - (90 - \theta_3)$$

$$N = B \cos \theta_4$$

$$O = B \sin \theta_4$$

Again θ_5, θ_6 and θ_7 can be found using the cosine rule.

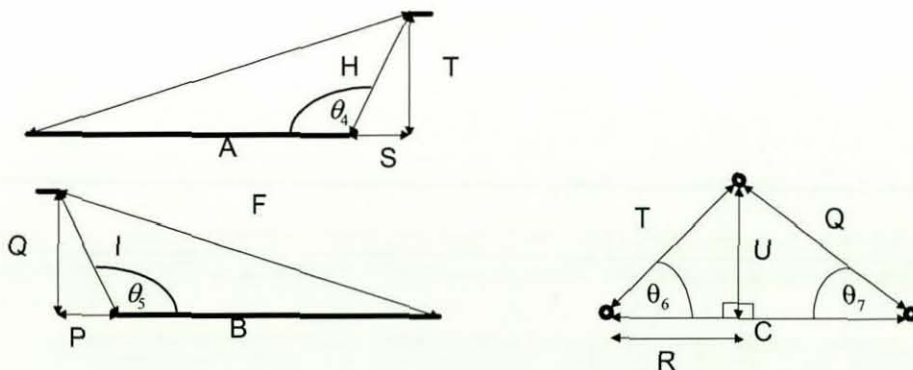


FIGURE 4.3-3 GEOMETRY OF CALIBRATION SYSTEM

From this:

$$P = I \cos(180 - \theta_5)$$

$$R = T \cos \theta_6$$

$$Q = I \sin(180 - \theta_5)$$

$$S = H \cos(180 - \theta_4)$$

$$T = H \sin(180 - \theta_4)$$

$$U = T \sin \theta_6$$

From all this information, each hydrophone can be located in x, y, and z.

$$H1=(0, 0, 0) \quad H2=(-A, 0,0) \quad H3=(M, L, 0) \quad H4=(-N, O, 0) \quad H5=(S, R, U)$$

4.3.2 TRANSMISSION AND PRE-DISTORTION

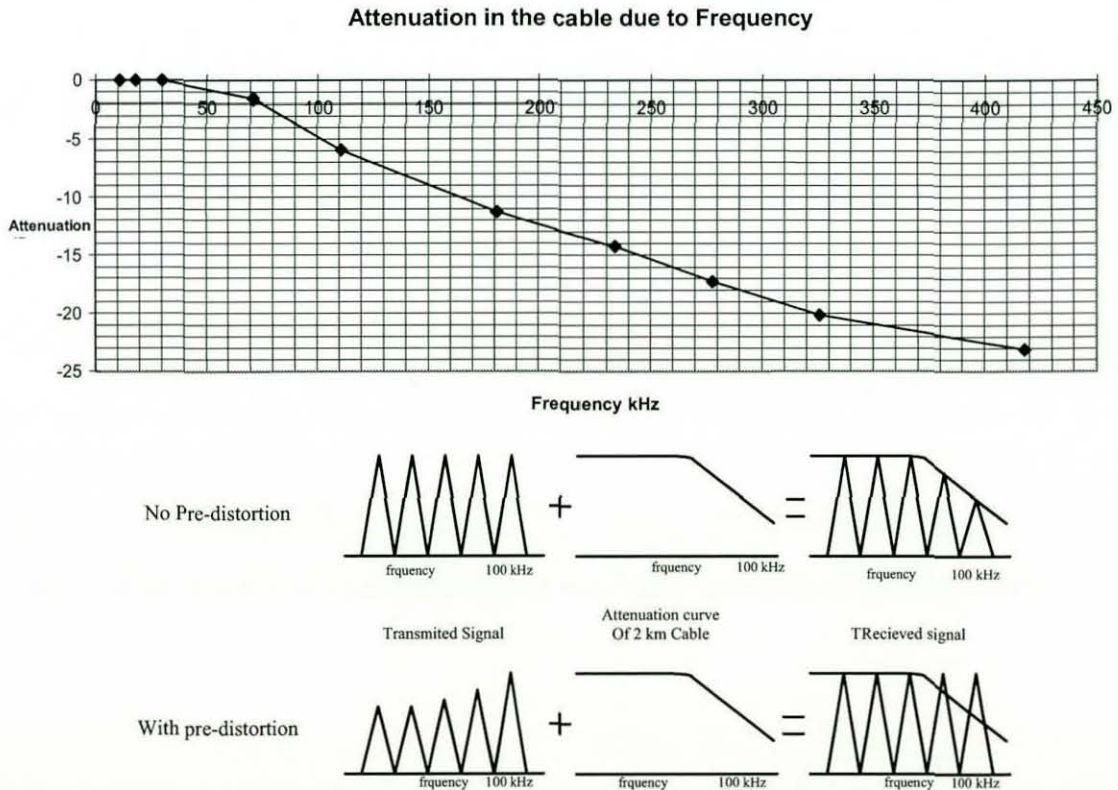


FIGURE 4.3-4 SIGNAL ATTENUATION ABOVE 100 kHz AND HOW PRE-DISTORTION CAN RECOVER SOME OF THE LOST BANDWIDTH

In the situation described in Chapter 5 (*CETASEL*), the transmission link provided the major limitations of the low accuracy system and so had to be used as efficiently as possible. The 2km coaxial cable attenuated any high frequency signals passed along it. It was tested during sea trial 1 and found to attenuate signals strongly above 100kHz. A maximum transmission frequency of 100kHz was therefore adopted. Even in this frequency range it was found necessary to add pre-distortion at the upper end of the range, as shown in Figure 4.3-4. This illustrates that the signals are pre-emphasised to the opposite of the cable attenuation, providing a flat response at the surface. The disadvantage is that noise can also be amplified.

Six channels of timing information are passed up the cable, five carry timing information which has to be sent at as high a frequency as possible to reduce timing errors. There is also one channel of audio information limited to a band of 4 - 25kHz containing information about trawl noise, cetacean whistles and the low frequency element of clicks including their envelopes. These signals are sent directly up the cable with the six channels of timing data being amplitude modulated at 10 kHz spacings below 100 kHz. Figure 4.3-5 shows an FFT showing the six channels of data and audio signals

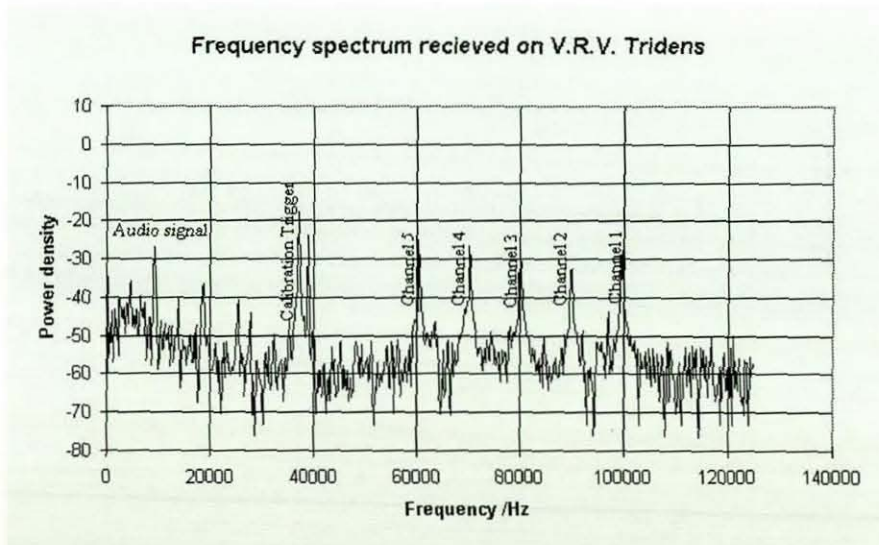


FIGURE 4.3-5 SPECTRUM OF TRANSMISSION SYSTEM IN USE AT SEA

Two modulation methods were tried, one with 90% and the other with 100% modulation. To decrease the random delay during demodulation a Phase Lock Loop

(PLL) circuit was designed. This relies on a local oscillator keeping in phase with the transmitter. With 100% modulation the receiver oscillator has to search continuously for the correct frequency. This is done with a ramp-like search over a user-specified range. When a signal arrives, the time for the local oscillator to lock is dependent on where in the search the system is. This error is unpredictable and leads to large timing errors (measured to be up to 16ms). Using 90% modulation a residue signal is always present, keeping the PLL demodulators continuously locked, removing these errors.

The simplest method of generating the modulation frequencies required for this operation is to generate a look-up table with each of the five frequencies. This table is continuously sent to a DAC and is amplified whenever a signal is received from the associated click circuit. The transmission system is shown in Figure 4.3-6.

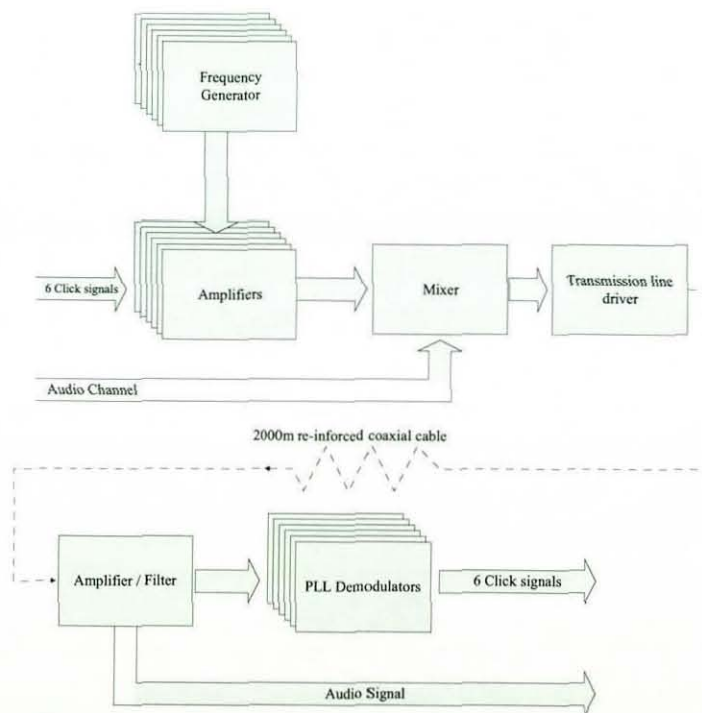


FIGURE 4.3-6 BLOCK DIAGRAM OF TRANSMISSION SECTION

Space considerations, and the number of channels involved, meant that the only way to implement the system was to use surface mount technology. This reduced the size of the circuitry from about five circuit board disks to three, allowing the whole system to be built into a proven Simrad Netsonde pressure housing. The risk of water ingress was thereby reduced and also made the unit a practical size for deployment.

4.3.3 DIVER AND PINGER TRACKING

The system is optimised to track echo-locating cetaceans. The nature of both the systems is such that they can track any impulse or click. If a diver were to carry a pinger, producing an echolocation type click, there is no reason the diver cannot be tracked in the same way as the cetacean. This could be particularly useful for monitoring divers from the surface, or indeed for monitoring the progress of an ROV/AUV. If the detection filter characteristics can be changed the system can be made to distinguish between sources so that a number of divers or vehicles could be tracked simultaneously. The design of the high accuracy correlating system has taken these potential uses into account and has a software adjustable filter on the trigger mechanism. This allows the user to track pingers of differing frequencies. The system is designed to take pingers with frequencies of 30 to 140 kHz at 10kHz steps, i.e.10 pingers. This could be improved with sharper filters or if pulses were coded.

4.3.4 HIGH-NOISE SITUATIONS

If noise becomes a limiting factor, for example if the range to the dolphin / diver is large, it is possible to increase the SNR using signal processing techniques. Matched filtering allows a significant SNR improvement. It is not suited to the click-tracking situation. However if the cetacean is producing vocalisations, it may be possible to track these also. Matched filtering relies on a frequency change with time. Typical dolphin whistles provide this pattern. If the first section of the whistle is captured by the system, it should be possible to use these techniques to improve the accuracy. It is however dependant on the initial signal being detectable by at least one channel. This method is even better suited to the diver case where the frequency pattern of a particular pinger will be known. In this case the trigger filter will need to be a real-time correlator, correlating the input with the expected signal. In this way signals could be recovered from within the noise. Pulse Compression techniques could also be employed to improve the SNR. It must be noted that there is a trade-off with this technique. The signal to noise gain is proportional to the time-bandwidth product, so if short pulses are used, as is the case in the high-speed system. The signal to noise gain is limited. If the signal is made longer the correlations also become longer and it takes longer to process the data.

Chapter 5

CASE STUDIES

This chapter considers three practical systems as case studies and describes their specification, development and implementation. It also presents some results obtained with each system.

5.1 PROJECT CETASEL: BY-CATCH REDUCTION OF SMALL CETACEANS IN PELAGIC TRAWLS.

The by-catch of marine mammals, particularly cetaceans, occurs to varying degrees in a number of commercial fisheries. The extent of the problem in gill-net fisheries is well known [1] but the by-catch of cetaceans in pelagic trawls has only recently attracted serious attention [2, 3]. The species shown to be at greatest risk from pelagic trawls in North-East Atlantic waters are the common dolphin (*Delphinus delphis*), Atlantic white-sided dolphin (*Lagenorhynchus acutus*), and the white-beaked dolphin (*Lagenorhynchus albirostris*) [4].

A study project funded by the European Commission (AIR III CT 94-2423) called *CETA-SEL* (**Cetacean Selectivity**) was tasked to investigate the by-catch problem and possible mitigation methods by technical means. Pelagic trawls operated near the continental shelf-break may be deployed at depths in excess of 100m and at a distance exceeding 800 m behind the vessel. In this environment cetacean interactions with these moving nets are particularly difficult to study. Methods used to gather information include: the use of observers watching for surfacings in daylight, a remotely operated vehicle (ROV) equipped with scanning sonar and low-light TV cameras, and passive acoustic methods involving individual hydrophones or arrays of hydrophones.

In this project, study and analysis of cetacean behaviour around fishing gear has only been possible for two captive species, the harbour porpoise (*Phocoena phocoena*)

and the bottlenose dolphin (*Tursiops truncatus*). For tests with wild cetaceans around fishing gear it is important that the study method has no influence on the animals' behaviour. Data capture systems must therefore be passive and non-intrusive, restricting the use of lights and most standard active sonar equipment.

The overall objectives of the project are to analyse the cetaceans' interaction with the pelagic trawl, to analyse the behaviour and to then attempt to influence the behaviour such that the cetaceans are less likely to be caught.

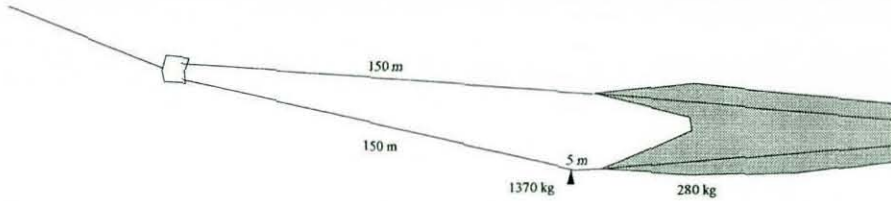
It is first necessary to understand both the advantages and the limitations of any underwater acoustic observation method. Acoustic detection and ranging methods can work at night and in sea-state conditions when observers have very limited visibility. Acoustic ranging can be significantly more accurate than simple visual estimates of distance. Information about the depth of the vocalising animal is also valuable as this can indicate the depth of preferred prey and hence the increased probability of a trawl interaction when this is operating at the same depth. As it is desirable that the ship's personnel on watch are aware of the presence of cetaceans within the study area both ahead and surrounding the vessel, the early detection of their vocalisations can be of great value. If a cetacean's track appears to converge with the vessel then all the information, before, during and immediately after a possible interaction, must be recorded for later analysis. Automatic data logging of technical parameters relating to the ship, the gear and the water environment is essential. If the vessel interacts with the same animal or pod on a later occasion, it may be possible to recognise this from a combination of visual and acoustic cues [5].

Photo-ID studies are not normally practical from a fishing boat, although the value of photographic or video material during an encounter may be considerable. The identification of the species and occasionally the recognition of gross marking on individuals may be useful. Normal surface observations can show an approximate range of an animal from the ship and may show a change in direction. Acoustic means allow a higher accuracy in the calculated range of an animal from the trawl

and will indicate the rate of approach. Changes in behaviour may be more noticeable when the animal is attracted to the trawl using this method. From studies of cetaceans both in captivity and in the wild on the sounds they make as they behave in particular ways and from an understanding of basic cetacean sonar, it is often possible to predict if a cetacean is foraging, fighting, or merely 'observing' an object. It is also possible to detect the range of the cetacean from its target. All this analysis can be carried out on data from a single hydrophone. With data from multiple hydrophones, not only can the previous analysis techniques be used, but also the direction to the cetaceans can be determined. With three hydrophones a position can be plotted in two dimensions and with four hydrophones, positions in the third dimension can be achieved.

5.1.1 THE SYSTEM

The system developed for this application is that described in section 4.2.1. The major limitations of this system are set by the environmental conditions. The pelagic trawl has an approximately conical shape (Figures 5.1-1); unlike the two-dimensional static nets, it cannot be traced using a two-dimensional tracking system placed on the sea-bed. The first developments on the system for pelagic trawls were to make the system capable of position fixing in three-dimensional space. This involved using a fourth hydrophone in the array displaced in the third dimension.



Test	No	1	2	3	4	5								
Towing speed	Knots	5.0	5.0	5.0	5.0	5.0								
Distance between doors	m	163.6	163.7	164.2	165.0	170.1								
Spread	Headline	m	99.1	99.4	99.5	99.6	99.1							
	Footrope	m	98.7	99.2	99.2	99.3	105.3							
Height	Wingend	m	32.3	32.9	33.7	35.0	42.9							
	Centre	m	36.4	36.4	36.4	37.5	44.6							
Tension per side	tons	8.44	8.34	8.01	7.32	5.20								

Test	Notes	Test	Notes
1	Trawl with codend, door spread app.165 m		
2	Codend and extension removed.		
3	The two aftmost belly sections removed		
4	Four aftmost belly sections removed		
5	All netting aft of shark teeth removed		



FIGURE 5.1-1 PELAGIC TRAWL

The proposed solution for this problem was to use a tetrahedron with one of the four hydrophones at each apex. It was proposed to connect this to a Remotely Operated Vehicle (ROV), which could be flown at a fixed distance from the net at the same time as filming using low light cameras. This allowed the system to be deployed on or near the net with fibre-optic links to the towing ship, where the data could be processed with no power or space restrictions.



FIGURE 5.1-2 TOWED ROV



FIGURE 5.1-3 FRV *TRIDENS* USED FOR THE TRIALS OF THE TRACKING SYSTEM

Sea trials in March 1995 included tests to ascertain the self-noise of the ROV, shown in Figure 5.1-2, with a view of ensuring that a system in the proximity of the ROV could achieve the sensitivity needed. Unfortunately, it was found that the noise emanating from the hydraulic pumps on the ROV was great enough to engulf biological signals when the hydrophones were nearby. This meant such a system would be able to function only if spatially separated from the vehicle. Removing the tetrahedron array from the vehicle presented its own problems. The only way this could be done would be to tow the array behind the vehicle. This presented stability and practical problems, such as rotation and deployment. Removing the array from the ROV totally was the obvious answer, but this gave a major disadvantage in that the reinforced fibre-optic cable then became unavailable and the ship was not equipped for an extra fibre directly connected to the net.

At present, electronic equipment on commercial fishing nets is connected to the ship in one of two methods, acoustically or via a reinforced coaxial cable. The trial's ship F.R.V. *Tridens* (Figure 5.1-3) uses both methods. On the trawl it has a vertical echo sounder, Simrad Netsonde, to measure the height of the net above the sea-bed. This sends information to the ship via a co-axial cable (Netsonde cable); for example, when the doors are being adjusted it has a form of a horizontal echo-sounder (Scanmar), to measure the distance between them. The information from this equipment is transmitted acoustically to a hull-mounted hydrophone.

The tracking algorithm needs to achieve a high accuracy in the timing data captured by the four hydrophones of the array. In using a fibre-optic link, it was possible to achieve bit rates in excess of 120 Mbps and to transmit many different channels at once using FM techniques. The water attenuates signals transmitted acoustically from the net to the ship (a distance of up to 1000m), and this attenuation is frequency dependent. To achieve the distance, low frequencies would have to be used and this would severely limit the accuracy of any system relying on time difference measurements rather than phase difference measurements. The co-axial cable provides a compromise between the two systems, because it can comfortably achieve frequencies into the 100 kHz region on a cable of the required length (2km).

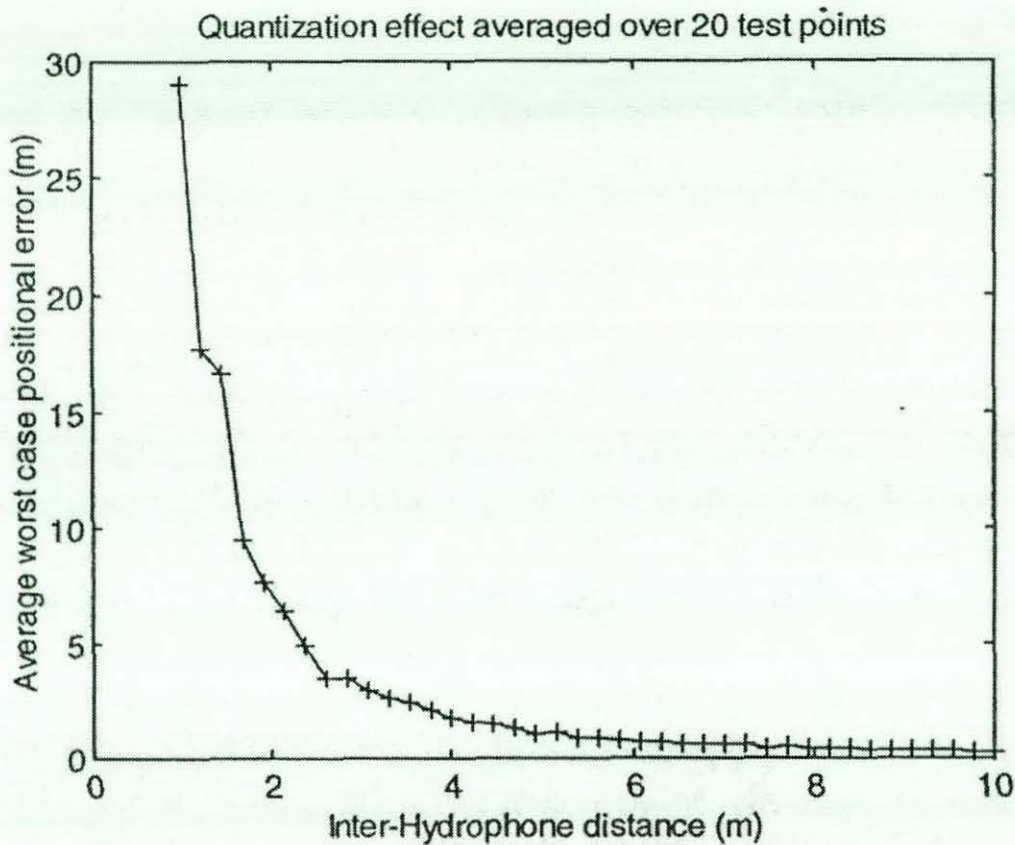


FIGURE 5.1-4 SYSTEM ACCURACY WITH RECEIVER SEPERATION

The F.R.V. *Tridens* can fish at speeds of approximately 1 - 8 knots in weather conditions as high as sea-state 8. To deploy a rigid frame on the top of the trawl net and expect it to be hydrodynamically stable in all conditions and speeds is unrealistic. It was decided that the system would have to be made physically flexible and streamlined to allow for these varying conditions.

Military and hydrographical survey vessels have long used streamers to give a stable, flexible system for the deployment of hydrophones. If streamers could be used it would provide a stable proven system for the development of the arrays. The main limitation of a streamer (here with two hydrophones) is that the positional error increases exponentially as the hydrophone separation is decreased, as shown in Figure 5.1-4. The streamers designed for this project are shown in Figure 5.1-5; these are specified to at least four times the maximum water depth to be used.

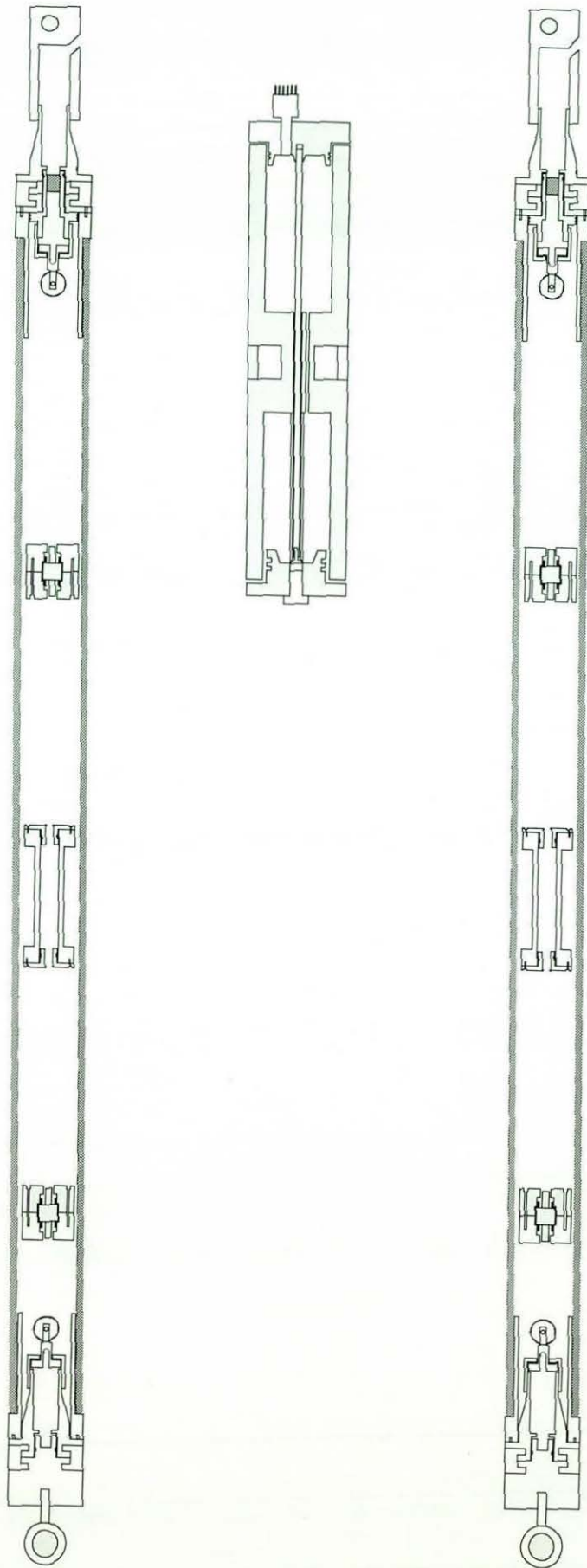


FIGURE 5.1-5 UNDERWATER HOUSING ASSEMBLIES

Such a system could be deployed on the pelagic trawl net and information sent to the surface via the Netsonde cable. Pelagic trawl nets are vast in comparison to the array size and the side of the net presents a virtually flat surface to the array. There is therefore a problem of how to get the fourth hydrophone out of the plane of the other three hydrophones to provide three-dimensional tracking. To run a cable around the net to the bottom side (footrope) 50m away would require over 100m of cable, which would be impracticable for the following reasons:

Deployment: The cables may be severely stretched as the net takes shape once in the water, as shown in Figure 5.1-6.



FIGURE 5.1-6 TRAWL DEPLOYMENT WITH STREAMERS

System accuracy: The net shape is by no means fixed, and changes particularly on deployment and with speed; any changes in inter-hydrophone distances result in large errors in the positions calculated by the algorithm.

Non-detection of the dolphin signals: The dolphin transmits its echolocation clicks in a relatively narrow beam so a large inter-hydrophone distance of up to 50m would make it unlikely that any one click would be detected by all four hydrophones.

Another more practical solution is to bring the fourth hydrophone down into the plane of the other three. This results in a permanent dual solution, as shown in

Figure 5.1-7. However, inter-hydrophone distances can be fixed, thereby reducing errors. To remove this duality a fifth hydrophone can be placed slightly out of the plane, for example further up the Netsonde cable. This fifth hydrophone need not be fixed in relation to the other four, but it can be used to remove the anomalous position fix.

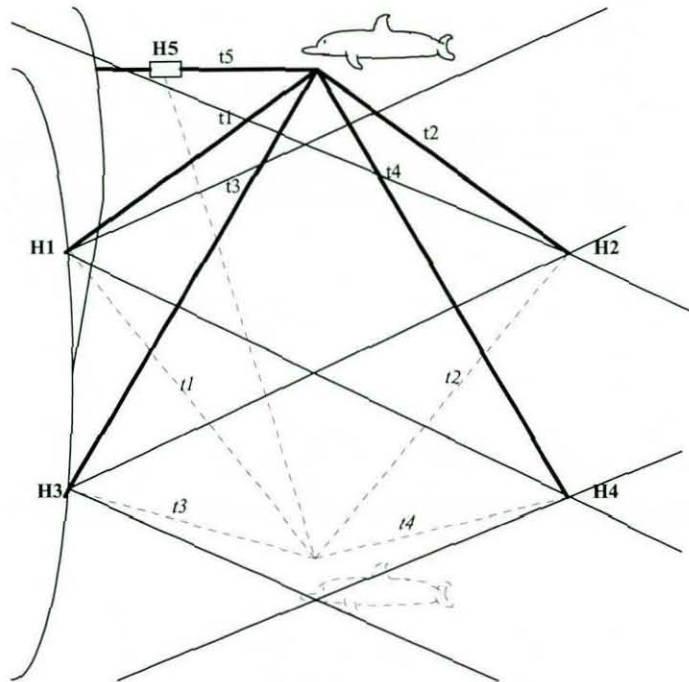


FIGURE 5.1-7 HYDROPHONE POSITIONS ON TRAWL

In summary, the system contains two streamers, each with two hydrophones separated by 3m (the distance of optimum definition that should allow the cetacean sonar beam to ensonify all four hydrophones), and a fifth hydrophone out of the plane of the other four, approximately 2m higher than the streamers. The system can be deployed at fixed points on the net and it has fixed spacings between the hydrophones in each streamer; however, the inter-streamer distance may change with speed. As it is not always possible to have the ROV in the water, a method was needed of accurately measuring the distance between the streamers. This can be done using a pinger in each streamer, which emits a signal that is detected on all four hydrophones. The signal needs to be similar to a dolphin click to ensure that it

passes through the circuitry. Since the position of the pinger will be fixed in relation to two of the hydrophones, the exact time of transmission can be determined, and the time of arrival at the other streamer and on the fifth hydrophone will allow the determination of the precise positions of all the hydrophones relative to each other.

It is usually possible to detect a dolphin's presence long before any clicks are detected by listening to its lower frequency (5-24kHz) whistles. These tend to travel farther and are easier to distinguish from gear noise (of the net). It is important that the final system would be able to detect these signals. This could be done using the single hydrophone, which is away from the net in less disturbed waters.

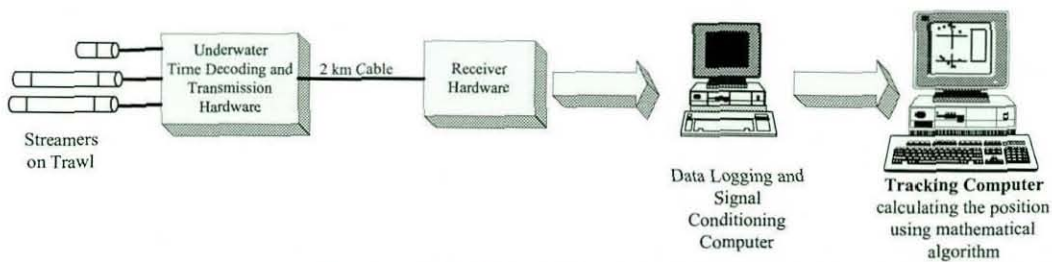


FIGURE 5.1-8 CETASEL SYSTEM

5.1.1.1 DEVELOPMENT OF UNDERWATER SYSTEM

The system has to be deployed by fishermen on virtually standard nets. It is important not to make the equipment too cumbersome or difficult to deploy. The housings presently used on many nets are Simrad Netsonde housings. These are cylindrical pressure housings, which are fixed inside fibreglass casings for ease of attachment to the net, as shown in Figure 5.1-9



FIGURE 5.1-9 NETSONDE HOUSING

These housings contain both a power pack and a space for the circuitry, which although restricted, should be enough if surface mount technology were to be used.

The circuitry used for the system is described in the previous chapter.

5.1.1.2 POWER SUPPLY UNIT

The initial circuit, streamers and the line driver were all powered via a battery pack consisting of eight D-cells. This gave a total of 12 volts with a nominal life of 18 ampere-hours. The system was quite current-greedy, in particular the transmission circuits, which used bipolar technology. In total, the circuit took just over 1.5A. Although the battery life was made as long as possible by using alkaline cells, it was restricted by the fact that many chips shut down at low voltages. By using a switched-mode supply the voltage was held high until the battery voltage totally collapsed. This was healthier for the circuit and made optimum use of the cells, but this method of voltage generation tended to induce noise into the circuits, especially at low battery voltages. To shield the noise from the sensitive amplifier stages of the circuit, the power supply circuit was made in such a format that it could fit into the narrow spaces between the cells in the battery section of the pressure housing, which was mechanically isolated from the main circuit housing. During the initial tests of this system in Sea Trial 2 the inconvenience of replacing batteries every 4-6 hours made it clear that a system to power the equipment down the cable was needed. Throughout the whole trial the noise generated by the switched-mode power supplies was apparent in the audio spectrum, at times swamping the vocalisations received.

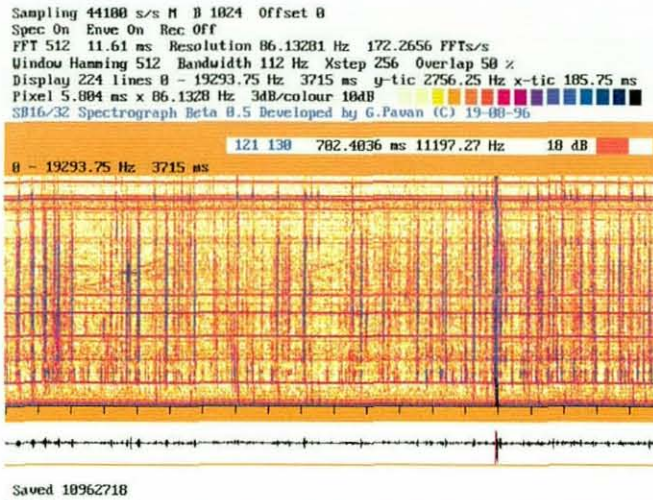


FIGURE 5.1-10 SPECTROGRAM OF SWITCHED-MODE POWER SUPPLY TONAL NOISE IN THE 0- 20KHZ RANGE DURING SEA TRIAL 2 [6]

A new system was designed for Sea Trial 3. This system was powered at 60V DC from the ship. With the use of transformers at either end of the coaxial cable, the signal perturbations were integrated onto the DC, such that the unit could be powered from the surface, yet signals could still be transmitted simultaneously. A high DC voltage was chosen to reduce the current passing through the cable, thereby increasing the efficiency of the transfer. In the place of the battery pod, the wet-end transformer and step-down switched-mode circuitry were inserted. Using regulators, positive and negative 5V supplies were created. The high power requirement of these components during start-up increased the potential across the coaxial cable to a point where the voltage on the circuit was too small to start the switched-mode circuits (55V). A starter therefore had to be built into the system to give an initial injection of higher potential until the system started; this had to be reduced again quickly when the system started, otherwise the circuit would be destroyed by following chain of events.

As the system started, the power requirement fell, along with the current, the potential across the cable fell from 55V to 8V. The voltage across the initial circuit

rose from 5V to 62V (assuming 70V start-up potential). The limit of the first stage supply was 60V and so the start-up potential had to be swiftly reduced. This method of powering provided a more convenient system and reduced the tonal noise. It also allowed continuous use for days at a time during the sea trials.

5.1.1.3 LOW FREQUENCY DETECTOR

The audio part of the spectrum provides useful information about the type of animal, as well as background noise from other sources, i.e. the Netsonde unit, the ROV when deployed or the net gear noise. Since we only hear this channel of information, it is important that it is 'clean' and includes as much information as possible. For these reasons the circuit contains a click detector whose output is mixed with the original signal after filtering to remove ship noise and high frequencies, therefore providing a combined audio/click channel. This circuit receives its signal from the fifth channel, which is displaced from the net and Netsonde unit, both potentially annoying sources of acoustic noise.

The circuit was adapted from an earlier version used as a stand-alone system to be used in the same pod but utilising the pod's own hydrophones, allowing a listening facility on the net. This circuit could also be used with the fifth hydrophone on its own to provide a very good, sensitive listening system. When combined, all these component parts made up the final system, which is shown as a block diagram in Figure 5.1-11.

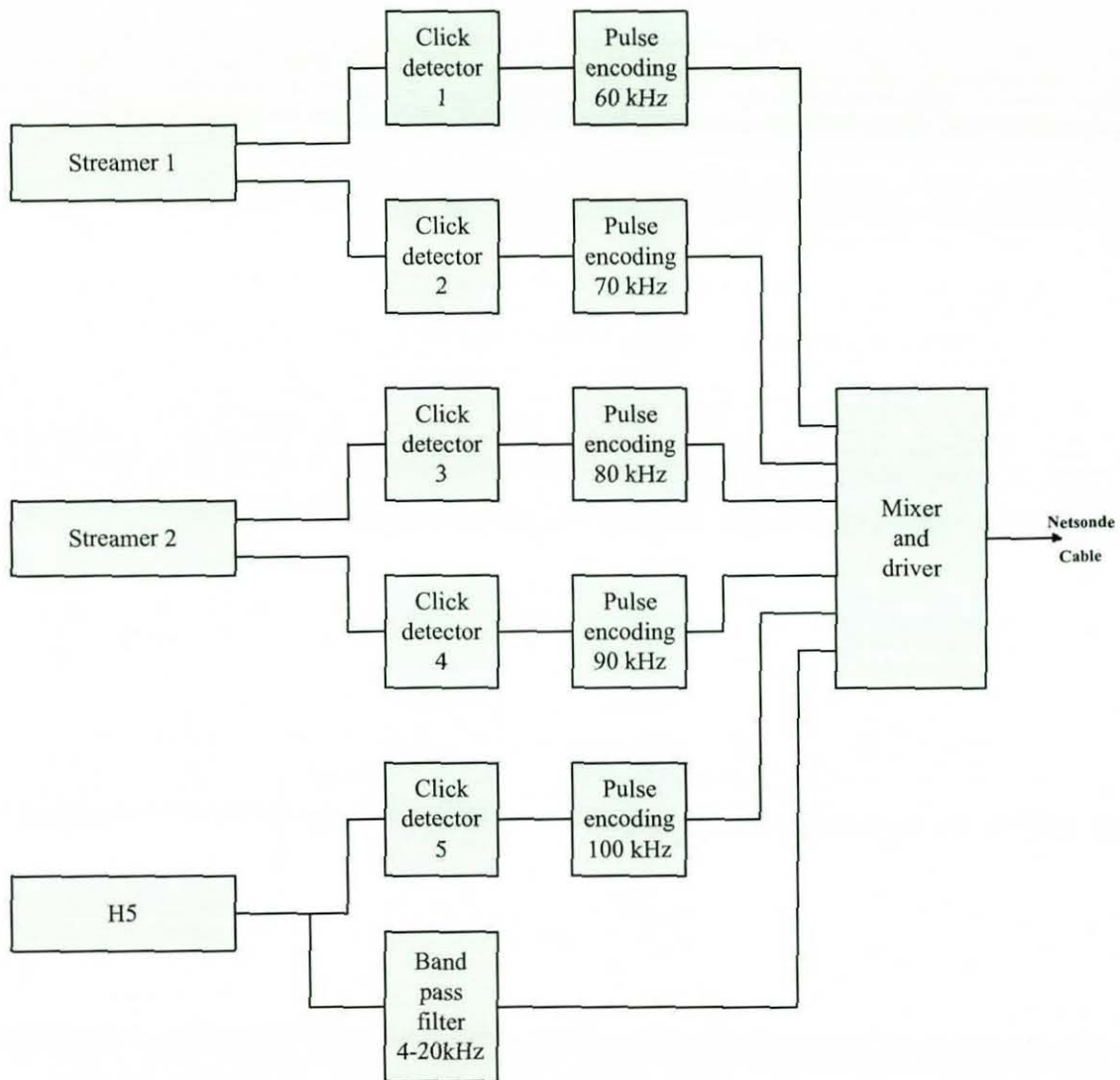


FIGURE 5.1-11 COMPLETE UNDERWATER TRACKING SYSTEM

The system was tested both in the laboratory and on six occasions at sea in various states of completion. Very few dolphins were sighted, and those that were did not always approach when the equipment was operational. Some clicks were recorded, but the timing accuracy achievable was not high enough to produce unique solutions at the ranges required. In these cases a vector was displayed, indicating bearing only. When combined with the range information from the system described in section 5.2, cetacean positions could be localised. Various setbacks during the *CETASEL* project led to the full system only being fully available during the final

trial in April 1997, although a limited system was available during the October 1997 trial, when the self-calibration section of the system failed. In case of this unit failing again a second simple 'fall-back' mode was added to the system to provide a very coarse vector to the sound source, and this required minimal calibration data.

During the April 1997 trial, impulsive sounds were detected from the trawl. These emanated from various places on the trawl itself, i.e. the footrope, headrope or bindings (Figures 5.1-12, 5.1-13) and from the Netsonde unit (Figure 5.1-14). During this trial there were no occasions when an echo-locating cetacean was within range of the functional tracking system. Post-analysis of the data from the October 1996 trial, using low-accuracy calibration, showed some data on a malfunctioning hydrophone channel, which has made analysis difficult (Figure 5.1-15).

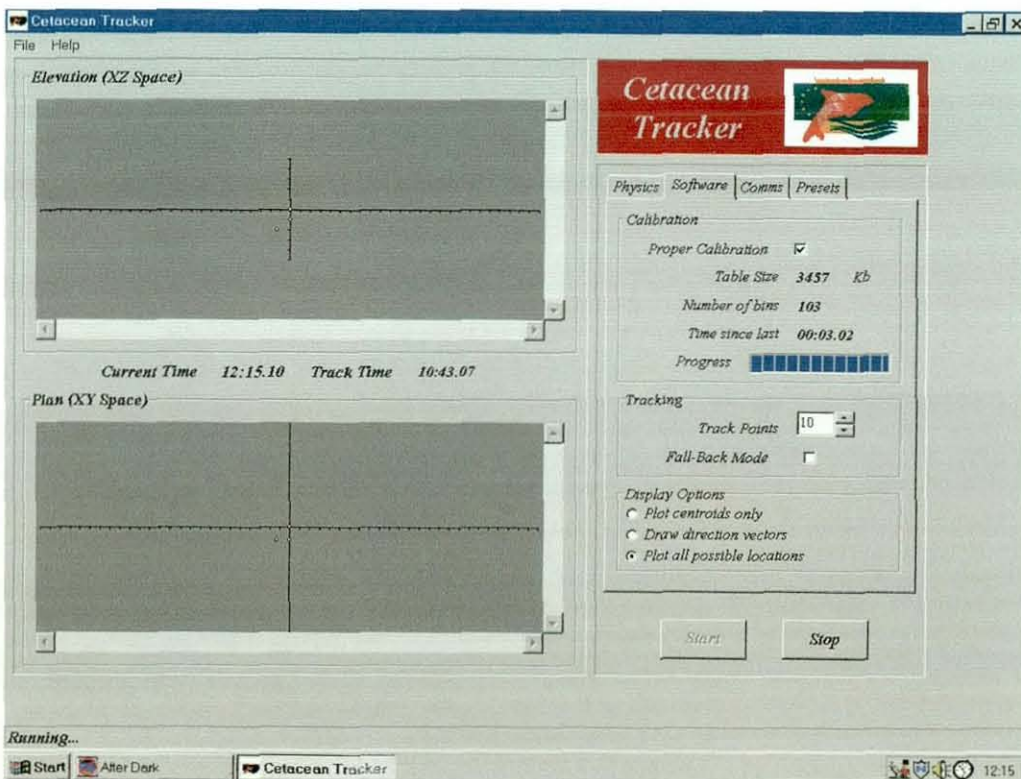


FIGURE 5.1-12 FULL SYSTEM, SHOWING TRAWL NOISE

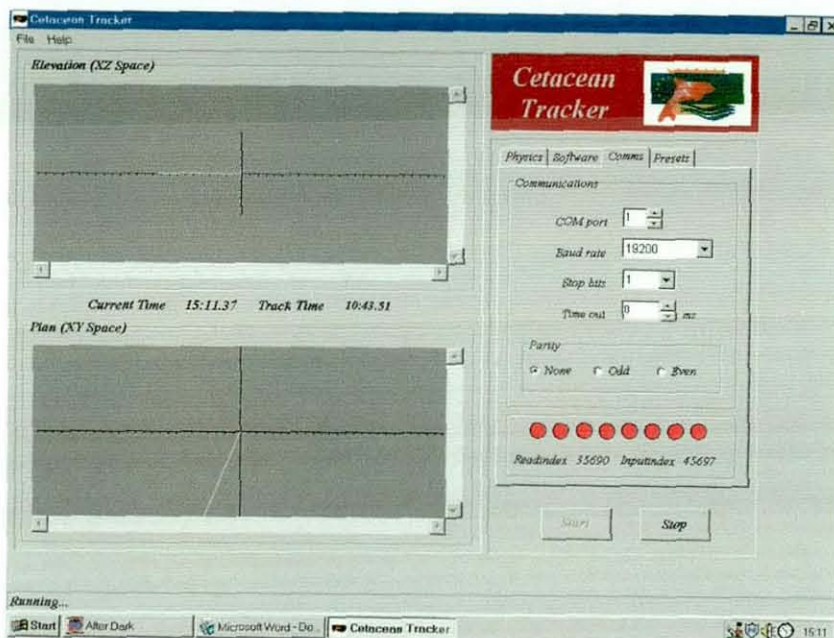


FIGURE 5.1-13 TRAWL NOISE VECTORS

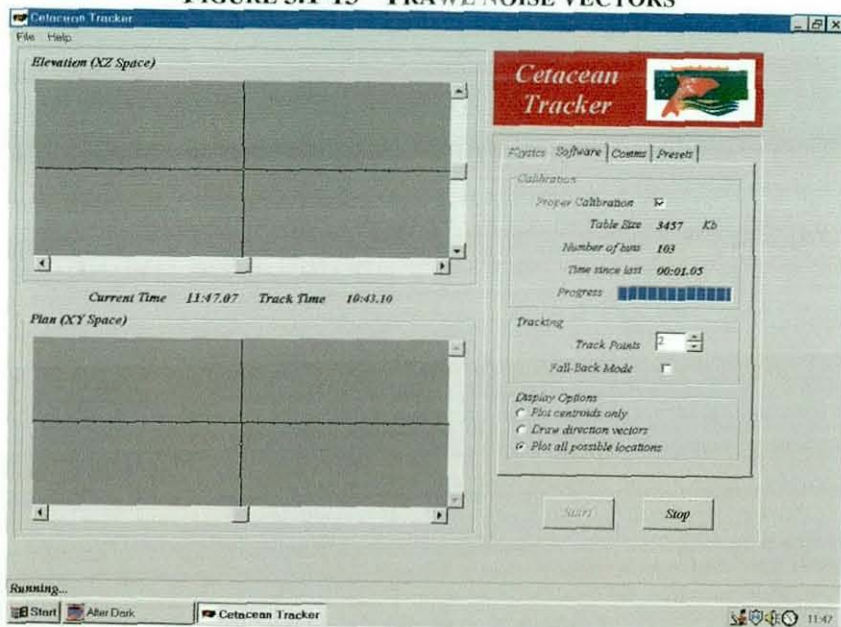


FIGURE 5.1-14 FULL SYSTEM, SHOWING NETSONDE AT A POSITION 7M AWAY

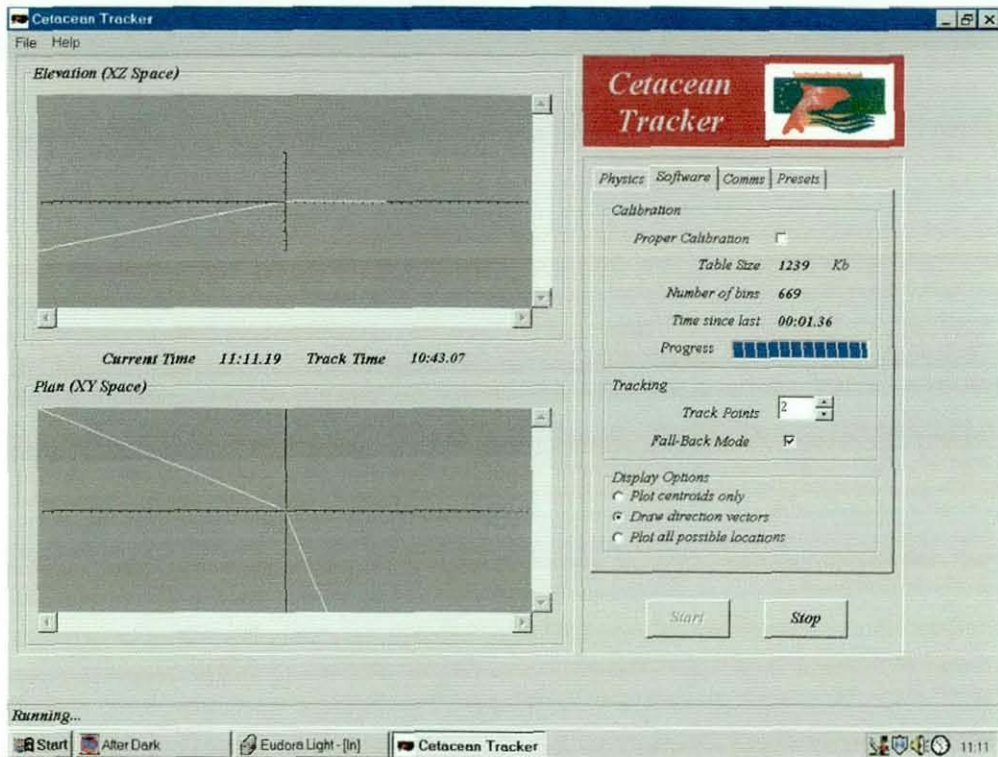


FIGURE 5.1-15 NON-CALIBRATION METHOD, SHOWING NOISE AND THE NETSONDE

5.2 A SIMPLE MEANS OF DETECTING CETACEAN PRESENCE AND RANGE

In the early stages of the *CETASEL* project it was necessary to have a simple system to detect the presence of vocalising cetaceans in the area when a trawl was deployed. A single hydrophone was connected to the trawl and its output was fed to a pass-band filter with a pass band in the vocalising range of most cetaceans (2-25kHz). Using this method, the whistle-like vocalisations can be clearly heard from a considerable distance, typically hundreds of metres. Using a spectrogram program, the vocalisations can be viewed as a function of time. It became obvious that a large proportion of the time that cetaceans were in the area a reverberation could be observed, often multiple reverberations. Assuming observers were able to

occasionally pinpoint the cetaceans, it was considered possible to find a range to the cetacean using the reverberation method described in section 2.5.1. Since the technology did not exist to extract the reverberations automatically in real time, the data was post-processed and ranges placed on charts. Together with visual observations and information regarding the velocity of the cetacean, it was in some cases possible to piece together tracks of passing cetaceans and to observe how close they passed the trawl. Several papers by the author and colleagues describe tracking by this method [7-9]. These papers are included in full as Appendix C.

5.3 DIRECT DIVER / CETACEAN TRACKING: HIGH DEFINITION SYSTEM OF TRACKING CETACEANS OR PINGERS

This test was performed to show that passive tracking works practically, and to provide data to compare with simulations. This aim is achieved via three objective, as follows:

1. To show that the system's signal processing techniques function correctly, and to show any weaknesses.
2. To show that the timing data collected in a tightly controlled situation can be used to generate positions, to verify those positions using spherical positioning techniques, and to demonstrate a physical measurement system.
3. To verify the flat array algorithms presented in Chapter 3, comparing the result with the simulations shown in that chapter.

A test was devised to allow these three objectives to be achieved. A controlled test was initiated to allow the technical limitations of the system described in section 5.1 to be reduced. Once the algorithms and base technology were proven it would be more realistic to invest time and funds in the system to allow a more diverse use at sea. Due to time limitations the testing was scaled down to a minimum. To provide the controlled situation necessary, the Loughborough tank was utilised; this tank, measuring 9x5x2m, is a little small to provide long-range data to fully prove the method but was considered sufficient for controlled testing. The major limitation of

this tank is depth, which made it extremely difficult to perform experiments at anything other than mid-water, thus limiting the test to two-dimensions. By sampling the whole signal, triggered by the electrical signal to the source, and using MatLab, it is possible to use spherical tracking to find the exact position of the source and then use passive tracking to verify the algorithms. These limitations were considered acceptable under the circumstances.

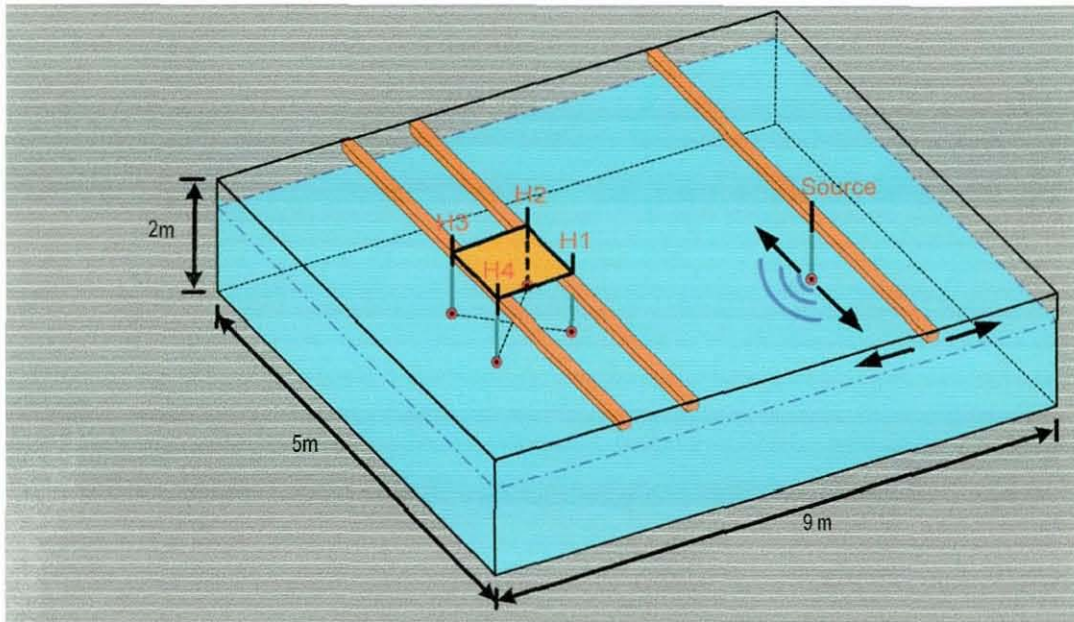


FIGURE 5.3-1 TEST ARRANGEMENT.

5.3.1 METHODOLOGY

The experimental set-up comprised a fixed array at one end of the tank, as shown in Figure 5.3-1, and a source attached at the same depth to a moveable gantry at the other end. The source could be moved in both the x and y axes in front of the array. In this way the angle of the source to the array was changed and a number of angles were covered. At each position the source was made to ping and the incoming data was recorded using a data capture system (Tektronix 420). The data was processed in a near-identical fashion to that performed in the previously described data capture system (section 4.1.2) but using MatLab.

The output is displayed as a spatial figure showing the spherical tracking position (taken to be a reference), which is detected by using the trigger pulse of the source and the arrival times on receiver 1 and 2. The predicted position using the specified algorithm with the time differences between the received pulses. To demonstrate how the algorithms perform and how accurate they are, the time differences are shown as three or more hyperbolae. Ideally these should all cross at a single point, but because of timing inaccuracies they may not intersect ideally. Figure 5.3-2 shows an example of a spatial plot of hyperbolae.

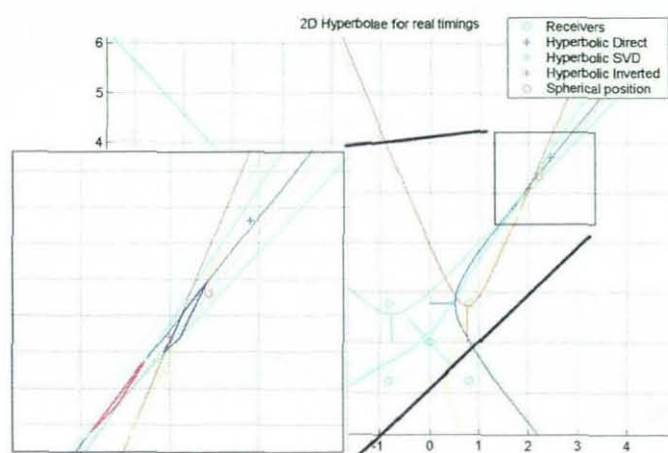


FIGURE 5.3-2 SPATIAL PLOT OF A CALCULATED LOCATION, WITH BOTH SPHERICAL AND HYPERBOLIC POSITIONS, AND HYPERBOLAE WITH IDEAL TIMINGS (DASHED) AND REAL (SOLID) FOR EACH HYDROPHONE PAIR. THE RELEVANT CROSS-OVER POINTS ARE MARKED IN THE INSERT IN BOLD

Data will be displayed for each of twelve recorded points, showing the timing errors for each point and how this affects the hyperbolae. To allow a comparison of the correlation and amplitude methods described in sections 4.1.1 and 4.1.2, plots are shown for hyperbolae of timings with both methods. For each algorithm a spatial plot shows the reference positions relative to the receiver array, together with the predicted positions. The difference between these positions will be plotted to show any error trends.

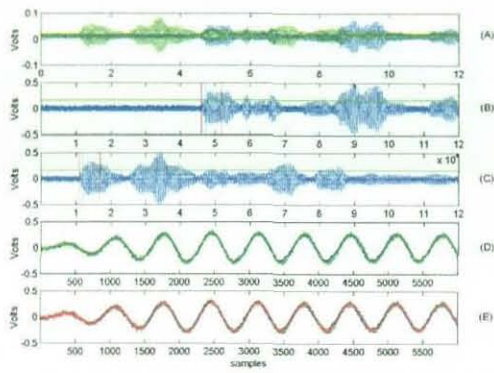


FIGURE 5.3-3 (I) H_{12}

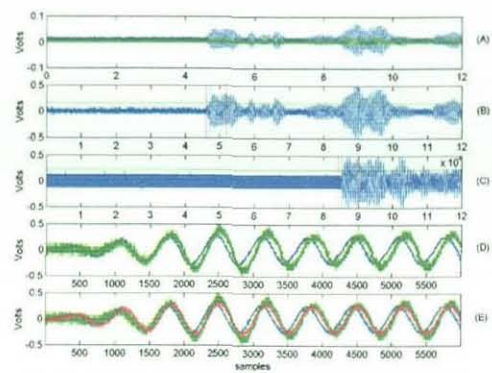


FIGURE 5.3-3 (II) H_{13}

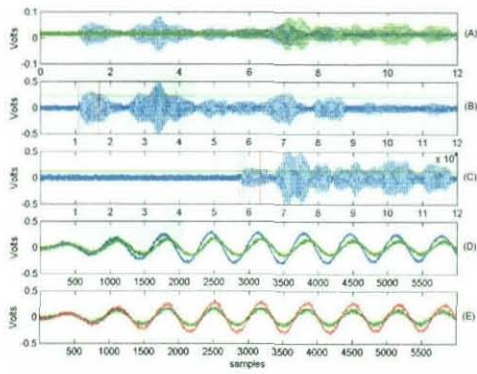


FIGURE 5.3-3 (III) H_{24}

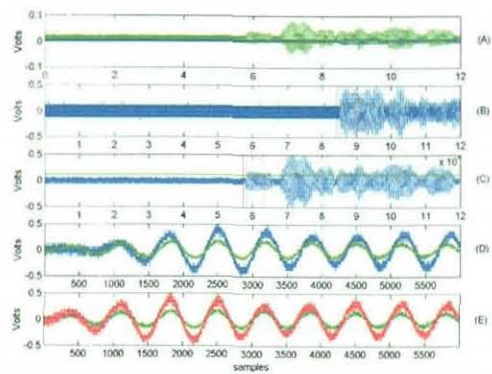


FIGURE 5.3-3 (IV) H_{34}

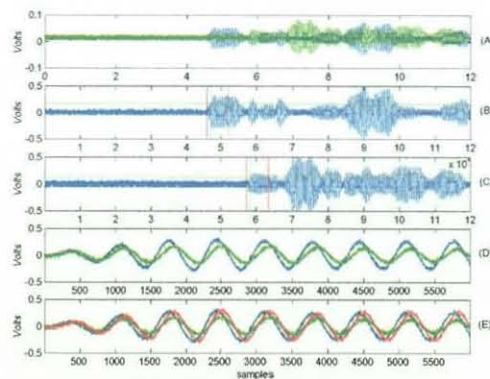


FIGURE 5.3-3 (V) H_{14}

STAGES OF PROCESSING FOR RECEIVERS
1&2(I), 1&3(II), 2&4(III), 3&4(IV) AND 1&4(V)

Each of the three relevant algorithms was applied to these data points and the results are plotted as crosses. In all cases the single value decomposition (SVD algorithm 6) and straight inversion techniques (Algorithm 5) have given identical solutions. This is to be expected as the SVD solution only differs in singularity cases.

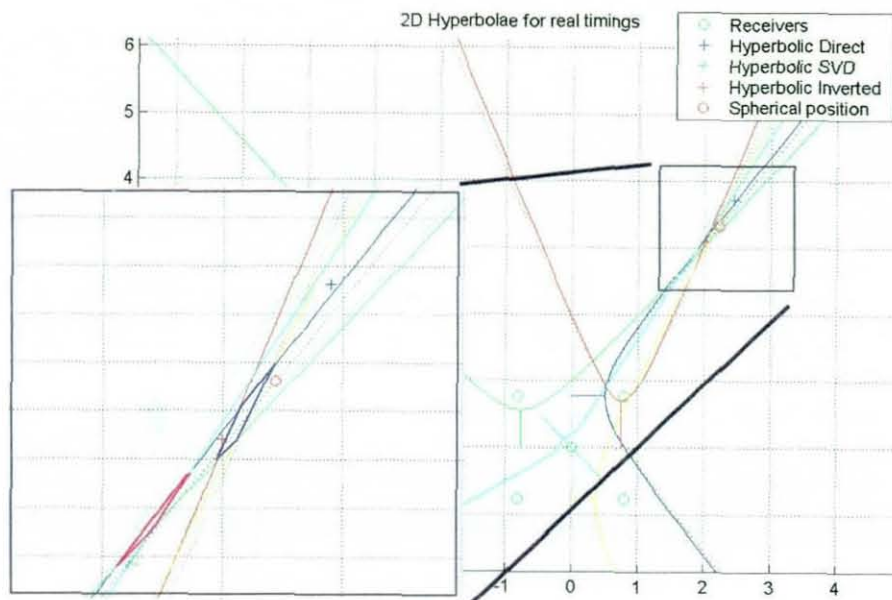


FIGURE 5.3-4 HYPERBOLAE FOR THE DATA OF THE POINT PRESENTED IN FIGURE 5.3-3 (POINT 1) DOTTED LINES INDICATES IDEAL TIMINGS (WITH 20MHZ SAMPLING) AND THE AREAS IN THE INSERT DEPICT THE INTERSECTION AREA. THE DIFFERENT CROSSES REPRESENT THE ALGORITHMS DESCRIBED EARLIER WITH DIRECT (ALGORITHM 2), SVD(ALGORITHM 6) AND INVERTED(ALGORITHM 5)

As the source draws closer to a receiver pair axis or orthogonal, it can be observed that relatively small errors in the timings of the sensitive axes (in the case of Figure 5.3-5, t_{24}) can result in large range differences in the crossing points of the loci. The effect of this is to spread the solutions along the bearing of the real solution.

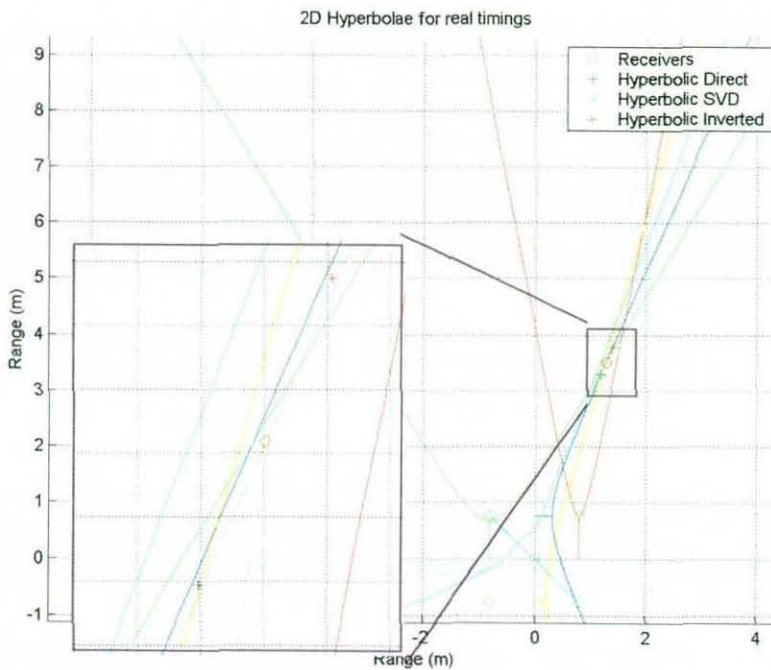


FIGURE 5.3-5 HYPERBOLAE FOR THE DATA OF POINT 2
THE DIFFERENT CROSSES REPRESENT THE ALGORITHMS DESCRIBED EARLIER WITH
DIRECT (ALGORITHM 2), SVD(ALGORITHM 6) AND INVERTED(ALGORITHM 5)

As the range increases it can be expected that the hyperbolae become straighter and may run near parallel, in this case small timing errors can give large range errors as seen in Figure 5.3-6 where errors are as large as 14m. Conversely, as the source moves closer to the array the intersection angles become greater and the accuracy improves.

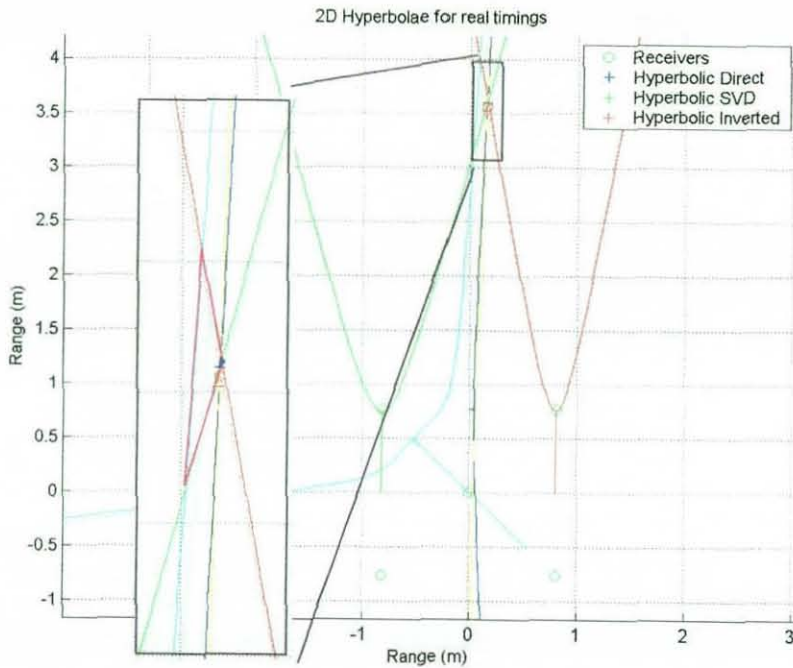


FIGURE 5.3-6 HYPERBOLAE FOR THE DATA OF POINT 3
THE DIFFERENT CROSSES REPRESENT THE ALGORITHMS DESCRIBED EARLIER WITH
DIRECT (ALGORITHM 2), SVD(ALGORITHM 6) AND INVERTED(ALGORITHM 5)

As the array is symmetrical it can be assumed that the sensitivity pattern will be repeated in the four quadrants around the zero point. In the case of Figure 5.3-7 a small error has caused the hyperbola for t_{13} to be the maximum for the receiver pair. A small error in position in this case will accentuate errors in this zone.

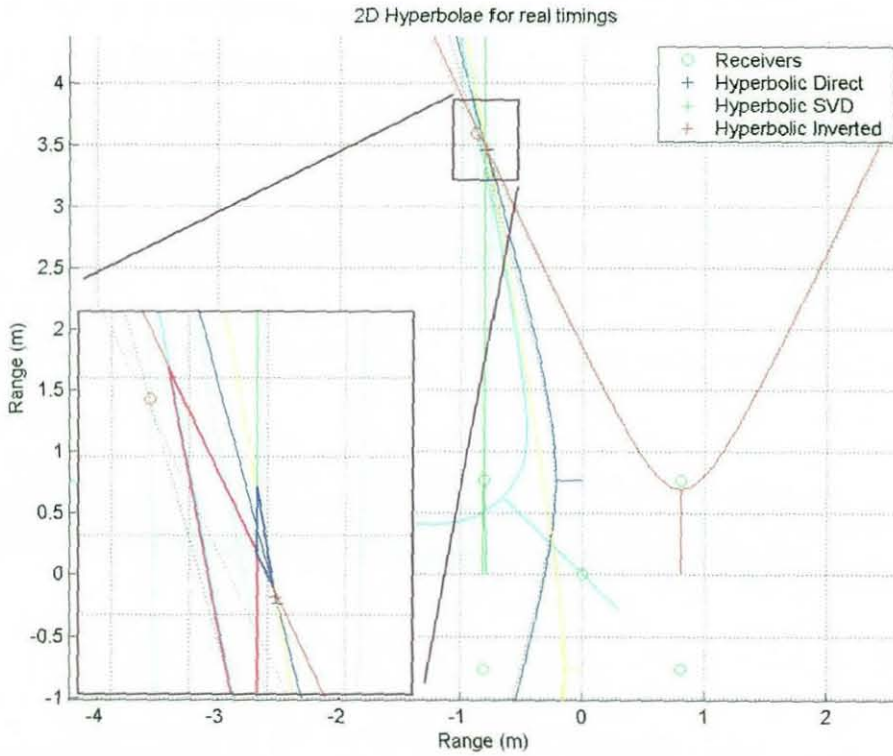


FIGURE 5.3-7 HYPERBOLAE FOR THE DATA OF POINT 4
THE DIFFERENT CROSSES REPRESENT THE ALGORITHMS DESCRIBED EARLIER WITH
DIRECT (ALGORITHM 2), SVD(ALGORITHM 6) AND INVERTED(ALGORITHM 5)

As the source nears the diagonal, the *inversion method*, which uses the t_{14} diagonal timing, begins to be sensitive to timing errors and in the case of Figure 5.3-8 this pulls the estimated position towards the array. The bold red area in the insert shows the area between the intersections of these three timing differences. The *direct method* does not use timing difference t_{14} ; the timing errors have a smaller effect and the estimate of position is better.

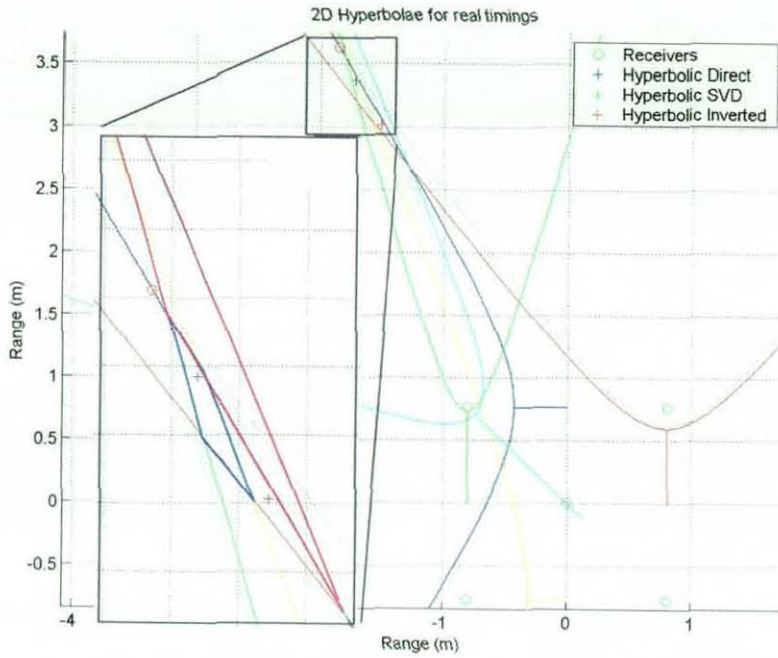


FIGURE 5.3-8 HYPERBOLAE FOR THE DATA OF POINT 5. THE DIFFERENT CROSSES REPRESENT THE ALGORITHMS DESCRIBED EARLIER WITH DIRECT (ALGORITHM 2), SVD(ALGORITHM 6) AND INVERTED(ALGORITHM 5)

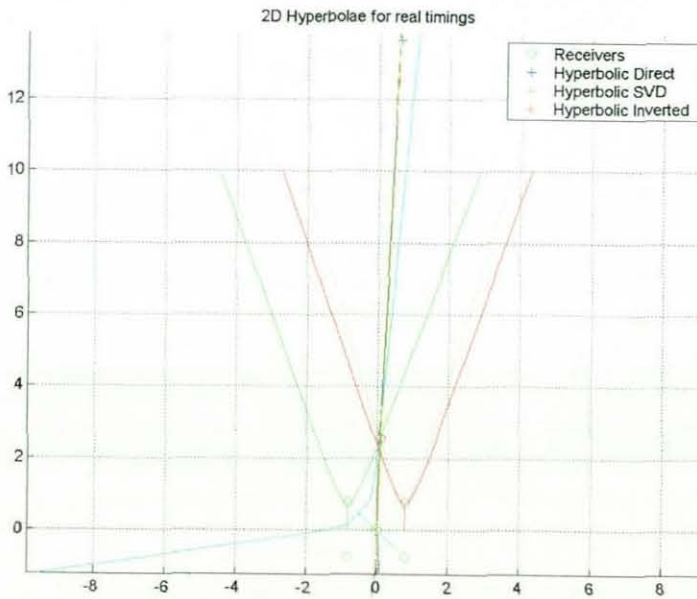


FIGURE 5.3-9 HYPERBOLAE FOR THE DATA OF POINT 8.

To show what happens with range in the sensitive areas a point 1m closer to the array and close to the orthogonal axis to timings h_{12} and h_{34} has been depicted in Figure 5.3-9. In this case the crossing of the hyperbolae for t_{13} and t_{24} are such that timing errors have little effect; however t_{12} , t_{34} and t_{14} are nearly parallel, and so small errors in timing give a large positional error, in this case up to 14m.

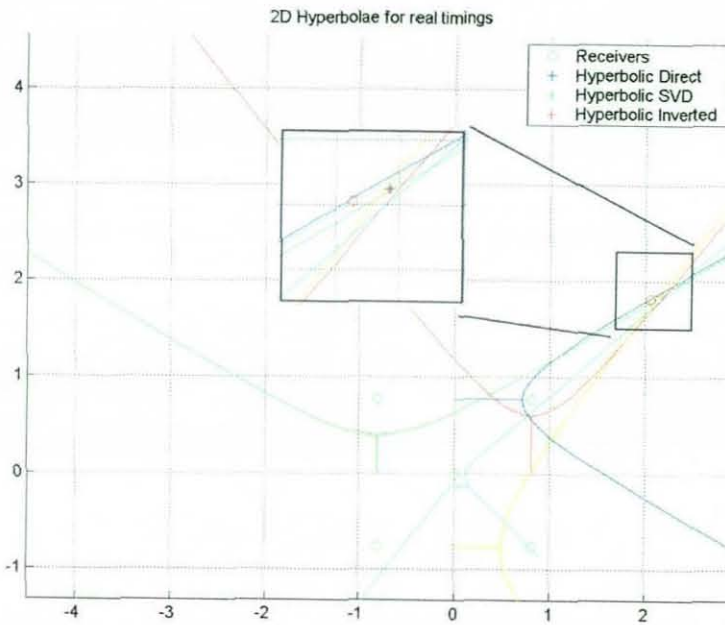


FIGURE 5.3-10 HYPERBOLAE FOR THE DATA OF POINT 11. THE DIFFERENT CROSSES REPRESENT THE ALGORITHMS DESCRIBED EARLIER WITH DIRECT (ALGORITHM 2), SVD(ALGORITHM 6) AND INVERTED(ALGORITHM 5)

Figures 5.3-10 and 5.3-11 show sources even nearer to the array and almost on the diagonals. In these cases positional errors would be expected to be present due to the source being near orthogonal to t_{14} , however in this case the source is so near the array that errors have less effect.

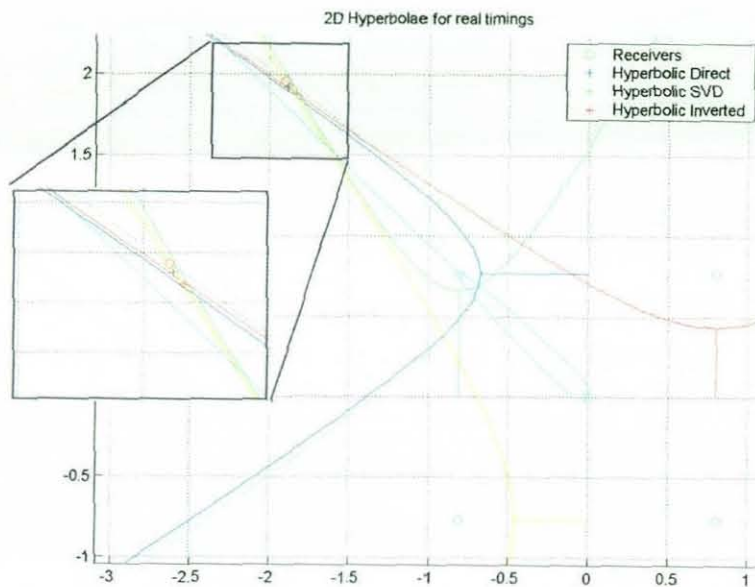


FIGURE 5.3-11 HYPERBOLAE FOR THE DATA OF POINT 12. THE DIFFERENT CROSSES REPRESENT THE ALGORITHMS DESCRIBED EARLIER WITH DIRECT (ALGORITHM 2), SVD(ALGORITHM 6) AND INVERTED(ALGORITHM 5)

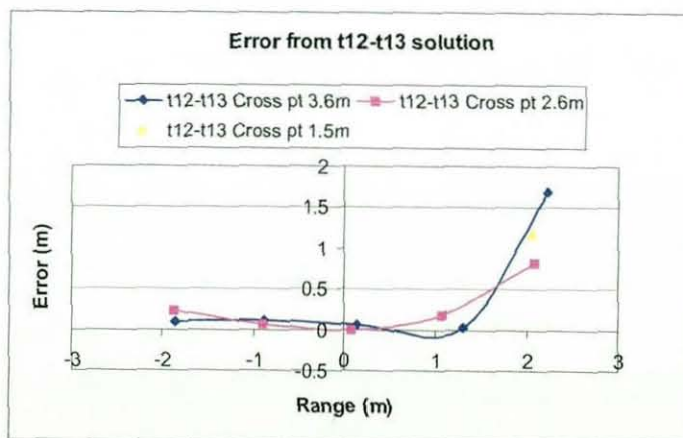


FIGURE 5.3-12 ERROR FROM INTERSECTION OF T_{12} AND T_{13} TO THE REFERENCE POSITION (BLUE $\gamma=2.6M$, PINK $\gamma=3.6M$)

The errors of the hyperbolae, especially of t_{24} and t_{34} , can be seen to have the greatest effect normal to the receiver axis. This corresponds to the pattern shown in the simulations performed in Chapter 3. The bearing to the source is, however, virtually unaffected. Taking the receiver pairs with best results, t_{12} , and t_{13} , and measuring the range from the cross point to the actual position, a figure can be plotted showing how range error changes with position relative to the array (Figure 5.3-12). It can be observed that as the source moves towards the diagonal, the error increases.

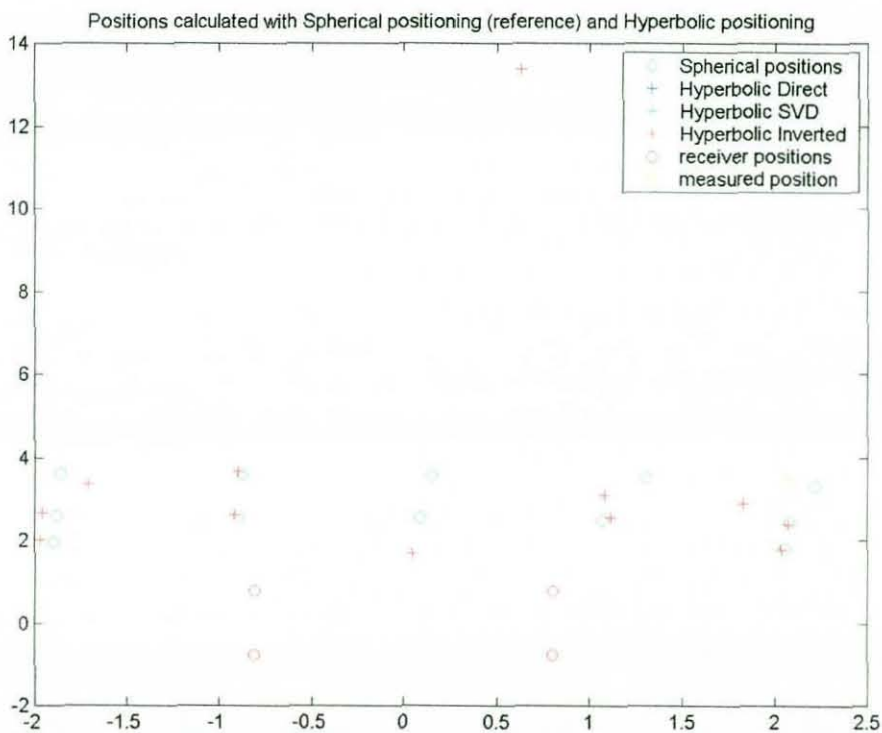


FIGURE 5.3-13(A) ESTIMATED POSITIONS OF ALL DATA POINTS FROM MANUAL MEASUREMENTS (YELLOW CIRCLE), SPHERICAL (GREEN CIRCLE), AND HYPERBOLIC USING SVD(6)/INVERSION(5) ALGORITHMS (RED CROSS) AND DIRECT(2) METHOD (BLUE CROSS) AMPLITUDE METHOD

Collating the results of all the test points a plot can be created depicting the points calculated using spherical and hyperbolic algorithms. In addition, the reference point measured by hand is included in yellow. To see the difference in timing

extraction algorithm Figure 5.3-13(A) shows the positions calculated using the initial amplitude calculations. Figure 5.3-13(B) shows the calculations using the correlated timings.

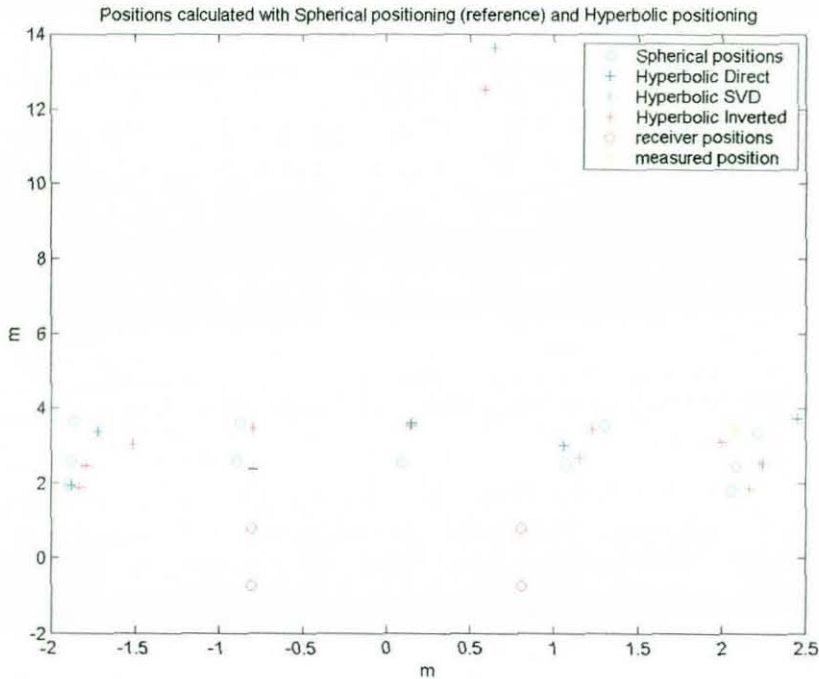
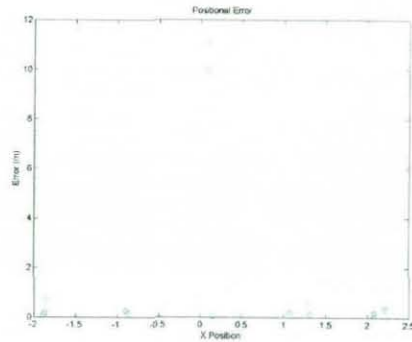


FIGURE 5.3-13(B) ESTIMATED POSITIONS OF ALL DATA POINTS FROM MANUAL MEASUREMENTS (YELLOW CIRCLE), SPHERICAL (GREEN CIRCLE), AND HYPERBOLIC USING SVD(6)/INVERSION(5) ALGORITHMS (RED CROSS) AND DIRECT METHOD(2) (BLUE CROSS). CORRELATION METHOD

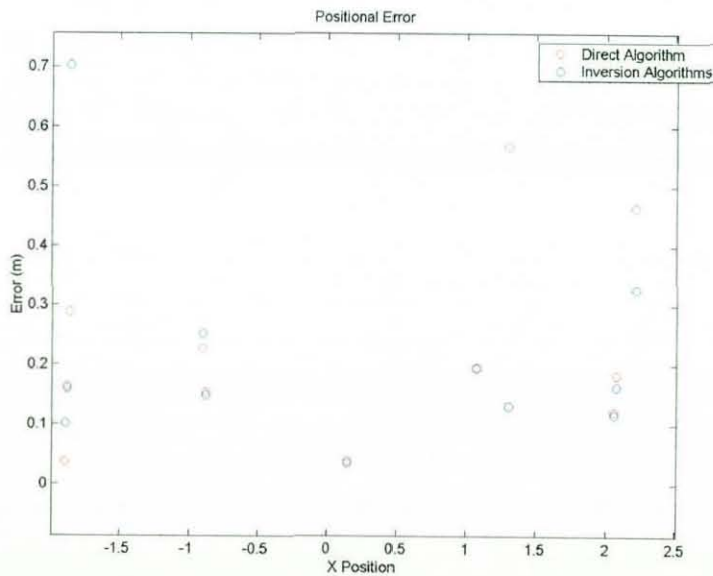
Figure 5.3-13(A) shows results of the amplitude detection method, the results are reasonable however the points at the orthogonal have greater error than Figure 5.3-13(B). In Figure 5.3-13(A) all the methods gave identical results in X and Y. Figure 5.3-13(B) is more consistent and although not all the points are as good as the amplitude method, most points are close to the target.

Concentrating now on the correlation method, if the positional errors are plotted versus the x range we get a picture of positional errors as a source crosses the face of

the array. According to simulation results we should expect to see a 'W'-shaped error pattern where the maxima are on the normal and orthogonal of each axis. In the case of Figure 5.3-14 we see a sharp peak at the orthogonal of t_{12} and possibly a slight rise towards the diagonals.

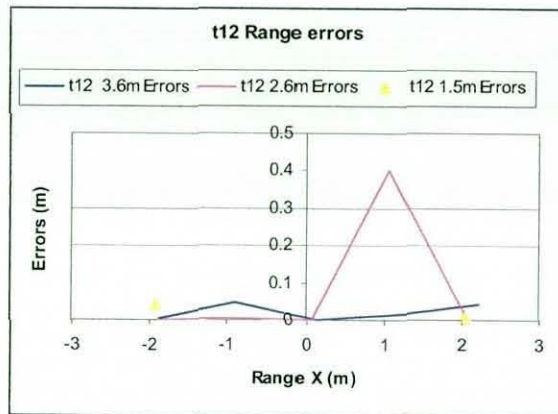


(A)



(B)

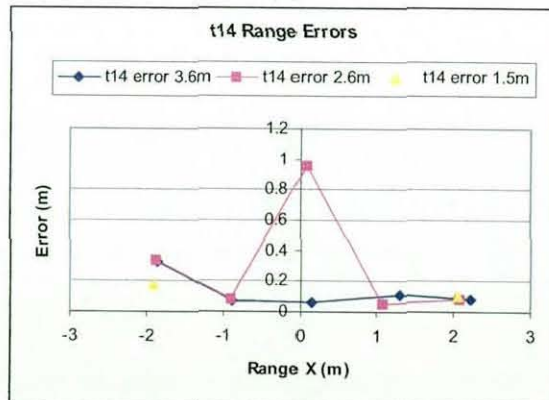
FIGURE 5.3-14 ERRORS OF THE PREDICTED AND REFERENCE POINTS USING ALGORITHM DESCRIBED IN SECTION 4.2. (B) IS A ZOOMED VERSION OF (A)



(A)



(B)



(C)

FIGURE 5.3-16 A - C RANGE FROM MEASURED HYPERBOLAE TO THE ACTUAL POSITION FOR EACH HYDROPHONE PAIR

Figure 5.3-16 (A) shows that errors are in the vicinity of 0-5cm although a peak is present at 1m (probably a bad point). In plot (B) t_{13} shows errors in the region of 0-7cm; this time a peak is present when the source passes in line with the receiver pair. Otherwise the results seem to describe a 'U' as could be expected as the source draws nearer to the orthogonal axes. In plot (C) t_{14} shows a source moving diagonally to line of the array. In this case the errors seem to increase towards the line of the array, and there is again an unusual peak near zero in x. A badly positioned hydrophone (H4) may be part of the reason that this axis has higher error rates.

5.3.3 CONCLUSION

Although this test is not comprehensive it does show some interesting trends. As expected it shows that the flat array method is sensitive to small timing errors, particularly in line and orthogonal to each axis. These errors appear to increase with range, although the data set is too small to show real trends. The test also shows that the bearing to the source is very accurate. We can also say that the system achieves general accuracies in bearing of within 1 degree and range accuracy of within 15cm in most cases, although this can be considerably larger in 'sensitive' areas. The experiment was interesting but by no means comprehensive. It appears that H4 may have been badly positioned, by up to 6cm (3 cycles). It is also apparent that the high noise level on H3 is unacceptable and limits the performance of the correlator. With these signal-to-noise ratios, the correlation method has little advantage over the amplitude method, but close examination of the signals at each stage of the processing has shown that the potential advantage of using this method is high. The amplitude method is potentially more vulnerable to lower quality data capture systems than the correlation method.

The study has shown that particular algorithms are more suitable for particular situations. A static array mounted on a vessel is ideally suited for the direct flat algorithm(2), however if the array is not static or fixed the SVD(6) algorithm is preferable. This algorithm seems more robust, and can deal with errors in hydrophone position. Algorithm (1) for the tetrahedron array works well if the array is static, but errors in hydrophone position can give large errors in position and/ or

dual solutions. The quantisation algorithm(4) gives varying accuracy in position mainly depending on quantisation size of the calibration, but it seems to give a good bearing to the source.

5.4 References in Chapter 5

- [1] W.F. Perrin and J.F. Hunter, Escape behavior of the Hawaiian springer porpoise (*Stenella cf. S. longirostris*), U.S. National Marine Fisheries Bulletin, Vol 70, p 49, 1972.
- [2] G.T. Waring, P.Gerrior, M.P. Payne, B.L. Parry and J.R. Nicolas, Incidental take of marine mammals in foreign fishery activities off the Northeast United States, 1977-1988, Fisheries Bulletin U.S. Vol 88, pp 347-360.
- [3] Y. Morizur, N. Tregenza, H. Heessen, S. Berrow and S. Pouvreau, By-catch and discarding in pelagic trawl fisheries, European Commission, DGXIV-C-1, Study Contract BIOECO 93/017 Final Report, 1995.
- [4] S.D.Berrow, N.J.C. Tregenza and P.S.Hammond, Marine mammal by-catch on the Celtic shelf, European Commission, DGXIV-C-1, Study Contract 92/3503 Final Report, 1994.
- [5] C.R. Sturtivant and S.Datta, Techniques to isolate dolphin and other tonal sounds from background noise, *Acoustic Letters*, Vol 18, No 10, pp 189-193.
- [6] G. Pavan, A real time FFT spectrogram display for bioacoustics, International Bioacoustics Council Symposium (XV IBAC 96); 24-26 October 1996, Pavia, Italy (unpublished).
- [7] P.R. Connelly, A.D. Goodson, K. Kaschner, P.A. Lepper and B. Woodward, Acoustic techniques to study cetacean behaviour around pelagic trawls; Proceedings of the Annual Science Conference of the International Council for the Exploitation of the Sea, *ICES 1997/Q: 15*, pp 137, Baltimore, Maryland, USA, 25 September - 1 October 1997 (Abstract)
- [8] K. Kaschner, A.D. Goodson, P.R. Connelly, and P.A. Lepper, Species characteristic features in communication signals of cetaceans: Source level estimates for some free ranging North Atlantic Odontocetes, *Proceedings of the Institute of Acoustics*, Vol. 19, No 9, pp 217-226, 1997, ISSN 0309-8117.
- [9] P.A. Lepper, K. Kaschner, P.R. Connelly, and A.D. Goodson, Development of a simplified ray path model for estimating the range and depth of vocalising marine mammals, *Proceedings of the Institute of Acoustics*, Vol. 19, No 9, pp 227-234, 1997, ISSN 0309-8117.

Chapter 6

COMPARATIVE ANALYSIS

This chapter does a comparative analysis of the results from the simulations in Chapter 3 and the practical results shown in Chapter 5.

6.1 THEORY AND PRACTICE

The simulations of Chapter 3 were very much more comprehensive than could be tested within the constraints of this project. Section 3.1 described the main factors causing errors to be

- i. Environmental, variations due to change of the sound speed;
- ii. Electronic, recognition and response time delays;
- iii. Residual timing errors, caused by phase shifts in electronics or random timings
- iv. Curvilinear acoustic ray paths;
- v. Image interference due to interference;
- vi. Baseline errors in initial calibration;
- vii. Multiplicative errors for speed of sound in slant-range measurements;
- viii. Square law errors from quadratic equations;
- ix. Transducer motion during reception.

The practical study was very limited by the environment, and it was not possible to study the effects of the errors described in i, iv, and vii. Simulations concentrated on the effect of unpredictably moving the receivers and the effect of errors in timing. Most of the error factors above result in these effects to varying degrees. The results of the simulations were varied with accuracies varying from the ludicrously small hundreds of microns in the perfect case, to hundreds of metres in the cases where reasonably large errors were added. The simulations showed trends of where the algorithms were most sensitive, in general along the axis of the hydrophone pairs and orthogonal. Errors in the diagonal were not observed in simulation, and these areas need further study to see if this is real.

In general the measured errors were larger than the simulated errors; however, the practical set-up was not perfect. The set-up was assumed perfect but certain assumptions proved wrong.

It seems there was a baseline error in the positioning of receiver 4, which although compensated for, introduced timing errors on the receiver pairs that included this receiver.

Spherical spreading was used as the reference for position, but only from receivers 1 and 2. This led to errors in timings involving receivers 3 and 4 being unpredictable and these timings causing errors in the final position.

To achieve the timing accuracy simulated, very low noise conditions are required. The hydrophones available for experimentation were not of this standard, and one in particular had very low signal-to-noise values, which was not conducive to accurate timings.

The practical test was severely limited in size. Simulations were performed over a range of 500m, but the practical test was to a maximum range of 5m. In this range the results were within 10cm in the non-sensitive areas, which is acceptable, but is many times larger than the theoretical values.

The results show that positional errors are mainly due to baseline errors in the calibration and electronic noise in the circuitry, both of which may be significantly reduced with greater control of the manufacturing and system set-up. Simulation showed that the flat array is sensitive to small errors in receiver positioning, although the error was not known in the practical experiment. The results seemed better than could be expected from the simulation results, but the larger ranges were not tested and so errors are likely to get significantly larger with greater range.

The algorithms performed well. In the case of the flat array, both algorithms performed satisfactorily, with no sign of multiple solutions. No points were measured on the singularity areas, but values in that region showed the same trend both practically and in simulation.

The tetrahedron array was not tested due to size and time constraints.

In general, the experimental results were not extensive or accurate enough to prove or disprove the simulations. The trends shown were similar, and this is useful to know for future work.

Project *CETASEL*, which used a dynamic flat array, suffered from technical and physical difficulties, resulting in very little data, and not enough to draw any conclusions from with respect to algorithms or accuracy. The test did show that the technology was possible, although it was impractical to produce an accurate system with this method.

Both methods did, however, show that bearing estimates are good even with the lower sampling rates. This is important as it could lead to other ways of configuring the array or arrays for greater coverage of a space.

Chapter 7

CONCLUSIONS

7.1 PASSIVE TRACKING OF DOLPHINS

This thesis has covered the basics of the physiology of cetaceans with regards to how they produce echolocation clicks and the most probable frequency range in which the target species produce them. Two systems have been developed to make use of these signals to attempt to locate the co-ordinates of one or more cetaceans.

7.1.1 DYNAMIC DEPLOYMENT

The first system was for a specific use in pelagic trawl by-catch research. This system had so many constraints that it became impractical to achieve the accuracy required. The stabilised movement of the passive array deployed was observed to be large enough to cause major errors in position fixing, although according to the simulations the bearing information was acceptable. Limitations of the calibration system led to too little data being collected to allow any detailed analysis.

7.1.2 STATIC DEPLOYMENT

By fixing the array and performing controlled experiments using a dolphin-like source at known points, new and original algorithms were simulated and tested. The tests were too limited in scope to draw any major conclusions but they highlighted the need for high quality, high speed, recording systems. Results of the study showed that the use of flat arrays is possible, although added levels of difficulty arise from use of this type of array, especially in the third (z) dimension. Bearing information seemed accurate using this type of array, and position information is potentially accurate in the less sensitive areas (not on the axis of receiver pairs).

7.2 PASSIVE TRACKING OF DIVERS

If a diver carries a source that emits similar impulsive sounds to those analysed here, a diver tracking system can be produced using this technique. The advantage is that the

diver only needs a pinger and not a transponder. The system could also be used for tracking anything large enough to carry a pinger, for example an autonomous underwater vehicle (AUV). The system developed in Chapter 4 was designed with this in mind, allowing the system to switch between pinger frequencies. This function was not tested due to time constraints.

7.3 THREE DIMENSIONS FROM TWO?

One aim of the project was to show the feasibility of retrieving three-dimensional positions from a two-dimensional array. The new algorithm developed during this project and simulated comprehensively has shown that this is indeed possible. The algorithm simplifies to a very simple general equation set and can be calculated on a simple processor at high speeds. Inaccuracies in the z-axis are however, likely to be significantly higher than in the x- and y-axes. Unfortunately it was not practical to test this in the practical experiment.

7.4 SUMMARY

This project has been very ambitious. One part of the research, the *CETASEL* project, suffered from its specification being dictated from an early stage by politics and available equipment rather than scientific analysis and methods. This resulted in the prototypes produced not always producing satisfactory results. In the last part of the project a step back was taken and the project re-thought from the experiences of the first part. This led to a system with the potential to track a sound source to the theoretical accuracy. Time and physical constraints did not allow this system to be tested to its full capacity, although the controlled experiments that were performed were positive and verified that it is possible to track a source by applying algorithms that already exist and those developed during this project.

As a spin-off from this work a second ranging method was developed. This method was used for determining the range of cetaceans from their vocalisations and has now been accepted in the field as a tool for this kind of monitoring.

In retrospect, the project has taken a number of blind alleys, which if it had been possible to avoid them, would have led to a much more advanced system. However, time and financial limitations have steered the latter course of the research, which became more a verification of passive tracking techniques than the development of a working system operating on a ship at sea.

Although the project has not advanced as far as the author would have liked it has shown the potential of the systems and has also highlighted the positive and negative points that need to be considered in the development of such a system.

7.5 FUTURE WORK

Future work is needed to analyse the full potential of a practical system. The electronics needs to be redesigned with noise issues in mind and a fixed array of known dimensions needs to be manufactured. In particular the front end and sampling circuitry should be laid out with more care taken to electronic noise elimination. Tests of the system in open water where greater ranges can be achieved should show the true errors of the system. The second measurement system using a fixed array and a higher frequency sampling system shows most potential. Future systems should be based on this type of sampling regime. However the designed system had a number of extra features that were not necessary for the proof of concept. Keeping it simple will allow any future work to progress more effectively.

Although some of the algorithms could at times be poor in finding accurate positions, they proved very reliable in achieving a bearing to the source with accuracy's within 0.5 degree in the simulations. If two such arrays were used, spaced apart from each other, the bearing information alone could provide enough information to locate the source. The range could then be used as verification. In addition, tracking algorithms such as Kalman filters could be introduced. These incorporate known factors such as maximum velocity of the source, and maximum depth, so by using the tracking system for an estimate of position these could be used to predict a track of the source's movement.

Future work should use the algorithms which seem best suited for the working environment. For flat arrays the new flat array algorithm presented here is the only viable choice found so far, for three dimensional arrays the SVD matrix method seems to be the most stable. In the industrial world it is often the case that physical limitations dominate decisions, and theory is forced to fit it, if possible. The best solution for this kind of situation would be to have a fixed 4 or more receiver flat array, and a fixed third dimension incorporated with as large a vertical spacing as possible. This will allow both algorithms to be used. If the receivers were placed in a number square configurations but offset in angle i.e. two squares offset at 45 degrees (8 receivers at 45 degrees to each other in a ring), the surplus of receivers will enable multiple solutions which can be incorporated in a best fit solution. This also allows a quality figure to be calculated for each data point.

AUTHOR'S PUBLICATIONS

Connelly PR, Woodward B, Goodson A D, Lepper P and Newborough D, Remote sensing methods for cetacean interactions with pelagic trawl fishing gear; Proceedings of the 11th Annual Conference of the European Cetacean Society, Stralsund, Germany, 10-12 March 1997, edited by Siebert U and Lick R, University of Kiel, Germany

Kaschner KA, Goodson AD, Connelly PR and Lepper PA, Species characteristic features in communication signals of cetaceans: Source level estimates for some free ranging North Atlantic Odontocetes, Proceedings of the Institute of Acoustics Symposium on Underwater Bio-Sonar and Bioacoustics, Loughborough University, 16-17 December 1997; in *Proceedings of the Institute of Acoustics*, Vol 19, Part 9, ISBN 1-901656-08-X, ISSN 0309-8117

Lepper PA, Kaschner K, Connelly PR and Goodson AD, Development of a simplified ray path model for estimating the range and depth of vocalising marine mammals; Proceedings of the Institute of Acoustics Symposium on Underwater Bio-Sonar and Bioacoustics, Loughborough University, 16-17 December 1997; in *Proceedings of the Institute of Acoustics*, Vol 19, Part 9, pp 227-234, 1997, ISSN 0309-8117.

Connelly P R, Goodson A D, Kaschner K, Lepper P A and Woodward B, Acoustic techniques to study cetacean behaviour around pelagic trawls; Proceedings of the Annual Science Conference of the International Council for the Exploitation of the Sea, *ICES 1997/Q: 15*, pp 66-71, Baltimore, Maryland, USA, 25 September - 1 October 1997

Connelly P R, Woodward B and Goodson A D, Tracking a moving acoustic source in a three-dimensional space; Proceedings of the IEEE Oceanic Engineering Society and the Marine Technology Society International Conference *Oceans '97*, Halifax, Nova Scotia, Canada, 6-9 October 1997, Vol 1, pp 447-450, ISBN 0-7803-4108-2

Connelly PR, Goodson AD and Coggrave CR, MatLab modelling of shallow water sound fields to explain the aversive behaviour of a harbour porpoise, *Proceedings of the Institute of Acoustics*, Vol 19, No 9, pp 185-192, 1997, ISSN 0309-8117.

Connelly P R and Woodward B, Real time tracking of divers and dolphins; 21st Scandinavian Symposium on Physical Acoustics, Ustaøset, Norway, 1 - 4 February 1998; in Scientific/Technical Report, pp 19-20, edited by H Hoboek, University of Bergen, May 1998, ISSN 0803-2696

Connelly P R, Woodward B and Goodson A D, A non-intrusive tracking technique for dolphins interacting with a pelagic trawl using a sparse array of hydrophones; Proceedings of the IOA Symposium on Underwater Bio-Sonar and Bio-Acoustics, Loughborough University, 16-17 December 1997; in *Proceedings of the Institute of Acoustics*, Vol 19, Part 9, pp 193-198, ISBN 1-901656-08-X

Woodward B, Connelly P R, Barson L, Bourne S, L Fish, Jackson C and Rawlings P, An autonomous underwater vehicle as a student project; Proceedings of the 1st IEEE Oceanic Engineering Society Pacific Rim Symposium - *Underwater Technology '98 - Key Issues in the Global Underwater Environment*, Institute of Industrial Science, University of Tokyo, Japan, 15-17 April 1998, pp 150-154, ISBN 0-7803-4273-9

Woodward B and Connelly P R, An autonomous underwater vehicle as an imaging platform; IEE Colloquium on Image Processing in Underwater Applications, London, 25 March 1998

Woodward B and Connelly P R, Project *CETASEL*: Tracking echo-locating dolphins in the vicinity of a trawl; IEE Colloquium on Recent Advances in Sonar applied to Biological Oceanography, London, 5 June 1998, Group E15 (Radar, sonar and navigation systems); in *IEE Digest* No 1998/227, pp 8/1-8/6, ISSN 0963-3308

The author has also made major contributions to the following reports:

Woodward B and Goodson A D, Enhancing the acoustic detectability of fishing nets to prevent the entrapment of cetaceans; Final report (36 months) for contract CSA2270, Ministry of Agriculture, Fisheries and Food, and De Haan D, Dremlere P-Y, Woodward B, Kastelein R, Amundin M and Hansen K, Prevention of by-catch of cetaceans in pelagic trawls by technical means (project *CETASEL*); Proceedings of the Annual Science Conference of the International Council for the Exploitation of the Sea, *ICES Fish Capture Committee*, Vol 1, pp. 1-14, 1997 *ICES '97*, Baltimore, Maryland, USA, 25 September - 1 October 1997

Final report (36 months) for contract CRO127, Department of the Environment, with contributions from Coggrave C R, Connelly P R, Datta S, Klinowska M, Lepper P A, Mayo R H and Newborough D, 1997 (February, re-submitted November);

De Haan D, Dremlere P-Y, Woodward B, Kastelein R A, Amundin M and Hansen K, Prevention of by-catch of small cetaceans in pelagic trawls by technical means; Final Report (36 months) for AIR-III *CETA-SEL* project, contract AIR3-CT94-2423, European Commission, 1998 (February)

De Haan D, Dremlere P-Y, Woodward B, Kastelein R A, Amundin M and Hansen K, Prevention of by-catch of small cetaceans in pelagic trawls by technical means; Final Report (condensed version) for AIR-III *CETA-SEL* project, contract AIR3-CT94-2423, European Commission, 1999 (10 April)

Van Biesen L, Adamy J, Bjorno L, Sessarego J-P, Taroudakis M I, Woodward B, Zakharia M E, Sediment Identification for Geotechnics by Marine Acoustics; Final Report (36 months) for MAST-III *SIGMA* project, contract PL96-1111, European Commission, 2000 (November)

APPENDIX A

EXPANSION OF THREE-DIMENSIONAL EQUATION SET

The following equations show the derivation of the three-dimensional equation set first performed by Hardman and Woodward [1], and later re-worked and tested in simulation by Coggrave [2]. They are presented here in full, including all the operations and expansions, starting with Fig. 6 from [1].

- [1] P.A. Hardman and B. Woodward, Underwater location fixing by a diver-operated acoustic telemetry system, *Acustica*, Vol 55, pp 34-44, 1984.
- [2] C.R. Coggrave, Performance analysis of 3D underwater tracking system using computer simulation techniques, Internal Report, Department of Electronic and Electrical Engineering, Loughborough University, UK.

Three Dimensional Equation Set

$$c \cdot t_1 = \sqrt{x^2 + (y - y_1)^2 + (z - z_1)^2} \quad \text{Equ 1}$$

$$c \cdot t_2 = \sqrt{x^2 + (y - y_2)^2 + (z - z_2)^2} \quad \text{Equ 2}$$

$$c \cdot t_3 = \sqrt{(x - x_3)^2 + (y - y_3)^2 + (z - z_3)^2} \quad \text{Equ 3}$$

$$c \cdot t_4 = \sqrt{(x - x_4)^2 + (y - y_4)^2 + (z - z_4)^2} \quad \text{Equ 4}$$

From equ 1 & 2

$$c \cdot \Delta t_2 = c \cdot t_1 - c \cdot t_2$$

$$c \cdot \Delta t_2 = \sqrt{x^2 + (y - y_1)^2 + (z - z_1)^2} - \sqrt{x^2 + (y - y_2)^2 + (z - z_2)^2} \quad \text{Equ A}$$

Rearranging

$$\sqrt{x^2 + (y - y_2)^2 + (z - z_2)^2} = \sqrt{x^2 + (y - y_1)^2 + (z - z_1)^2} - c \cdot \Delta t_2$$

$$\sqrt{x^2 + (y - y_2)^2 + (z - z_2)^2} = \frac{c \cdot \Delta t_2 \cdot \sqrt{x^2 + (y - y_1)^2 + (z - z_1)^2} - (c \cdot \Delta t_2)^2}{c \cdot \Delta t_2}$$

And substituting equ A

$$\sqrt{x^2 + (y - y_2)^2 + (z - z_2)^2} = \frac{\left[\sqrt{x^2 + (y - y_1)^2 + (z - z_1)^2} - \sqrt{x^2 + (y - y_2)^2 + (z - z_2)^2} \right] \cdot \sqrt{x^2 + (y - y_1)^2 + (z - z_1)^2} - (c \cdot \Delta t_2)^2}{c \cdot \Delta t_2}$$

Multiplying out the bracket

$$\sqrt{x^2 + (y - y_2)^2 + (z - z_2)^2} = \frac{\left[x^2 + (y - y_1)^2 + (z - z_1)^2 \right] - \left[\sqrt{x^2 + (y - y_2)^2 + (z - z_2)^2} \cdot \sqrt{x^2 + (y - y_1)^2 + (z - z_1)^2} \right] - (c \cdot \Delta t_2)^2}{c \cdot \Delta t_2} \quad \text{Equ B}$$

Now to evaluate square root product term go back to equ 4 and square both sides, giving

$$c \cdot \Delta t_2 = \sqrt{x^2 + (y - y_1)^2 + (z - z_1)^2} - \sqrt{x^2 + (y - y_2)^2 + (z - z_2)^2}$$

$$(c \cdot \Delta t_2)^2 = \left[x^2 + (y - y_1)^2 + (z - z_1)^2 + x^2 + (y - y_2)^2 + (z - z_2)^2 \right] - 2 \cdot \sqrt{x^2 + (y - y_1)^2 + (z - z_1)^2} \cdot \sqrt{x^2 + (y - y_2)^2 + (z - z_2)^2}$$

So rearranging

$$\sqrt{x^2 + (y - y_1)^2 + (z - z_1)^2} \cdot \sqrt{x^2 + (y - y_2)^2 + (z - z_2)^2} = \frac{\left[x^2 + (y - y_1)^2 + (z - z_1)^2 + x^2 + (y - y_2)^2 + (z - z_2)^2 \right] - (c \cdot \Delta t_2)^2}{2} \quad \text{Equ C}$$

Substituting equ C into equ B gives

$$\sqrt{x^2 + (y - y_2)^2 + (z - z_2)^2} = \frac{\left[x^2 + (y - y_1)^2 + (z - z_1)^2 \right] - \left[\frac{\left[x^2 + (y - y_1)^2 + (z - z_1)^2 + x^2 + (y - y_2)^2 + (z - z_2)^2 \right] - (c \cdot \Delta t_2)^2}{2} \right] - (c \cdot \Delta t_2)^2}{c \cdot \Delta t_2}$$

Put over a common denominator

$$\sqrt{x^2 + (y - y_2)^2 + (z - z_2)^2} = \frac{\left[x^2 + (y - y_1)^2 + (z - z_1)^2 \right] \cdot 2 - \left[x^2 + (y - y_1)^2 + (z - z_1)^2 + x^2 + (y - y_2)^2 + (z - z_2)^2 - (c \cdot \Delta t_2)^2 \right] - (c \cdot \Delta t_2)^2 \cdot 2}{2 \cdot c \cdot \Delta t_2}$$

Expand the numerator

$$\sqrt{x^2 + (y - y_2)^2 + (z - z_2)^2} = \frac{-2 \cdot y \cdot y_1 + y_1^2 - 2 \cdot z \cdot z_1 + z_1^2 + 2 \cdot y \cdot y_2 - y_2^2 + 2 \cdot z \cdot z_2 - z_2^2 - c^2 \cdot \Delta t_2^2}{2 \cdot c \cdot \Delta t_2}$$

Factorize the numerator

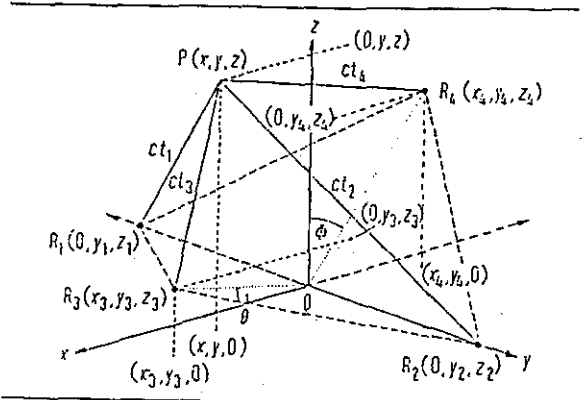


Fig. 6. Receiver arrangement for development of 3-D equation set.

Now combining equ 2 and equ 3 we obtain

$$c \cdot \Delta 32 = c \cdot 13 - c \cdot 12$$

$$c \cdot \Delta 32 = \sqrt{(x-x3)^2 + (y-y3)^2 + (z-z3)^2} - \sqrt{x^2 + (y-y2)^2 + (z-z2)^2} \quad \text{Equ D}$$

Rearranging

$$\sqrt{x^2 + (y-y2)^2 + (z-z2)^2} = \sqrt{(x-x3)^2 + (y-y3)^2 + (z-z3)^2} - c \cdot \Delta 32$$

$$\sqrt{x^2 + (y-y2)^2 + (z-z2)^2} = \frac{(c \cdot \Delta 32) \cdot \sqrt{(x-x3)^2 + (y-y3)^2 + (z-z3)^2} - (c \cdot \Delta 32)^2}{c \cdot \Delta 32}$$

Now substituting equ D

$$\sqrt{x^2 + (y-y2)^2 + (z-z2)^2} = \frac{\sqrt{(x-x3)^2 + (y-y3)^2 + (z-z3)^2} - \sqrt{x^2 + (y-y2)^2 + (z-z2)^2} \cdot \sqrt{(x-x3)^2 + (y-y3)^2 + (z-z3)^2} - (c \cdot \Delta 32)^2}{c \cdot \Delta 32}$$

Multiply out the bracket

$$\sqrt{x^2 + (y-y2)^2 + (z-z2)^2} = \frac{[(x-x3)^2 + (y-y3)^2 + (z-z3)^2] - [\sqrt{x^2 + (y-y2)^2 + (z-z2)^2} \cdot \sqrt{(x-x3)^2 + (y-y3)^2 + (z-z3)^2}] - (c \cdot \Delta 32)^2}{c \cdot \Delta 32} \quad \text{Equ E}$$

Now to evaluate square root product term go back to equ D and square both sides, giving

$$c \cdot \Delta 32 = \sqrt{(x-x3)^2 + (y-y3)^2 + (z-z3)^2} - \sqrt{x^2 + (y-y2)^2 + (z-z2)^2}$$

$$(c \cdot \Delta 32)^2 = [(x-x3)^2 + (y-y3)^2 + (z-z3)^2] + [x^2 + (y-y2)^2 + (z-z2)^2] - 2 \cdot \sqrt{(x-x3)^2 + (y-y3)^2 + (z-z3)^2} \cdot \sqrt{x^2 + (y-y2)^2 + (z-z2)^2}$$

So rearranging

$$\sqrt{(x-x3)^2 + (y-y3)^2 + (z-z3)^2} \cdot \sqrt{x^2 + (y-y2)^2 + (z-z2)^2} = \frac{[(x-x3)^2 + (y-y3)^2 + (z-z3)^2] + [x^2 + (y-y2)^2 + (z-z2)^2] - (c \cdot \Delta 32)^2}{2} \quad \text{Equ F}$$

Substituting equ F into equ E gives

$$\sqrt{x^2 + (y-y2)^2 + (z-z2)^2} = \frac{[(x-x3)^2 + (y-y3)^2 + (z-z3)^2] - \left[\frac{[(x-x3)^2 + (y-y3)^2 + (z-z3)^2] + [x^2 + (y-y2)^2 + (z-z2)^2] - (c \cdot \Delta 32)^2}{2} \right] - (c \cdot \Delta 32)^2}{c \cdot \Delta 32}$$

Put over a common denominator

$$\sqrt{x^2 + (y-y2)^2 + (z-z2)^2} = \frac{[(x-x3)^2 + (y-y3)^2 + (z-z3)^2] \cdot 2 - [(x-x3)^2 + (y-y3)^2 + (z-z3)^2] + [x^2 + (y-y2)^2 + (z-z2)^2] - (c \cdot \Delta 32)^2}{2 \cdot c \cdot \Delta 32} - (c \cdot \Delta 32)^2 \cdot 2$$

Expand the numerator

$$\sqrt{x^2 + (y-y2)^2 + (z-z2)^2} = \frac{2 \cdot x \cdot x3 + x3^2 - 2 \cdot y \cdot y3 + y3^2 - 2 \cdot z \cdot z3 + z3^2 + 2 \cdot y \cdot y2 - y2^2 + 2 \cdot z \cdot z2 - z2^2 - c^2 \cdot \Delta 32^2}{2 \cdot c \cdot \Delta 32}$$

Factorize the numerator

$$\sqrt{x^2 + (y-y2)^2 + (z-z2)^2} = \frac{-2 \cdot x \cdot x3 + 2 \cdot y \cdot (y2 - y3) + 2 \cdot z \cdot (z2 - z3) + x3^2 - y2^2 + y3^2 - z2^2 + z3^2 - c^2 \cdot \Delta 32^2}{2 \cdot c \cdot \Delta 32} \quad \text{Equ 6}$$

Now combining equ 2 and 4

$$c \cdot \Delta t^2 = c \cdot t_1 - c \cdot t_2$$

$$c \cdot \Delta t^2 = \sqrt{(x-x_4)^2 + (y-y_4)^2 + (z-z_4)^2} - \sqrt{x^2 + (y-y_2)^2 + (z-z_2)^2} \quad \text{Equ G}$$

Rearrange

$$\sqrt{x^2 + (y-y_2)^2 + (z-z_2)^2} = \sqrt{(x-x_4)^2 + (y-y_4)^2 + (z-z_4)^2} - c \cdot \Delta t^2$$

$$\sqrt{x^2 + (y-y_2)^2 + (z-z_2)^2} = \frac{c \cdot \Delta t^2 \cdot \sqrt{(x-x_4)^2 + (y-y_4)^2 + (z-z_4)^2} - (c \cdot \Delta t^2)^2}{c \cdot \Delta t^2}$$

Now substituting equ G

$$\sqrt{x^2 + (y-y_2)^2 + (z-z_2)^2} = \frac{\sqrt{(x-x_4)^2 + (y-y_4)^2 + (z-z_4)^2} - \sqrt{x^2 + (y-y_2)^2 + (z-z_2)^2}}{c \cdot \Delta t^2} \cdot \sqrt{(x-x_4)^2 + (y-y_4)^2 + (z-z_4)^2} - (c \cdot \Delta t^2)^2$$

Multiply out the bracket

$$\sqrt{x^2 + (y-y_2)^2 + (z-z_2)^2} = \frac{[(x-x_4)^2 + (y-y_4)^2 + (z-z_4)^2] - [\sqrt{x^2 + (y-y_2)^2 + (z-z_2)^2} \cdot \sqrt{(x-x_4)^2 + (y-y_4)^2 + (z-z_4)^2}] - (c \cdot \Delta t^2)^2}{c \cdot \Delta t^2} \quad \text{Equ H}$$

Now to evaluate square root product term go back to equ G and square both sides, giving

$$c \cdot \Delta t^2 = \sqrt{(x-x_4)^2 + (y-y_4)^2 + (z-z_4)^2} - \sqrt{x^2 + (y-y_2)^2 + (z-z_2)^2}$$

$$(c \cdot \Delta t^2)^2 = [(x-x_4)^2 + (y-y_4)^2 + (z-z_4)^2] + [x^2 + (y-y_2)^2 + (z-z_2)^2] - 2 \cdot \sqrt{(x-x_4)^2 + (y-y_4)^2 + (z-z_4)^2} \cdot \sqrt{x^2 + (y-y_2)^2 + (z-z_2)^2}$$

So rearranging

$$\sqrt{(x-x_4)^2 + (y-y_4)^2 + (z-z_4)^2} \cdot \sqrt{x^2 + (y-y_2)^2 + (z-z_2)^2} = \frac{[(x-x_4)^2 + (y-y_4)^2 + (z-z_4)^2 + x^2 + (y-y_2)^2 + (z-z_2)^2] - (c \cdot \Delta t^2)^2}{2} \quad \text{Equ J}$$

Substituting equ J into equ H gives

$$\sqrt{x^2 + (y-y_2)^2 + (z-z_2)^2} = \frac{[(x-x_4)^2 + (y-y_4)^2 + (z-z_4)^2] - \frac{[(x-x_4)^2 + (y-y_4)^2 + (z-z_4)^2 + x^2 + (y-y_2)^2 + (z-z_2)^2] - (c \cdot \Delta t^2)^2}{2} - (c \cdot \Delta t^2)^2}{c \cdot \Delta t^2}$$

Put over a common denominator

$$\sqrt{x^2 + (y-y_2)^2 + (z-z_2)^2} = \frac{[(x-x_4)^2 + (y-y_4)^2 + (z-z_4)^2] \cdot 2 - [(x-x_4)^2 + (y-y_4)^2 + (z-z_4)^2 + x^2 + (y-y_2)^2 + (z-z_2)^2] - (c \cdot \Delta t^2)^2 \cdot 2}{2 \cdot c \cdot \Delta t^2}$$

Expand the numerator

$$\sqrt{x^2 + (y-y_2)^2 + (z-z_2)^2} = \frac{-2 \cdot x \cdot x_4 + x_4^2 - 2 \cdot y \cdot y_4 + y_4^2 - 2 \cdot z \cdot z_4 + z_4^2 + 2 \cdot y \cdot y_2 - y_2^2 + 2 \cdot z \cdot z_2 - z_2^2 - c^2 \cdot \Delta t^4}{2 \cdot c \cdot \Delta t^2}$$

Factorize the numerator

$$\sqrt{x^2 + (y-y_2)^2 + (z-z_2)^2} = \frac{-2 \cdot x \cdot x_4 + 2 \cdot y \cdot (y_2 - y_4) + 2 \cdot z \cdot (z_2 - z_4) + x_4^2 - y_2^2 + y_4^2 - z_2^2 + z_4^2 - c^2 \cdot \Delta t^4}{2 \cdot c \cdot \Delta t^2} \quad \text{Equ 7}$$

Now equate equ 5 and equ 6.

$$\frac{2 \cdot y \cdot (y_2 - y_1) + 2 \cdot z \cdot (z_2 - z_1) + y_1^2 - y_2^2 + z_1^2 - z_2^2 - (c \cdot \Delta t_1)^2}{2 \cdot c \cdot \Delta t_1} = \frac{-2 \cdot x \cdot x_3 + 2 \cdot y \cdot (y_2 - y_3) + 2 \cdot z \cdot (z_2 - z_3) + x_3^2 - y_2^2 + y_3^2 - z_2^2 + z_3^2 - c^2 \cdot \Delta t_3^2}{2 \cdot c \cdot \Delta t_3}$$

$$2 \cdot y \cdot (y_2 - y_1) + 2 \cdot z \cdot (z_2 - z_1) + y_1^2 - y_2^2 + z_1^2 - z_2^2 - (c \cdot \Delta t_1)^2 = \frac{\Delta t_1}{\Delta t_3} \left[-2 \cdot x \cdot x_3 + 2 \cdot y \cdot (y_2 - y_3) + 2 \cdot z \cdot (z_2 - z_3) + x_3^2 - y_2^2 + y_3^2 - z_2^2 + z_3^2 - c^2 \cdot \Delta t_3^2 \right]$$

Define $K_1 = \frac{\Delta t_1}{\Delta t_3}$

$$2 \cdot y \cdot (y_2 - y_1) + 2 \cdot z \cdot (z_2 - z_1) + y_1^2 - y_2^2 + z_1^2 - z_2^2 - (c \cdot \Delta t_1)^2 = K_1 \cdot \left[-2 \cdot x \cdot x_3 + 2 \cdot y \cdot (y_2 - y_3) + 2 \cdot z \cdot (z_2 - z_3) + x_3^2 - y_2^2 + y_3^2 - z_2^2 + z_3^2 - c^2 \cdot \Delta t_3^2 \right]$$

$$2 \cdot y \cdot (y_2 - y_1) - K_1 \cdot (2 \cdot y \cdot (y_2 - y_3)) = K_1 \cdot \left[-2 \cdot x \cdot x_3 + 2 \cdot z \cdot (z_2 - z_3) + x_3^2 - y_2^2 + y_3^2 - z_2^2 + z_3^2 - c^2 \cdot \Delta t_3^2 \right] - \left[2 \cdot z \cdot (z_2 - z_1) + y_1^2 - y_2^2 + z_1^2 - z_2^2 - (c \cdot \Delta t_1)^2 \right]$$

Now collect y terms on lhs

$$2 \cdot y \cdot (y_2 - y_1 - K_1 \cdot (y_2 - y_3)) = K_1 \cdot \left[-2 \cdot x \cdot x_3 + 2 \cdot z \cdot (z_2 - z_3) + x_3^2 - y_2^2 + y_3^2 - z_2^2 + z_3^2 - c^2 \cdot \Delta t_3^2 \right] - \left[2 \cdot z \cdot (z_2 - z_1) + y_1^2 - y_2^2 + z_1^2 - z_2^2 - (c \cdot \Delta t_1)^2 \right]$$

Make y the subject

$$y = \frac{K_1 \cdot \left[-2 \cdot x \cdot x_3 + 2 \cdot z \cdot (z_2 - z_3) + x_3^2 - y_2^2 + y_3^2 - z_2^2 + z_3^2 - c^2 \cdot \Delta t_3^2 \right] - \left[2 \cdot z \cdot (z_2 - z_1) + y_1^2 - y_2^2 + z_1^2 - z_2^2 - (c \cdot \Delta t_1)^2 \right]}{2 \cdot (y_2 - y_1 - K_1 \cdot (y_2 - y_3))}$$

Expand numerator

$$y = \frac{-2 \cdot K_1 \cdot x \cdot x_3 + 2 \cdot K_1 \cdot z \cdot z_2 - 2 \cdot K_1 \cdot z \cdot z_3 + K_1 \cdot x_3^2 - K_1 \cdot y_2^2 + K_1 \cdot y_3^2 - K_1 \cdot z_2^2 + K_1 \cdot z_3^2 - K_1 \cdot c^2 \cdot \Delta t_3^2 - 2 \cdot z \cdot z_2 + 2 \cdot z \cdot z_1 - y_1^2 + y_2^2 - z_1^2 + z_2^2 + c^2 \cdot \Delta t_1^2}{2 \cdot (y_2 - y_1 - K_1 \cdot (y_2 - y_3))}$$

Now rearrange to the form

$$y = \alpha \cdot x + \beta \cdot z + \phi$$

Equ 8

$$y = \frac{(-2 \cdot K_1 \cdot x \cdot x_3) + (2 \cdot K_1 \cdot z \cdot z_2 - 2 \cdot K_1 \cdot z \cdot z_3 - 2 \cdot z \cdot z_2 + 2 \cdot z \cdot z_1) + (K_1 \cdot x_3^2 - K_1 \cdot y_2^2 + K_1 \cdot y_3^2 - K_1 \cdot z_2^2 + K_1 \cdot z_3^2 - K_1 \cdot c^2 \cdot \Delta t_3^2 - y_1^2 + y_2^2 - z_1^2 + z_2^2 + c^2 \cdot \Delta t_1^2)}{2 \cdot (y_2 - y_1 - K_1 \cdot (y_2 - y_3))}$$

$$y = \left[\frac{-K_1 \cdot x_3}{y_2 - y_1 - K_1 \cdot (y_2 - y_3)} \right] \cdot x + \left[\frac{K_1 \cdot (z_2 - z_3) - (z_2 - z_1)}{y_2 - y_1 - K_1 \cdot (y_2 - y_3)} \right] \cdot z + \left[\frac{K_1 \cdot (x_3^2 - y_2^2 + y_3^2 - z_2^2 + z_3^2 - c^2 \cdot \Delta t_3^2) - (y_1^2 - y_2^2 + z_1^2 - z_2^2 - c^2 \cdot \Delta t_1^2)}{2 \cdot (y_2 - y_1 - K_1 \cdot (y_2 - y_3))} \right]$$

That is

$$\alpha = \frac{-K_1 \cdot x_3}{y_2 - y_1 - K_1 \cdot (y_2 - y_3)}$$

Equ 11

$$\beta = \frac{K_1 \cdot (z_2 - z_3) - (z_2 - z_1)}{y_2 - y_1 - K_1 \cdot (y_2 - y_3)}$$

Equ 12

Now equate equ 5 and equ 7

$$\frac{2 \cdot y \cdot (y_2 - y_1) + 2 \cdot z \cdot (z_2 - z_1) + y_1^2 - y_2^2 + z_1^2 - z_2^2 - (c \cdot \Delta t_1)^2}{2 \cdot c \cdot \Delta t_1} = \frac{-2 \cdot x \cdot x_4 + 2 \cdot y \cdot (y_2 - y_4) + 2 \cdot z \cdot (z_2 - z_4) + x_4^2 - y_2^2 + y_4^2 - z_2^2 + z_4^2 - c^2 \cdot \Delta t_2^2}{2 \cdot c \cdot \Delta t_2}$$

$$2 \cdot y \cdot (y_2 - y_1) + 2 \cdot z \cdot (z_2 - z_1) + y_1^2 - y_2^2 + z_1^2 - z_2^2 - (c \cdot \Delta t_1)^2 = \frac{\Delta t_1}{\Delta t_2} \left[-2 \cdot x \cdot x_4 + 2 \cdot y \cdot (y_2 - y_4) + 2 \cdot z \cdot (z_2 - z_4) + x_4^2 - y_2^2 + y_4^2 - z_2^2 + z_4^2 - c^2 \cdot \Delta t_2^2 \right]$$

Define $K_2 = \frac{\Delta t_1}{\Delta t_2}$

$$2 \cdot y \cdot (y_2 - y_1) + 2 \cdot z \cdot (z_2 - z_1) + y_1^2 - y_2^2 + z_1^2 - z_2^2 - (c \cdot \Delta t_1)^2 = K_2 \left[-2 \cdot x \cdot x_4 + 2 \cdot y \cdot (y_2 - y_4) + 2 \cdot z \cdot (z_2 - z_4) + x_4^2 - y_2^2 + y_4^2 - z_2^2 + z_4^2 - c^2 \cdot \Delta t_2^2 \right]$$

Now collect y terms on lhs

$$2 \cdot y \cdot (y_2 - y_1) - K_2 \cdot (2 \cdot y \cdot (y_2 - y_4)) = K_2 \left[-2 \cdot x \cdot x_4 + 2 \cdot z \cdot (z_2 - z_4) + x_4^2 - y_2^2 + y_4^2 - z_2^2 + z_4^2 - c^2 \cdot \Delta t_2^2 \right] - \left[2 \cdot z \cdot (z_2 - z_1) + y_1^2 - y_2^2 + z_1^2 - z_2^2 - (c \cdot \Delta t_1)^2 \right]$$

Separate y term

$$2 \cdot y \cdot (y_2 - y_1 - K_2 \cdot (y_2 - y_4)) = K_2 \left[-2 \cdot x \cdot x_4 + 2 \cdot z \cdot (z_2 - z_4) + x_4^2 - y_2^2 + y_4^2 - z_2^2 + z_4^2 - c^2 \cdot \Delta t_2^2 \right] - \left[2 \cdot z \cdot (z_2 - z_1) + y_1^2 - y_2^2 + z_1^2 - z_2^2 - (c \cdot \Delta t_1)^2 \right]$$

Make y the subject

$$y = \frac{K_2 \left[-2 \cdot x \cdot x_4 + 2 \cdot z \cdot (z_2 - z_4) + x_4^2 - y_2^2 + y_4^2 - z_2^2 + z_4^2 - c^2 \cdot \Delta t_2^2 \right] - \left[2 \cdot z \cdot (z_2 - z_1) + y_1^2 - y_2^2 + z_1^2 - z_2^2 - (c \cdot \Delta t_1)^2 \right]}{2 \cdot (y_2 - y_1 - K_2 \cdot (y_2 - y_4))}$$

Expand numerator

$$y = \frac{-2 \cdot K_2 \cdot x \cdot x_4 + 2 \cdot K_2 \cdot z \cdot z_2 - 2 \cdot K_2 \cdot z \cdot z_4 + K_2 \cdot x_4^2 - K_2 \cdot y_2^2 + K_2 \cdot y_4^2 - K_2 \cdot z_2^2 + K_2 \cdot z_4^2 - K_2 \cdot c^2 \cdot \Delta t_2^2 - 2 \cdot z \cdot z_2 + 2 \cdot z \cdot z_1 - y_1^2 + y_2^2 - z_1^2 + z_2^2 + c^2 \cdot \Delta t_1^2}{2 \cdot (y_2 - y_1 - K_2 \cdot (y_2 - y_4))}$$

Now rearrange to the form $y = \gamma \cdot x + \zeta \cdot z + \psi$ Equ 9

$$y = \frac{(-2 \cdot K_2 \cdot x \cdot x_4) + (2 \cdot K_2 \cdot z \cdot z_2 - 2 \cdot K_2 \cdot z \cdot z_4 - 2 \cdot z \cdot z_2 + 2 \cdot z \cdot z_1) + (K_2 \cdot x_4^2 - K_2 \cdot y_2^2 + K_2 \cdot y_4^2 - K_2 \cdot z_2^2 + K_2 \cdot z_4^2 - K_2 \cdot c^2 \cdot \Delta t_2^2 - y_1^2 + y_2^2 - z_1^2 + z_2^2 + c^2 \cdot \Delta t_1^2)}{2 \cdot (y_2 - y_1 - K_2 \cdot (y_2 - y_4))}$$

$$y = \left[\frac{-K_2 \cdot x_4}{(y_2 - y_1) - K_2 \cdot (y_2 - y_4)} \right] \cdot x + \left[\frac{K_2 \cdot (z_2 - z_4) - (z_2 - z_1)}{(y_2 - y_1) - K_2 \cdot (y_2 - y_4)} \right] \cdot z + \left[\frac{K_2 \cdot (x_4^2 - y_2^2 + y_4^2 - z_2^2 + z_4^2 - c^2 \cdot \Delta t_2^2) - (y_1^2 - y_2^2 + z_1^2 - z_2^2 - c^2 \cdot \Delta t_1^2)}{2 \cdot ((y_2 - y_1) - K_2 \cdot (y_2 - y_4))} \right]$$

That is

$$\gamma = \frac{-K_2 \cdot x_4}{(y_2 - y_1) - K_2 \cdot (y_2 - y_4)} \quad \text{Equ 14}$$

$$\zeta = \frac{K_2 \cdot (z_2 - z_4) - (z_2 - z_1)}{(y_2 - y_1) - K_2 \cdot (y_2 - y_4)} \quad \text{Equ 15}$$

$$\psi = \frac{K_2 \cdot (x_4^2 - y_2^2 + y_4^2 - z_2^2 + z_4^2 - c^2 \cdot \Delta t_2^2) - (y_1^2 - y_2^2 + z_1^2 - z_2^2 - c^2 \cdot \Delta t_1^2)}{2 \cdot ((y_2 - y_1) - K_2 \cdot (y_2 - y_4))} \quad \text{Equ 16}$$

for equ 6 and 7

$$\frac{2 \cdot y \cdot (y_2 - y_3) + 2 \cdot z \cdot (z_2 - z_3) + x_3^2 - y_2^2 + y_3^2 - z_2^2 + z_3^2 - c^2 \cdot \Delta 32^2}{2 \cdot c \cdot \Delta 32} = \frac{-2 \cdot x \cdot x_4 + 2 \cdot y \cdot (y_2 - y_4) + 2 \cdot z \cdot (z_2 - z_4) + x_4^2 - y_2^2 + y_4^2 - z_2^2 + z_4^2 - c^2 \cdot \Delta 42^2}{2 \cdot c \cdot \Delta 42}$$

$$K_3 = \frac{\Delta 32}{\Delta 42} \left[\frac{2 \cdot y \cdot (y_2 - y_3) + 2 \cdot z \cdot (z_2 - z_3) + x_3^2 - y_2^2 + y_3^2 - z_2^2 + z_3^2 - c^2 \cdot \Delta 32^2}{\Delta 42} \cdot \frac{\Delta 32}{\Delta 42} - \frac{-2 \cdot x \cdot x_4 + 2 \cdot y \cdot (y_2 - y_4) + 2 \cdot z \cdot (z_2 - z_4) + x_4^2 - y_2^2 + y_4^2 - z_2^2 + z_4^2 - c^2 \cdot \Delta 42^2}{\Delta 42} \right]$$

$$y \cdot (y_2 - y_3) + 2 \cdot z \cdot (z_2 - z_3) + x_3^2 - y_2^2 + y_3^2 - z_2^2 + z_3^2 - c^2 \cdot \Delta 32^2 = K_3 \cdot [-2 \cdot x \cdot x_4 + 2 \cdot y \cdot (y_2 - y_4) + 2 \cdot z \cdot (z_2 - z_4) + x_4^2 - y_2^2 + y_4^2 - z_2^2 + z_4^2 - c^2 \cdot \Delta 42^2]$$

terms on lhs

$$-K_3 \cdot (2 \cdot y \cdot (y_2 - y_4)) = K_3 \cdot [-2 \cdot x \cdot x_4 + 2 \cdot z \cdot (z_2 - z_4) + x_4^2 - y_2^2 + y_4^2 - z_2^2 + z_4^2 - c^2 \cdot \Delta 42^2] - [-2 \cdot x \cdot x_3 + 2 \cdot z \cdot (z_2 - z_3) + x_3^2 - y_2^2 + y_3^2 - z_2^2 + z_3^2 - c^2 \cdot \Delta 32^2]$$

term

$$K_3 \cdot (y_2 - y_4) = K_3 \cdot [-2 \cdot x \cdot x_4 + 2 \cdot z \cdot (z_2 - z_4) + x_4^2 - y_2^2 + y_4^2 - z_2^2 + z_4^2 - c^2 \cdot \Delta 42^2] - [-2 \cdot x \cdot x_3 + 2 \cdot z \cdot (z_2 - z_3) + x_3^2 - y_2^2 + y_3^2 - z_2^2 + z_3^2 - c^2 \cdot \Delta 32^2]$$

subject

$$+ 2 \cdot z \cdot (z_2 - z_4) + x_4^2 - y_2^2 + y_4^2 - z_2^2 + z_4^2 - c^2 \cdot \Delta 42^2 - [-2 \cdot x \cdot x_3 + 2 \cdot z \cdot (z_2 - z_3) + x_3^2 - y_2^2 + y_3^2 - z_2^2 + z_3^2 - c^2 \cdot \Delta 32^2]$$

$$2 \cdot (y_2 - y_3 - K_3 \cdot (y_2 - y_4))$$

erator

$$\frac{-2 \cdot K_3 \cdot z \cdot z_2 - 2 \cdot K_3 \cdot z \cdot z_4 + K_3 \cdot x_4^2 - K_3 \cdot y_2^2 + K_3 \cdot y_4^2 - K_3 \cdot z_2^2 + K_3 \cdot z_4^2 - K_3 \cdot c^2 \cdot \Delta 42^2 + 2 \cdot x \cdot x_3 - 2 \cdot z \cdot z_2 + 2 \cdot z \cdot z_3 - x_3^2 + y_2^2 - y_3^2 + z_2^2 - z_3^2 + c^2 \cdot \Delta 32^2}{2 \cdot (y_2 - y_3 - K_3 \cdot (y_2 - y_4))}$$

to the form $y = s \cdot x + t \cdot z + u$

Equ 10

$$\frac{-2 \cdot x \cdot x_3 + (2 \cdot K_3 \cdot z \cdot z_2 - 2 \cdot K_3 \cdot z \cdot z_4 - 2 \cdot z \cdot z_2 + 2 \cdot z \cdot z_3) + (K_3 \cdot x_4^2 - K_3 \cdot y_2^2 + K_3 \cdot y_4^2 - K_3 \cdot z_2^2 + K_3 \cdot z_4^2 - K_3 \cdot c^2 \cdot \Delta 42^2 - x_3^2 + y_2^2 - y_3^2 + z_2^2 - z_3^2 + c^2 \cdot \Delta 32^2)}{2 \cdot (y_2 - y_3 - K_3 \cdot (y_2 - y_4))}$$

$$\left[\frac{x_3}{y_2 - y_4} \right] + \left[\frac{K_3 \cdot (z_2 - z_4) - (z_2 - z_3)}{(y_2 - y_3 - K_3 \cdot (y_2 - y_4))} \right] \cdot z + \left[\frac{K_3 \cdot (x_4^2 - y_2^2 + y_4^2 - z_2^2 + z_4^2 - c^2 \cdot \Delta 42^2) - (x_3^2 - y_2^2 + y_3^2 - z_2^2 + z_3^2 - c^2 \cdot \Delta 32^2)}{2 \cdot (y_2 - y_3 - K_3 \cdot (y_2 - y_4))} \right]$$

$\frac{x_3}{y_2 - y_4}$

Equ 17

$\frac{(z_2 - z_3)}{(y_2 - y_4)}$

Equ 18

Equating equ 8 and equ 9 gives

$$\alpha x + \beta z + \psi = \gamma x + \zeta z + \mu$$

Collect x terms on the lhs

$$x(\alpha - \gamma) = (\zeta z + \mu) - (\beta z + \psi)$$

Make x the subject

$$x = \frac{(\psi - \psi) + z(\zeta - \beta)}{(\alpha - \gamma)} \quad \text{Equ 20}$$

Now substituting equ 20 into equ 10

$$y = z \left[\frac{(\psi - \psi) + z(\zeta - \beta)}{(\alpha - \gamma)} \right] + \sigma z + \mu$$

Collect z terms

$$y = \left[\frac{z(\zeta - \beta)}{(\alpha - \gamma)} + \sigma \right] z + \frac{z(\psi - \psi)}{(\alpha - \gamma)} + \mu$$

Multiply through by $(\alpha - \gamma)$

$$(\alpha - \gamma)y = (z(\zeta - \beta) + \sigma(\alpha - \gamma))z + z(\psi - \psi) + \mu(\alpha - \gamma)$$

Make z the subject

$$z = \frac{(\alpha - \gamma)y - \mu(\alpha - \gamma) - z(\psi - \psi)}{z(\zeta - \beta) + \sigma(\alpha - \gamma)}$$

Separate the y term

$$z = \left[\frac{\alpha - \gamma}{z(\zeta - \beta) + \sigma(\alpha - \gamma)} \right] y + \left[\frac{-\mu(\alpha - \gamma) - z(\psi - \psi)}{z(\zeta - \beta) + \sigma(\alpha - \gamma)} \right] \quad \text{Equ 21}$$

Which has the form $z = G \cdot y + W$

Equ 22

Where

$$G = \frac{\alpha - \gamma}{z(\zeta - \beta) + \sigma(\alpha - \gamma)}$$

$$W = \left[\frac{-\mu(\alpha - \gamma) - z(\psi - \psi)}{z(\zeta - \beta) + \sigma(\alpha - \gamma)} \right]$$

if we go back to equ 20 we can rearrange to collect z terms

$$x = \frac{(\zeta - \beta)}{(\alpha - \gamma)} z + \frac{(\psi - \phi)}{(\alpha - \gamma)}$$

Multiply through by $(\alpha - \gamma)$

$$x(\alpha - \gamma) = (\zeta - \beta)z + (\psi - \phi)$$

Make z the subject

$$z = \frac{x(\alpha - \gamma) - (\psi - \phi)}{(\zeta - \beta)}$$

Now substitute this into equ 10

$$y = z + \sigma \frac{x(\alpha - \gamma) - (\psi - \phi)}{(\zeta - \beta)} + \mu$$

Collect x terms

$$y = \left[z + \sigma \frac{(\alpha - \gamma)}{(\zeta - \beta)} \right] x - \sigma \frac{(\psi - \phi)}{(\zeta - \beta)} + \mu$$

Multiply through by $(\zeta - \beta)$

$$y(\zeta - \beta) = (z(\zeta - \beta) + \sigma(\alpha - \gamma))x - \sigma(\psi - \phi) + \mu(\zeta - \beta)$$

Make x the subject

$$x = \frac{y(\zeta - \beta) + \sigma(\psi - \phi) - \mu(\zeta - \beta)}{z(\zeta - \beta) + \sigma(\alpha - \gamma)}$$

Separate out the y terms

$$x = \left[\frac{\zeta - \beta}{z(\zeta - \beta) + \sigma(\alpha - \gamma)} \right] y + \left[\frac{\sigma(\psi - \phi) - \mu(\zeta - \beta)}{z(\zeta - \beta) + \sigma(\alpha - \gamma)} \right] \quad \text{Equ 23}$$

Which has the form $x = T \cdot y + S$

Equ 24

Where

$$T = \frac{(\zeta - \beta)}{z(\zeta - \beta) + \sigma(\alpha - \gamma)}$$

$$S = \frac{\sigma(\psi - \phi) - \mu(\zeta - \beta)}{z(\zeta - \beta) + \sigma(\alpha - \gamma)}$$

Thus, knowing x and z in terms of y, substitution of equ 22 and equ 24 into equ 5 should yield a quadratic in y:

$$\sqrt{x^2 + (y - y_2)^2 + (z - z_2)^2} = \frac{2 \cdot y(y_2 - y_1) + 2 \cdot z(z_2 - z_1) + y_1^2 - y_2^2 + z_1^2 - z_2^2 - (c \cdot \Delta t)^2}{2 \cdot c \cdot \Delta t}$$

$$\sqrt{(T^2 + 1 + G^2) \cdot y^2 + (-2 \cdot y_2 - 2 \cdot z_2 \cdot G + 2 \cdot W \cdot G + 2 \cdot S \cdot T) \cdot y + (y_2^2 + S^2 + z_2^2 + W^2 - 2 \cdot W \cdot z_2)} = \frac{(2 \cdot y_2 - 2 \cdot y_1 + 2 \cdot G(z_2 - z_1)) \cdot y + 2 \cdot W(z_2 - z_1) - z_2^2 + y_1^2 + z_1^2 - c^2 \cdot \Delta t^2}{2 \cdot c \cdot \Delta t}$$

Which is of the form $\sqrt{J \cdot y^2 + K \cdot y + L} = M \cdot y + N$ Equ K

Where

$$J = T^2 + 1 + G^2$$

$$K = 2 \cdot W \cdot G + 2 \cdot S \cdot T - 2 \cdot y_2 - 2 \cdot z_2 \cdot G$$

$$L = (y_2^2 + S^2 + z_2^2 + W^2 - 2 \cdot W \cdot z_2)$$

$$M = \frac{2 \cdot y_2 - 2 \cdot y_1 + 2 \cdot G(z_2 - z_1)}{2 \cdot c \cdot \Delta t}$$

$$N = \frac{2 \cdot W(z_2 - z_1) - y_2^2 - z_2^2 + y_1^2 + z_1^2 - c^2 \cdot \Delta t^2}{2 \cdot c \cdot \Delta t}$$

Rearrange equ K into standard quadratic form

$$\sqrt{J \cdot y^2 + K \cdot y + L} = M \cdot y + N$$

$$J \cdot y^2 + K \cdot y + L = (M \cdot y + N)^2$$

$$J \cdot y^2 + K \cdot y + L = M^2 \cdot y^2 + 2 \cdot M \cdot y \cdot N + N^2$$

$$y^2 (J - M^2) + y(K - 2 \cdot M \cdot N) + (L - N^2) = 0$$

Which is now of the form $A \cdot y^2 + B \cdot y + C = 0$ Equ 25

Where

$$A = J - M^2 = T^2 + 1 + G^2 - \frac{1}{4} \frac{(2 \cdot y_2 - 2 \cdot y_1 + 2 \cdot G(z_2 - z_1))^2}{(c \cdot \Delta t)^2}$$

Rearranging $A = G^2 + 1 + T^2 - \frac{(G(z_2 - z_1) + (y_2 - y_1))^2}{c^2 \cdot \Delta t^2}$ Equ 26

$$B = K - 2 \cdot M \cdot N = 2 \cdot y_2 - 2 \cdot z_2 \cdot G + 2 \cdot W \cdot G + 2 \cdot S \cdot T - 2 \left[\frac{(2 \cdot y_2 - 2 \cdot y_1 + 2 \cdot G(z_2 - z_1))}{2 \cdot (c \cdot \Delta t)} \right] \left[\frac{2 \cdot W(z_2 - z_1) - y_2^2 - z_2^2 + y_1^2 + z_1^2 - c^2 \cdot \Delta t^2}{2 \cdot (c \cdot \Delta t)} \right]$$

Rearranging $B = 2 \cdot G(W - z_2) - 2 \cdot y_2 + 2 \cdot T \cdot S - \left[\frac{G(z_2 - z_1) + (y_2 - y_1)}{c \cdot \Delta t} \right] \left[\frac{2 \cdot W(z_2 - z_1) + y_1^2 - y_2^2 + z_1^2 - z_2^2 - c^2 \cdot \Delta t^2}{c \cdot \Delta t} \right]$

$$B = 2 \cdot G(W - z_2) - 2 \cdot y_2 + 2 \cdot T \cdot S - \frac{(G(z_2 - z_1) + (y_2 - y_1)) \cdot [2 \cdot W(z_2 - z_1) + y_1^2 - y_2^2 + z_1^2 - z_2^2 - c^2 \cdot \Delta t^2]}{c^2 \cdot \Delta t^2}$$
 Equ 27

$$C = L - N^2 = (y_2^2 + S^2 + z_2^2 + W^2 - 2 \cdot W \cdot z_2) - \left[\frac{2 \cdot W(z_2 - z_1) - y_2^2 - z_2^2 + y_1^2 + z_1^2 - c^2 \cdot \Delta t^2}{2 \cdot c \cdot \Delta t} \right]^2$$

Rearranging $C = (W - z_2)^2 + y_2^2 + S^2 - \frac{[2 \cdot W(z_2 - z_1) + y_1^2 - y_2^2 + z_1^2 - z_2^2 - c^2 \cdot \Delta t^2]^2}{c^2 \cdot \Delta t^2}$ Equ 28

APPENDIX B

B1: COMPREHENSIVE SIMULATION RESULTS

A comprehensive set of results was obtained using MatLab to simulate space surrounding the receiver array. Six different position-fixing algorithms were used, as described in Chapters 2 and 3, although MatLab's own method (QR) of inverting a matrix produced too many singularities to be useful and is not shown here. The results augment those presented in Chapter 3, but they are not included in the thesis for reasons of brevity. Instead they are available, along with the text of the complete thesis, on a CD-ROM on request to Loughborough University. The reason for carrying out the simulations was to give a wider perspective of the errors occurring in different situations. In all the cases considered, various receiver spacings are simulated with each of the algorithms.

THE PERFECT SITUATION

The initial work was to carry out simulations of the algorithms with the full definition of MatLab and the IBM PC's 32-bit mathematical capabilities. No external errors were injected, so these results can be taken as the baseline. Although the figures for the 0m and 100m cases seem similar, this is due to symmetry within the system. On closer inspection it can be seen that the errors in the diagrams are often in the order of 10 to 100 times greater in the 100m case.

B-2 TRACKING CONFIGURATIONS WITH RECEIVER POSITIONAL ERRORS

This part of the study gives the full results of simulations in which a receiver positional error is introduced, on the basis that such an error could be introduced in a practical system.

B-3 TRACKING CONFIGURATIONS WITH RECEIVER TIMING ERRORS

This part of the study gives the full results of simulations in which a receiver timing error is introduced. In the experimental systems developed in this research the timing is extremely accurate but this depends on the sampling rate used. The errors introduced here correspond to achievable sampling rates.

B-4 TRACKING CONFIGURATIONS WITH VELOCITY PROFILE-INDUCED ERRORS

This part of the study gives the full results of simulations in which a receiver timing error is introduced as a result of the time of flight of an acoustic signal being altered by the change of sound velocity in the water with depth. A baseline is obtained in the first set of results, showing similar errors in timings to the previous baselines. Timing errors and time difference errors are shown that are more relevant to the passive forms of tracking. With this data, Algorithm 1 only has been used. The timing error data can be compared with the errors obtained in Appendix B3 to see the positional error effects with the other algorithms.

B-5 SIMULATIONS OF THE SINGLE RECEIVER REVERBERATION METHOD

In this part of the study the source is moved through the space around the receiver and its position calculated. This method gives only range and depth, although by using two receivers it is possible to detect the position of the source in three-dimensional space. The simulations assume the receiver is placed in mid-water and only simulates the space above its position. Any errors are mirrored below the receiver's position. If the first and second reverberations are inadvertently swapped the source position is also mirrored below the receiver.

APPENDIX C

SINGLE HYDROPHONE RANGING TECHNIQUE

The following papers present full details of the single hydrophone ranging technique, which was developed from data obtained during sea trials for the European Commission *CETASEL* project.

P.R. Connelly, A.D. Goodson, K. Kaschner, P.A. Lepper, C.R. Sturtivant and B. Woodward, Acoustic techniques to study cetacean behaviour around pelagic trawls, Theme session *By-catch of Marine Mammals*: Proceedings of the Annual Science Conference of the International Council for the Exploitation of the Sea, *ICES* (CM 1997/Q15), September 1997, Baltimore, USA.

K. Kaschner, A.D. Goodson, P.R. Connelly and P.A. Lepper, Species characteristic features in communication signals of cetaceans: source level estimates for some free ranging North Atlantic odontocetes. Proceedings of 11th Annual Conference of the European Cetacean Society *ECS 97*, Stralsund, Germany, 10-12 March, 1997, edited by U. Siebert and R. Lick, University of Kiel, Germany.

P.A. Lepper, K. Kaschner, P.R. Connelly, and A.D. Goodson, Development of a simplified ray path model for estimating the range and depth of vocalising marine mammals, *Proceedings of the Institute of Acoustics*, Vol. 19, No 9, pp 227-234, 1997, ISSN 0309-8117.

Acoustic techniques to study cetacean behaviour around pelagic trawls

Connelly P.R., Goodson A.D., Kaschner K., Lepper P.A., Sturtivant C.R. & Woodward B.

ABSTRACT

As part of the European Commission's DGXIV *CETASEL* project, new cetacean tracking techniques have been developed to investigate the risks of small cetacean by-catch in pelagic trawls. Interactions between cetaceans and pelagic trawls are particularly difficult to study unobtrusively since these trawls may be operated more than 1 km behind the vessel in water depths greater than 100 m. ROV investigations with TV cameras, a Tritech scanning sonar, and attached hydrophones were judged unsuitable for this work since the ROV's power pack was noisy, the cameras required lights at night or in deep water, and the 325 kHz sonar had been shown to affect harbour porpoise behaviour in earlier work. To aid this study two passive acoustic systems have been developed that employ hydrophones directly attached to the trawl. The first utilises an array of 5 hydrophones placed near the headrope to localise and track the spatial positions of echolocating cetaceans in three dimensions, and displays this information in real-time relative to the net. The second method exploits a single hydrophone to detect the presence of vocalising animals in the general area around the vessel, which is especially useful at night or when seastate conditions hinder visual observation. In addition, when analysed off-line, this single channel data can be used to estimate range to the animal whenever measurable multi-path echoes are present. Echolocation *click* rates indicate the different stages of foraging activity, and analysis of the cetacean's FM whistles has shown that pod identities can be isolated and repeat encounters with the same group of animals recognised.

Key words : acoustic, bycatch, dolphin, pelagic trawl, tracking, ranging.

P.R.Connelly, A.D.Goodson, P.A. Lepper, B. Woodward & C.R.Sturtivant: Underwater Acoustics Group, Electronic & Electrical Engineering Department, Loughborough University LE11 3TU, UK.

Tel +44 1509 222846, email: P.R.Connelly@lboro.ac.uk

K.Kaschner : University of Frieberg, Germany. email: kaschner@ruf.uni-frieberg.de

INTRODUCTION

By-catch of marine mammals, in particular of cetaceans, occurs to varying degrees in a number of commercial fisheries. The extent of the problem in gill-net fisheries is well known, [Perrin *et al.*, 1994], and although the pelagic trawl is known to have a by-catch of cetaceans, it has only recently attracted serious attention [Waring *et al.*, 1990][Morizur *et al.*, 1996]. The species shown to be at greatest risk from pelagic trawls in N.E. Atlantic waters are the common dolphin (*Delphinus delphis*), Atlantic white-sided dolphin (*Lagenorhynchus acutus*), and the white-beaked dolphin (*Lagenorhynchus albirostris*) [Berrow *et al.*, 1994].

A study project funded by the European Commission (AIR III CT 94-2423) called CETA-SEL (Cetacean Selectivity) is tasked to investigate the problem and possible mitigation methods by technical means. Pelagic trawls operated near the shelf-break may be deployed at depths in excess of 100m and at a distance exceeding 800 m behind the vessel, and in this environment cetacean interactions with these moving nets are particularly difficult to study. Methods used to gather information include: the use of observers watching for surfacings in daylight; a remotely operated vehicle (ROV) equipped with scanning sonar and low light TV cameras; and passive acoustic methods involving individual or arrays of hydrophones.

Study and analysis of cetacean behaviour around fishing gear has only been possible for two captive species as part of this project, specifically the harbour porpoise (*Phocoena phocoena*) and the bottlenose dolphin (*Tursiops truncatus*). For tests with wild cetaceans around fishing gear it is important that the study method has no influence on the animals behaviour. Data capture systems must therefore be passive and non-intrusive, restricting the use of lights and most standard active sonar equipment. This paper will discuss passive acoustic techniques that have been developed within this project.

TECHNIQUES

It is necessary to understand both the advantages and the limitations of any underwater acoustic observation method. Acoustic detection and ranging methods can work at night and in seastate conditions when observers have very limited visibility. Acoustic ranging can be significantly more accurate than simple visual estimates of distance. Information about the depth of the vocalising animal is also valuable, since this can indicate the depth of preferred prey and hence the increased probability of a trawl interaction when this is operating at the same

depth. Since it is desirable that the ship's personnel on watch are aware of the presence of cetaceans within the study area both ahead and surrounding the vessel, the early detection of their vocalisations can be of great value. If a cetacean's track appears to converge with the vessel then all the information, before, during, and immediately after a possible interaction must be recorded for later analysis. Automatic data logging of technical parameters relating to the ship, the gear, and the water environment is essential. If the vessel interacts with the same animal or pod on a later occasion it may be possible to recognise this from a combination of visual and acoustical cues [Sturtivant and Datta, 1997].

Photo-ID studies are not normally practical from a fishing boat, but the value of photographic or video material during an encounter may be considerable. The identification of the species and occasionally the recognition of gross marking on individuals may be useful. Normal surface observations can indicate an approximate range of an animal from the ship, and may also show changes in direction. Acoustic means allow a higher accuracy in calculated range of an animal from the trawl and will indicate the rate of approach. When the animal is attracted to the trawl, changes in behaviour may be more noticeable using this method. From studies in captivity and the wild on the sounds cetaceans make as they behave in particular ways [Herman & Tavolga, 1980] and from an understanding of basic cetacean sonar, it is often possible to predict if a cetacean is foraging, fighting, or merely 'observing' an object. It is also possible to infer the range of the cetacean from its target. All this analysis can be carried out on data from a single hydrophone. With data from multiple hydrophones, not only can the previous analysis techniques be used, but also the direction to the cetaceans can be obtained. With three hydrophones a position can be plotted in two dimensions, and with a fourth hydrophone positions in the third dimension can be achieved [Hardman & Woodward, 1984].

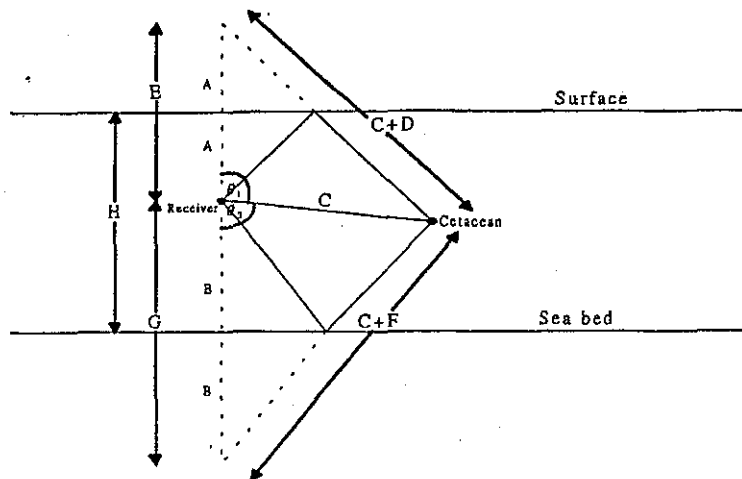
Single hydrophone methods

The presence of a cetacean can be detected as long as the animal is vocalising. Apart from the harbour porpoise, all of the target species produce whistles in the frequency range 2-24kHz [Evans, 1973], and these signals can travel considerable distances in good acoustic conditions. Detection ranges were impaired by the self noise of the trawler and of the gear, but detection of dolphin calls was obtained at ranges well in excess of 1km by implementing suitable filters to remove acoustic energy below 4 kHz. Certain of these whistles appear to carry information on identity [Caldwell *et al.*, 1990] and may be used in this way by the dolphins, although mimicry by animals in the same group has been observed. By using this data, the identity of individual dolphin groups can be ascertained from one encounter to the next [Sturtivant and Datta, 1997].

Automatic whistle detection, extraction, isolation, and classification techniques have been developed whereby the whistles' time-frequency contours are classified. The contours are encoded into segments by basic whistle shape, and a hidden Markov model is used to represent the segment sequences that make up each whistle class. More detailed comparisons of the contours are made using three distance measures between segments in the candidate whistle contour and those in existing classes. The product of the segment sequence probability and contour similarity percentages then can be used to calculate the probability that the whistle contour belongs to a pre-existing whistle class. By calculating class membership probabilities for a number of whistles from the same group of dolphins, a quantitative answer can be calculated to the question of whether the group has previously been recorded.

Sounds other than whistles can sometimes be coupled to behaviour seen in captivity. Using a single hydrophone it is possible to distinguish social buzzes from echolocation click trains, and changes in such vocalisations may be useful in detecting changing behaviour as dolphins approach a trawl.

Since most of the sea trial recordings were obtained at the edge of the continental shelf in water depths between 100 m and 200 m, most of the cetacean whistles captured also included measurable multi-path echoes caused by reflections from both the bottom and surface of the water. Comparing these signal delays permits a range to be calculated as follows:



$$\theta_1 = 180 - \theta_2$$

$$\cos \theta_1 = -\cos \theta_2$$

$$G = 2B = 2(H - A)$$

$$D = vel \times t_{rev1}$$

$$F = vel \times t_{rev2}$$

Figure 1 Showing geometry of multi-path signals

Using the Cosine rule: and

$$\cos \theta_1 = \frac{E^2 + C^2 - (C+D)^2}{2EC} \quad \cos \theta_2 = -\cos \theta_1 = \frac{G^2 + C^2 - (C+F)^2}{2GC}$$

Equating these equations gives: and:

$$C = \frac{G^2 E - F^2 E + E^2 G - D^2 G}{2(GD + EF)} \quad \theta_1 = \cos^{-1} \left(\frac{4A^2 - 2CD - D^2}{4AC} \right)$$

This calculation indicates both the range of the cetacean from the hydrophone as well as the depth at which the cetacean was vocalising. For this algorithm to work it is necessary to know the depth of the hydrophone, the water depth, and to be able to distinguish the echoes from the surface from those from the bottom (although reversing surface and bottom echoes yields an ambiguous solution). Errors can also be introduced due to changes in sound velocity in the sea due to salinity or temperature.

Analysis of the echolocation click rates can reveal information about the different stages of foraging behaviour (Goodson & Datta, 1992). During target interception, the dolphin's click rate can be used to show the range to the animal's target, whether trawl or prey. In addition, if the range is known from the hydrophone to a vocalising animal the source level for whistles can be calculated, enabling whistles to be correctly assigned to groups when more than one are present at different ranges.

Multiple Hydrophone Techniques

A track can be obtained in three dimensions with a three dimensional array of four hydrophones. The rigidity of a three dimensional array is limited by the pelagic trawl and the turbulent water flow surrounding it, so instead a system which can track in three dimensions using a flat array of four hydrophones is being developed. The ambiguities produced by such a system can be overcome by the use of a fifth hydrophone out of the plane that requires less stability than the main array. The algorithms required to retrieve a position using such a system are complicated and involve calculating crossing points of intersecting hyperboloids. A requirement of the system is to provide real-time data, and due to the complexity of the calculations a look-up table approach is used. The system is made up of three streamers. Two of these are connected to the hydrophone and front sections of a specially adapted trawl containing two hydrophones and a calibration pinger, the other containing a single fifth hydrophone and calibration pinger connected to an armoured electrical cable to the ship above the plane of the other streamers (Fig.2)

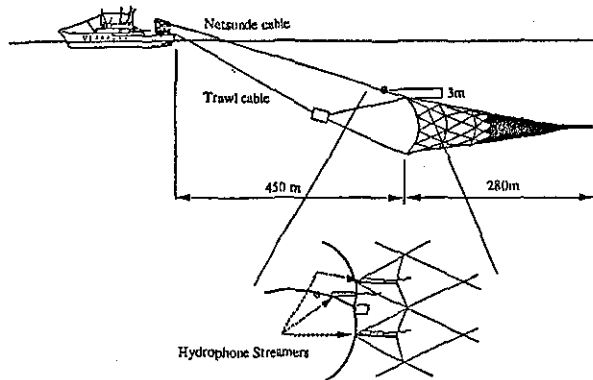


Figure 2 Showing the tracking array positioned on the trawl.

The time information from these hydrophones is extracted, modulated and transmitted to the surface via a coaxial cable formerly used for the ship's second Netsonde echo sounder. The information is demodulated at the surface, and the low frequency audio signal from the fifth hydrophone is extracted for analysis as mentioned above. All the information is stored at this stage, both in an analogue form and digitally. The five channels of information can be used in one of two ways at the surface. If the fifth hydrophone is proving to be stable its data can be included in the main tracking array, simplifying the algorithms to those developed by Hardman and Woodward [1984]. If it is not stable the computers go through a process of generating a large look-up table that effectively splits the space around the trawl into discrete zones, each zone having a set of time delays which are calculated by the computer. These zones are sorted such that as the set of time delays arrives, the associated position can be retrieved by the fastest possible method. The number of zones that have to be calculated is dependent on the accuracy of the arrival time of the information.

If the streamers are stable, the generation of this table occurs only once at the beginning of the period. As is more often the case, however, the array tends to move with changes of speed and warp length. Each time this occurs, the system has to re-calibrate and regenerate the table. If the accuracy of the time delays decreases, the zones tend to start overlapping and so more than one position is found. As it decreases further the calculated positions tend towards a vector display. The system used for CetaSel is restricted by the bandwidth of the cable transmitting the time information to the surface, and this tends to produce multiple positions in the calculations. (Fig 3)

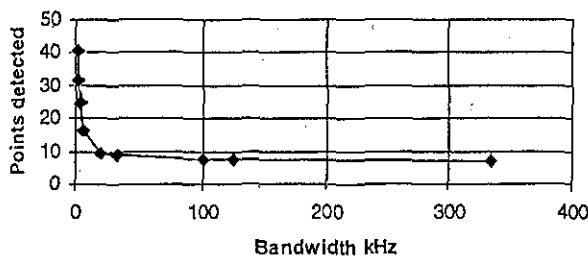


Figure 3 The average number of positions generated for different bandwidth restrictions.

METHODS

The Dutch Fisheries Research Ship 'Tridens', used for the sea trials for Ceta-Sel, is equipped with rigging for most types of trawling. It is capable of towing the 4200 and 5600 trawls used in these tests, and the most important variables about the ship, its environment and the trawl, are recorded automatically. In addition to this data, the ship is equipped with a towed ROV with scanning sonar and low light video. Ceta-Sel employs experienced observers to detect and plot any cetacean surfacings around the ship. The trawl has been adapted to hold the three streamers of the tracking system and the associated circuitry, and the information from this system is passed to the surface by way of the ship's spare Netsonde cable. A single hydrophone can be placed on the trawl for times when the tracking system is not available, and is designed to detect the audio spectrum (whistles and buzzes) and to fold the high frequencies (echolocation clicks) down to make them audible. Signals up to 24 kHz are recorded on Sony RDAT (TCD-D7), and up to 100 kHz on Racal VSTORE for tracking purposes. A picture of the movement of the target species as they approach, interact with, and leave the trawl can be built up

by comparing notes made by the observers, and recordings made from the tracking system and the single hydrophone.

RESULTS

The tracking system has been developed throughout the project and is beginning to show results, although acoustic analysis of data collected at sea is still ongoing. Simulation shows that vector plotting is available within the limits set by this project (limited by transmission bandwidth) even though the situations are few where the working tracking system and the target species are both present at the same time. In addition, there are some cases where positions can be detected. The single hydrophone techniques have served both to confirm observers' sightings, and also to detect many cases where observers did not sight the animals. It also indicates animals coming close to the trawl and interacting and foraging in its vicinity.

Figure 4 shows a situation where three groups of cetaceans passed the ship. The acoustic techniques combined with the observer sightings showed how the first group passed the trawl relatively quickly, whereas the second group stayed with the trawl briefly and then fell back to be replaced by the third group who stayed with the trawl for longer than 10 minutes.

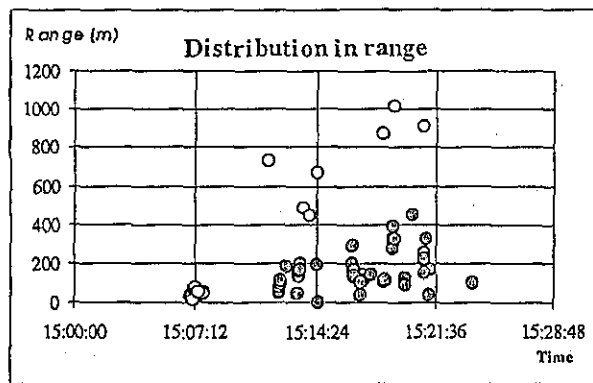


Figure 4a

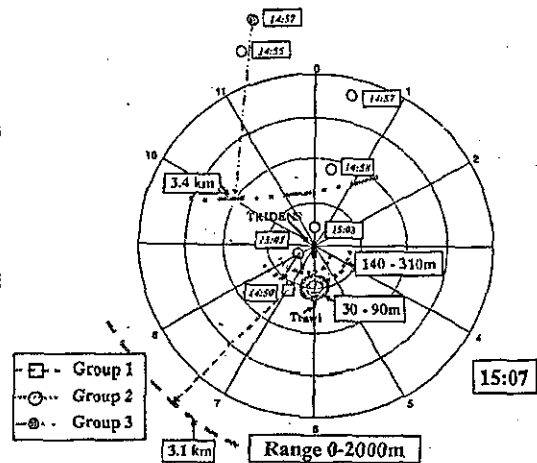


Figure 4b

Figure 4a Showing the distribution of cetaceans over time, showing that as group 2 falls behind, a new group approach and stay with the trawl for some time.

Figure 4b Showing how the range estimates based on multi-path signals (solid circles around the hydrophone attached to the trawl gear) can be used to further clarify group movements. The different symbols represent the various sightings of different groups, and the semicircles represent the respective possible positions for each group at 15:07. (Distances are referred to the position of the last sighting and were calculated assuming a constant swimming speed and direction for the animals and taking the ships movement into consideration).

CONCLUSIONS

The large amount of data recorded during Ceta-Sel sea trials with these passive acoustic systems is still being analysed in the laboratory. The simple single hydrophone technique has provided valuable behavioural information supporting the hypothesis that some small cetaceans are attracted to the vicinity of the trawl. The self-noise of the fishing gear would seem to ensure that such interactions are non-accidental. The fine detail of these interactions, where the path of the animal into and out of the trawl has been studied, has proved to be a more difficult exercise. The algorithms to study these interactions have been refined, and a design for a high-resolution digital system to utilise these in real time was built in the laboratory. However it was unable to be tested at sea since the fibre optic link needed to carry the very high data rates was not available on the vessel. The performance of the reduced band-width system that was developed was severely restricted by the data rate limitations of the 2 km long netsonde coaxial cable, and it resolved the animal's position at the intersections between relatively coarse quantised blocks of space around the net. This 3 D tracking system has considerable potential for this type of work, but the hardware also requires a lot of handling expertise by deck crew when

attaching the streamer arrays to the trawl. Since this activity proved to be time consuming it is unlikely that it could reasonably be exploited on a commercial trawler in its present form. For future studies directly involving the commercial fishery, refinement of the single hydrophone methodology is worth further consideration. For off-line analysis, a self-contained pod incorporating an internal R-DAT recorder could be operated on a commercial net without the restriction of a cable link back to the vessel. Data capture periods would be limited by recording time, but this pod could be activated remotely to sample data at specific times, e.g. just before and during hauling or when animals have been detected in the vicinity. The need to detect the presence of the animals is important and a bow mounted hydrophone — even one deployed inside a fully flooded buoyancy bow compartment — could be used to inform the watch personnel on the ships bridge of their presence. This approach has the advantage of reduced self-noise conditions (unless the bow breaks out of the water) and can be operated continuously with or without fishing gear in the water. However, a hydrophone placed in this position, effectively at the surface, will not permit this echo-ranging method to operate. When supported by the co-ordinated data from the ship and observer logs, off-line acoustic analysis is providing valuable behavioural information needed for the development of methods to reduce cetacean by-catch.

ACKNOWLEDGEMENTS

This work has been supported by the European Commission DGXIV, our partners in the CETASEL project: RIVO, NL; IFREMER, FR; DIFTA, DK; Kolmarden Djurpark, SE; Harderwijk, NL. The UK Ministry of Agriculture, Fisheries and Food, the UK Department of the Environment. Technical assistance from Professor T. Curtis (DERA-Winfrith) D. Anthony, C. Richards (Loughborough University EE Dept.) with the construction and the software of the tracking system is gratefully acknowledged.

REFERENCES

- Berrow, S.D, Tregenza, N.J.C., Hammond, P.S. (1994) Marine Mammal Bycatch on the Celtic Shelf. European Commission, DGXIV/C/1 Study contract 92/3503.
- Caldwell, M.C., Caldwell, D.K., and Tyack, P.L. (1990). Review of the signature-whistle hypothesis for the Atlantic bottlenose dolphin. In *The Bottlenose Dolphin* (S. Leatherwood and R.R. Reeves, eds.), Academic Press, pp. 199–234.
- Evans, W.E. (1973). Echolocation by marine delphinids and one species of freshwater dolphin. *Journal of the Acoustical Society of America* 54(1): 191-199.
- Goodson A.D. & Datta S. (1992) Acoustic detection of gill-nets, the dolphin's perspective. *Acoustic Letters* 16(6) pp129-133.
- Hardman P.A. and Woodward B., Underwater location fixing by a diver-operated acoustic telemetry system, *Acustica*, Vol. 55(1), pp. 34-44, 1984
- Herman, L.M. & Tavorga, W.N. (1980). The Communication System of Cetaceans. In *Cetacean Behavior: Mechanisms and Functions*, L.M. Herman (ed.), Kreiger, Florida. pp 149–210.
- Morizur Y., Tregenza N., Heesen H., Berrow S., Pouvreau S. By-catch and discarding in pelagic trawl fisheries *BIOECO* 93/17, Report to the EC (DG XIV-C-1), 1996
- Perrin W.F., Donovan, G.P., & Barlow J. (eds): *Gillnets and cetaceans*. Rep. Int. Whal. Commn. (Special Edition 15) pp629. ISSN 0255-2760
- Sturtivant, C.R. & Datta, S. (1995a). Techniques to isolate dolphin whistles and other tonal sounds from background noise *Acoustics Letters* 18(10): 189–193.
- Sturtivant, C.R. & Datta, S. (1995b). The isolation from background noise and characterisation of bottlenose dolphin (*Tursiops truncatus*) whistles. *Journal of the Acoustical Society of India* 23(4): 199–205.
- Sturtivant, C., and Datta, S. (1997). An acoustic aid for population estimates. *European Research on Cetaceans* — 11 (in press).
- Waring, G.T., Gerior, P. Payne, M.P. Parry, B.L. Nicolas, J.R. (1990) Incidental Take of Marine Mammals in Foreign Fishery Activities off the Northeast United States, 1977-88. *Fishery Bulletin, U.S.* 88, 347-360

SPECIES CHARACTERISTIC FEATURES IN COMMUNICATION SIGNALS OF CETACEANS: SOURCE LEVEL ESTIMATES FOR SOME FREE RANGING NORTH ATLANTIC ODONTOCETES

K Kaschner (1), A D Goodson (2), P R Connelly (2), P A Lepper (2)

(1) Biologie I, Abtl. Tierphysiologie, Albert-Ludwigs-Universität Freiburg, Hauptstr. 1, 79104 Freiburg, DE

(2) Underwater Acoustic Group, Electronic & Electrical Engineering Dept., Loughborough University, LE11 3TU, UK

1. INTRODUCTION

It is known that the acoustic signals of cetaceans vary considerably among species, Schevill & Lawrence [1], and these differences may be useful when discriminating species in the wild, Schevill [2]. Extensive studies have compared odontocete echolocation signals to establish characteristic features, e.g. Evans & Awbrey [3], Kamminga & Wiersma [4], Wiersma [5]. In recent years research into the structure of the comparatively narrow-band low-frequency communications signals of different odontocetes has focussed on attempts to identify distinctive individuals, e.g. Buck & Tyack [6], Caldwell, Caldwell & Tyack [7], McCowan [8], Sayigh *et al.* [9], pod, McCowan & Reiss [10], or simply species-specific features, Wang *et al.* [11], Evans [12], Steiner [13], that might assist in acoustic identification and discrimination. So far most of these studies have concentrated on the frequency modulated signal by examining these for characteristic features in the frequency-time domain using FFT analysis. Such analysis has concentrated on the centre frequency, frequency deviation, number of inflection points, and more significantly the general shape or contour of the call, McCowan [10], Buck & Tyack [6], Sturtivant [14].

To our knowledge research has not been carried out (?) to compare the absolute intensity or Source Level (SL), i.e. the Sound Pressure Level (SPL) in dB re 1 μ Pa at 1 m, of these communication signals. The neglect of this parameter as a possible classifier may be explained. Most studies of individual or pod signature whistles have been based on data obtained either from captive animals, e.g. McCowan [10], Sayigh *et al.* [9], where it is reasonable to expect that in short range, reverberant conditions, animals will not vocalise at their highest intensity and whistle or echolocation click amplitude data may not be representative of the SLs obtained in more anechoic, open water conditions, Goodson *et al.* [15]; Sturtivant & Goodson [16]. Other studies comparing species characteristic features of whistles, e.g. Wang *et al.* [11], Steiner [13], used data obtained from free-ranging animals, however, in these cases the distance of the vocalising animal from the hydrophone is unknown. Knowledge of both range and received SPL from a specific animal is essential if the Source Level is to be estimated. The SL of different odontocete echolocation signals has been extensively studied, Au *et al.* [17], Akamatsu *et al.* [18], Goodson *et al.* [15], Woods & Evans [19] and this parameter appears to reflect some body size dependency, indicating its potential as a tool for species discrimination. However, the high directivity of the pulses make reliable measurement problematic in wild. Whistles, on the other hand, are far less directional (see 2.3.1.) and would be better candidates for an attempt to determine a species

SPECIES CHARACTERISTIC FEATURES IN COMMUNICATION SIGNALS

related characteristic SL for free-ranging animals.

A novel acoustic ranging technique for diving vocalising animals based on multi-path signals (created by specula reflections of the signal via the sea surface and the seabed) has been developed while post processing acoustic data obtained during 1996 and 1997 in the CETASEL pelagic trawl cetacean bycatch study, Kaschner *et al.* [20], Lepper [21]. CETASEL (AIR III-CT94-2423), De Haan [22], was an EC funded project 'to reduce the by-catch of small cetaceans in pelagic trawls by technical means' which included 14 weeks of sea trials carried out in relatively deep water (100-200 m depth) along the edge of the continental shelf in the Eastern North Atlantic sea areas SW of Ireland, through Biscay and towards Finnisterre. This paper discusses the feasibility of establishing the maximum SL in the wild of the lower frequency social calls based on a simplified multi-path echo ranging method, and the potential of this SL estimation method to provide a inter-species classifier when operating at night or in sea state conditions where visual observation is not possible.

2. MATERIAL AND METHODS

2.1. Passive Acoustics

The acoustic data used for analysis was recorded from a 75 m long Dutch fishing research vessel (FRV Tridens). Data obtained in five different experimental set-ups was processed in order to test the validity of the developed method. Hydrophone signals were preamplified, buffered and transmitted to the ship via a 1.8 km netsonde coaxial cable (2.1.1., 2.1.3-5)

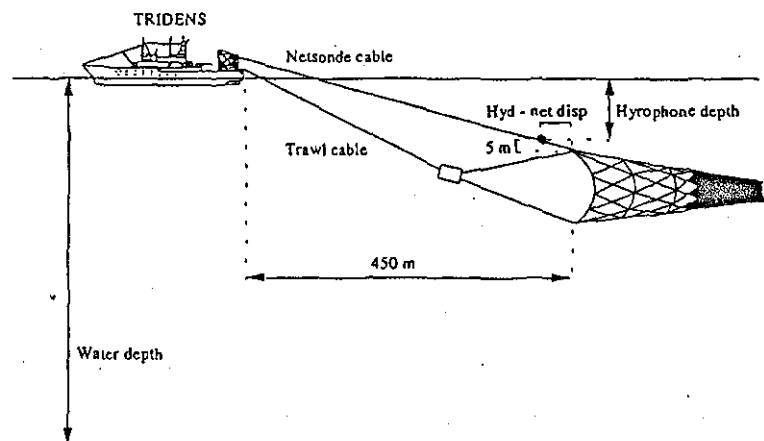


Fig. 1. Trial set-up for the CETASEL trials showing the position of the hydrophone for T1, T3 & T4a,b.

(Fig.1) or received using wide band VHF sonobuoys (2.1.2). In most cases the frequency response of the hydrophone pre-amplifier was rolled off below 4 kHz to reduce the masking effect of the fishing vessel's self-noise. All data was further band limited to 20 kHz when recorded onto a Sony (TCD-D7) DAT recorder. Additional data regarding the species, depth of the hydrophone etc. were taken from the corresponding trial logs. Data from the following trial set-ups was used:

SPECIES CHARACTERISTIC FEATURES IN COMMUNICATION SIGNALS

2.1.1. Trial set-up 1 (referred to as T1 in the following) (24.04.96): 10-20 Atlantic White-sided Dolphins, (*Lagenorhynchus acutus*) accompanied the ship for more than one hour, staying in close vicinity of the pelagic trawl towed some 500 m astern of the vessel. The acoustic data was recorded using a Benthos AQ4 hydrophone attached to the trawl which was part of a multiple hydrophone array developed to track cetaceans at short range in 3 dimensions, Connelly *et al.* [23]. A 13 kHz 'Netmark 1000' pinger (Dukane) was attached to the netsonde cable at a known distance from the hydrophone to provide a calibration reference.

2.1.2. Trial set-up 2 (T2) (08.05.96): A group of Common Dolphins (*Delphinus delphis*) was recorded on a sonobuoy (SSQ 904a) which was moored to the drifting vessel at a distance of app. 100 m with its hydrophone set at a known depth. At the same time a static test was in progress with another hydrophone deployed directly over the stern at varying depths. A 'Netmark 1000' pinger was attached to the cable 10m above the hydrophone.

2.1.3 Trial set-up 3 (T3) (19.04.96): Two bow riding Common Dolphins were recorded on the dual channel hydrophone unit (DHU1) deployed with the trawl.

2.1.4. Trial set-up 4 (T4a, T4b) (10.10.96): There are two different data sets from this day. One (T4a) consists of Common Dolphin signals recorded on an improved version of the dual hydrophone unit with Benthos AQ4 hydrophones (DHU2) deployed on the trawl. T4b was obtained in a situation when a group of bow riding Common Dolphins were filmed with a video camera from directly above, while their whistles were recorded on the DHU2 underwater.

2.1.5. Trial set-up 5 (T5) (22.04.97): In this set-up a group of bow riding Common Dolphins were recorded on a single ½" ball hydrophone (HS150) only a few metres away from the animals. This hydrophone was deployed directly inside the fully flooded bow trim tank which formed the bulbous bow of the vessel. A signal from a transducer attached to the outside surface of the bow tank casing was available when required as a calibration reference.

2.2. Spectral analysis

The RDAT tapes were analysed using a real time frequency analysis software (SB 16/32 spectrograph) developed by Dr Pavan from the University of Pavia [24]. For the two main data sets (T1&T2) only signals with multi-path reverberations from the surface and seabed were selected for analysis (see below). The selected whistles were divided into categories of different intensity and an approximately equal number of whistles out of each category was chosen for analysis, in order to reduce the bias towards higher SPLs of animals closer to the hydrophone. For each individual whistle the maximum SPL received was extracted, taking the varying sensitivities at different frequencies of the respective hydrophone system into account. Time delays between arrivals of multi-path signals which were required for the ranging technique were extracted using the spectrograph's cursor facility. For the remaining data sets all whistles could be used for analysis and were treated the same way.

SPECIES CHARACTERISTIC FEATURES IN COMMUNICATION SIGNALS

2.3. Source Level calculations

The extracted maximum sound pressure levels of social calls were converted into Source Levels (SL re 1 μ Pa at 1 m) using the simplified sonar equation for transmission loss (TL) due to direct path attenuation, i.e. spherical spreading and absorption:

$$SL = SPL + 20\log (R/1m) + \alpha * R \quad \text{Urick [25]}$$

SL = Source Level in dB re 1 μ Pa at 1 m : SPL = Sound Pressure Level in dB re 1 μ Pa
R = Range in metres : α = absorption coefficient in dB/m

The knowledge of both, the actual SPL of the recorded signal and the distance of the source producing this signal from the hydrophone is thus required.

2.3.1. Determination of the actual SPL of a signal.

For data sets T1 and T2 a 13 kHz pulsed cw pinger ('Netmark 1000', 300 ms pulse at 4 s) with a known SL (calibrated SL v battery voltage) provided a reference. These data sets are considered to be the ones with the highest confidence. However, the overall gain of the whole recording system for all the other set-ups was also established with reasonable confidence by calibration of each individual part of the recording chain. However, in a number of the original recordings information was missing for the exact settings of some of the vital parts. Since the possibility of an error being introduced by this in the second method is comparatively high, these data sets are treated with less confidence and are only used as a back-up for set-up T1 and T2.

The effect of different orientations of vocalising animals in respect to the hydrophone on the SPL has been considered negligible in this study as the directivity of the communication signals is believed to be very low. At 10 kHz (the centre frequency range of most selected whistles) the wavelength in seawater is 0.375 m which is not dissimilar from the maximum cross-section of a dolphin's head. This physical limitation restricts any significant beam formation ensuring a low Directivity Index (DI). This belief is supported by a comparison of SPLs between the direct path signal from a dolphin approaching the hydrophone at relatively close range (<100 m) in deep water and the echo amplitudes received from the surface and the bottom reverberation paths. The included vertical angle between these two multi-paths approached 150 degrees in this water depth. Since the reflection at the water/air boundary approaches 100% the attenuation along this path was compared to that of the direct path signal. The reduced SPL, after range correction, was found to be around 4 to 5 dB. Front-to-back ratios may be higher but generally there should be less than 12 dB variation in the polar radiated pattern in both azimuth and elevation and less than 6 dB variation in the forward looking 180 degree sector.

2.3.2. Determination of distance from source to hydrophone.

Again two different methods were used to obtain this information. For data set T1, T2, T3 and T4b the distance of the vocalising animal to the hydrophone was established using the echo-ranging technique, Kaschner *et al.* [20], Lepper [21]. In general the major advantages of this acoustic method over visual range estimates are its independence of surface weather conditions and its higher accuracy, Kaschner *et al.* [26], although under certain

SPECIES CHARACTERISTIC FEATURES IN COMMUNICATION SIGNALS

circumstances it can produce ambiguous results (as can be seen in Fig. 2 the effect of this on the SL results is relatively small). In respect to obtaining a SL the advantage lies in the certainty that both, distance and intensity information relate to the same signal. When more than one group of animals is in the area correlation of a particular whistle with visually obtained range estimates becomes a difficult if not impossible task.

Unfortunately the use of the multi-path echo-ranging method is limited by the depth of water and the best results were obtained in water depths between 50 and 300 m and the resulting range estimates deteriorate progressively at ranges above 1 km. For the remaining data sets (T4b&T5) the requirements were not met, but the animals at these particular times were observed bow riding so that the distance to the hydrophone could be established with certainty. The data set T4b was recorded on one occasion when a very vocal group of bow riding common dolphins was recorded simultaneously in air, using a standard Hi-8 camcorder microphone deployed directly above them on the bow, and underwater using the hydrophone attached to the trawl at a distance of 485 m behind them. Individual characteristically shaped whistles could be identified in both recordings. The results of the SL calculation of this data set further supported the validity of this method.

2.3.3. Determination of species.

Since the aim of this study was to investigate possible differences in SL among different species, data was only used when the animals had been visually identified. There were encounters with a variety of typical North Atlantic odontocete species during the CETASEL trials, among them Bottlenose dolphins (*Tursiops truncatus*), Pilot Whales (*Globicephalus melaena*), Atlantic White-sided Dolphins and Common Dolphins. All parameters necessary for the calculation of SLs were available for Common Dolphins (T2, T3, T4a,b, T5) and White-sided Dolphins (T1).

2.4. Statistical analysis

The results of the two main data sets (T1&T2) were analysed with the aid of a software program (CSS:STATISTICA, StatSoft™) using a Kruskal-Wallis test (ANOVA by ranks) in order to determine the significance of the variation in SL estimates for different species.

2.5. Further analysis

Using the equation cited in 2.3. a first attempt was made to obtain range estimates of animals based on the knowledge of the absolute intensity of their communication signals.

3. RESULTS

3.1. Constant maximum Source Levels

As can be seen in Figure 2. the resulting maximum SL estimates are more or less constant for one species, even though ranges of vocalising animals varied by more than 500 m and a variety of recording systems were used under varying circumstances. The observable intra-specific variation in SL may be explained by the different orientations of the vocalising animals in respect to the hydrophone (see above) or simply by the possibility that the whistles are not always emitted with the maximum possible intensity.

SPECIES CHARACTERISTIC FEATURES IN COMMUNICATION SIGNALS

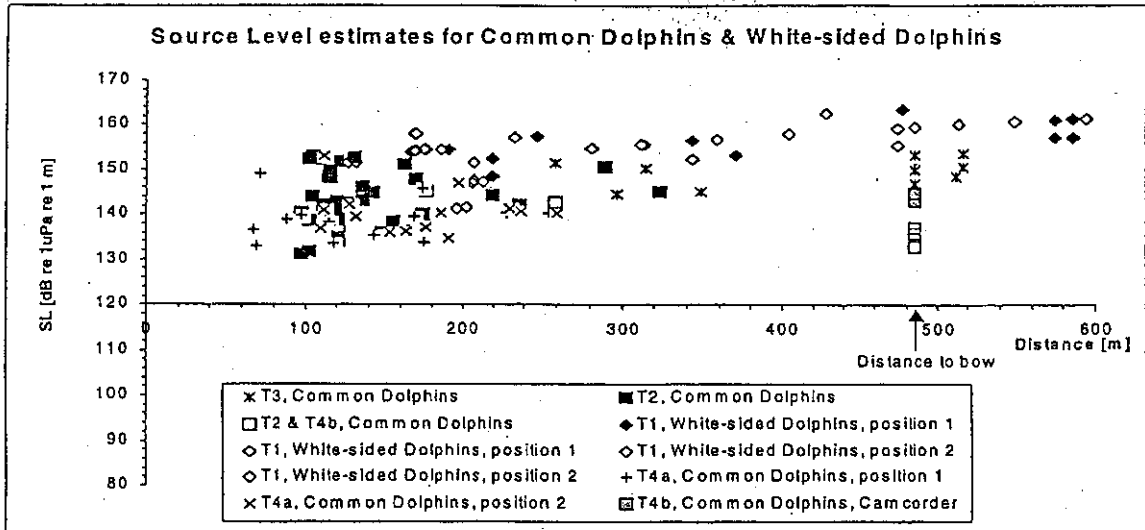


Fig 2. Source Level estimates for White-sided Dolphins (diamonds ?) and Common Dolphins (cubes). Solid black and dark grey symbols represent results with the highest confidence. Symbols in lighter shades of grey represent less confident results. In case of ambiguous results in range from the echo-ranging method SL estimates for both possible positions were shown.

Deteriorating signal to noise ratios (SNR) in higher seastates might encourage a louder vocalisation. That the noise floor is relevant is suggested by the data set with the lowest average maximum SL (T4a) which was recorded under very quiet, low seastate, conditions. The effect that the ambient noise floor may have on the intensity of the whistles will require further study.

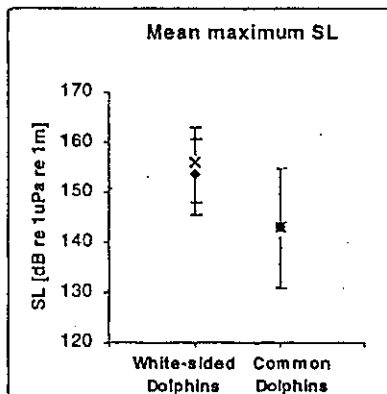


Fig. 3 Statistical results for the mean max. SL of White-sided (positions 1 & 2) and Common Dolphins and the respective standard deviations.

3.2. Source Levels as an acoustic species-characteristic feature

The statistical analysis of the results with the highest confidence (T1&T2, which were recorded in similar sea state conditions!) has established that the Source Level of these social calls are indeed a characteristic feature for these two species at least (Kruskal-Wallis test: $H(1, N=54) = 30.38793, p < 0.0001$ (position 1 of two possible positions for White-sided Dolphins or $H(1, N=52) = 25.33806, p < 0.0001$ (position 2)). is shown in Figure 3. As such it might be useful in the future when studying free-ranging cetaceans in several ways:

3.2.1 Aiding acoustic species identification. Under circumstances of low visibility conditions, the knowledge of the typical maximum SL of a certain species can be used as an additional classifier for species discrimination.

SPECIES CHARACTERISTIC FEATURES IN COMMUNICATION SIGNALS

3.2.2. Establishing maximum ranges. If a species has been visually identified at some stage, a known maximum SL typical for that species can be used to determine the maximum range of a vocalising animal. This is demonstrated with the help of the example in Figure 4: Even though the confidence in the absolute values for this data set (T5) is not very high (due to high directivity of the transducer which emitted the signal used for calibration) the relative values still serve as an example to illustrate this method.

The only information available on the position of the animals was that they were bow riding at the very beginning of this data set, so when first analysing this distance had been assumed to remain at a constant 3 m (an estimate for the average distance to hydrophone inside the bulbous bow chamber when animals were bow riding). These first results are shown on the left hand side of Figure 4. A definite decrease in max. SL over time was observed, which appears to be too evenly distributed to be simply due to the intraspecific variation. So, assuming that the animals were falling behind the ship (which was moving at over 5.5 ms^{-1} , or 11 knots), after the first 30 s, the max. SL measured was used to predict the range to these animals, as it is demonstrated on the right hand side of Figure 4.

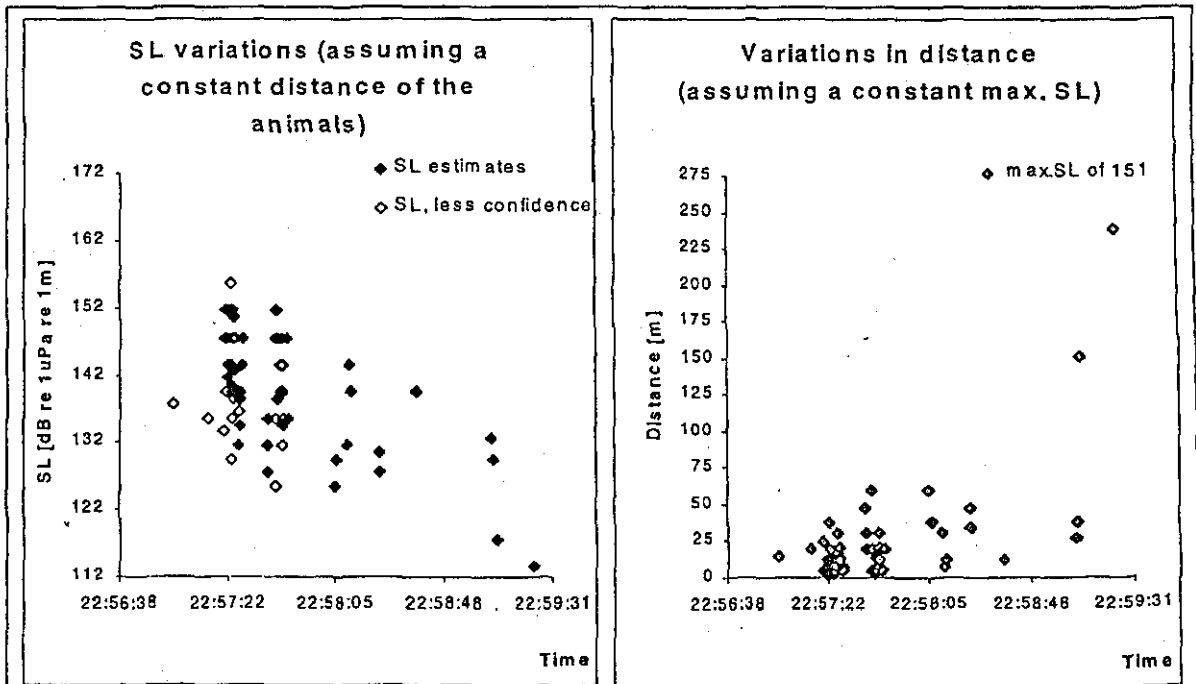


Fig. 4. An example for a first attempt to use maximum SL as a ranging method. For the results shown on the left hand side of this graph a constant distance of 3 m from the hydrophone was assumed. On the right hand side the decrease in measured SPL was assumed to be caused by an increase in distance instead, which was calculated based on a constant SL of 151dB.

Due the decreasing rate of spreading loss attenuation with increasing distances (Fig. 5), this unusual methodology is limited to data obtained at close range. At distances below 250 m the attenuation will be in the order of several dBs, detectable even when using this comparatively coarse method, which will in turn allow for a good approximation in distance.

SPECIES CHARACTERISTIC FEATURES IN COMMUNICATION SIGNALS

4. LIMITATION OF METHODS

SPREADING LOSS AND ABSORPTION

SPL dB re 1 μ Pa (SL=151 dB at 1m)

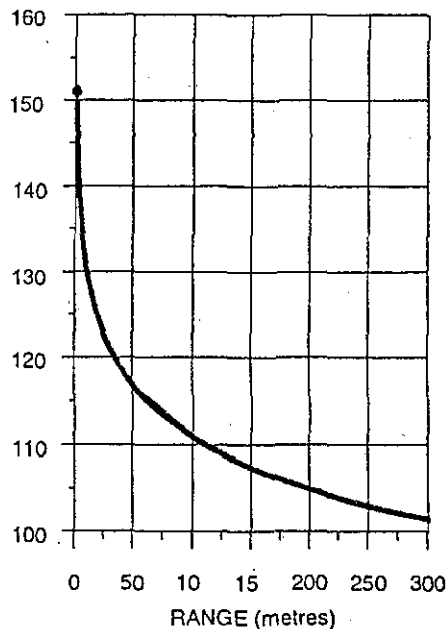


Fig. 5. Spreading loss - The rapid initial attenuation rate reduces with range due to square law spreading and absorption

Since the accuracy of the SL estimate is entirely dependent on the estimation of the source to hydrophone distance, any limitation or significant error introduced by the ranging technique will effect the SL estimate (see 2.3.2., Kaschner *et al.* [20]). Minor errors in range estimates are introduced by the assumption of a constant sound velocity profile and inaccuracy in measurements of water and hydrophone depth or time delays in the spectrogram. However, at ranges in excess of 100 m such errors usually introduce a difference in the order of about 1 dB when calculating the maximum SL. Another problem effecting the SL estimate is caused by the ambiguity of the results obtained from the echo-ranging when bottom and surface paths are incorrectly identified. As can be seen in Figure 2. the effect of this is similarly quite small. Further systematical errors may be introduced through the analysis software used to measure the intensity of a whistle in a spectrogram. Effects introduced by the DI, as the orientation of the vocalising animal changes, can usually be resolved while monitoring the same animals over the normal duration of an interaction which can extend to many minutes.

5. CONCLUSIONS

The results of post-processing this large tape archive of cetacean calls have been shown to include species specific features. The first results obtained by this relatively simple technique suggest that SL estimation is possible in open sea conditions and indicate that SL estimation may provide an additional tool to assist in discriminating between different species. The technique is independent of daylight and reasonable sea state conditions and can usefully extend data obtained from the associated visual observer records. Although primarily intended as an off-line processing technique this methodology could be applied during actual sea trials and the accuracy can be improved especially if additional environmental parameters are included in the technical log.

SPECIES CHARACTERISTIC FEATURES IN COMMUNICATION SIGNALS

6. FUTURE IMPROVEMENTS

In future sea trials additional parameters, such as the hydrophone position in the water column and the actual water depth should be continuously logged. Temperature and salinity records need to be exploited and the temperature profile in the water column should be sampled at intervals using expendable bathythermographs (X-BTs). With these additional parameters commercial ray tracing programmes can be employed to increase the accuracy of the echo-ranging technique. A semi-permanent installation of a calibrated bow chamber hydrophone will be valuable for use at close range and, in conjunction with one or two hydrophones (with known separations) towed behind the vessel at depth. The introduction of correlation signal processing to the echo-ranging technique will also improve these estimates. However, alternative quieter platforms than a pelagic trawler are strongly recommended for such work. The construction of a data base of such SL estimates for different species would allow these values to be used when attempting to discriminate between species especially at night. The procedures described require further investigation to assess the value of maximum SL estimation as a tool for inter-species classification and future studies should attempt to assess the possible effect of such external factors as signal to noise ratio, e.g. sea state conditions, and such internal relationships as body size. Comparison of SLs obtained in open water conditions with results obtained from pattern recognition techniques focussing on the analysis of whistle contour methods will be of interest.

7. REFERENCES

- [1] W E SCHEVILL & B LAWRENCE, 'Underwater listening to the porpoise *Delphinaterus leucas*', *Sci*, 109 pp143-144 (1949)
- [2] W E SCHEVILL, 'Underwater sounds of cetaceans'. In: *Marine Bio-Acoustics* (Ed. Tavolga, W.N.), Pergamon Press, Oxford, pp307-316 (1964)
- [3] W E EVANS & F T AWBREY, 'Natural history aspects of marine mammal echolocation: feeding strategies and habitat'. In: *Animal Sonar: Processes and Performance*, (Eds. P E Nachtigall & P W B Moore) Plenum Press, New York, pp521-534 (1988)
- [4] C KAMMINGA & H WIERSMA, 'Investigations on cetacean sonar. II. acoustical similarities and differences in odontocete sonar signals'. *Aquatic Mammals*, 8 (2), pp41-62 (1981)
- [5] H WIERSMA, 'A comparison of wave shapes of odontocete sonar signals', *Aquatic Mammals*, 9 (2), pp57-66 (1982)
- [6] J R BUCK & P L TYACK, 'Quantitative measure for similarity for *Tursiops truncatus* signature whistles' *J Acoust Soc Am*, 94 (5), pp2497-2505 (1993).
- [7] M C CALDWELL, D K CALDWELL & P L TYACK, 'Review of the signature whistle hypothesis for the Atlantic bottlenose dolphin', in *The Bottlenose Dolphin*, (Eds. S Leatherwood & R R Reeves) Academic, San Diego, CA Chap. 10 pp199-234 (1990)
- [8] B McCOWAN, 'A new quantitative technique for categorizing whistles using simulated signals and whistles from captive bottlenose dolphins (Delphinidae, *Tursiops truncatus*)', *Etho*, 100 pp177-193 (1995)
- [9] L S SAYIGH, P L TYACK, R S WELLS & M D SCOTT 'Signature whistles of free-ranging bottlenose dolphins *Tursiops Truncatus*: stability and mother-offspring comparisons', *Behav Ecol Sociobiol*, 26 pp247-260 (1995)
- [10] B McCOWAN & D REISS, 'Quantitative comparison of whistle repertoires from captive adult bottlenose dolphins (*T. truncatus*): a re-evaluation of the signature whistle hypothesis'. *Etho*, 100 pp194-209 (1995)
- [11] D WANG, B WÜRSIG & W EVANS, 'Comparisons of whistles among seven odontocete species. In: *Sensory Systems of Aquatic Mammals*, (Eds. R A Kastelein, J A Thomas & P E Nachtigall), DeSpil Publishers, Woerden, The Netherlands, pp299-332 (1995)

SPECIES CHARACTERISTIC FEATURES IN COMMUNICATION SIGNALS

- [12] W E EVANS, 'Vocalization among marine mammals'. In: Marine Bio-acoustics, (Ed. W N Tavolga), Pergamon Press, Oxford and New York Vol. 2, pp159-186 (1967)
- [13] W STEINER 'A comparative study of the pure tonal whistle vocalisation from five western north Atlantic dolphin species', Behav Ecol Sociobiol, 9 pp241-246 (1981)
- [14] C R STURTIVANT, 'Techniques to isolate dolphin whistles and other tonal sounds from background noise', Acoustic Letters, 18 (10) pp189-193 (1995)
- [15] A D GOODSON; R A KASTELEIN & C R STURTIVANT, 'Source Levels and echolocation signal characteristics of juvenile Harbour porpoises (*Phocoena phocoena*) in a pool'. In: *Harbour porpoises - laboratory studies to reduce bycatch*, (Eds. P E Nachtigall, J Lien, W W L Au & A J Read), DeSpil Publishers, Woerden, The Netherlands, pp41-53 (1995)
- [16] C R STURTIVANT & A D GOODSON, 'Literature available on the echolocation characteristics of the Harbour Porpoise (*Phocoena phocoena*) and Common Dolphins (*Delphinus delphis*)' Proc. European Association for Aquatic Mammals Conference, Kolmardens, SE., Abstract, (1994)
- [17] W W L AU, R W FLOYD, R H PENNER and A E MURCHISON. 'Measurement of echolocation signals of the Atlantic bottlenose dolphin, *Tursiops truncatus* Montagu, in open waters', J. Acoust Soc. Am. 56 pp1280-1290 (1974)
- [18] T AKAMATSU, Y HATAKEYAMA; T KOJIMA & H SOEDA, 'Echolocation rates of two Harbour porpoises (*Phocoena phocoena*)', Mar Mamm Sci, 10 (4) pp401-411 (1994)
- [19] F G WOOD & W E EVANS; 'Adaptiveness and ecology of echolocation in toothed whales'. In: *Animal Sonar Systems*, pp381-425 (1980)
- [20] K KASCHNER, P A LEPPER & A D GOODSON, 'Analysis and interpretation of cetaceans sounds obtained from a hydrophone attached to a pelagic trawl'. In European Research on Cetaceans - 11. Proc. 11th Ann. Conf. ECS, Stralsund Germany (Ed. P.G.H. Evans) European Cetacean Society, Cambridge (1997)
- [21] P A LEPPER et al. 'Development of a simplified ray path model for estimating the range and depth of vocalising marine mammals', this volume (1997)
- [22] D deHAAN, P Y DREMIERE; B WOODWARD; R A KASTELEIN; M AMUNDIN & K HANSEN, 'Prevention of by-catch of small cetaceans in pelagic trawls by technical means (Project CETASEL), ICES J Mar Sci (1997)
- [23] P R CONNELLY, B WOODWARD, A D GOODSON, P A LEPPER & D NEWBOROUGH, 'Remote sensing methods for cetacean interactions with pelagic trawl fishing gear'. In: *European Research on Cetaceans - 11*. Proc. 11th Ann Conf ECS, (Ed. P.G.H. Evans), European Cetacean Society, Cambridge (1997)
- [24] G PAVAN, 'A real time FFT spectrographic display for bioacoustics'. International Bioacoustics Council Symposium (XV IBAC 96) - 24-26 October Pavia, Italy. (1996) unpub.
- [25] R J URICK, *Principles of Underwater Sound for Engineers*, McGraw-Hill p342 (1967)
- [26] K KASCHNER, C R STURTIVANT & S DATTA. 'Acoustic assessment of the accuracy of ship-based visual observation of small cetaceans'. European Association for Aquatic Mammals Conference, Duisburg, Germany 18-22 March (1997). Abstract.

Proceedings of the Institute of Acoustics

DEVELOPMENT OF A SIMPLIFIED RAY PATH MODEL FOR ESTIMATING THE RANGE AND DEPTH OF VOCALISING MARINE MAMMALS

P A Lepper (1), K Kaschner (2), P R Connelly (1), A D Goodson (1).

(1) Underwater Acoustics Group, Electronic & Electrical Engineering Dept.,
Loughborough University, LE11 3TU, UK.

(2) Biologie II, Abteilung Teirphysiologie / Zoologie, Albert-Ludwigs-Universitat Freiburg, DE.

1. ABSTRACT

As part of a pelagic trawl fishery study investigating the causes of small cetacean bycatch a simplified ray path model was developed to simulate various sound source and single hydrophone receiver geometry's to predict a vocal target's range and depth. The computed differences in the arrival time of first order multi-path signals (surface and seabed reflections) were compared with those measured from a recorded data set obtained during sea trials. A number of assumptions were made in the initial model, which included: limited range and water depth, a constant sound velocity-depth profile and the treatment of the surface and seabed as a simple parallel reflecting surfaces. Initial results provided examples with reasonable correlation between the estimated range of submerged vocalising cetaceans and the associated surface sightings. In addition, cetacean behaviour within the water column very close to the pelagic trawl could be detected. Some examples of ambiguous solutions were noted which may result from incorrect identification of the surface and bottom returns, inaccurate hydrophone or water depth data and/or resolution limitations in the multi-path timing measurement method. The use of correlation signal processing techniques and stand-alone depth measurement devices is proposed for future studies. Within constraints, this relatively simple ranging technique provides valuable additional information regarding cetacean behaviour in the wild and can be applied off-line to recorded data sets to validate observer records. The method allows cetacean detection and localisation in both range and depth to be obtained at night or in increasing seastate conditions when visual sighting methods become impracticable. The introduction of more precise time measurement techniques and better ray path modelling should provide greater accuracy and this technique may be developed for on-line application.

2. INTRODUCTION

As part of the European Commission's DGXIV CETASEL project a study of small cetaceans was made along the edge of the continental shelf between SW Eire, Biscay and Northern Spain. A main objective being to investigate the behaviour of small cetaceans interacting with pelagic trawls and to look for technical means which might reduce the incidental catch of these mammals in the commercial fishery. A large mid-water trawl was operated by Dutch fisheries research vessel (FRV Tridens), typically in water depths in excess of 100m near the shelf break. Study techniques included the use of surface observers, various passive acoustic listening devices, and the use of a remotely operated vehicle (ROV) equipped with scanning sonar and low light TV cameras.

A multiple hydrophone system has been developed in order to track echolocating cetaceans at short range, Connelly [1]. Comparison of the arrival times of high frequency echolocation 'clicks' received on a sparse hydrophone array attached to a fishing trawl, allow the spatial position of a cetacean to be localised as it interacts with fish herded in the open mouth of the net. This tracking array was formed using 5 hydrophones, 4 contained in two oil filled *streamers*, which were directly attached to the headrope of the pelagic trawl which was deployed at distances up to 800m behind the vessel and at depths around 100m, fig .1. Signal processing to extract the 'click' timing data was carried out underwater on all 5 hydrophone channels. This timing data was then coded and modulated before transmission to the ship via a 1.8 km

Proceedings of the Institute of Acoustics

A SIMPLIFIED RANGING METHOD FOR VOCALISING MARINE MAMMALS

long coaxial 'Netsonde' cable. Analysis of the difference in arrival time for signals received on the different hydrophone channels was carried out using a data set spanning over 14 weeks of sea trials. This short range system was developed to compute the positions and track echolocating animals interacting with the fishing trawl in three-dimensional space.

Additional low frequency (4-20 kHz) recordings were made of cetacean 'communication' calls vocalisations as these could be detected at much longer ranges (typically >1km) using the fifth hydrophone of the sparse array tracking system which was positioned a few metres above and forward of the plane of the two streamers. This hydrophone comprised a preamplified single Benthos AQ4 element contained within a small oil filled pod. The masking effect of the fishing vessel's self-noise was reduced by the use of a high-pass filter, which desensitised the system to noise below 4 kHz. The signals were then 'band-split' and separately processed into HF 'click' data and LF 'whistle' or 'vocalisation' signals. Both low and high frequency data were then transmitted to the surface via the Netsonde cable.

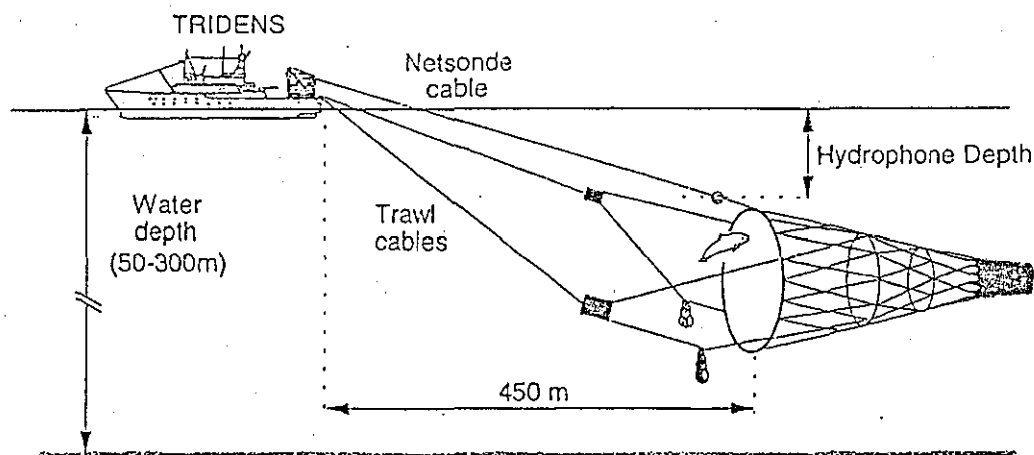


Figure .1. Hydrophone position on the pelagic trawl.

During several encounters of cetaceans during a trial held in October 1996 both 'click' and 'whistle' signals were observed from animals in the vicinity of the ship. A number of examples of the lower frequency 'whistle' signals (< 20 kHz) were found during analysis to include strong multi-path echoes, i.e. delayed echoes resulting from the longer propagation paths formed by reflections via the seabed and the sea surface. With knowledge of the hydrophone position and the water depth, comparison of the arrival time of the direct and multi-path components of a signal has allowed the estimation of both the range to, and the depth of, the signal source from the receiver.

Although intended to supplement and validate the visual observer's records of events this off-line tool has proved useful as it provides underwater behavioural data in conditions where surface visual observation is range limited by sea state or by darkness. This paper concerns the exploitation of a digitally recorded data set obtained using the single hydrophone receiver.

3. MULTI-PATH SIGNALS

Acoustic signals arriving at a receiver are joined by acoustic radiation outside the main path of the direct signal after reflection at either the surface or the seabed. Multi-path phenomena of this type are characteristic of acoustic propagation underwater. The study of the problem of image interference in man

Proceedings of the Institute of Acoustics

A SIMPLIFIED RANGING METHOD FOR VOCALISING MARINE MAMMALS

made acoustic systems due to multi-path echoes, dates back to the early developments in underwater telemetry and communication systems, Caruthers [2]. The increased path lengths resulting in a delayed arrival time and interference with the direct signal.

Many authors have also studied reflection and scattering effects at both the surface and seabed. A perfectly smooth sea-surface would form a near perfect reflector, more realistic situations however resulting in reflection losses of around 3dB at frequencies of 25 – 30kHz, Urick and Saxton [3] and Liebermann [4]. The degree of scattering at the surface in relation to reflection can be described in terms of the Rayleigh parameter $R = kH \sin \theta$ where k is the wave number ($2\pi/\lambda$), H the rms 'wave height' and θ is the grazing angle, Urick [5]. For $R \ll 1$ the surface acts as primarily as a reflector and $R \gg 1$ as a scatterer. The degree of coherent reflection on an identical reflection and incident angle is therefore increased at lower frequencies and under smoother conditions. In the case of a 10 kHz signal and a 1m wave height both scattering and reflection take place, sufficient acoustic radiation may however be reflected at a similar incident to reflected angle to allow the detection of simple reflected multi-path signals.

Reflection, scattering and transmission losses must be considered in the case of incident sound radiation arriving at the seabed. The predictions of reflection losses are however more complex than the surface due to a greater variety of seabed materials and multi-layering of the seabed itself. Additional reflected signal level may be lost due to transmission of sound into the seabed. This radiation may then be re-reflected from a sub-bottom layer of differing material. The study of sound propagation at and in the seabed has also had considerable attention, Cron and Schumacher [6], Mackenzie [7], Eyring, Christenson and Raitt [8].

Refraction effects due to variations in sound velocity with depth may also cause a bending of the propagation path seen by an acoustic signal. In the case of source and receiver placed close to the seabed in deep water, ranges may be limited to several km. Variations in sound velocity with depth and the travelling of curved paths results in a variation in propagation times for signals travelling different routes, Cestone [9]. The application of Snell's law to refraction effects, Mackenzie [10], when applied to sound propagation in water of varying sound velocities has become one of the most important features of ray path models. Models for sound velocity prediction in terms of temperature, salinity and pressure have been developed over several years, reviewed Mackenzie [11] and later refined by Ross [12].

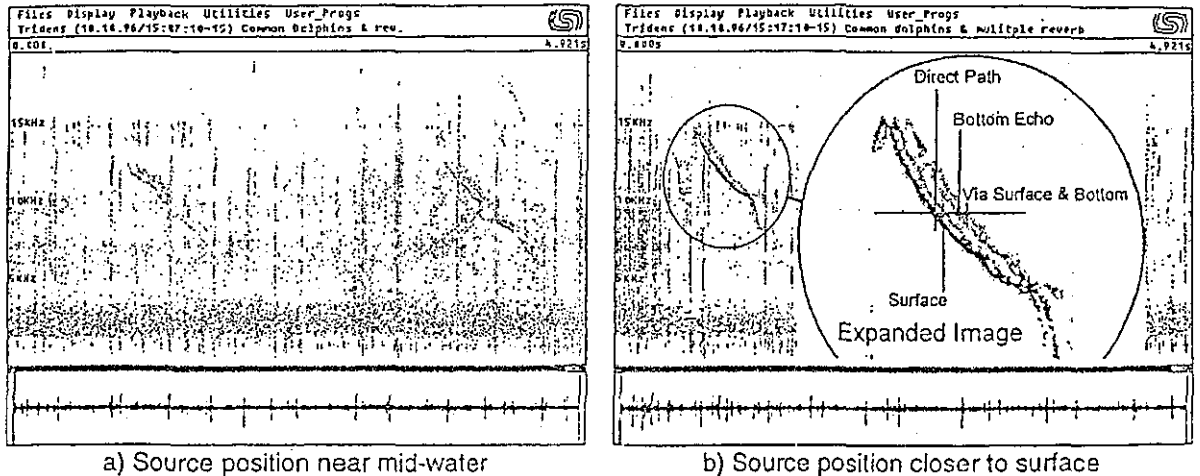
Although exact prediction of sound behaviour at the surface and seabed is complex, the treatment of both the surface and seabed as parallel plane reflectors was felt valid in the conditions considered as relative time of arrival, rather than amplitude, forms the basis of the ray path model in this study. Additional effects such as phase shifting, frequency smearing (due to the frequency of the wave movement, Roderik and Cron [13]) and refraction were ignored for this application as the resultant variations in received signals at the relatively short ranges of interest, <1km, were not believed to be significant.

4. METHOD

The higher frequency component (typically =120 kHz) of echolocation signals observed in bottlenose dolphins (*Tursiops truncatus*) exhibit a high degree of directivity. Typical -3dB beam-widths in the order of 10° have been measured in both the horizontal and vertical plane at these frequencies, Au [14]. Lower frequency vocalisation signals, typically less than 22 kHz, are often observed during interactions with cetaceans. These social calls are projected with a much lower directivity than that of the high frequency echolocation emissions. The probability of the simultaneous generation of multi-path echoes reflected from the sea surface and sea bed is increased for these low frequency vocalisations.

Proceedings of the Institute of Acoustics

A SIMPLIFIED RANGING METHOD FOR VOCALISING MARINE MAMMALS



a) Source position near mid-water
 b) Source position closer to surface
Figure 2. Rolling map FFT of vocalisation signals of cetaceans including multi-path signals.
 Note - Signals filtered below 2 kHz to reduce self-noise of observation platform. Broadband transients are derived from the pelagic trawl gear

Off-line analysis of possible multi-path signals obtained during the October 1996 trial was carried out in both time and frequency domains. A rolling map spectrograph - Fast Fourier Transform (FFT) frequency analysis - was used to display the signals, fig .2., and peak signal levels for both the direct and each multi-path for a given frequency modulated 'whistle' were observed. A single frequency point, with a steep frequency gradient and good signal to noise ratio, for both the direct and multi-path signals was selected and expanded on the display. Arrival time differences of these peaks at a specific frequency could then be measured with the analyser's measurement cursors.

Simple ray path models were developed in software for known depths and hydrophone positions assuming reflections of the signal at the surface and seabed. The peak signal observed for the multi-paths were assumed to have identical angles of incidence and reflection and a constant sound velocity profile with depths. Comparisons of the measured and modelled arrival time differences was then made to measure the echo delays .

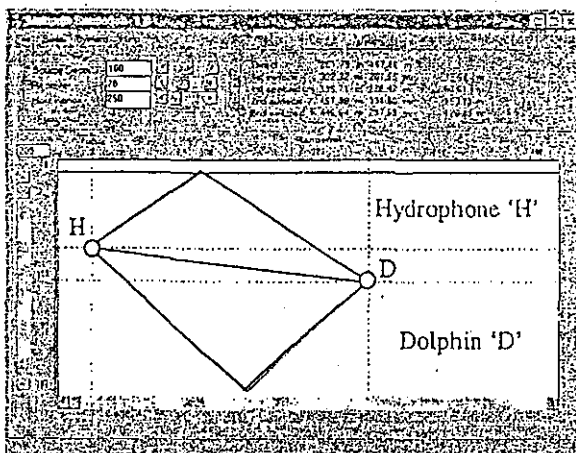


Figure 3a. Surface and seabed multi-path simulation.

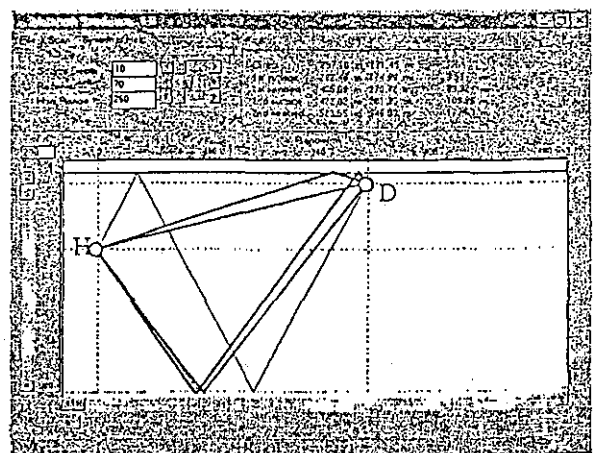


Figure 3b. Source near surface - additional multi-path

Proceedings of the Institute of Acoustics

A SIMPLIFIED RANGING METHOD FOR VOCALISING MARINE MAMMALS

Although used initially while exploring the methodology, manual adjustment of the geometry to match measured timings was time consuming and prone to error. Scanning software was therefore developed,

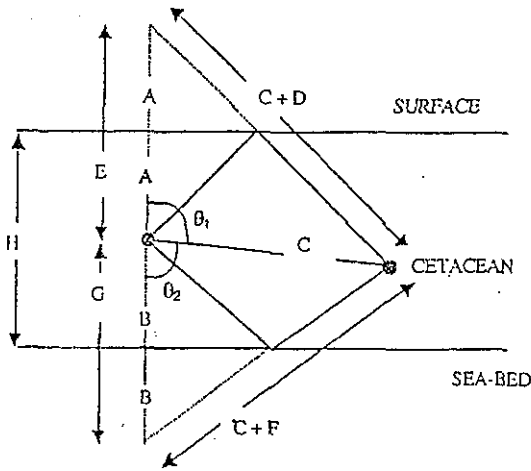


Figure 4. Geometry of simple multi-path signals.

fig.3a. to evaluate all possible permutations of the ray geometry in discrete resolution steps. All the geometric paths within defined ranges were therefore evaluated and prioritised for the closest matches to the observed timings. Several examples were also seen which included second order delays resulting from a path which included both surface/bottom and bottom/surface reflections. Sources which vocalised close to the surface were characterised by double echo traces, Fig.2b, resulting from the ray geometry modelled in Fig.3b.

Within this simple geometry, a mathematical solution for positions can also be found. Knowledge of water depth (H) hydrophone depth (A) and multi-path propagation differences (D and F) allows the derivation of angle θ_1 and range to the source (C), fig.4.

$$\theta_1 = 180 - \theta_2$$

$$\cos \theta_1 = -\cos \theta_2$$

$$G = 2B = 2(H - A)$$

$$D = vel \times t_{rev1}$$

$$F = vel \times t_{rev2}$$

Using the Cosine rule:

$$\cos \theta_1 = \frac{E^2 + C^2 - (C+D)^2}{2EC}$$

and

$$\cos \theta_2 = -\cos \theta_1 = \frac{G^2 + C^2 - (C+F)^2}{2GC}$$

Equating these equations gives:

and:

$$C = \frac{G^2 E - F^2 E + E^2 G - D^2 G}{2(GD + EF)}$$

$$\theta_1 = \cos^{-1} \left(\frac{4A^2 - 2CD - D^2}{4AC} \right)$$

Calculation of both source range and source depth is possible. The algorithm does however require knowledge of which received echo is associated with which multi-path. Reversal of which can yield alternate solutions. Comparison is possible with solutions found using the scanning technique, covering all

Proceedings of the Institute of Acoustics

A SIMPLIFIED RANGING METHOD FOR VOCALISING MARINE MAMMALS

possible ray path geometry's. The closest matched solutions from the scanning technique were then compared to similar geometry's applied to the above algorithm as validation.

5. RESULTS

A large number of multi-path signals similar to those shown in fig .2. were subsequently analysed using the scanning technique, Kaschner [15, 16]. In most cases a single unambiguous solution was produced and these range circles were compared with the surfacing positions recorded in the observer's log. In most cases the computed range to the vocalising animal could be interpolated between the observed surfacing positions. Where the calculated range clearly did not match the observed animal's position a careful analysis of all the signals in the same time period demonstrated that the sound sources would usually cluster at two different ranges indicating that a second group of animals was also being detected. Establishing the precision of this ranging technique at longer ranges is a little difficult. However, accurate ranging was possible whenever animals crossed ahead of the ship and passed very close to the bow. In these conditions the distance between the surfacing animal and the hydrophone attached to the trawl was determined by the length of the ship and by the trawl warps. By taking the ship's speed and its course into account, relative to the typical swimming speed of the cetaceans, permits a track plot to be constructed which can frequently be extended well beyond the observers sighting range. During the CETASEL study this non-intrusive methodology was able to confirm that some dolphins had an affinity for the pelagic fishing gear and would deviate from their course and stay in close proximity to the trawl for extended periods lasting many minutes before moving on. It was also noted that dolphins appeared to dive repeatedly to a similar depth, at which they were very vocal. This behaviour, which may suggest the presence of prey at this depth, requires further study Kaschner [15].

Example:

Water depth = 200 m;

Trawl mounted hydrophone = 70 m depth;

1st Surface reflected path delayed echo

arrives 3.59 ms after the direct path signal;

1st Bottom reflection arrives after 99.8 ms.

A = 70m; B = 130m; E = 140m; G = 260m

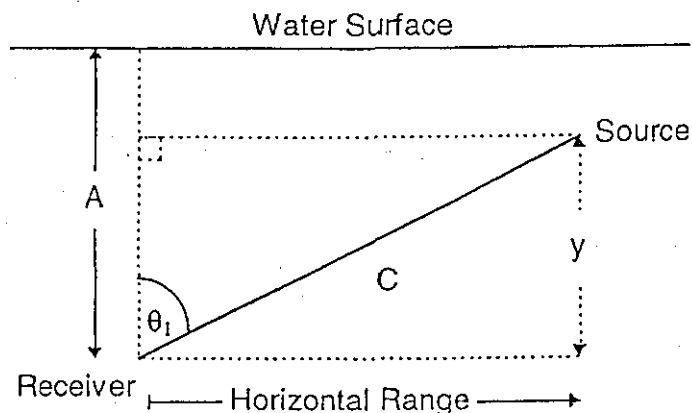
D = $1500 \times 3.59 \text{ ms} = 5.385 \text{ m}$;

F = $1500 \times 99.32 \text{ ms} = 148.98 \text{ m}$

\therefore Horizontal Range = 250m and $y = 60\text{m}$,

Receiver Depth (A) = 70

\therefore Source Depth = $(A - y) = 70 - 60 = 10\text{m}$



Several examples of multiple solutions, with two 'good fits' to the measured arrival time differences were found. This ambiguity becomes problematic when both the source position and the hydrophone approach mid-water depth and relative echo intensity cues make discrimination between the surface and bottom echo paths more difficult. As the vocalisations made by individual animals are frequently stereotyped, plotting the results of several sequential range estimates usually resolves such ambiguities. In future such multiple solutions could be eliminated through the use of a second hydrophone placed in the vicinity of the first. Only a single matching solution for both receivers should then exist. Small variations in the water and receiver depth measurements of just a few metres can cause relatively large variations in the target range/depth solution obtained and may also result in the generation of ambiguous or multiple solutions. Improvements in the accuracy of the measurements will minimise both the ranging errors and the

Proceedings of the Institute of Acoustics

A SIMPLIFIED RANGING METHOD FOR VOCALISING MARINE MAMMALS

generation of ambiguous results. In future the use of a stand alone depth measurement system, placed near the hydrophone, which can be synchronised to an automatic log of the echosounder depth recorded on board the vessel will provide greater accuracy.

Errors may also be introduced due to inaccuracies in the measurement of arrival times. Better accuracy is achieved when a suitable part of the signal spectrum can be selected where the signal frequency is changing rapidly and where an adequate signal to noise ratio exists for both the direct and multi-path signals, Rosenberger [17]. Difficulties may also arise if the arrival times of both surface and bottom multi-path echoes coincide. There is a particular problem when both the source and receiver approach mid-water. Correlation signal processing techniques are now being developed in order to remove the limitations of the manual cursor measurement. This approach exploits the time/bandwidth product of the signal and can achieve much better echo timing and relative amplitude measurement accuracy. Other errors can be introduced by local variations in sound velocity within the water column which may cause refractive deviations from the predicted ray path. The inclusion of ray path correction's within models is feasible if the sound velocity profile is known, Mackenzie [11]. However, the measurement of sound velocity profiles from the moving fishing vessel was not possible at the time these recordings were made. The application of standard profile models, Ross [12], is proposed to allow comparison with the straight-line models presented here in order to assess the magnitude of such errors.

6. CONCLUSIONS

Although a simplistic approach to sound propagation underwater has been applied in the models developed, this technique has been used to provide some valuable information concerning cetacean behaviour around a pelagic fishing vessel operating at the continental shelf edge in 100-200 m water depth. The archive of acoustic data examined was recorded between 1995 and 1997 in a series of sea trials mainly carried out to the SW of Ireland, through Biscay and along the N Spanish coast as part of the European Commission DGXIV project CETASEL. A large part of this data set contained vocalisations with significant multi-path echo components. Refraction effects due to temperature and salinity variations in the water column have been ignored as at shorter ranges in these depths the reflection angles tend to become acute. Sound velocity variations may be expected to introduce increasingly significant errors at longer ranges and shallower reflection angles. Within the data set examined, such errors are believed to be quite small when compared with the simple visual range estimates made by observers. Also, within the limited observation time window created by the moving vessel, the accuracy of relative range estimates made from the ship to the different vocalising animals can be expected to remain consistent. This technique has successfully allowed calls from individual animals to be assigned to different range groups and indicate probable cetacean pod associations. In addition the spectrum and the envelope shape of the individual calls detected has been analysed separately and this data used when determining the number of vocalising animals present in these groups. Multi-path range estimates can be used to validate, and in some cases correct, the visual observer record of events. The use of more sophisticated ray path prediction methods to improve the absolute accuracy will probably require a *velocimeter* which can be dipped at intervals to explore the sound velocity characteristics of the water column. Alternatively, accurate temperature and salinity measurements in the water column will need to be obtained to predict the sound velocity variations. In either case such measurements are difficult to obtain from a moving pelagic fishing trawler and the information was not available with this recorded data set. This simple non-intrusive ranging technique has shown good correlation with observed surfacing behaviour and, together with the associated depth estimates, should assist in the study of cetacean behaviour in situations whenever clear multi-path signals are obtained. With better knowledge of water column conditions and the use of correlation signal processing techniques some improvement in the accuracy of this ranging method appears likely and on-line processing at sea should be possible.

Proceedings of the Institute of Acoustics

A SIMPLIFIED RANGING METHOD FOR VOCALISING MARINE MAMMALS

7. REFERENCES

- [1] CONNELLY P, WOODWARD B, GOODSON D, LEPPER P and NEWBOROUGH D, 'Remote Sensing Methods for Cetacean Interactions with Pelagic Trawl Fishing Gear', 10 - 12th March, Proc. 11th Annual Conference European Cetacean Society, Stralsund, Germany, in: P.G.Evans (ed), *European Research on Cetaceans - 11*, (1997) in press.
- [2] CARUTHERS J.W, 'Fundamentals of Marine Acoustics', Elsevier Oceanography Series 18, Elsevier Scientific Publishing Co., Amsterdam. (1977).
- [3] URICK R.J and SAXTON H.L, 'Surface Reflection of Short Supersonic Pulses in the Oceans', *J. Acoust. Soc. Am*, 19:8. (1947).
- [4] LIBERMANN L.N, 'Reflection of Underwater Sound from the Sea Surface', *J. Acoust. Soc. Am*, 20:498. (1948).
- [5] URICK R.J, 'Principals of Underwater Sound', McGraw-Hill. (1967).
- [6] CRON B.F and SCHUMACHER W.R, 'Theoretical and Experimental Study of Underwater Sound Reverberation', *J. Acoust. Soc. Am*, Vol. 33 No 7, p881-888. (1961).
- [7] MACKENZIE K.V, 'Reflection of Sounds From Coastal Bottoms', *J. Acoust. Soc. Am*, Vol. 32 No 3, p351-355. (1960).
- [8] EYRING C.F, CHRISTENSEN R.J and RAITT, 'Reverberation in the Sea', *J. Acoust. Soc. Am*, Vol. 20 No 4, p462-475. (1948).
- [9] CESTONE J.A, 'Sensors and Navigation Systems for Deep Water Submergence Program', IEEE International Convention Record. (1966).
- [10] MACKENZIE K.V, 'The Acoustic Behaviour of Near-Bottom Sources Utilised for Navigation of Manned Deep Submergence Vehicles', *Marine Technol. Soc. J.* 3(2), 45-56. (1969).
- [11] MACKENZIE K.V, 'Formulas for the Computation of Sound Speed in Sea Water', *J. Acoust. Soc. Am.* 32:100. (1960)
- [12] ROSS D, 'Revised Simplified Formula for Calculating the Speed of Sound in Sea Water', Memorandum SM-107, Saclant ASW Research Centre, USA. (1978).
- [13] RODERICK W.I and CRON B.F, 'Frequency Spectra of Forward Scattered Sound from the Ocean Surface', *J. Acoust. Soc. Am*, 48:759. (1970).
- [14] AU W.W.L, 'THE SONAR OF DOLPHINS', Springer - Verlag, New York, Inc. (1993).
- [15] KASCHNER K, LEPPER P.A and GOODSON A.D, 'Analysis and Interpretation of Cetacean Sounds Obtained from a Hydrophone Attached to a Pelagic Trawl', 10 - 12th March, Proc. 11th Annual Conference European Cetacean Society, Stralsund, Germany, in: *European Research on Cetaceans*, (ed) P.G.Evans. (1997).
- [16] KASCHNER K, GOODSON A D, CONNELLY P R, LEPPER P A. 'Species characteristic features in communication signals of cetaceans: Source Level estimates for some free ranging North Atlantic odontocetes'. Proc. Institute of Acoustics Symposium on Underwater Bio-Sonar and Bioacoustics. Loughborough University, December 1997. (This volume)
- [17] ROSENBERGER J.C. 'Passive localization'. In: *Underwater Acoustic Data Processing*. Y T Chan (ed), NATO ASI Series E. Vol.161 pp511-522 (1988).

